DOUBLE SEISMIC ZONES:
A FIRST ORDER FEATURE OF PLATE TECTONICS

A DISSERTATION

SUBMITTED TO THE DEPARTMENT OF GEOPHYSICS

AND THE COMMITTEE ON GRADUATE STUDIES

OF STANFORD UNIVERSITY

IN PARTIAL FULFILLMENT OF THE REQUIREMENTS

FOR THE DEGREE OF

DOCTOR OF PHILOSOPHY

By

Hitoshi Kawakatsu

March 1985

I certify that I have read this thesis and that in my opinion it is fully adequate, in scope and quality, as a dissertation for the degree of Doctor of Philosophy.

Robert Nelle

(Principal Adviser)

I certify that I have read this thesis and that in my opinion it is fully adequate, in scope and quality, as a dissertation for the degree of Doctor of Philosophy.

Robert L Knach

I certify that I have read this thesis and that in my opinion it is fully adequate, in scope and quality, as a dissertation for the degree of Doctor of Philosophy.

Norman H. Sleep

Approved for the University Committee on Graduate Studies:

Dean of Graduate Studies & Research

I certify that I have read this thesis and that in my opinion it is fully adequate, in scope and quality, as a dissertation for the degree of Doctor of Philosophy.

(Principal Adviser)

I certify that I have read this thesis and that in my opinion it is fully adequate, in scope and quality, as a dissertation for the degree of Doctor of Philosophy.

I certify that I have read this thesis and that in my opinion it is fully adequate, in scope and quality, as a dissertation for the degree of Doctor of Philosophy.

Approved for the University Committee on Graduate Studies:

Dean of Graduate Studies & Research

ACKNOWLEDGMENTS

I was lucky to be able to work with such extra-ordinary people, Bob Geller, Tetsuzo Seno, and Norm Sleep, as my senior scientists. Bob-sensei, Seno-san and Norm have taught me what is a true scientist and not; what is a true Japanese and not; what is a true human being and not; not respectively and maybe respectably. Bob made me to realize that asking questions was the most important thing in geophysics and that whether or not you find answers did not matter. Seno-san showed me that there were no difference between questions and answers. Norm proved me that every question had infinite number of answers and that what was important was to choose the right one.

I thank Bob Geller for his general deep understanding of me as an advisor and for his support of my work. He let me to do whatever I wanted to do and let me to say whatever I wanted to say. I appreciate his tolerance and am very happy that my tongue is still here. Nobody on this Earth except him could be my advisor. Although none of my work with Bob is presented in this thesis, his influence can be seen everywhere. Nagai Aida Arigato Gozaimasita !!

I thank Seno-san for being a co-worker on Chapter 2. He let me to use some of his data in this thesis. He also introduced me that there was something called 'double seismic zone', which turned out to be the theme of this thesis.

I thank Norm for just being Norm. You are so wonderful, Norm! I wish you knew how to cook fish, though.

I enjoyed being with my graduate fellows of the Geller/Sleep 385G/H group; Shi-Chen Wang, Glenn Kroeger, Joe Stefani, Sandra Morris, Rick Schult, Jan Morton, Eric Peterson, Rob Haar, Andy Michael, Paul Layer, Doug Wilson and Les Nakae. I thank them for their friendship and encouragements. I especially thank Glenn, my ghost office-mate, for letting me to use his computer program and for his selfish and un-selfish devotion to our computer as a system programmer; Joe for number of stimulating discussions on geophysics and science in general and for 'the moon'; and Rick for picking me up at the S.F. airport on the first day of my stay at Stanford and for everything. I also thank the faculty members and the secretarial staff of the Geophysics Department for general help and J. Daniel, J. Walker and Mr. Smirnoff for their companionship. The ways of life of M. Miyamoto and Miss Oshin also encouraged me

very much. I thank Stevie Wonder. I liked your song from the bottom of my heart.

I am grateful to the Japan Ministry of Education and NSF for supporting me through their fellowship and grants EAR80-19457, EAR80-19463, EAR81-08718, EAR82-18961, EAR83-06555, respectively.

I thank Dr. D. Giardini of Harvard University for sending me a tape of CMT solutions and Dr. Fumiko Tajima of University of Texas for JHD program. Eric Peterson and Gay Bradshaw kindly read this thesis and made a lot of comments. I deeply appreciate their help.

I especially thank my parents and brother for their understanding, encouragements and love. It was my four-years-older brother (not Carl Sagan) who showed me all the wonderful world of physical sciences in my childhood and had lead me there, although I ended up struggling in the jungle of geophysics. I would like to dedicate this thesis to them and to everything that has been broken, including my left clavicle, my heart and the subducted slabs.

Finally, I thank my wife for her loving support and all the ..... woops, I forgot to have one.

DOUBLE SEISMIC ZONES: A FIRST ORDER FEATURE OF PLATE TECTONICS

Hitoshi Kawakatsu, Ph.D.
Stanford University, 1985

In this thesis, I study the seismicity of subducting slabs above 200 km depth in detail to investigate the origin of double seismic zones and stresses in the subducting lithosphere.

The regional and temporal variation of seismicity along the northern Honshu arc, Japan, is first studied using accurate focal depths and focal mechanism types. Out of more than 900 well-located earthquakes selected from the bulletins of the International Seismological Centre, I determine the types of the focal mechanisms of ~ 210 events using P wave first motion data reported from local stations. The main conclusions are: (1) the zone of large interplate thrust earthquakes extends deeper (down to ~ 60 km) than those of other subduction zones (~ 40 km); (2) in some areas, double seismic zones extend seaward beyond the so-called 'aseismic front' and the overlap of the double seismic zone and interplate thrust zone creates a 'triple seismic zone'; (3) there appears to be a correlation between the state of stress accumulation at the interplate thrust zone and the activity of earthquakes in the double seismic zone.

The seismicity of the northern Tonga arc, which has been regarded as the prototype of a compressionally loaded slab, is studied next. A careful examination of major ($m_b > 5.3$) earthquakes reveals a rather unexpected result: the presence of a double seismic zone between depth of 70km - 200km. This discovery of the Tonga double seismic zone suggests that the double seismic zone is a more general feature of subducting slabs in the intermediate depth range than previously thought.

The seismic strain rate estimated from earthquake activity in the intermediate depth range is of the same order as the strain rate expected from geometrical unbending of subducted slabs, and much higher than that expected from thermo-elastic strain. Thus thermal stress cannot be the main cause of the double seismic zone, while unbending of the subducting slab can. Oceanic lithosphere bends above a depth of ~ 60 km when it subducts into the mantle.

The fact that the subducting lithosphere is almost straight in the mantle below a depth of ~ 200 km indicates that the lithosphere must therefore unbend in a depth range from ~ 60 km to ~ 200 km to become straight below a depth of ~ 200 km. Plate tectonics, therefore, requires the unbending of subducting slabs and the presence of double seismic zones at intermediate depth range of subducting slabs.

Approved for publication:

By Robert Dell
For Major Department

By _____
Dean of Graduate Studies and Research

昭和六十年三月二十八日

川勝君

君のような ろん文は とっても少ないので、
読む気持ちは 本当に すごく楽しかった。
学生として良くて、今から研究者として良く
成れる。おめでとう。

ケビラー

TABLE OF CONTENTS

to subducted oceanic lithospheres

CHAPTER I

INTRODUCTION

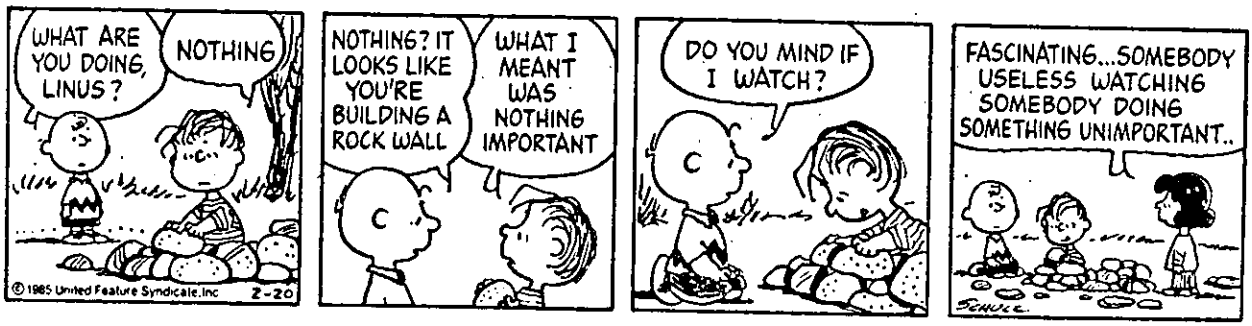

The aim of this thesis is to describe and explain the nature of earthquake activity (so-called **double seismic zone**) in the intermediate depth range within the framework of **plate tectonics**.

In the theory of plate tectonics, the zone of intermediate depth and deep earthquakes[†] (Wadati, 1935; Gutenberg and Richter, 1954; Benioff, 1955) is considered the trace of subducting oceanic lithosphere. Isacks and Molnar (1969, 1971) investigated the faulting mechanisms of 204 intermediate depth and deep focus earthquakes globally, and found a general parallel trend between one of the principal stress axes and the dip direction of the Wadati-Benioff zone. I will refer to orientations of the stress axes in which the P or T axis is parallel to the local dip of the slab as '**down-dip compression**' or '**down-dip tension**', respectively, as used by Isacks and Molnar (1969, 1971).

Figure 1.1 (Isacks and Molnar, 1971) shows the variation of down-dip stress type as a function of region and depth. They concluded that deep earthquakes (>300 km) were strongly down-dip compressional, while intermediate-depth earthquakes were more variable. They also suggested a correlation between the down-dip stress type at intermediate depths and the gross nature of the distribution of seismicity as a function of depth. These observations led them to the model shown in Figure 1.2, in which the stress distribution within slabs is determined by the gravitational force acting on the excess mass within the slabs and the support from the viscous mantle. They noted the imperfection of this model for intermediate depths, where down-dip compression and down-dip tension earthquakes sometimes exist in close proximity, but did not further investigate the possible cause of the model's imperfection.

The discovery of double-planed seismicity at intermediate depths - i.e, a double seismic zone - beneath Japan (Tsumura, 1973; Umino and Hasegawa, 1975; Hasegawa et al., 1978a,b) based on the data from local seismograph networks brought a new view to the problem. The two planes of this double seismic zone are separated by about 40 km at the shallow end (a depth of ~ 60 km), and gradually merge at depth (~ 180 km) (Figure 1.3a). The focal mechanisms of the upper and lower planes are characterized by down-dip compression and down-dip tension, respectively (Figure 1.3b). Hasegawa et al. (1978b) showed that the upper plane appeared to coincide with the upper boundary of the slab by measuring the difference between the arrival

[†]I will call this a 'Wadati-Benioff zone' in this thesis. Although this is not an attractive naming, it certainly should not be called a 'Benioff' zone, as is often done (for the argument, see Le Pichon et al., 1976 or Ustu, 1977).

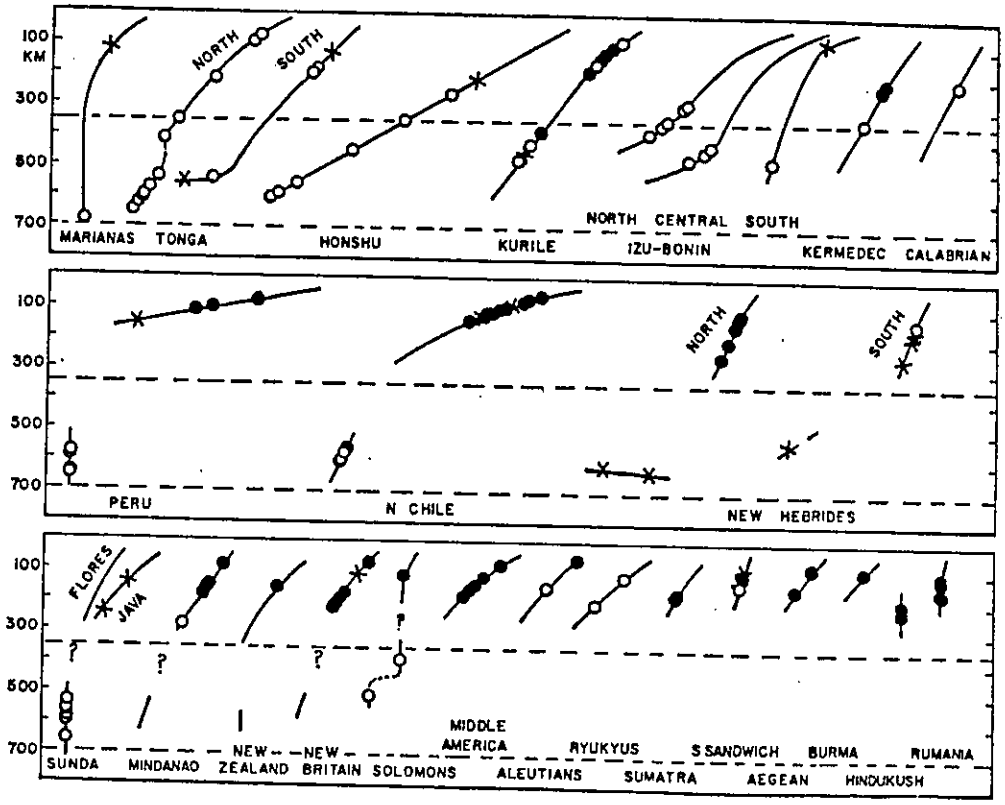

Figure 1.1. Global summary of the distribution of down-dip stresses in Wadati-Benioff zone (after Isacks and Molnar, 1971). Open circles and closed circles represent earthquakes with down-dip compressional and down-dip tensional axes, respectively. Crosses are the events which have neither axis in the down-dip direction. For each region, the solid line represents the seismic zone in a vertical section aligned perpendicular to the strike of the zone.

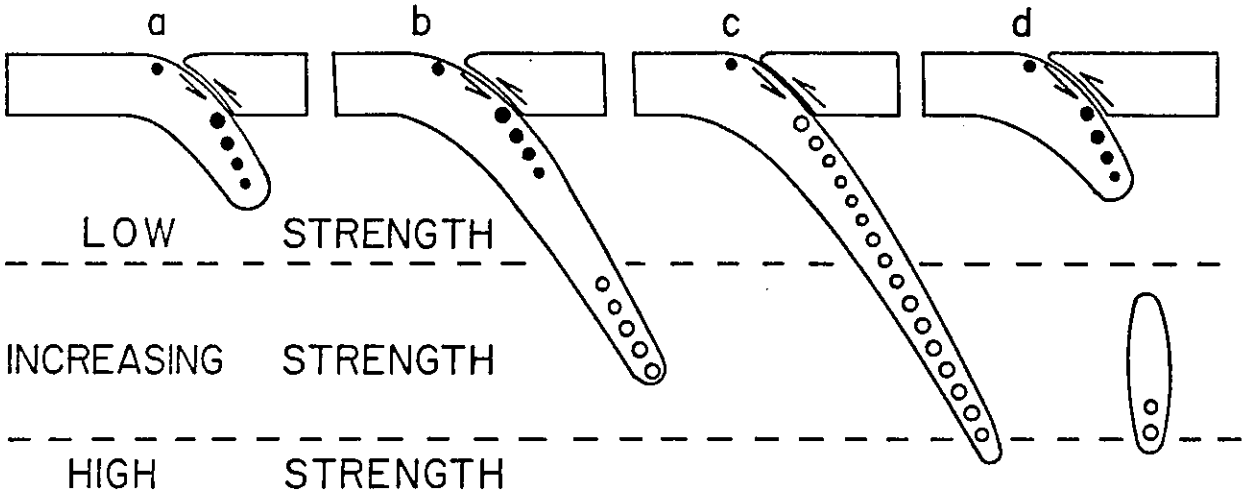

Figure 1.2. A model (proposed by Isacks and Molnar, 1969, 1971) showing plausible distributions of stresses within slabs where gravitational forces act on excess mass within the slabs. The symbols are the same as in Figure 1.1. The size of the circle qualitatively indicates the relative amount of seismic activity. In (a) the slab sinks into the asthenosphere, and the load of excess mass is mainly supported by forces applied to the slab above the sinking portion; in (b) the slab penetrates into stronger material, and part of the load is supported from below, part from above; the stress changes from extension to compression as a function of depth. In (c) the entire load is supported from below, and the slab is under compression throughout. In (d) a piece has broken off. (Figure after Isacks and Molnar, 1969 and caption after Isacks and Molnar, 1971)

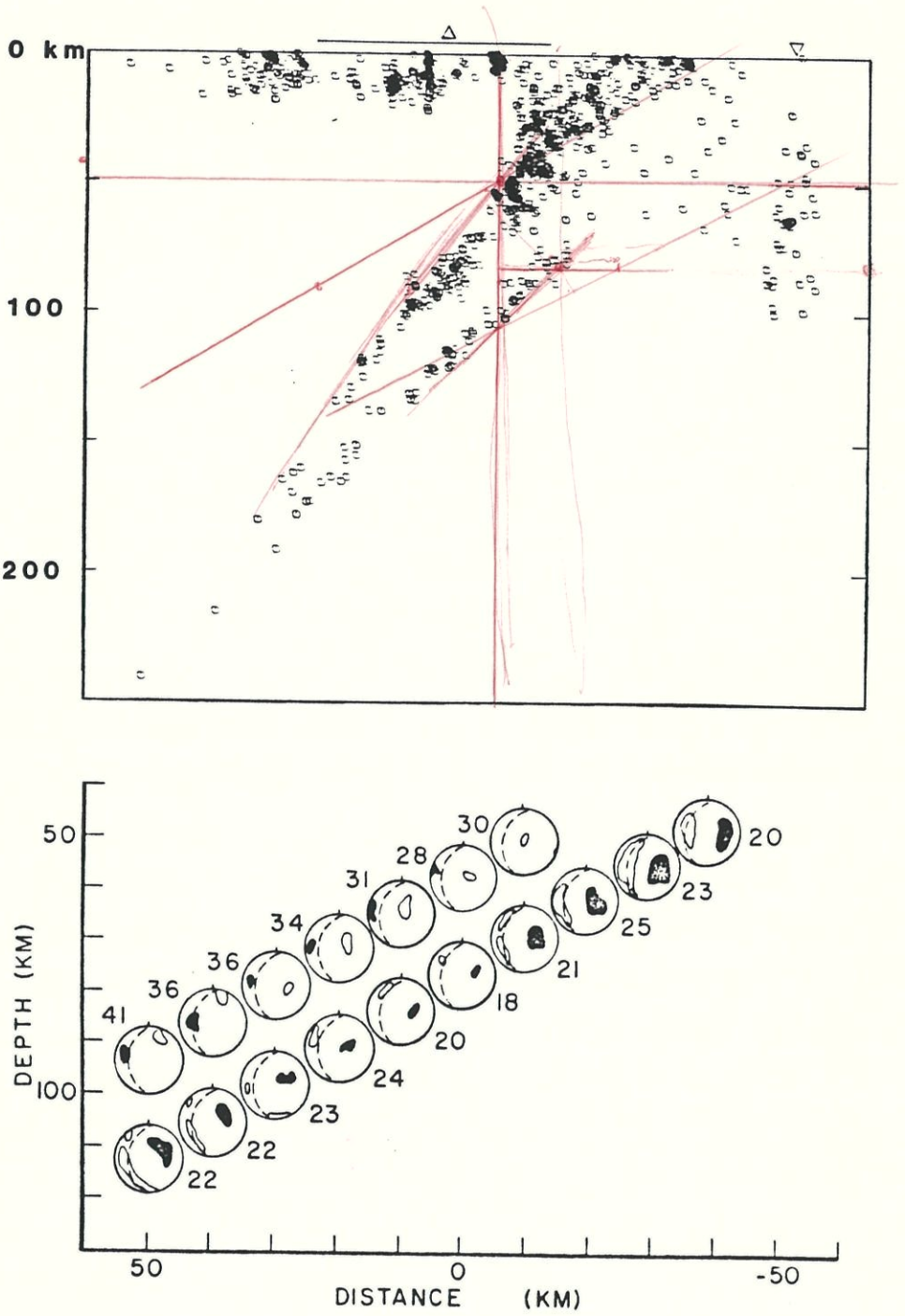

Figure 1.3. (a) Double seismic zone beneath the northern Honshu arc, Japan (after Hasegawa et al., 1978a). The precise determination of the microearthquake hypocenters using data from the seismic network of Tohoku University revealed a clear separation of two seismic zones. The figure is vertically exaggerated by a 2:1 ratio. (b) Composite lower hemisphere focal mechanisms from the Tohoku Microearthquake Network at 10 km intervals for the upper and lower planes of the double seismic zone. Numbers denote the percentage of inconsistent first motions for the best solution. The dashed curve shows the dip of the subducting slab. The black areas denote the range of solutions possible for the P-axis if five more stations are allowed to be inconsistent additional to the best solution; white regions represent the same for the T-axis. (Figure after Hasegawa and Umino, 1978 and caption after Fujita and Kanamori, 1981)

times of precursors of the *ScS* phase (*ScSp*) and *ScS* itself.

This discovery, combined with the earlier suggestions of the presence of a two-layered seismic zone in the Kuriles (Sykes, 1966; Veith, 1974), led to speculation that double seismic zones are a general feature of Wadati-Benioff zones worldwide (Engdahl and Scholz, 1977). Many attempts have been made to search for double seismic zones in other subduction zones - some have been successful and some have not.

Based on the results of previous workers, and compiling a large number (about 2.5 times the amount available to Isacks and Molnar, 1971) of focal mechanism solutions for intermediate depth earthquakes, Fujita and Kanamori (1981) suggested that double seismic zones were not a feature common to all subduction zones. They compared the stress state of the slabs at intermediate depths with the arc-normal convergence rate and the age of subducting lithosphere (Figure 1.4). In their model, slow convergence rate and old age both make the stress state relatively tensional compared to some equilibrium state, while a fast rate and young age make it compressional. Noting that most double seismic zones had been observed only in subduction zones with fast convergence rate and old lithosphere, they concluded that double seismic zones existed only in slabs which were not dominated by tensile or compressive stresses.

Double seismic zones have been observed beneath Tohoku, Japan (e.g., Umino and Hasegawa, 1975; Hasegawa et al., 1978a,b; Yoshii, 1979a), Hokkaido, Japan (Suzuki et al., 1983), Kurile-Kamchatka (Veith, 1974; Stauder and Mualchin, 1976), eastern Aleutians (Reyners and Coles, 1982; House and Jacob, 1983) and Peru (Isacks and Barazangi, 1977). Suggestions of double seismic zones beneath the central Aleutians (Engdahl and Scholz, 1977) and Marianas (Samowitz and Forsyth, 1981) are rather questionable (Topper, 1978; Engdahl and Fujita, 1981).

Previous global surveys of double seismic zones suffer from the fact that the quality of data different subduction zones varies too much to compare seismicity on the same basis. Fujita and Kanamori (1981) made an attempt to do this by using only teleseismic data, but sampling earthquakes for only ~ 20 years is not long enough to draw plausible conclusions concerning where double seismic zones exist and where they do not.

The cause of the double seismic zones has also been discussed by many researchers but no consensus has been reached as yet. Proposed mechanisms are: stresses associated with phase changes (Veith, 1974), unbending of the slabs (Engdahl and Scholz, 1977; Isacks and Barazangi, 1977; Tsukahara, 1977, 1980; Samowitz and Forsyth, 1981), sagging of the plate (Yoshii, 1977; Sleep, 1979), and thermo-elastic stresses (Goto and Hamaguchi, 1978, 1980; House and Jacob,

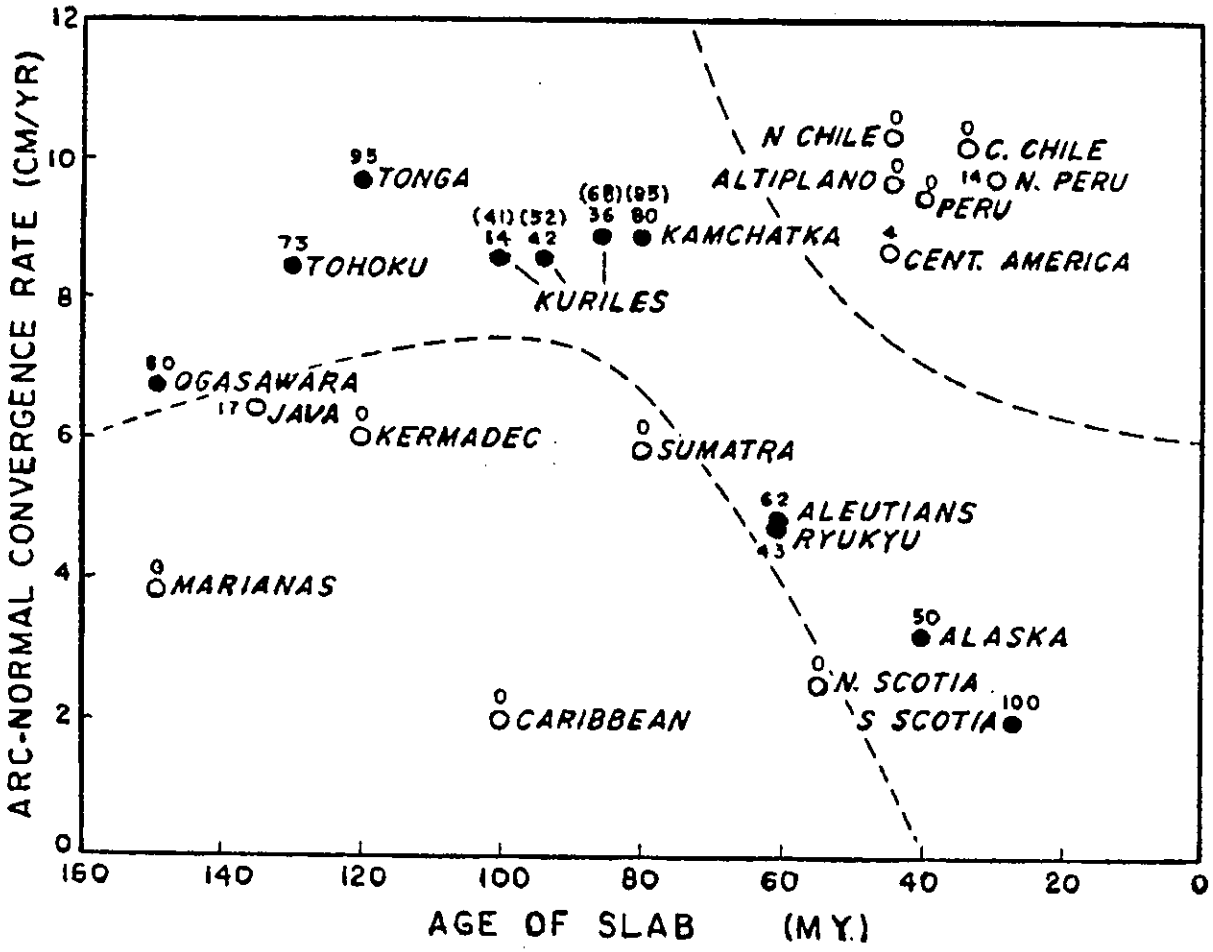

Figure 1.4. Correlation between the arc-normal convergence rate, the age of the subducting lithosphere, and the percentage of in-plate compressive events. (After Fujita and Kanamori, 1981)

1982).

Our understanding of the nature of seismicity of the subducting slabs at intermediate depths has progressed significantly since the advent of the theory of plate tectonics. However, there still exist problems to be solved regarding the nature of double seismic zones. In this thesis, I will attempt to solve these problems from both observational and theoretical considerations. My view of the subduction process here is essentially two dimensional and there are many problems that cannot be treated as two dimensional. Nevertheless, if a simple view can explain certain properties, it should be applied first. As I will show, double seismic zones are actually simple manifestations of this two dimensional deformation. The goal of this thesis is to demonstrate that the existence of double seismic zones is a logical and straightforward consequence of the theory of plate tectonics.

Chapter 2 discusses a new aspect of a double seismic zone - the spatial and temporal variation of its activity. The double seismic zone beneath the northern Honshu arc, Japan is studied extensively. It will be suggested that some causal relations exist between the behavior of the double seismic zone and the accumulated stress state at the thrust zone where large earthquakes occur.

Chapter 3 presents the discovery of a double seismic zone beneath the Tonga arc, which had previously been thought of as the prototype of a compressionally loaded slab. The presence of a double seismic zone beneath the Tonga arc implies that a double seismic zone is a persistent and general feature of all subducting slabs at the intermediate depths.

Chapter 4 discusses the origin of double seismic zones. Estimating the strain release rate from earthquakes and the geometrical unbending strain rate of subducting slabs, I will suggest that the unbending of subducting oceanic lithosphere at intermediate depths is the cause of double seismic zones. By modeling the double seismic zone beneath Tohoku, Japan, I will also show that the currently available flow law of 'dry' olivine does not properly describe the double seismic zone. It will be suggested that some weakening mechanism is required, if the rheology of 'dry' olivine determines the thickness of a double seismic zone.

In Chapter 5, based on observational and theoretical considerations, I will speculate on where double seismic zones may exist. I will suggest that if better data become available, double seismic zones should be seen in most subduction zones where deformation is taking place in a two dimensional manner.

CHAPTER II

TRIPLE SEISMIC ZONE ALONG THE JAPAN TRENCH

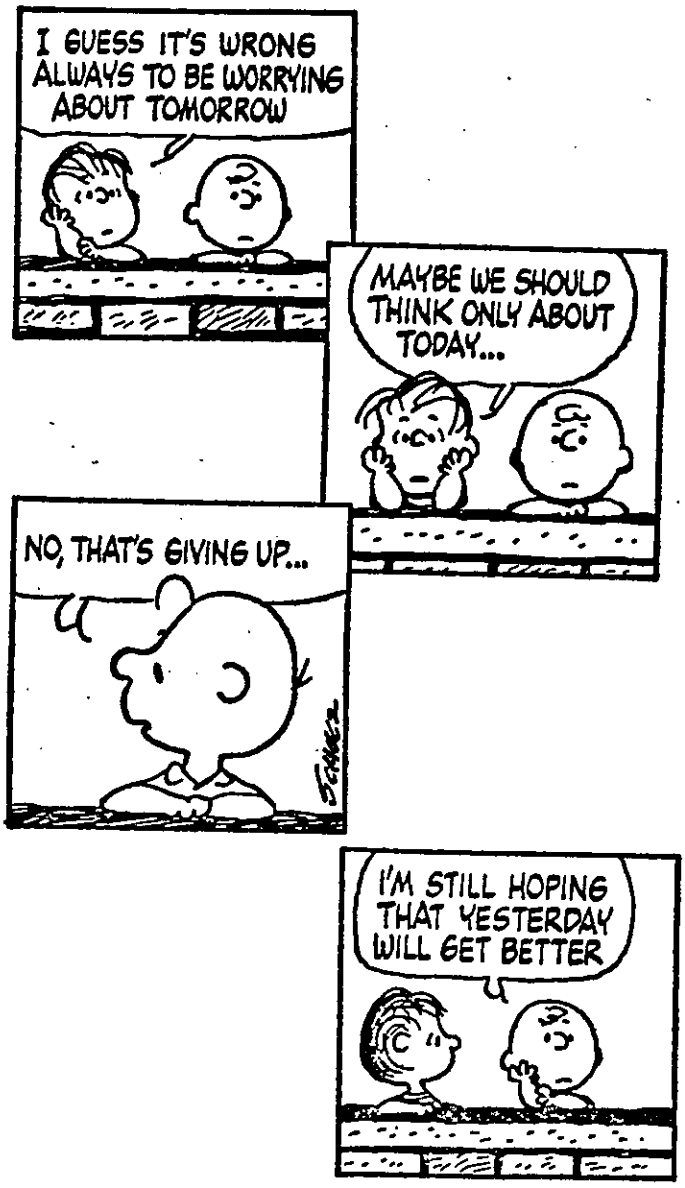

Introduction

The discovery of the double seismic zone beneath trench-island arc systems, revealed by detailed analyses of seismicity (Tsumura, 1973; Veith, 1974; Umino and Hasegawa, 1975; Hasegawa et al., 1978a,b) has become a new aspect of our understanding of the subduction processes (Engdahl and Scholz, 1977; Isacks and Barazangi, 1977; Goto and Hamaguchi, 1978; Sleep, 1979; Yoshii, 1979a; Fujita and Kanamori, 1981; House and Jacob, 1982). Similarly, a detailed analysis of the spatial and temporal distribution of earthquakes with focal mechanism solutions and accurate hypocentral locations has the potential to contribute to our understanding of subduction processes (e.g., the stress state in the slab, rheological properties of the upper mantle at the subduction zone, the occurrence of large earthquakes, etc.).

Most work on the double seismic zone considered intermediate or deep events (>70 km). The results of these studies have helped in understanding the stress state within descending slabs and the rheological properties of the upper mantle around and within the slabs. They do not, however, properly reveal the nature of the seismic coupling at the interface between the two converging plates and its effect on the seismic activity and the stress state within the slabs. Difficulties arise because for shallower offshore earthquakes, hypocentral locations (especially focal depths) are scattered and unreliable even for the data of local networks, and focal mechanism solutions are available only for major (m_b >5.5) earthquakes. In this chapter, the main topic is the seismic activity at the uppermost part of the double seismic zone and at the deeper (40-60 km)† part of the interface of two converging plates. A causal relation between these activities will be suggested. Through this, information on the seismic coupling at the plate interface and the forces which act on the slab at the uppermost edge of the Wadati-Benioff zone is obtained.

Seno and Pongsawat (1981) made a detailed cross section of the seismicity and determined focal mechanisms for events prior to the occurrence of, and in the vicinity of, the Miyagi-Oki M_s =7.5 earthquake of 1978, northern Honshu, Japan. They studied the occurrence of moderate size earthquakes near the interface between the two converging plates (30-150 km depth) to determine the pattern of seismicity which might be related to the occurrence of the large earthquake. They used earthquakes with focal depths determined from depth phases and

†The reader is cautioned that throughout this chapter, 'deeper' refers to the 40-60 km depth range, while elsewhere in this thesis 'deep' events are >300 km. Similarly, in this chapter, 'deep thrust zone' refers to interplate thrust events in the 40-60 km depth range.

decided the types of focal mechanism by using a method which allows a larger number of earthquakes with $m_b > 4.0$ to be analyzed. They found a triple-planed structure of seismicity which will be called a **triple seismic zone**, at the seaward edge of the double seismic zone, where the double seismic zone extends seaward beyond the aseismic front and overlaps with the zone of low-angle thrust type earthquakes at the interface of two converging plates. They related this to the stress concentration around the focal region of the Miyagi-Oki earthquake prior to its occurrence.

In this chapter, I extend their work in space to distinguish the regional and temporal variation of seismicity along the subduction zone of the northern Honshu arc, Japan. The subduction zone is divided into four regions based on the pattern of occurrence of historical great and large earthquakes. The differences in the seismicity of each region will be illustrated in terms of the pattern of occurrence of both large and intermediate size earthquakes. It will be proposed to separate the zone of low-angle thrust earthquakes at the plate interface into two parts: the shallow thrust zone (0-40 km), where *great* earthquakes ($M_s \sim 8.0$) occur, and the deep thrust zone (40-60 km), where *large* earthquakes ($M_s \sim 7.4$) occur. The regional variation of seismic activity at the seaward edge of the double seismic zone is discussed with regard to its relation to the coupling at the deep thrust zone. Another triple seismic zone is found in the region offshore of Fukushima prefecture immediately to the south of the region where Seno and Pongsawat (1981) found the triple seismic zone. The possibility of a future large earthquake in this region will be discussed on the basis of the seismic coupling at the deep thrust zone and historical seismicity data.

Historical Seismicity

Historical and recent seismicity along the Japan trench represents typical subduction seismicity. Although it is typical, there is a great variety of modes of seismicity. Historically, great ($M_s \geq 7.8$) or large ($M_s \geq 7.4$) earthquakes have recurred, but occurrence of these events has never been uniform over the entire length of the arc. In this section, the historical seismicity for great and large earthquakes is summarized. Characteristics of the historical seismicity data will be related to the seismicity and focal mechanisms during the past few decades along the Japan trench in a later section.

From the local intensity distribution and many other sources of information including the reports from the seismological bulletins of the Central Meteorological Observatory (formerly Japan Meteorological Agency, JMA), Utsu (1979b, 1982) recompiled the epicentral location and magnitude of all earthquakes, $M > 6$ (in the rest of the chapter M denotes a magnitude determined with respect to JMA magnitude scale), which occurred around Japan from 1885 to 1925. Combining his data with other earthquake catalogues (JMA, ISS, ISC, PDE, Gutenberg and Richter, 1954; Geller and Kanamori, 1977; Abe, 1981) yields a very good record of seismicity of large earthquakes around Japan for about the last 100 years (1885-1980). Figure 2.1 shows the seismicity of large ($M_s \geq 7.4$) earthquakes along the Japan trench during this period, and they are also listed in Table 2.1. The closed areas represent the focal regions of large earthquakes. From the pattern of occurrence of these earthquakes, the subduction zone along the Japan trench is divided into four sections, A, B, C, and D, as seen in Figure 2.1. Because the subduction of the Philippine Sea plate along the Sagami Trough (Figure 2.1) makes seismicity complex at the southernmost part of the arc, the region south of region D is not included in this study. For similar reasons, the region north of region A, where the Kuril arc meets the northern Honshu arc, is not included in this study.

Region A

The 1968 $M_s = 8.1$ Tokachi-Oki earthquake, which is a great thrust type event (Kanamori, 1971a) occurred offshore of Aomori prefecture in this region. The rupture zone is shown in Figure 2.1 as the enclosed area 'a' (the 2-day aftershock area based on preliminary determination of epicenter (PDE) data). Studies of historical earthquakes (Utsu, 1974; Usami, 1975; Hatori, 1975) show that similar events have occurred in this zone very regularly since 1677: 1677, 1763, 1853, and 1968. Thus great earthquakes have been occurring in this zone every ~ 80-100 years. In zone 'a' ', immediately landward of zone 'a', relatively smaller but still large ($M_s \sim 7.4$) events occur often , e.g., in 1901 and 1945. Zone 'a' ' is the rupture area of the 1901, $M = 7.4$, earthquake determined from tsunami data (Hatori, 1975).

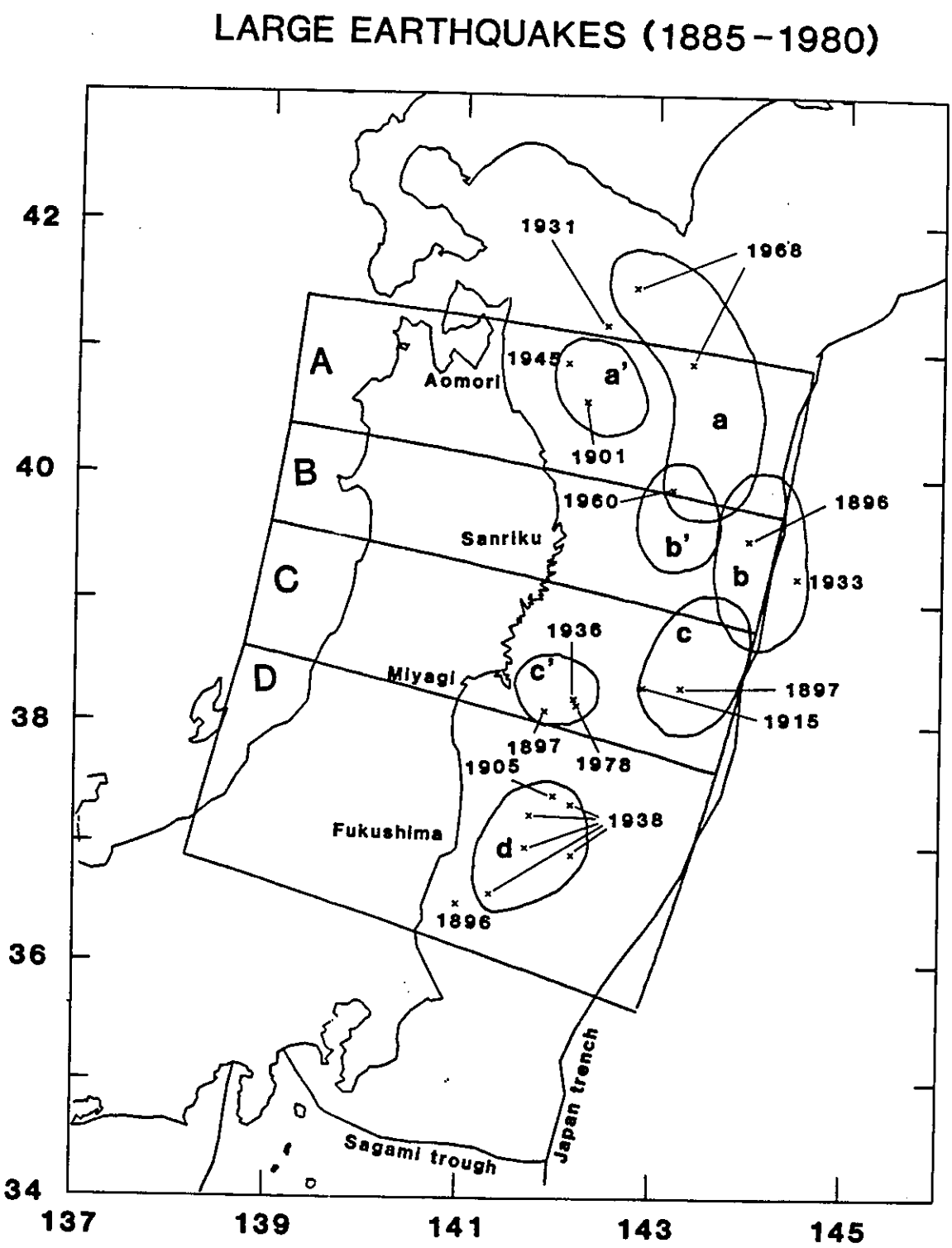

Figure 2.1. Summary of large offshore earthquakes along the Japan trench (1885-1980). The subduction zone is divided into four segments from the occurrence of these events. Enclosed areas correspond to the rupture zones of 1968 (a), 1901 (a'), 1933 (b), 1960 (b'), 1897 (c), 1978 (c'), and 1938 (d) earthquakes.

TABLE 2.1. Large Earthquakes (1885-1980)

Year	Latitude, °N	Longitude, °E	Region	Magnitude	
				M_j	M_s
1896	36.5	141.	D	6.6	7.4[a]
1896	39.5	144.	B	6.8	8.6[b]
1897	38.1	141.9	C	7.4	-
1897	38.3	143.3	C	7.7[c]	-
1901	40.6	142.3	A	7.4	-
1905	37.4	141.8[c]	D	7.0	7.8
1915	38.3	142.9	C	7.5	7.6
1931	41.2	142.5	A	7.6	7.7
1933	39.2	144.5[d]	B	8.1	8.5
1936	38.15	142.13	C	7.5	7.2
1938	36.58	141.34[e]	D	7.0	7.6
1938	36.97	141.71[e]	D	7.5	7.7
1938	37.24	141.75[e]	D	7.3	7.7
1938	37.33	142.18[e]	D	7.4	7.6
1938	36.91	142.19[e]	D	6.9	7.0
1945	41.00	142.07	A	7.1	7.1
1960	39.9	143.2	B	7.2	7.7
1968	40.9	143.4	A	7.9	8.1
1968	41.5	142.8	A	7.5	7.7
1978	38.15	142.22[f]	C	7.4	7.5

Epicentral locations are obtained from Utsu (1979b), JMA, ISS, and ISC for the periods 1885-1925, 1926-1954, 1954-1963, and 1964-1980, respectively. M_j represents JMA magnitude; for the events before 1925, they are obtained from Utsu (1979b). M_s denotes surface wave magnitude of Abe (1981).

[a] Utsu (1980).
[b] Tsunami magnitude (M_t) (Abe, 1979).
[c] Utsu (1982).
[d] Kanamori (1971b).
[e] Abe and Tsuji (1976).
[f] Seno et al. (1980).

Region B

The tsunami generated by the 1896, M_t =8.6 (tsunami magnitude, Abe, 1979), earthquake caused a great disaster along the coast. This event is a low-frequency tsunami earthquake; the magnitude determined from intensity distribution is only about 6.8 (Utsu, 1979b), although this event has a seismic moment comparable to that of great earthquakes (Kanamori, 1972). The 1933 M_s =8.5 Sanriku earthquake, which may have broken the entire lithosphere by normal faulting (Kanamori, 1971b), occurred on the seaward edge of this region (zone 'b'). In 1960 a large earthquake (M_s =7.7) occurred west of the previous two great events. The aftershock area (zone 'b' ') overlaps with the rupture zone of the 1968 earthquake. Utsu (1974) suggested that there had been a possible overestimation of magnitude for the 1960 event. Both the size of the rupture area and the size of the generated tsunami show that this event is smaller than the two great earthquakes which occurred in the adjacent regions: 1968 in region A and 1897 in region C. Two historical tsunamigenic earthquakes (869 and 1611) have been located in zone 'b' (Utsu, 1974; Usami, 1975; Hatori, 1975); however, the nature of faulting and precise locations are not well known.

Therefore, region B is anomalous in the activity of great or large earthquakes; although the 1896 earthquake may have been a thrust event, this region lacks typical great thrust type earthquakes for at least the past 200 years. The occurrence of the great normal fault type event and the tsunami event suggests that the plate interface in region B is not coupled strongly. This is also supported by the activity of smaller magnitude events, as will be shown later.

Region C

Zone 'c' is the rupture area of the 1897 M =7.7 earthquake determined from tsunami data (Hatori, 1975; Aida, 1977). Historical data suggest that a similar event occurred in 1793 (Hatori, 1975; Aida, 1977; Seno, 1979). From tsunami analysis, Aida (1977) estimated the minimum seismic moments of these two earthquakes to be 5.6×10^{27} and 6.3×10^{27} dyne-cm, respectively, corresponding to a magnitude M_w (Kanamori, 1977) of 7.8. Zone 'c' is known as a seismic gap and considered as a possible site of a near-future great earthquake (Seno, 1979; Utsu, 1979a). Smaller events often occur landward of this zone. In particular, the rupture zone of the 1978 Miyagi-Oki earthquake (zone 'c' '), which represents thrust faulting at the relatively deeper

(30-60 km) interface of the two plates (Seno et al., 1980), has experienced large earthquakes ($M_s \sim 7.4$) about every 40 years at least since 1835: 1835, 1897, 1936, and 1978. Thus, the activity for great and large earthquakes in this region is similar to that in region A; great earthquakes recur in far offshore, and landward of this area large earthquakes occur more frequently.

Region D

A series of five large earthquakes occurred in 1938; M_s ranges from 7.0 to 7.7. Three of these are of thrust type and two are of normal fault type (Abe, 1977). The rupture zone of this series of earthquakes (Abe, 1977), which is indicated by 'd' in Figure 1, is located more landward than those of great thrust type events in regions A and C. The 1905 M_s =7.8 event is located in the rupture zone of the 1938 events by Utsu (1979b). This event and the 1896 M_s =7.4 event have characteristics of low-frequency earthquakes (Utsu, 1980) because magnitudes determined from the data recorded in Japan are much smaller than those determined at the teleseismic stations (Utsu, 1979b). No historical earthquake is known to have occurred in the farther offshore area in this region.

Deep and Shallow Thrust Zones

As mentioned earlier, the pattern of occurrence of great and large earthquakes changes from region to region. Although it should be noted that the interpretation of the data (especially the rupture zone) for historical earthquakes is biased by the data of recent large events for which many pieces of information are available, the regional variation of seismicity of large events along the northern Honshu arc can be summarized as follows: (1) decrease of great earthquake activity from north to south, (2) the rupture zones of great earthquakes ($M_s \sim 8.0$) are located on the offshore landward side of the trench (the zones 'a' and 'c'), (3) frequent occurrence of large events ($M_s \sim 7.4$) near the coast (the zones 'a' ', 'c' ' and 'd'), and (4) absence of great thrust type earthquakes and occurrence of a great normal fault earthquake and a great tsunami earthquake in region B.

Based on the above observations, it is proposed here to divide the zone of thrust type earthquakes into two parts: the shallow thrust zone where great ($M_s \sim 8.0$) earthquakes occur,

and the deep thrust zone, which is located more landward and where large ($M_s \sim 7.4$) earthquakes occur. The cross section of seismicity of recent moderate size earthquakes, shown in a later section, defines the depth range of these two zones as 0-40 km and 40-60 km, respectively.

It will be shown next that the pattern of occurrence of recent smaller size earthquakes also changes from region to region, reflecting the above-mentioned regional variation of the pattern of occurrence of great and large earthquakes. The nature of the shallow and deep thrust zones and the double seismic zone will be discussed in detail in a later section in conjunction with the recent seismicity and mechanism type.

Method of Analysis

Data

The earthquakes are selected from the International Seismology Centre (ISC) bulletins for the period of 1964-June, 1978, and satisfy the following conditions: (1) events have focal depths which are determined by the pP phase, and (2) events have not less than 20 P wave arrival time observations.

For the events deeper than 50 km, those whose depths have a standard error of not more than 5.0 km are also included. For the period 1964-1975, data are selected from Yoshii's file, EQ1, which includes events with the above conditions (Yoshii, 1979b). For the period 1976-June, 1978, events are listed from the ISC bulletins. For region C the results of Seno and Pongsawat (1981) and T. Seno (unpublished manuscript, 1982) are incorporated; thus the time period treated is terminated at the occurrence of the June 12, 1978, Miyagi-Oki earthquake, as in their study. It should be noted that region C of this study is not exactly identical with the region they studied. With the above procedure there are more than 600 earthquakes with minimum magnitude $m_b \sim 4.0$.

For submarine earthquakes, the depth determined from the pP phase by ISC is corrected by taking account of the effect of the ocean water layer after Yoshii (1979a). This is because the pwP phase (water reflection) is very likely to be misidentified as the pP phase (Fujita et al., 1981) for these shallow submarine earthquakes. This will be discussed in more detail in a later

section.

Focal Mechanism

Focal mechanisms of earthquakes which occurred in region D and are large enough (m_b >5.4), are determined by the conventional method: the initial motions of P wave and polarization angles of the initial half cycles of S waves are read from film chips of the long-period records at World-Wide Standard Seismographic Network (WWSSN) stations. When the long-period data are insufficient, first motions of short-period P waves are used as a supplement. P wave data recorded at the JMA stations and reported in the ISC bulletins are added to the WWSSN data. The earthquakes for which new nodal plane solutions are determined are summarized in Table 2.2, and their focal mechanisms are shown in Appendix B[†]. In this table, mechanisms which were already determined from long-period data by previous workers are also included.

In other regions, focal mechanisms for major events are compiled from previous studies (Yoshii, 1979a, b; Kanamori, 1971a; Sasatani, 1971; Stauder and Mualchin, 1976; Seno and Pongsawat, 1981). Some of these were revised by Seno and Kroeger (1983) using body wave synthetics, and their results are used for those events. Some of the focal mechanism solutions obtained by Nakajima (1974) are used in regions A and B, although they were obtained from short-period first motion data.

The earthquakes (m_b <5.5) for which it is not possible to produce reliable nodal plane solutions from long-period data are classified according to the type of faulting, using the following method of Seno and Pongsawat (1981). Assuming that there exist only three types of faulting: low-angle thrusting, down-dip compression, and down-dip tension, the events are classified into one of the above three types which is consistent with the P wave first motion data reported in the ISC bulletins. P wave first motion data are taken from JMA stations with epicentral distance less than 450 km, for which large amplitudes of first motions are expected. Although the first motion data in the ISC bulletins are often found to be inconsistent for teleseismic stations, they are reliable and consistent for local stations (see Figure 2.2). Figure 2.3 shows examples of the classification of focal mechanism types (see also Figure 5 of Seno and

[†]In this thesis, an equal-area projection is always used to represent the focal spheres.

TABLE 2.2. Solutions of Focal Mechanism for Earthquakes Off Fukushima Prefecture During 1964-1978

Solution	Date	Latitude, °N	Longitude, °E	Depth, km	m_b	A		B		P		T	
						$\phi°$	$\delta°$	$\phi°$	$\delta°$	AZ°	PL°	AZ°	PL°
1	Feb. 5, 1964	36.47	141.02	51	5.6	124	74	304	16	124	29	304	61
2	May 30, 1964	36.23	141.29	36	5.7	108	80	288	10	108	35	288	55
3[a]	Sept. 17, 1965	36.35	141.38	31	6.1	129	69	309	21	129	24	309	66
4	Sept. 22, 1965	36.44	141.37	42	5.8	113	78	293	12	113	33	293	57
5	Nov. 14, 1965	36.61	141.08	39	5.5	113	70	293	20	113	25	293	65
6	April 3, 1966	36.66	141.06	44	5.6	131	70	311	20	131	25	311	65
7	Nov. 4, 1967	37.39	141.71	39	5.5	112	82	292	08	112	37	292	53
8	Nov. 19, 1967	36.47	141.17	39	5.7	106	78	286	12	106	33	286	57
9	Aug. 8, 1968	36.40	141.50	31	5.5	107	76	287	14	107	31	287	59
10	April 9, 1969	36.84	139.77	109	5.5	235	40	338	80	7	24	123	43
11	July 20, 1973	36.45	141.05	46	5.8	113	70	293	20	113	25	293	65
12	Aug. 23, 1973	37.22	142.18	32	5.6	92	72	331	33	121	16	229	46
13[b]	May 5, 1974	37.78	141.77	41	5.7	116	70	285	20	113	24	303	65
14[c]	July 8, 1974	36.44	141.17	40	6.0	120	66	327	27	128	20	277	67
15[b]	April 8, 1975	37.75	141.75	42	5.7	108	70	285	20	107	24	289	64
16	Aug. 14, 1975	37.13	141.11	60	5.5	105	70	285	20	105	25	285	65
17	Dec. 16, 1977	36.65	141.07	45	5.6	115	60	295	30	115	15	295	75

Depth is pP-P depth corrected for water layer (see text).

[a] Solution after Sasatani (1971).

[b] Solution after Seno and Pongsawat (1981).

[c] Solution after Yoshii (1979b).

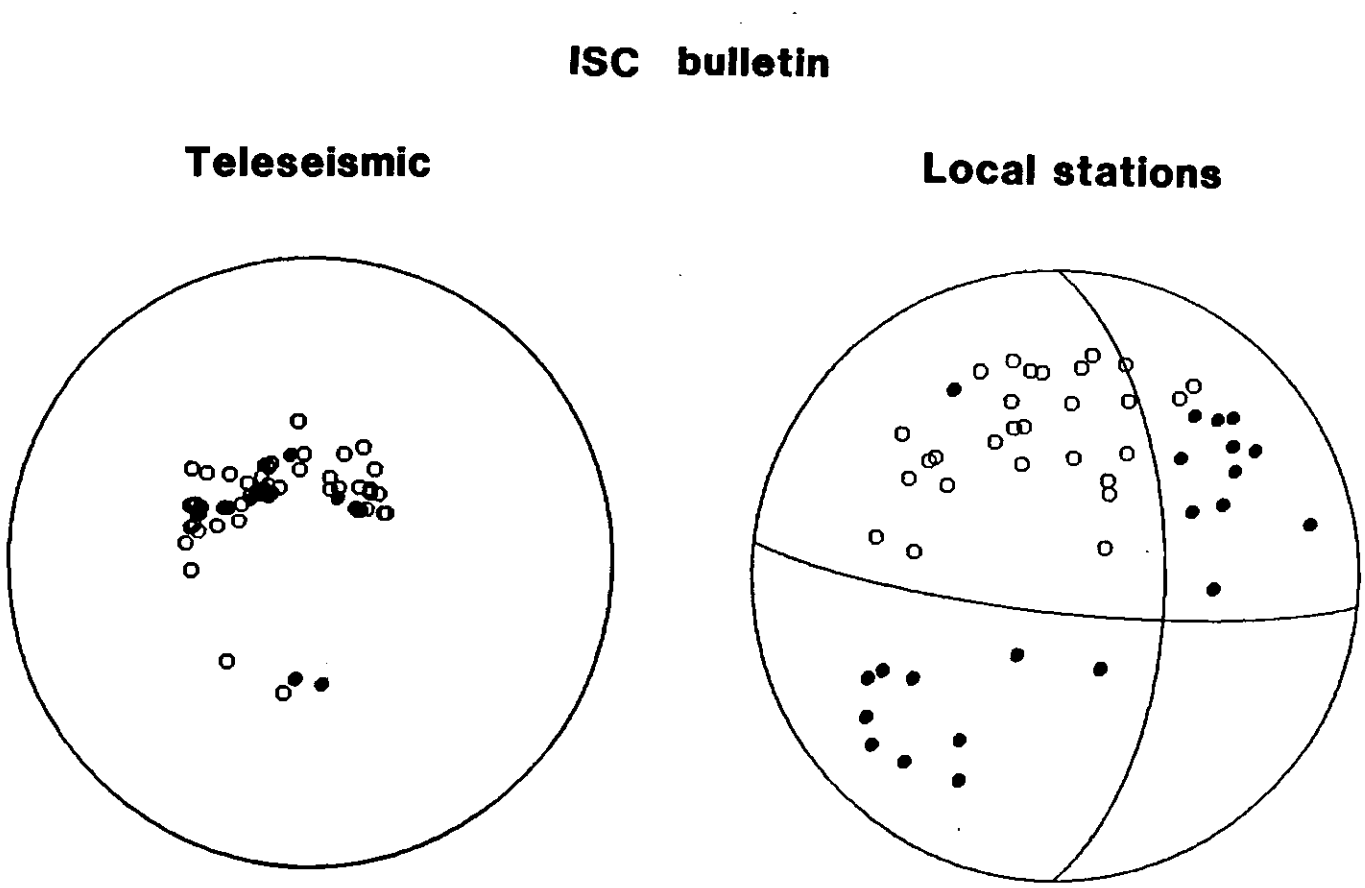

Figure 2.2. Comparison of two types of first motion data reported in the ISC bulletin for a typical event. (left) Teleseismic stations. (right) Local stations whose epicentral distance is less than 450 km. Note that the teleseismic data are totally inconsistent, while the local data are self-consistent (with only insignificant exceptions) and enable us to determine a focal mechanism type.

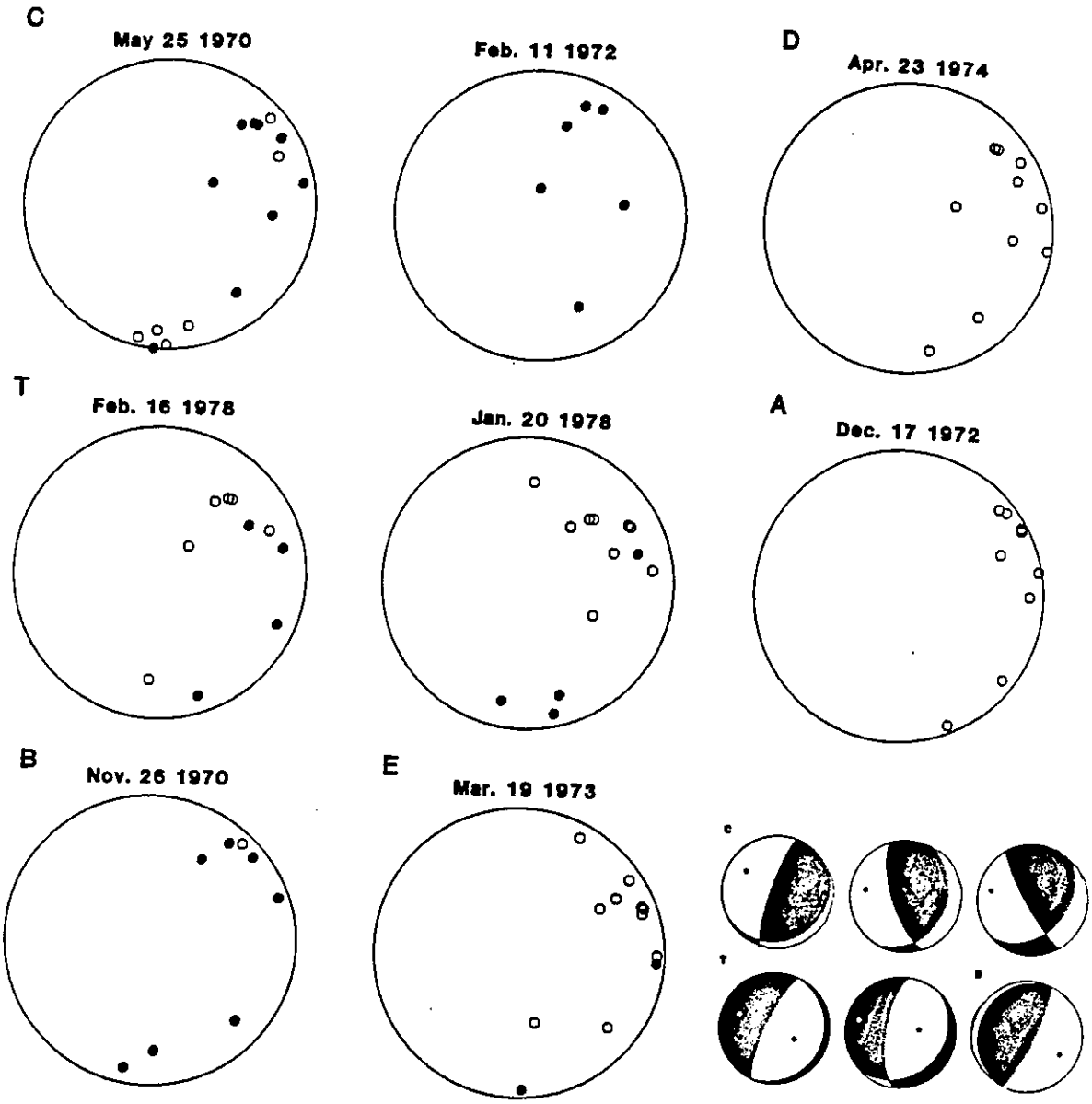

Figure 2.3. Examples of the classification of focal mechanism types. C, T, and D denote the events classified into down-dip compression, down-dip tension, and thrust types, respectively. For A, B, and E, see Table 3. Possible focal mechanism diagrams of the above three types are shown at the bottom right.

Pongsawat, 1981). For this analysis only those events which are located more than 140 km landward of the trench axis are used. This is because the hypocentral locations of the events distant from the coast are less reliable, and this could cause a serious error in the computation of the take-off angles. It is also difficult to determine the type of the mechanism for these shallower earthquakes since most of the rays travel horizontally westward and they cover only the edge of a focal sphere plot. The take-off angles are computed by assuming a spherically symmetric, layered earth model with crustal structure obtained by seismic refraction studies (Yoshii, 1979a; Asano et al., 1979). The possible errors in depth determination are taken into account in the computation of the take-off angles. The focal mechanism types are determined for 184 earthquakes in all.

For the earthquakes which cannot be classified definitely into one of the above three types, a further weak classification is provided. Those events whose data are consistent with two of the three types are classified into another category (see Table 2.3 and Figure 2.3). Although the above procedure reduces the minimum magnitude of event that can be analyzed down to about m_b ~4.0, there still are earthquakes which cannot be classified into any of the above groups.

Results

The results of the analysis are shown in Figures 2.4-2.7. The symbols 'D', 'C', and 'T' represent thrust type, down-dip compression and down-dip tension type events, respectively. The larger symbols correspond to those events of which the nodal plane solutions are obtained from long-period records. Symbols, 'A', 'B', and 'E' are summarized in Table 2.3. The cross marks indicate the earthquakes which could not be classified into any group.

Map Views

Map views of the entire result and of each type of event are shown in Figures 2.4 and 2.5, respectively. The landward edge of thrust type events, i.e., 'D' type events (Figure 2.5a), is parallel to the trench axis and almost identical to the 'aseismic front,' proposed by Yoshii (1975). Yoshii (1975) proposed that the thrust type events did not occur landward of the aseismic front. Thus the results support this. Further, it is noted that the edge of 'D' type

TABLE 2.3. Summary of Symbols.

Symbol	Mechanism
D	low-angle thrust
C	down-dip compression
T	down-dip tension
A	D or C
B	C or T
E	T or D

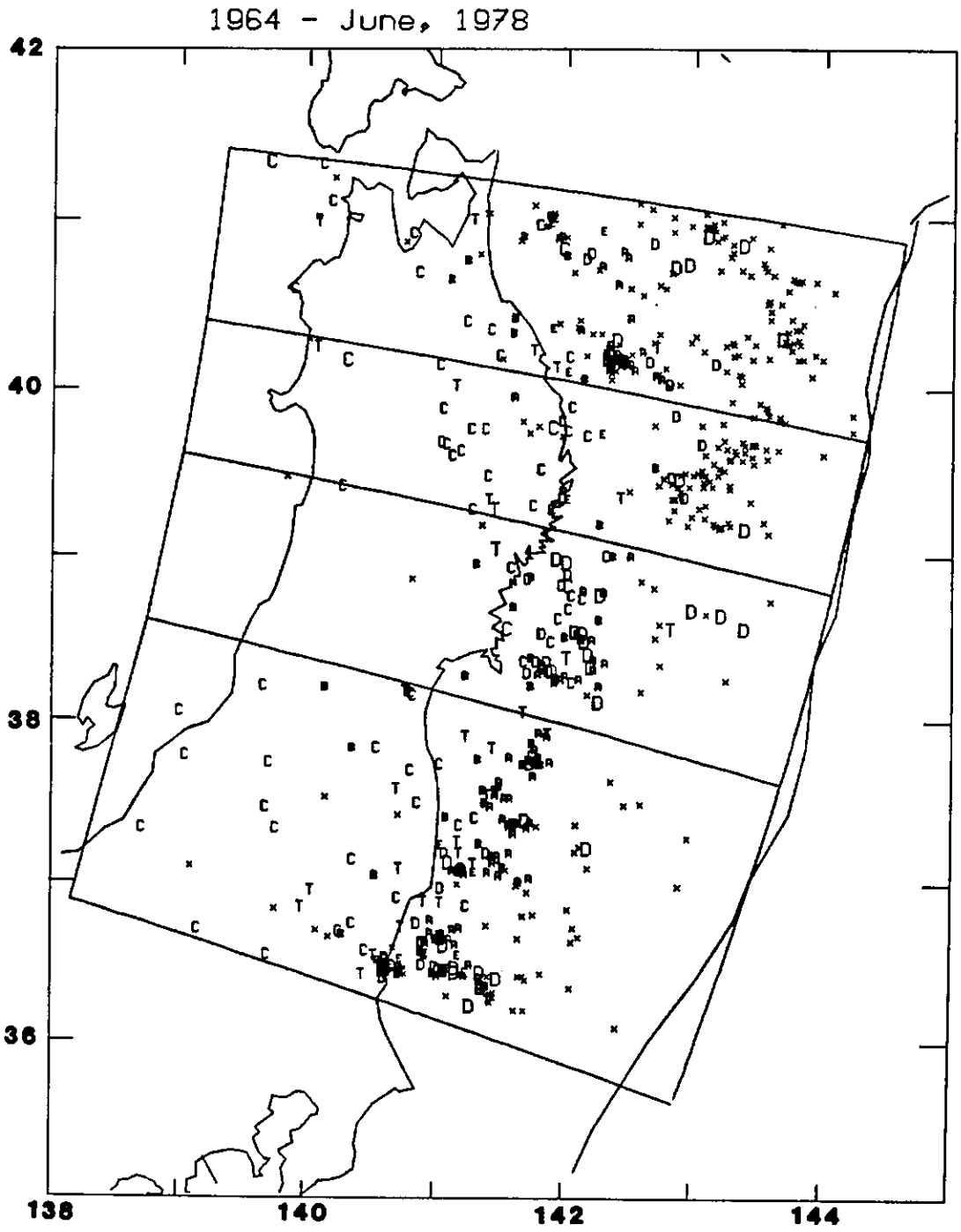

Figure 2.4. Map view of the well-located earthquakes with focal mechanism types. Symbols are summarized in Table 2.3. The larger symbols correspond to those events for which the nodal plane solutions are obtained from long-period records.

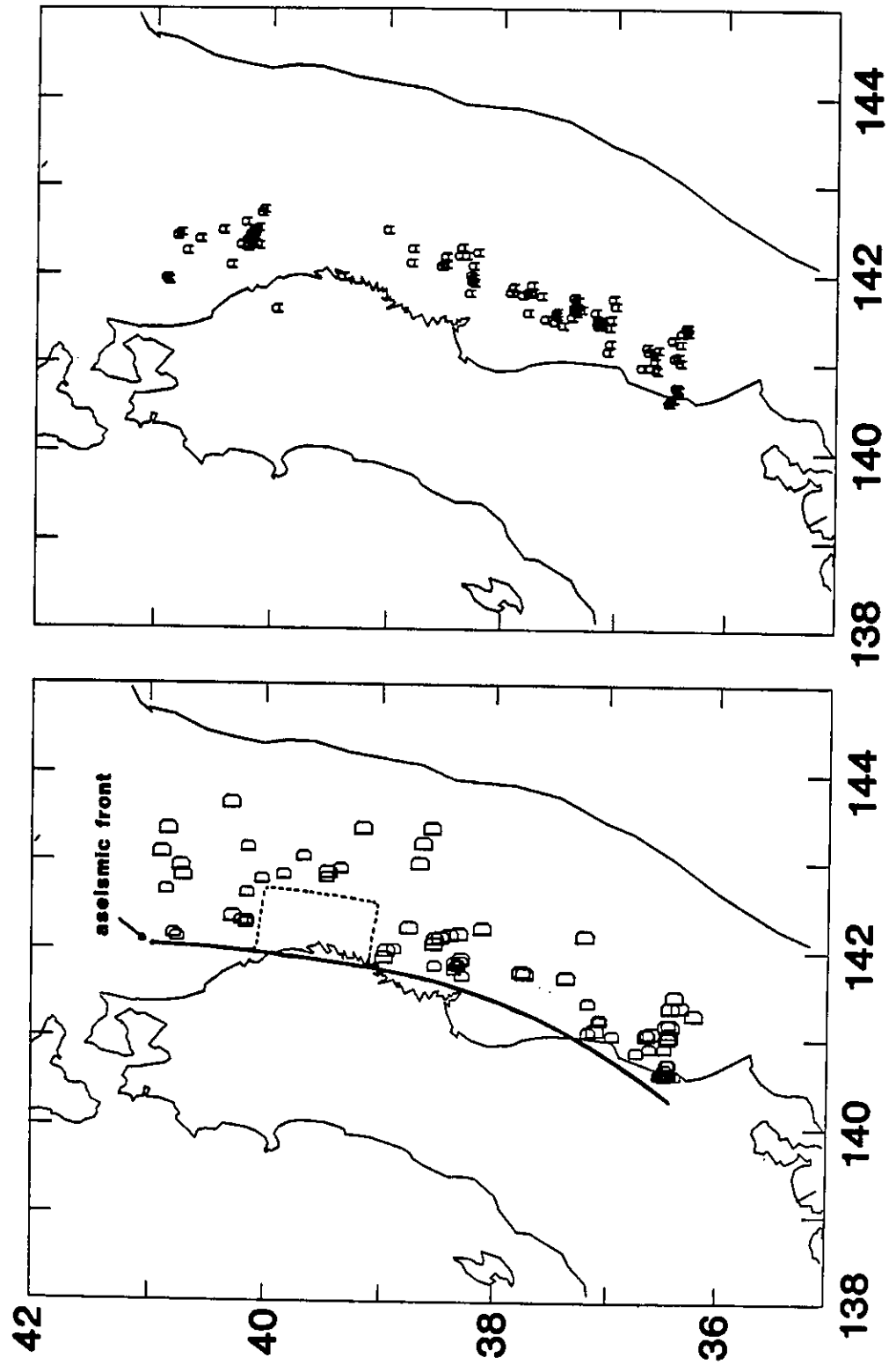

Figure 2.5. The events of each type are plotted in separate map views. (a) Thrust type. (b) Type 'A'. (c) Down-dip compression. (d) Down-dip tension. The line in Figure 2.5a represents the aseismic front. Note the gap in 'D' and 'A' type event activity in region B in Figures 2.5a and 2.5b, respectively. Figure 2.5c shows the lack of type 'C' events in the western half of region C.

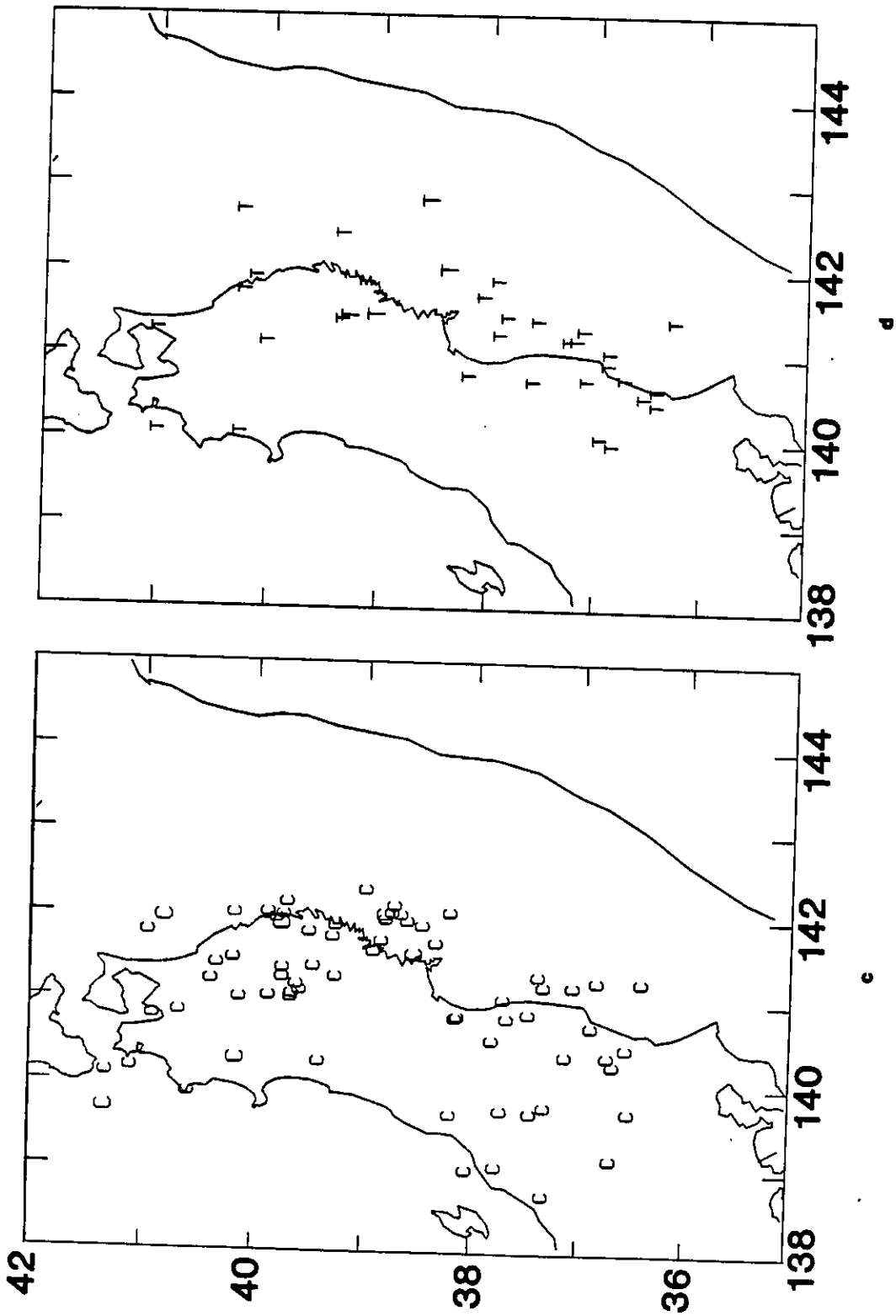

Figure 2.5. continued

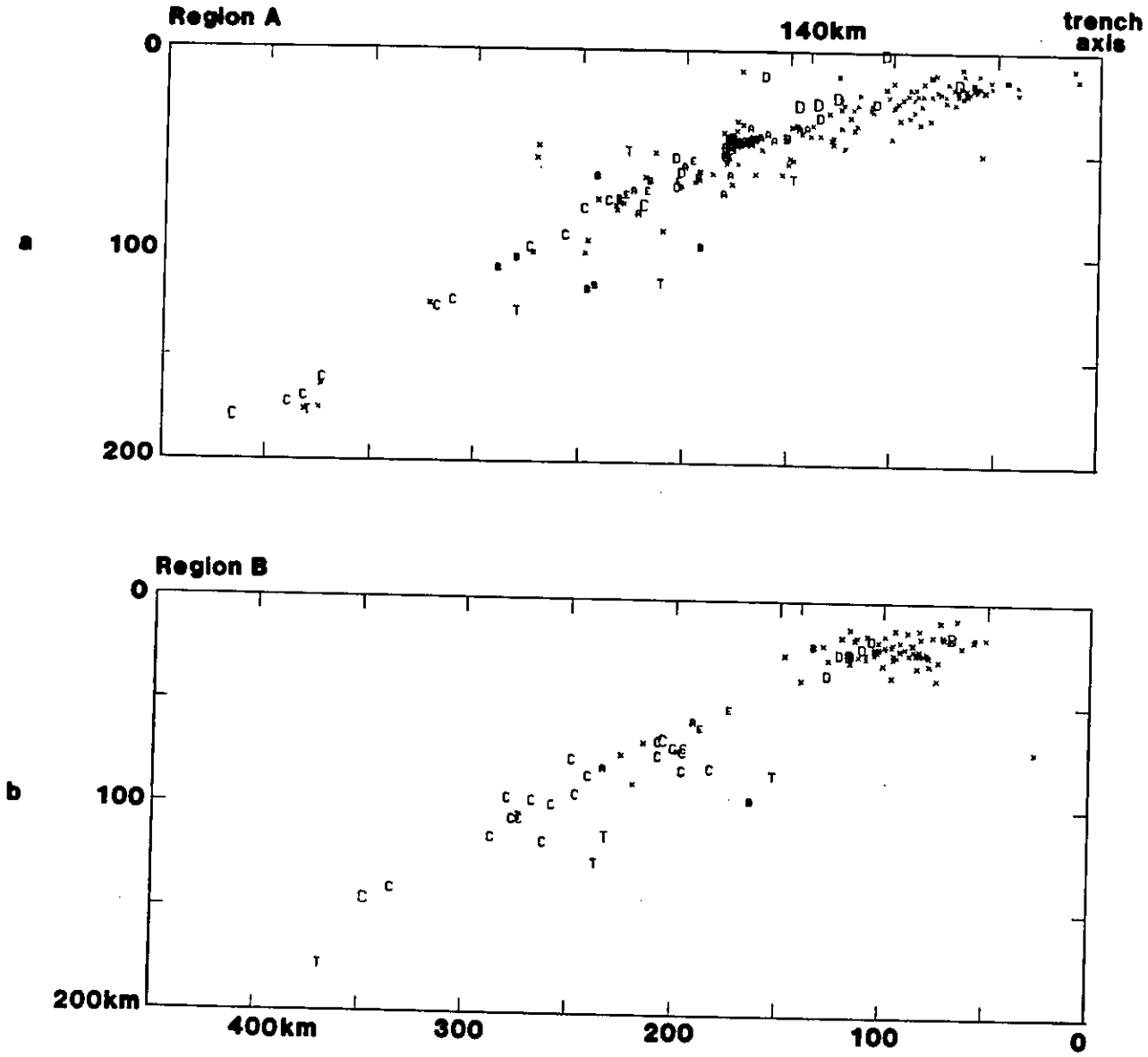

Figure 2.6. Cross sections of each region. Double seismic zones are seen in each region. The seismicity just beneath the deep thrust zones in regions C and D are much more active than in the other regions. The gap in region B is clearly seen in Figure 2.6b.

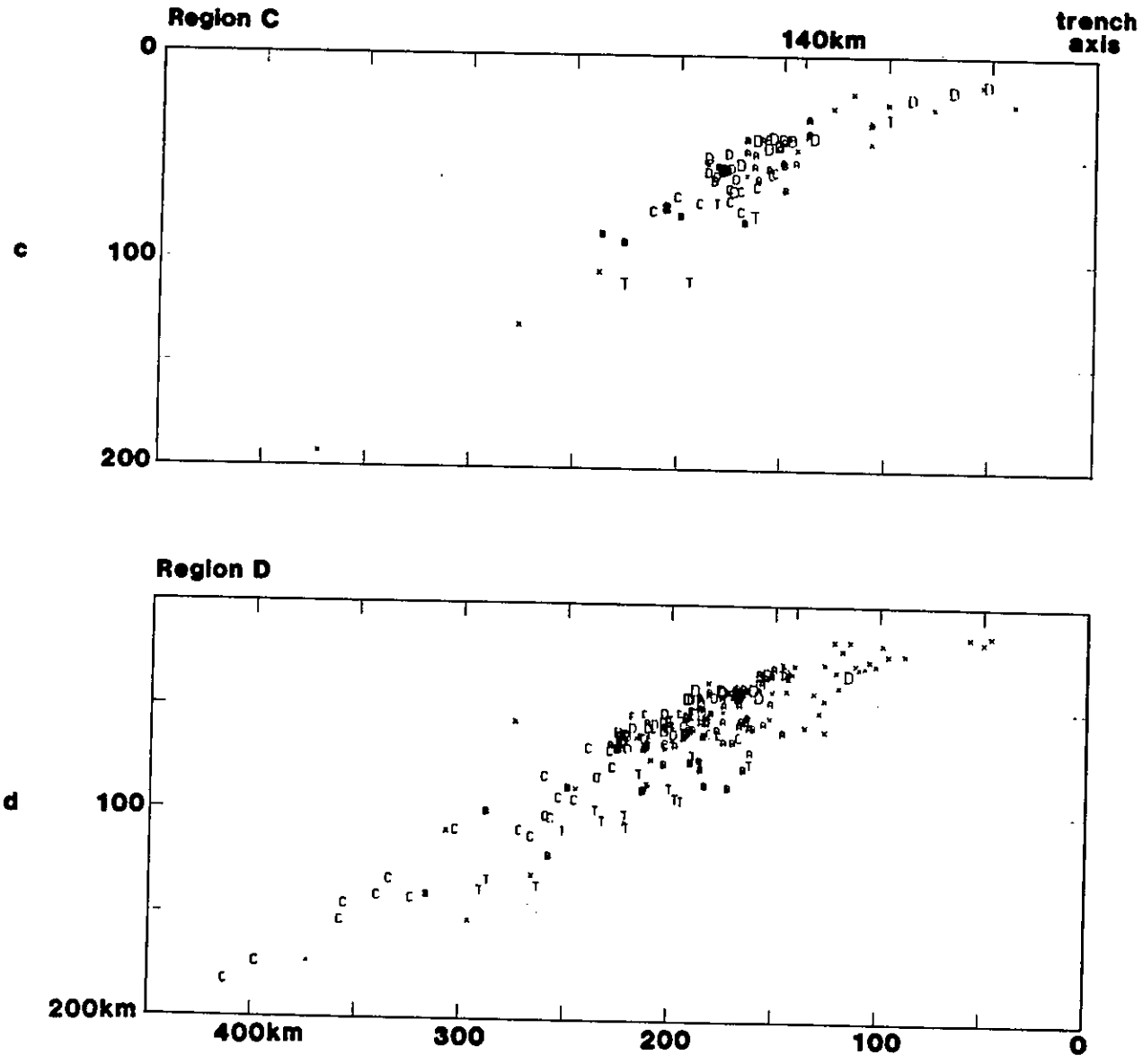

Figure 2.6. continued

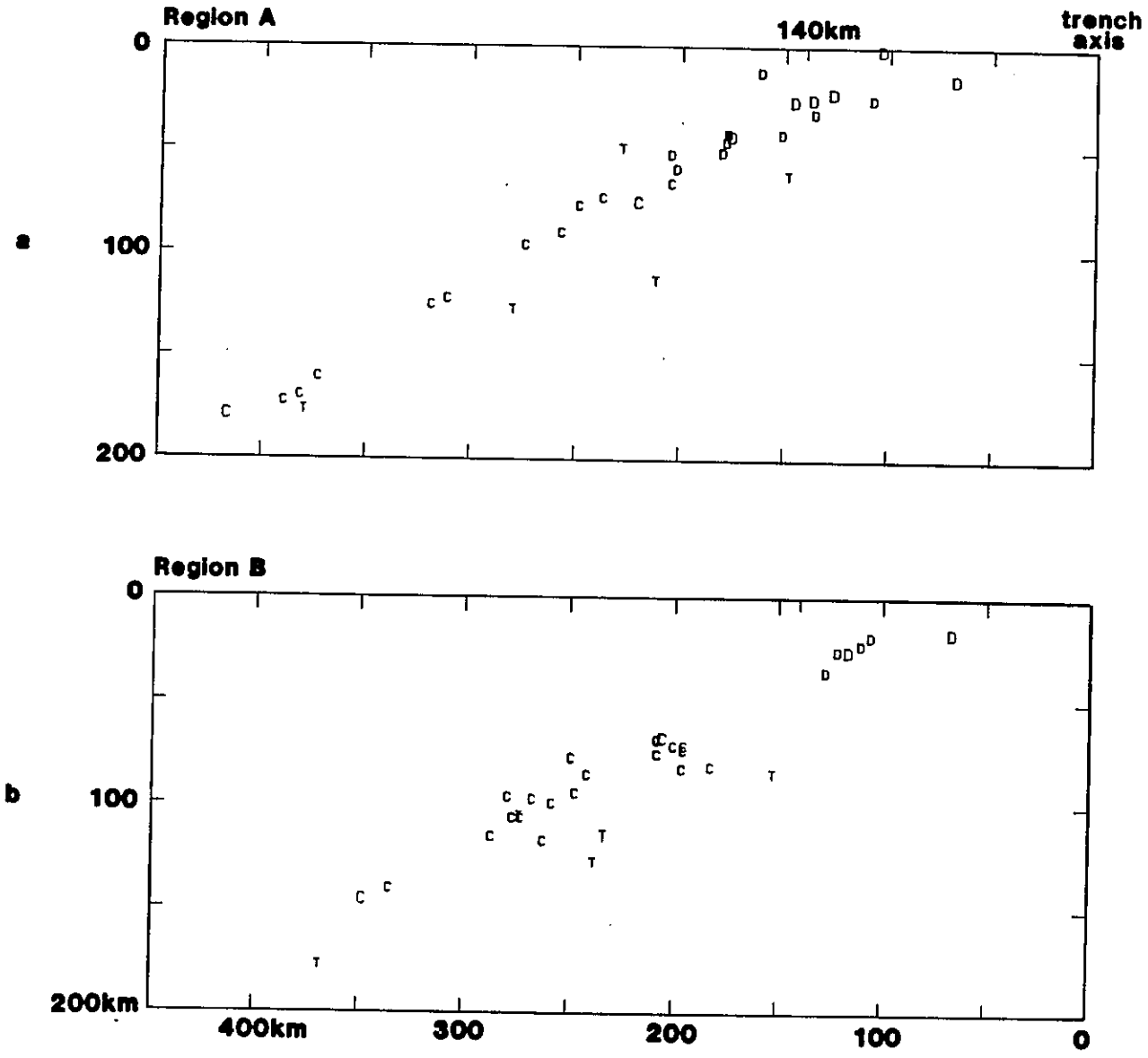

Figure 2.7. Cross sections of the events which are classified into type 'D', 'C', or 'T'. Triple seismic zones are seen in the regions C and D. Note the lack of 'C' type event below 80 km in region C.

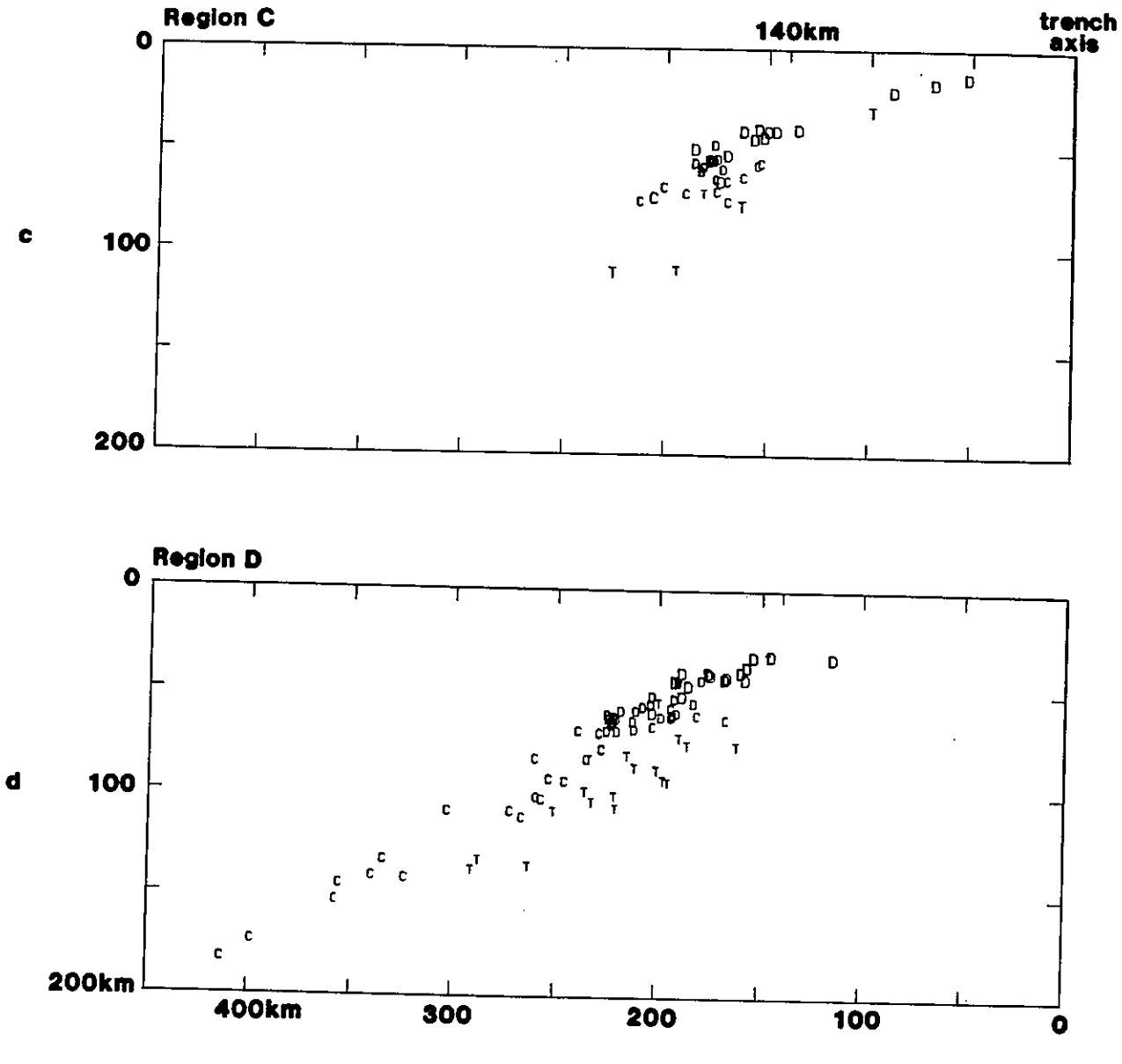

Figure 2.7. continued

events is indented seaward in region B, where no large earthquake is known in historical time (Figure 2.1). Type 'A' ('D' or 'C' type) events also show the same feature (Figure 2.5b) and this suggests that most type 'A' events are actually of thrust type. The map view of compression ('C') type events (Figure 2.5c) also shows a variation of activity; they extend seaward of the aseismic front in regions C and D. It should be also noted that the activity beneath the land area of region C is very low. It is not proper to draw a strong conclusion from the map view of tension ('T') type events because the level of activity of this type of event is not as high as other types of events; however, it seems worthwhile to note that a number of events occurred in the offshore area well beyond the aseismic front (see Figure 2.5a for the location). Although Yoshii (1979a) proposed that the aseismic front marks the edge of the double seismic zone along the northern Honshu arc, Figure 2.5 shows clearly this is not true.

Cross Sections

To draw the cross sections, the center of the small circle of the Japan trench was located at (40.15°N, 111.00°E), as determined by a least squares fit to the trench axis between 41°N and 36°N. Figure 2.6 shows a cross section of seismicity and mechanism type in each region. In Figure 2.7, only those earthquakes which could be classified into one of the three main types are plotted.

In region A, the overall seismicity level is very high, with a slight indication of the double seismic zone deeper than 60 km (Figure 2.6a). 'D' type events are distributed from the shallow zone near the trench to the 60 km depth. Although there is some seismicity immediately below the deep thrust zone, it is much less active than that seen in regions C and D. Most events belonging to this activity did not provide the information on the type of mechanism. It should be noted that region A and the northern part of region B have experienced the great 1968 Tokachi-Oki earthquake, which is the only great earthquake within the time period of this study. Therefore many shallow events should be considered the aftershocks of that event. However, the plot without those aftershocks does not basically change the pattern seen in Figures 2.6a and 2.7a.

Region B shows an interesting feature: the presence of a seismic gap at the deep thrust zone while activity in the shallow thrust zone is rather high. The same feature can also be noticed in the map views of 'D' and 'A' type events (Figures 2.5a and 2.5b). The double seismic

zone can be seen here as in other regions; however, it does not extend seaward beneath the deep thrust zone. Both the seismicity at the deep thrust zone and immediately beneath the zone are very low in this region. The nature of this gap will be discussed in detail later.

In region C, the double seismic zone which is characterized by 'C' and 'T' type events, extends immediately beneath the deep thrust zone and forms a triple seismic zone (Figures 2.6c and 2.7c). The 1978 M_s=7.5 Miyagi-Oki earthquake occurred in the deep thrust zone of region C. The time period treated in this study is just until the occurrence of this large event. Seno and Pongsawat (1981) suggested that the triple seismic zone was one of the precursory phenomena. The activity in the shallow thrust zone is low, which may reflect the gap in the activity prior to a great earthquake in this region; the region has been monitored as one of the possible areas of near-future occurrences of great earthquakes (Seno, 1979; Utsu, 1979a). The other prominent feature is the lesser activity in the deeper part (>100 km) of the double seismic zone in region C compared with that of other regions (Figures 2.5c, 2.6c, and 2.7c).

Region D is characterized by the presence of a triple seismic zone and less activity in the shallow thrust zone. It should be noted that the high density of distribution of the earthquakes in the cross section (Figure 2.6d) is primarily because the width of this zone is about twice as large as those of other regions.

Discussion

Depth Phases

It has been noticed that for submarine events, pP phases reported in the ISC bulletins are often actually pwP phases, the reflection from the ocean surface (Mendiguren, 1971; Yoshii, 1979a, b; Hong and Fujita, 1981; Fujita et al., 1981). Detailed studies of body wave synthetics with the local structure around the earthquake source (Seno and Kroeger, 1983; Kroeger and Geller, 1985) indicate that in many cases the reflection from the ocean surface (pwP phase) can be as large as that from the ocean bottom (pP phase). Since for shallow events, the arrival of the pP phase is much closer to the direct P phase and its amplitude is often smaller than that of the pwP phase, the pwP phases are often misidentified as pP phases in the ISC bulletins. Yoshii's (1979a, b) method of depth correction, which is used in this study, therefore, seems to

be proper. Fujita et al. (1981) showed that correcting the depth using pwP phases reduces the depth error to less than 10 and 15 km for large and moderate size events, respectively, from the analysis at the Aleutian trench. It is known that reported hypocentral locations determined by the standard method have a better resolution along the Japan trench than in the Aleutian trench (Barazangi and Isacks, 1979), and therefore the depth correction here gives more accurate focal depths than those which Fujita et al. (1981) reported. Seno and Kroeger (1983) determined precise focal depths for six moderate size events in the region studied using synthetic seismograms. For five of them, the corrected pP-P depth was in agreement with the depth determined by the synthetics within 4 km.

Triple Seismic Zone

The triple seismic zone is defined as the zone where the double seismic zone extends seaward of the aseismic front and overlaps with the zone of thrust type events at the interface of two converging plates (Seno and Pongsawat, 1981). As shown in the last section, triple seismic zones were found in both regions C and D. The upper zone of the double seismic zone is characterized by down-dip compression type ('C' type) events and the lower zone by the down-dip tension type ('T' type) events. There is a separation of about 10 km between the thrust zone and 'C' type events in Figures 2.7c and 2.7d. However, there is a possibility that the separation between the thrust zone and the zone of down-dip compression type events is caused by the inhomogeneity of the selection of earthquakes at a depth of 50 km. As described earlier, the most earthquakes used are those whose depths are determined from pP-P time difference with water depth corrections. These depths are often shallower than those determined routinely. For the events deeper than 50 km, the events determined routinely and having a small standard error in depth are included. However, if the accuracy is not good enough, this variation of focal depth determination could cause an artificial separation of one zone. Figure 3 of Seno and Pongsawat (1981) suggests this possibility because this figure demonstrates that the depths of the events at the deep thrust zone are mostly determined by depth phases while, in contrast, those of down-dip compression type events are mostly from routine determination.

In order to examine whether the apparent separation of the deep thrust zone and the 'C' type zone is true, the events in region D which compose the triple seismic zone are relocated by using a master event relocation technique. Six earthquakes which are relatively large ($m_b > 5.4$) and are expected to be better located are selected as the master events. Each event is relocated

relative to the closest of the six master events. This is because relative relocation methods such as the master event technique or the joint hypocenter determination technique seem to work properly for only events which have nearly equal distances from the center of the arc at subduction zones (Fujita et al., 1981). Figure 2.8 shows the result in a cross section. Large symbols denote the earthquakes chosen as master events and medium size symbols represent those relocated. The down-dip compression type events are still located about 10 km beneath the thrust type events. Although this does not completely eliminate the possibility of depth bias, within the resolution of the data this result should be considered as strong evidence against such a bias.

Figure 2.9 is the cross section of all the events which are classified into one of the three main types. This clearly shows the presence of the double seismic zone and the triple seismic zone at the seaward edge of the double seismic zone.

Seno and Pongsawat (1981) speculated that the triple seismic zone was caused by a stress disturbance within the slab beneath the deep thrust zone prior to the occurrence of a large thrust event. Because the stress distribution within the slab is more or less continuous, the similar stress pattern which can be seen in the double seismic zone should continue seaward of the double seismic zone. However, because the stress there is less than the critical stress required for triggering earthquakes, seaward continuation of the double seismic zone is not seen. At the plate interface of the deep thrust zone where large earthquakes recur, coupling between the plates at the rupture zone would produce a gradual stress buildup there which would approach the strength of the zone just prior to the occurrence of the large event. This stress buildup would also load the slab near the rupture zone and disturb the preexisting stress pattern, which could result in earthquakes within the slab farther seaward of the double seismic zone and beneath the deep thrust zone, resulting in a triple seismic zone.

In region B, neither activity at the deep thrust zone nor a double seismic zone beneath the deep thrust zone is seen. Historical seismicity data show that no large earthquakes are known near the coast in this region for at least the past 200 years (Usami, 1975). This shows a distinct contrast with the regions north and south of this zone where at least two large events occurred near the coast in this century in each region (Figure 2.1). Thus, it is proposed that the deep thrust zone in region B is totally aseismic and the decoupling at the deep thrust zone, i.e., no extra stress buildup, results in no extension of the double seismic zone beneath it. It is interesting to note that the shallow thrust zone in region B also shows an aseismic character.

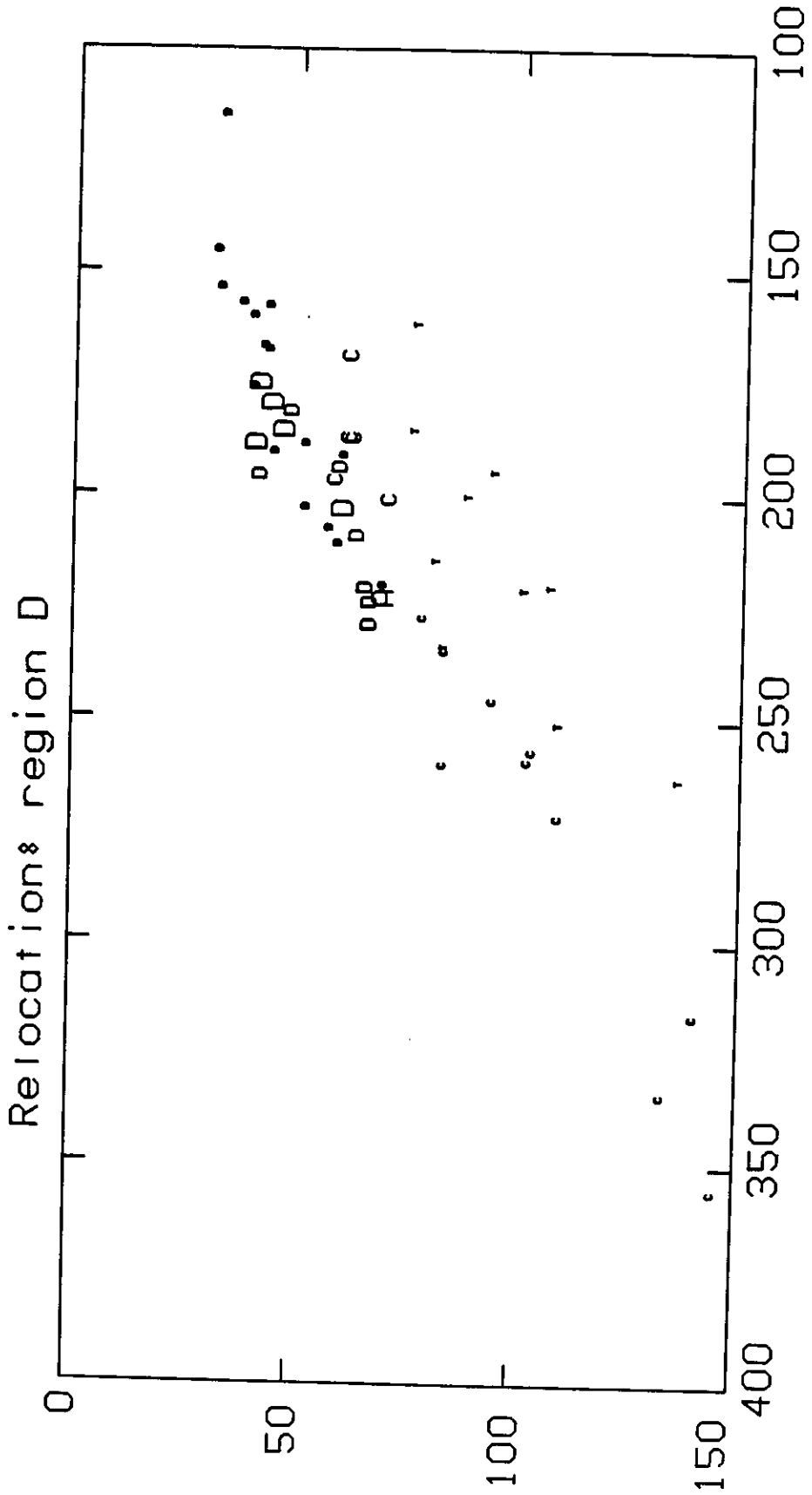

Figure 2.8. Master event relocation of the events at the triple seismic zone in the region D. The six large symbols denote the master events, and medium size symbols are those which are relocated. The vertical separation of 'D' and 'C' type events at the deep thrust zone is seen.

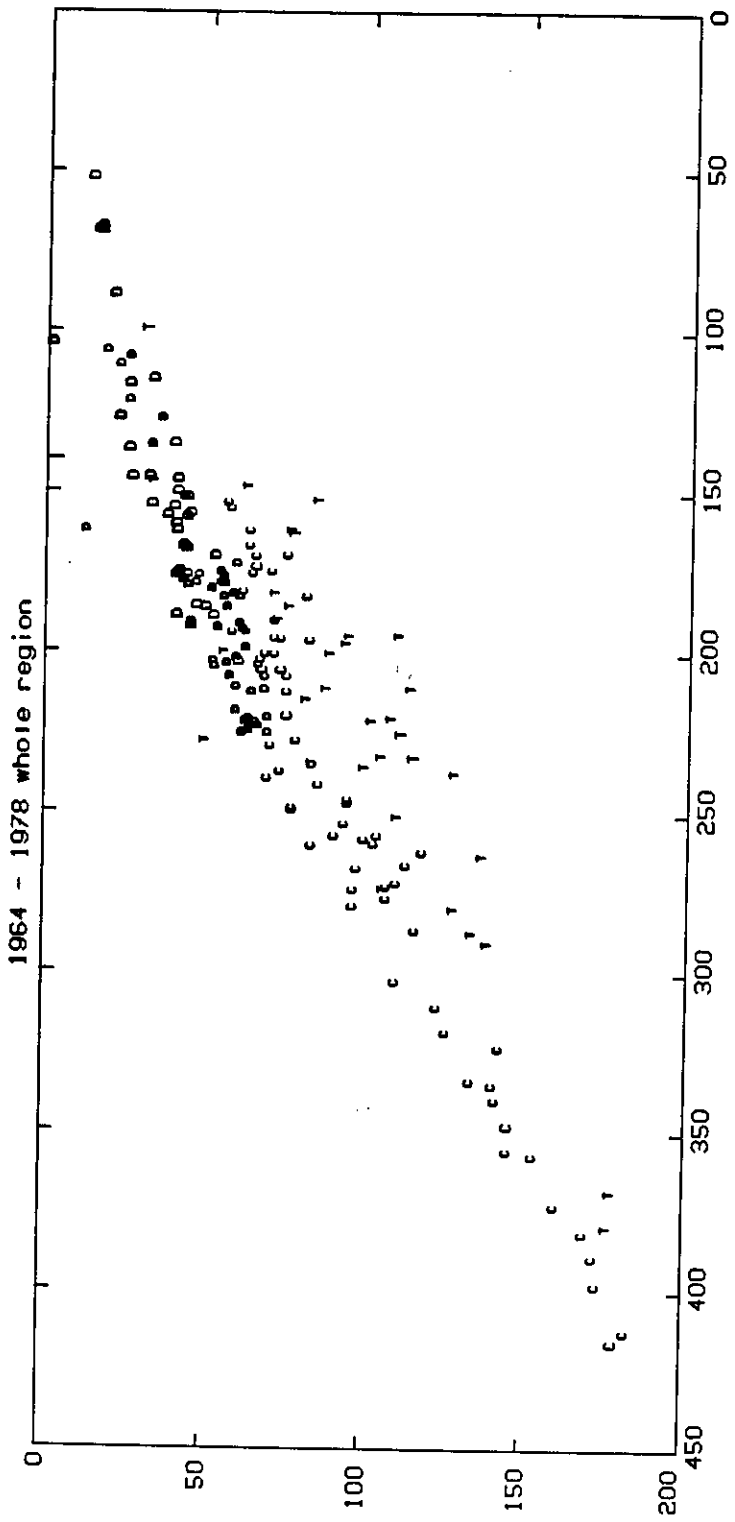

Figure 2.9. Cross section of the whole arc. Only those events which are classified into type 'D', 'C', or 'T' are plotted. Overall feature of subduction seismicity are seen clearly; the shallow and deep thrust zone, the double seismic zone, and the triple seismic zone which is an overlap of the double seismic zone and the deep thrust zone.

Here at the trench, a great normal fault, the 1933 M_s=8.5 Sanriku earthquake, occurred and a large tsunami earthquake occurred farther landward in 1896. No typical great thrust type earthquake has been known to occur at the shallow thrust zone in this region.

An alternative explanation for the triple seismic zone seen in regions C and D is that the unbending of the subducting lithosphere, which will be shown to be the cause of the double seismic zone in Chapter 4, starts at a shallower depth there than in the other regions. In this case the triple seismic zone is not a temporary but a permanent feature in these regions. It is, however, still expected that the earthquake activity in the triple seismic zone is sensitive to the stress state at the deep thrust zone.

The Possibility of a Large Earthquake in the Near Future

If the above hypothesis that the triple seismic zone is caused by the stress concentration prior to the occurrence of a large earthquake is correct, the presence of the triple seismic zone in region D suggests the existence of a stress concentration around the deep thrust zone and a possible near-future occurrence of a large earthquake in the deep thrust zone of this region. Abe (1977) stated that there has been no large earthquake in this region for the last 800 years except one series of five large earthquakes in 1938, and that a large portion of the relative plate motion is taken up by aseismic slip. However, this is probably incorrect. Utsu (1979b) located the 1896 M_s=7.4 and the 1905 M_s=7.8 event in this zone (see Figure 2.1). Both events show characteristics of low-frequency earthquakes which occurred in the deep thrust zone. The magnitude determined from the intensity distribution in Japan is much smaller than that from teleseismic stations, which suggests that these events are low-frequency earthquakes (Utsu, 1980). They did not cause large tsunamis, which suggests that their foci were deep. If historical large earthquakes in this region have the same character, it is likely that those events were overlooked in the ancient literature. Therefore this region, especially the deep thrust zone, should not be considered aseismic.

The possibility of occurrence of a large earthquake near the coast in region D has already been discussed by Mogi (1979) on the basis of a seismicity gap seen there for the past few decades. Mogi (1979) pointed out that a gap in activity for earthquakes whose magnitudes were greater than 5.6 for the past 30 years could be seen near the coast in the rupture zone of the large events in 1938. He also noted that the epicenters of large earthquakes tended to migrate to

the south along the northern Honshu arc and argued that there was a possibility of a migration of large events to the south from the region off Miyagi prefecture which ruptured in 1978. Katsumata and Yamamoto (1982) also noted seismic potential in the rupture zone of the 1938 events because the seismic activity has been very low in this zone since 1960. Thus the triple seismic zone seen in this zone may provide another line of evidence for the possibility of occurrence of a large earthquake in the near future off Fukushima prefecture (region D).

Another possible precursor to the Miyagi-Oki earthquake is the absence of down-dip compression type events in the deeper part of the double seismic zone (>100 km) in region C (Figures 2.4, 2.5c, 2.6c, and 2.7c). Strong coupling prior to the large earthquake could sustain the rest of the slab in the asthenosphere, thus creating a down-dip tensional stress field in the slab. This could counteract the preexisting down-dip compressional field in the upper plane of the double seismic zone, which would reduce the number of 'C' type events.

In region D, successive cross sections covering 5-year intervals (Figure 2.10) reveal a tensional stress feature in the slab during the latest interval (Figure 2.10c). This is consistent with the idea of current strong coupling at the deep thrust zone. Reyners and Coles (1982) and House and Jacob (1983) made a similar argument regarding the eastern Aleutian arc; the former explained the observed down-dip tension in the upper zone of the double seismic zone as a result of the coupling at the thrust zone in the Shumagin gap, and the latter explained the predominance of the T-type events in the eastern half of the eastern Aleutian arc by the seismic coupling in the thrust zone. Thus the degree of seismic coupling at thrust zones appears to play an important role in defining the stress field in the subducting slab at intermediate depths (80-200 km) on a relatively short time scale in contrast to the effects of tectonic features (e.g., age of the slab, convergence speed, etc.). This suggests the possibility of detecting the current degree of seismic coupling at the thrust zone by studying the stress pattern in the slab at intermediate depth. It is also important to include the possible perturbing effects of shallow coupling on deeper seismicity for studying the relative forces acting on the descending slabs. Since our knowledge about the state of stress within the slabs is obtained from the source mechanisms of earthquakes that occurred in the past two decades (e.g., Fujita and Kanamori, 1981), any short term temporal effects could significantly affect our interpretations.

In region A, the extension of the double seismic zone seaward beyond the aseismic front cannot be seen clearly. The seismic activity immediately beneath the deep thrust zone is lower than those of regions C and D. Therefore, although there have not been large earthquakes for

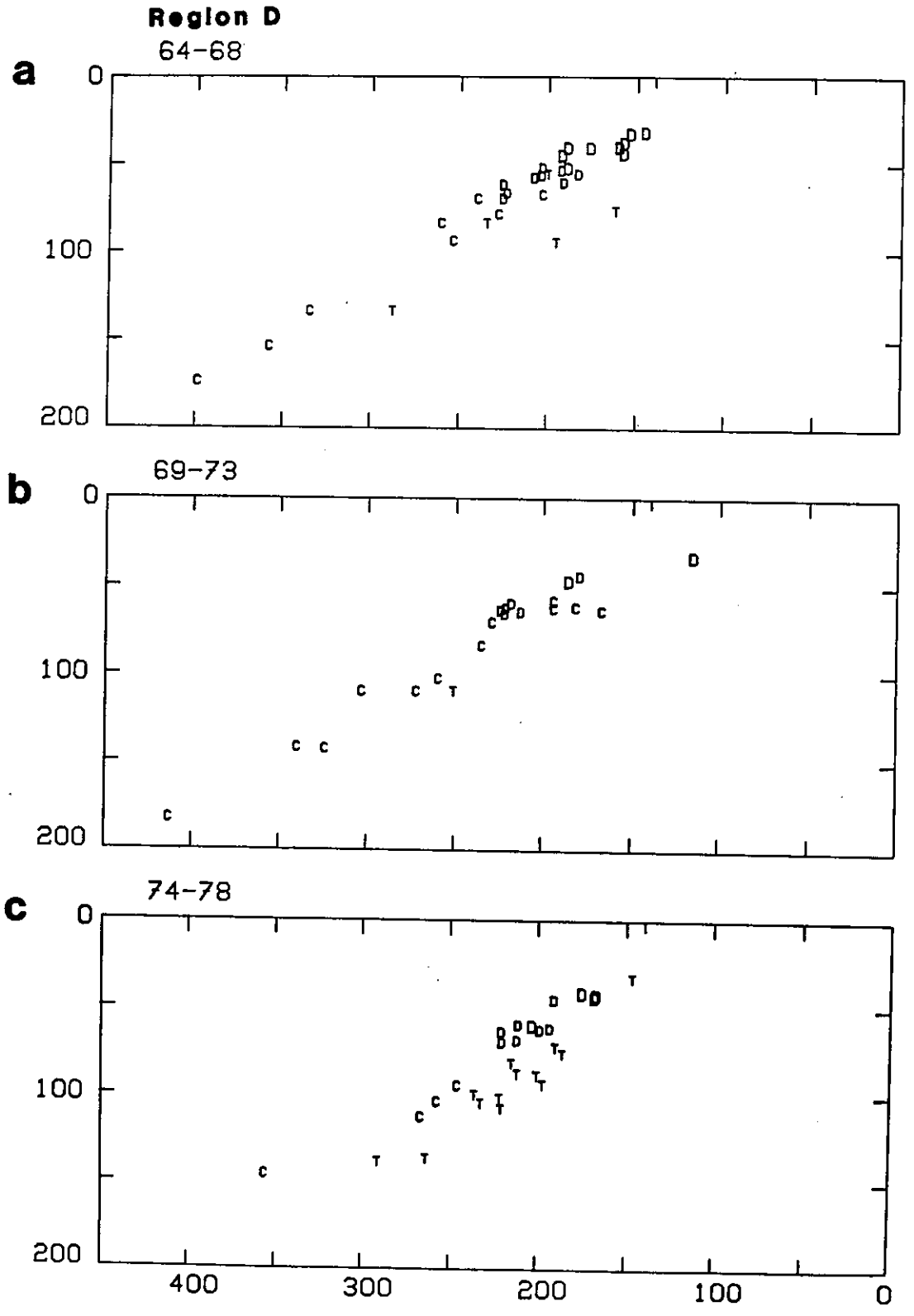

Figure 2.10. Successive cross sections of seismicity in region D in 5-year intervals. (a) 1964-1968. (b) 1969-1973. (c) 1974-1978. There are fewer compressional events and more tensional events in the latest interval than the two earlier ones.

about the last 40 years, there is no evidence of phenomena precursory to a large earthquake in this region. The possibility of a near-future large earthquake in the deep thrust zone of region A may be very small.

Deep Thrust Zone

It has been proposed in the chapter to characterize the subduction seismicity along the northern Honshu arc in terms of the shallow and deep thrust zones and the double seismic zone. Figure 2.11 shows a schematic characterization of this activity. The shallow thrust zone (0-40 km) is where great thrust type earthquakes occur regularly (100-year interval). The deep thrust zone (40-60 km) is characterized by the frequent occurrence of large thrust earthquakes.

The most recent deep thrust earthquake is the June 12, 1978, Miyagi-Oki earthquake. Seno et al. (1980) gave a depth of 27.8 km for the main-shock, referring to the data of a local network. The focal depth is redetermined by synthesizing long-period P waves, using a technique developed by Kroeger and Geller (1985), which allows to include the effect of local crustal structure around the source. Since the rupture process of the main-shock is too complicated to allow the application of body wave synthetics, the depth of the foreshock which occurred 8 minutes before the main-shock is determined. The depth of the foreshock was determined as 35 km. Because the focal depth of the main-shock is a few kilometers deeper than that of the foreshock and the rupture propagated westward (Seno et al., 1980), the Miyagi-Oki earthquake must have ruptured the thrust zone deeper than at least 35 km, i.e., the deep thrust zone. The depth obtained by Engdahl et al. (1979) using short-period depth phases is consistent with this result.

Although the physical difference between the shallow thrust zone and the deep thrust zone is not clear, the phase change of basalt/gabbro to eclogite in the crust of the oceanic plate may be responsible for the change of sliding characteristics at the 40-km depth of the plate interface, as proposed by Ruff and Kanamori (1981). Although they contended that no large thrust type earthquake occurred beneath a depth of 40 km, this is clearly not the case for the northern Honshu arc.

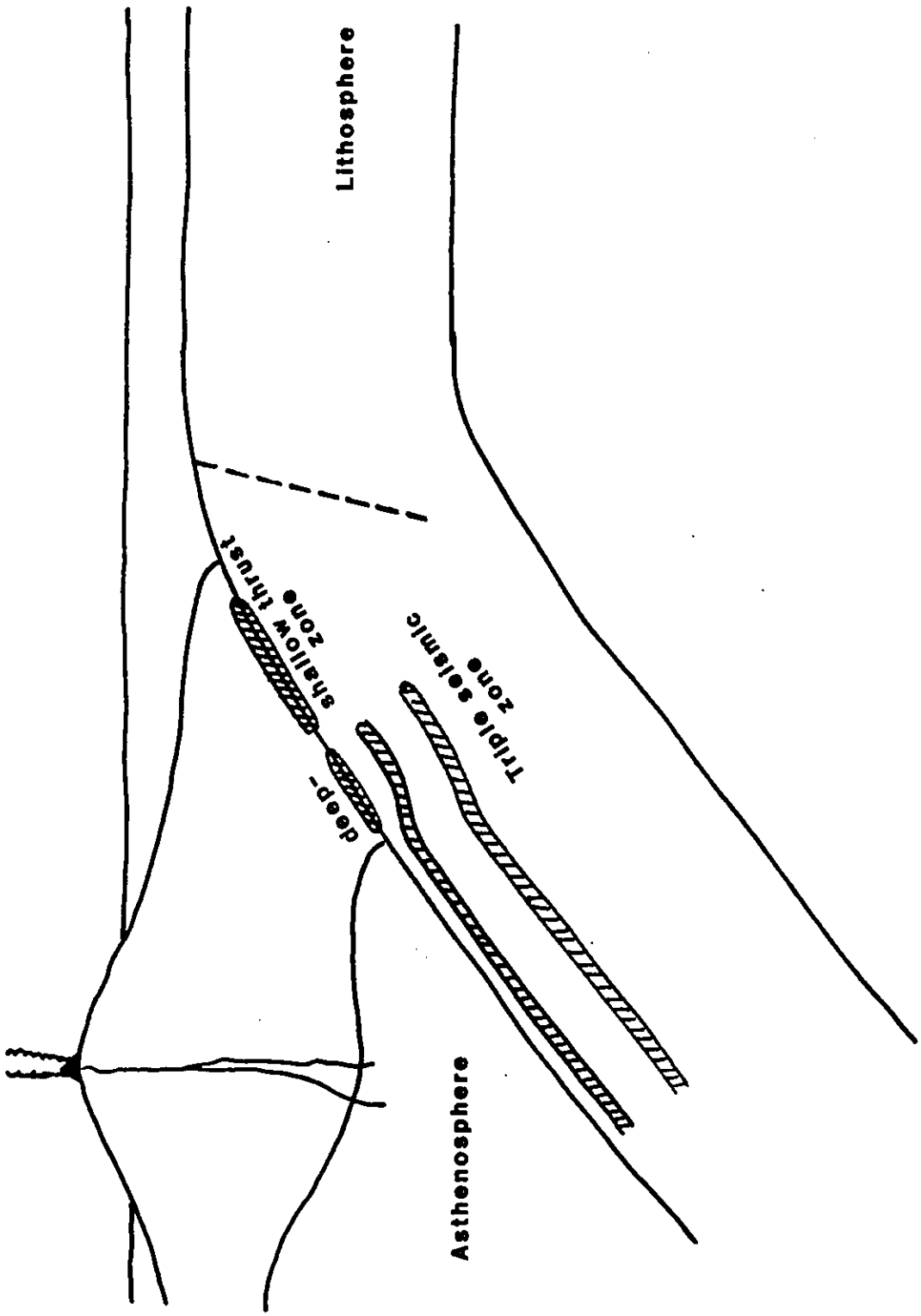

Figure 2.11. A schematic figure of the subduction seismicity along the northern Honshu arc. The dashed line represents the large normal fault earthquake that occurred in region B in 1933.

Conclusions

Regional variation of seismicity along the northern Honshu arc was studied in detail along with the types of focal mechanism. It is proposed to separate the interface of two converging plates into the shallow thrust zone (0-40 km) and the deep thrust zone (40-60 km). The regional variation of the seaward edge of the double seismic zone was found; in some regions, the double seismic zone constitutes a triple seismic zone with the overlapping deep thrust zone. The subduction zone was segmented into four regions A, B, C, and D from north to south, and each region was characterized by different activity in those thrust zones and the double seismic zone. Triple seismic zones were observed in regions C and D, where large historic earthquakes are recorded in the deep thrust zone. No triple seismic zone was observed in region A, although large earthquakes have occurred there historically in the deep thrust zone. In region B, there is a gap in activity for historic large and recent smaller earthquakes in the deep thrust zone. There the double seismic zone does not extend beneath the deep thrust zone. It is suggested that this variation of activity is related to spatial and temporal variation of the degree of the seismic coupling at the deep thrust zone. In regions C and D, the triple seismic zones may be caused by the stress buildup prior to the occurrence of large interplate earthquakes at the deep thrust zone. In region C, the large event has already occurred in 1978, and in region D, the occurrence may be in the near future. In region A, the low activity within the slab beneath the deep thrust zone may indicate the low level of the stress buildup in this zone. The aseismic character of the deep thrust zone in region B indicates that the seismic coupling is quite weak in this zone, and this is consistent with the lack of activity within the slab beneath the deep thrust zone in this region.

It is shown that the fine structure of the seismicity at the uppermost part of the Wadati-Benioff zone provides a key to understanding the seismic coupling at the plate interface, especially at the deep thrust zone. This may also give us information on the subduction process, stresses within the slab, and driving forces of plates.

New Data

New data (June, 1978 - 1980) have been analyzed since the publication of the paper by Kawakatsu and Seno (1983) which is substantially equivalent to the above. The result from the newly analyzed data are summarized below.

Figures 2.12 and 2.13 show the map view and the cross sections of the seismicity in this two and a half year time period. Since the time interval is very short, nothing conclusive can be stated. In region A, the shallow thrust zone is relatively quiet. Compared to region C, the intraplate seismicity in region D is very high. In particular, the T-type (and B-type) event activity beneath the deep thrust zone is continuously high from the previous time period (Figure 2.10c). Thus, the high stress built up at the deep thrust zone, which causes this down-dip extensional stress field, appears to exist.

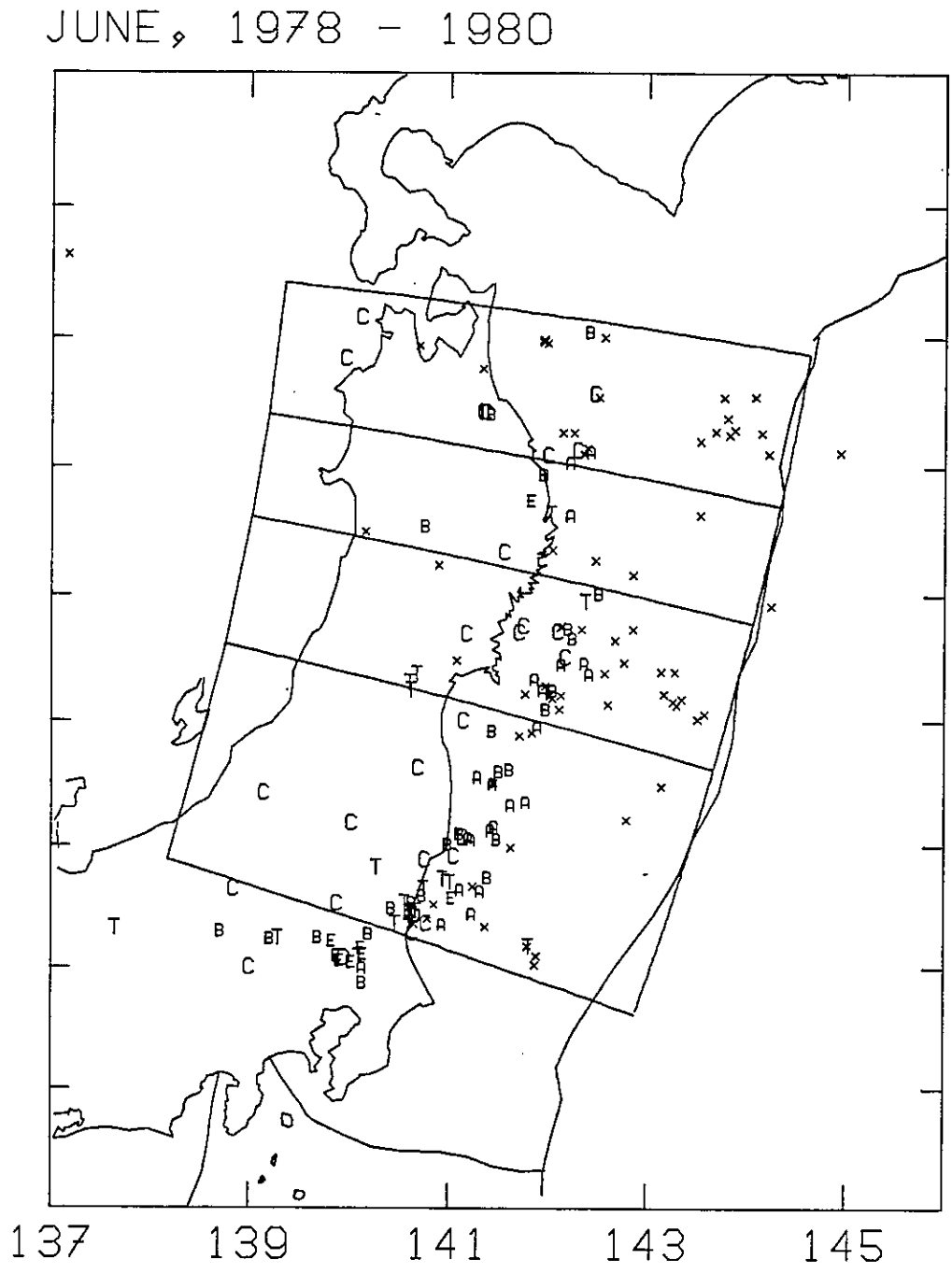

Figure 2.12. Map view for the new data.

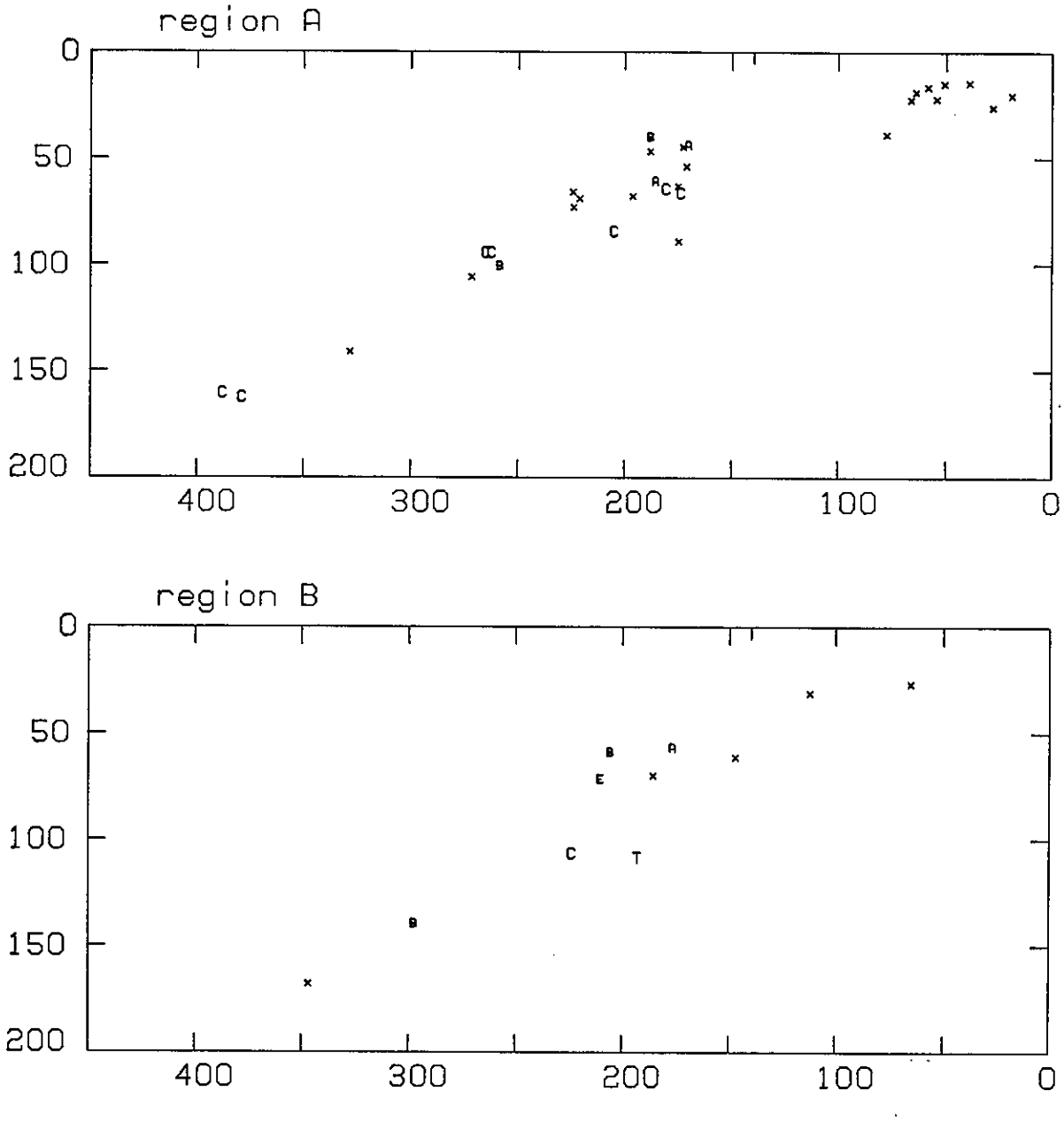

Figure 2.13. Cross sections for the new data.

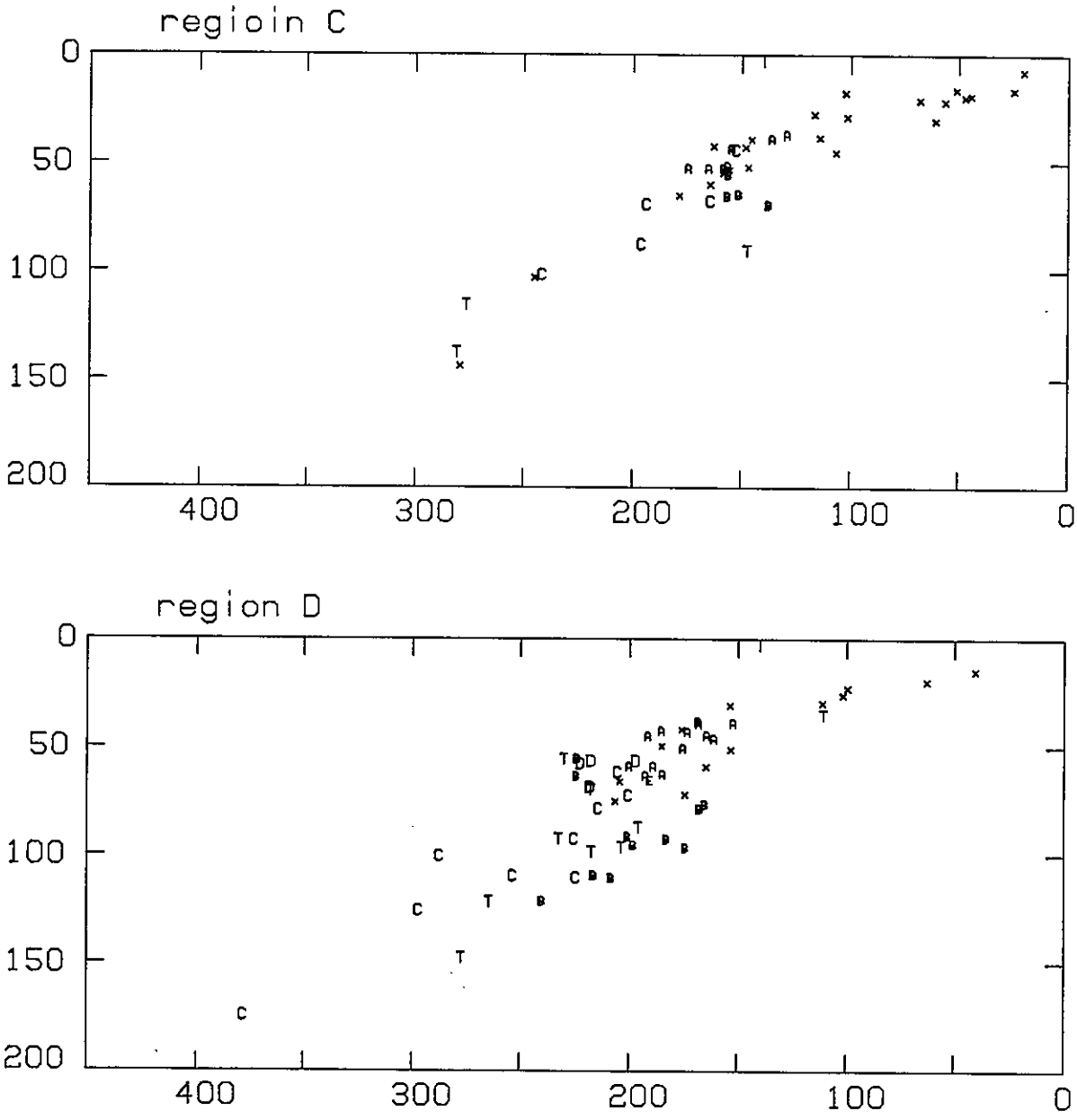

Figure 2.13. Cross sections for the new data (continued).

CHAPTER III

DOUBLE SEISMIC ZONE UNDER THE TONGA ARC

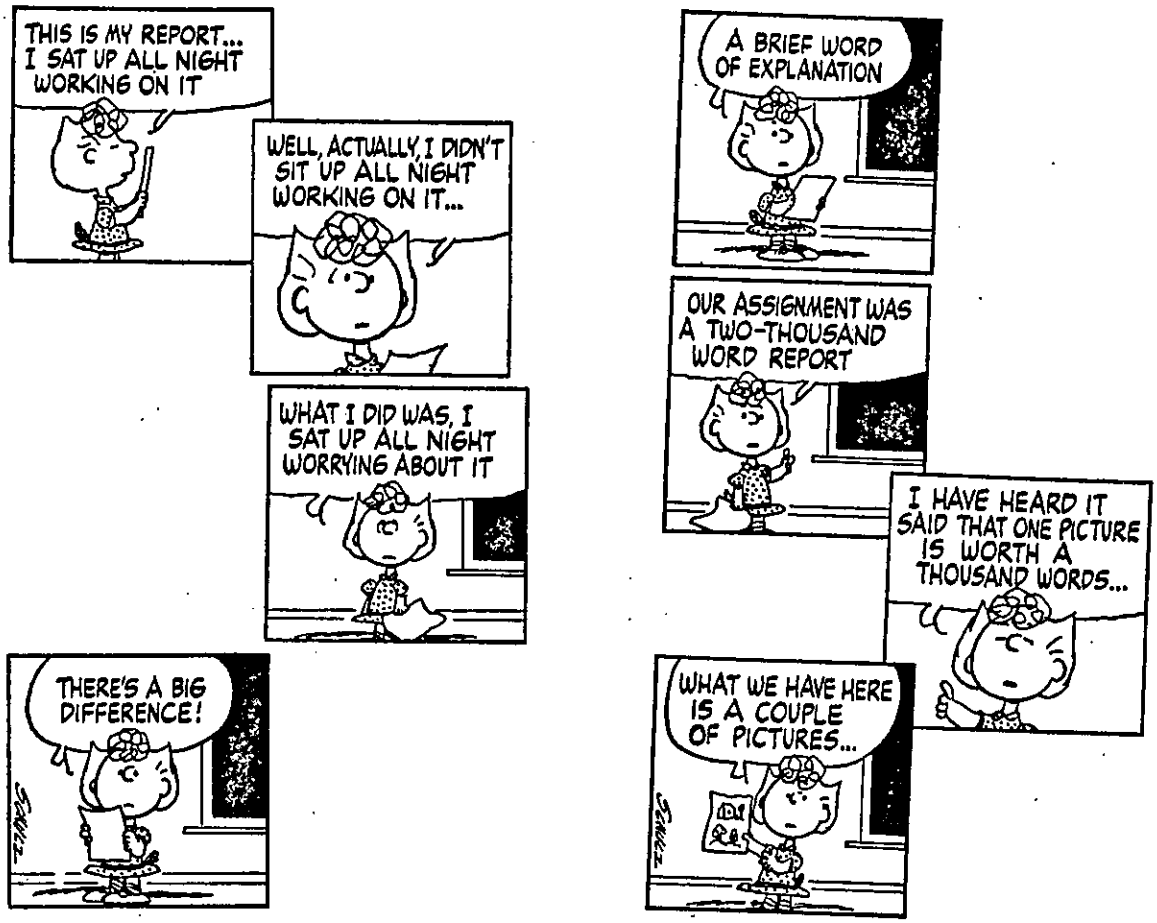

Introduction

Because of the large number of deep and intermediate earthquakes, the subduction zone along the Tonga-Kermadec arc has drawn much attention from seismologists. For example, in the early days of the development of the theory of plate tectonics, Barazangi, Isacks, Oliver and their coworkers (e.g., Oliver and Isacks, 1967; Barazangi et al., 1972) used the transmission of short-period S-waves to delineate the existence of a high velocity and low attenuation zone, and showed it coincided with the zone of deep and intermediate earthquakes.

The seismicity of this area has been also studied extensively by researchers at Cornell University. The most recent and complete summary of the seismicity can be found in Billington (1980). After selecting well-located earthquakes, she concluded that the thickness of the Wadati-Benioff zone is about 40km. In the intermediate depth range (70-300km), the stress state inferred from earthquake focal mechanisms indicates strong down-dip compression and down-dip tension in the Tonga and Kermadec subduction zones, respectively (Isacks and Molnar, 1971; Billington, 1980, Fujita and Kanamori, 1981). The activity of deep earthquakes under the Tonga arc is extremely high and the stress state is strongly down-dip compressional. Richter (1979) and Giardini and Woodhouse (1984) attributed this to the failure of the slab to penetrate into the lower mantle.

Therefore, all previous work on the seismicity of the Wadati-Benioff zone under the Tonga arc suggests that the stress pattern of the intermediate depth part of this slab is strongly down-dip compressional. In this chapter, however, by carefully examining earthquake focal mechanisms and locations, I will show that there is a double seismic zone beneath the Tonga arc. Although there are more down-dip compressional events than tensional events in the double seismic zone, the compressional stress (or strain) transmitted from below 200 km depth does not seem to completely overprint and erase the preexisting stress (or strain) feature of a double seismic zone. This discovery of a Tonga double seismic zone suggests that the double seismic zone is a more general and persistent feature of subducting slabs in the intermediate depth range than previously thought and that careful studies of seismicity of other Wadati-Benioff zones will probably reveal other as yet undiscovered double seismic zones.

Data

Depths of earthquakes are, in general, the least well constrained parameter of reported (ISC or PDE) hypocenters. The relative epicentral location of earthquakes in small areas can, on the other hand, usually be well determined. Therefore, as in the previous chapter, it is essential to have accurate depth estimates in order to study the detailed seismicity of shallow and intermediate depth earthquakes in subducting slabs and in order to determine the possible existence of a double seismic zone.

We use three different data sets (listed in Appendix C). The first set consists of events for which the focal mechanisms are determined by P-wave first motions and S-wave polarizations. The depth of these events is constrained by either checking the WWSSN seismograms by myself or pP-P time differences reported in the ISC bulletin. These events will be denoted by the list number in the table preceded by 'F' in the rest of this chapter.

The second data set consists of the events for which Harvard Centroid Moment Tensor (Dziewonski et al., 1981, Dziewonski and Woodhouse, 1983) solutions are available. The Harvard catalog is nearly complete for shallow events with $M_s \geq 6.5$ and deeper events (h>80km) with $m_b \geq 5.5$ after 1977. Their best double couple solutions are used. Since the moment tensor is determined from body-wave wave-form inversion (for large events, surface waves are also used), the depth of these events are reliable. The pP-P depths reported by ISC and Harvard centroid depths are usually the same within a few kilometers. For the crucial down-dip tensional events, which may be located in the lower plane of a double seismic zone, however, I checked the depths using WWSSN long period seismograms (Figure 3.5 and Appendix E). For some events, the CMT solutions are also compared with the WWSSN first motion data. Both tests suggest that Harvard CMT solutions are sufficiently reliable in both depth and earthquake mechanism for the purpose of this study (Appendix E). These events will be denoted by 'H'.

These two data sets include most of the intermediate depth events (350km>h>60km) with m_b greater than 5.5, for which focal mechanism solutions are available in the Tonga-Kermadec region.

The events of the third data set are selected from ISC bulletins from 1971 to 1979 under the following conditions; more than 30 observations of P arrivals and depth determined from pP-P time difference. From 1964 to 1970, events are added from Billington's file (Billington,

1980). Only events with pP-P depth between 70 km and 250km are selected from her file. The events of this data set will be called 'depth constrained ISC events' and will be plotted as background seismicity. In order to keep the consistency of the epicentral parameters, the epicentral locations reported by the PDE are used consistently for the events of all data sets.

Seismicity

Map View

All the depth constrained ISC events are plotted in Figure 3.1 with tectonic features in the Tonga-Kermadec area. The numbers in figure indicate the orientation of great circles connecting a point on the trench and the pole of the arc. The azimuth of these great circles is measured clockwise from north at the pole of the arc. The pole of the arc is located at $20.6^{o}\,N$,$102.8^{o}\,E$, so that the 100 km iso-depth contour under the Tonga arc of Isacks and Barazangi (1977) is 90 degrees distant away from the pole. The pole of the arc is thus chosen to best describe the seismicity in the Tonga region and may not be appropriate for the Kermadec region. The broken line denotes the trench. The lines perpendicular to the strike of the trench are drawn every degree from azimuth 109^{o} to 129^{o}. The lines parallel to the strike of the arc are at distances of 87.5^{o} and 92.5^{o} from the pole. It is well known that there is a complication in the geometry of the subducting plate (e.g., Isacks and Barazangi, 1977; Billington, 1980), possibly due to the subduction of the Louisville ridge, which also complicates the study of seismicity in this area.

Figure 3.2 shows the map view of the seismicity of the Tonga-Kermadec area. All the events for which earthquake focal mechanisms are available are plotted. Although the purpose of this chapter is primarily to study events shallower than 200 km, some of the interesting features of the deeper seismicity will nevertheless be summarized here.

For the events deeper than 350km, planar seismicity associated with nodal planes of earthquakes, for which focal mechanisms are obtained, has been identified (Billington, 1980; Giardini and Woodhouse, 1984). Using CMT solutions, Giardini and Woodhouse (1984) showed that large scale shear failure due to shortening of the slab might be taking place and interpreted it as evidence for the slab not being able to penetrate into the lower mantle.

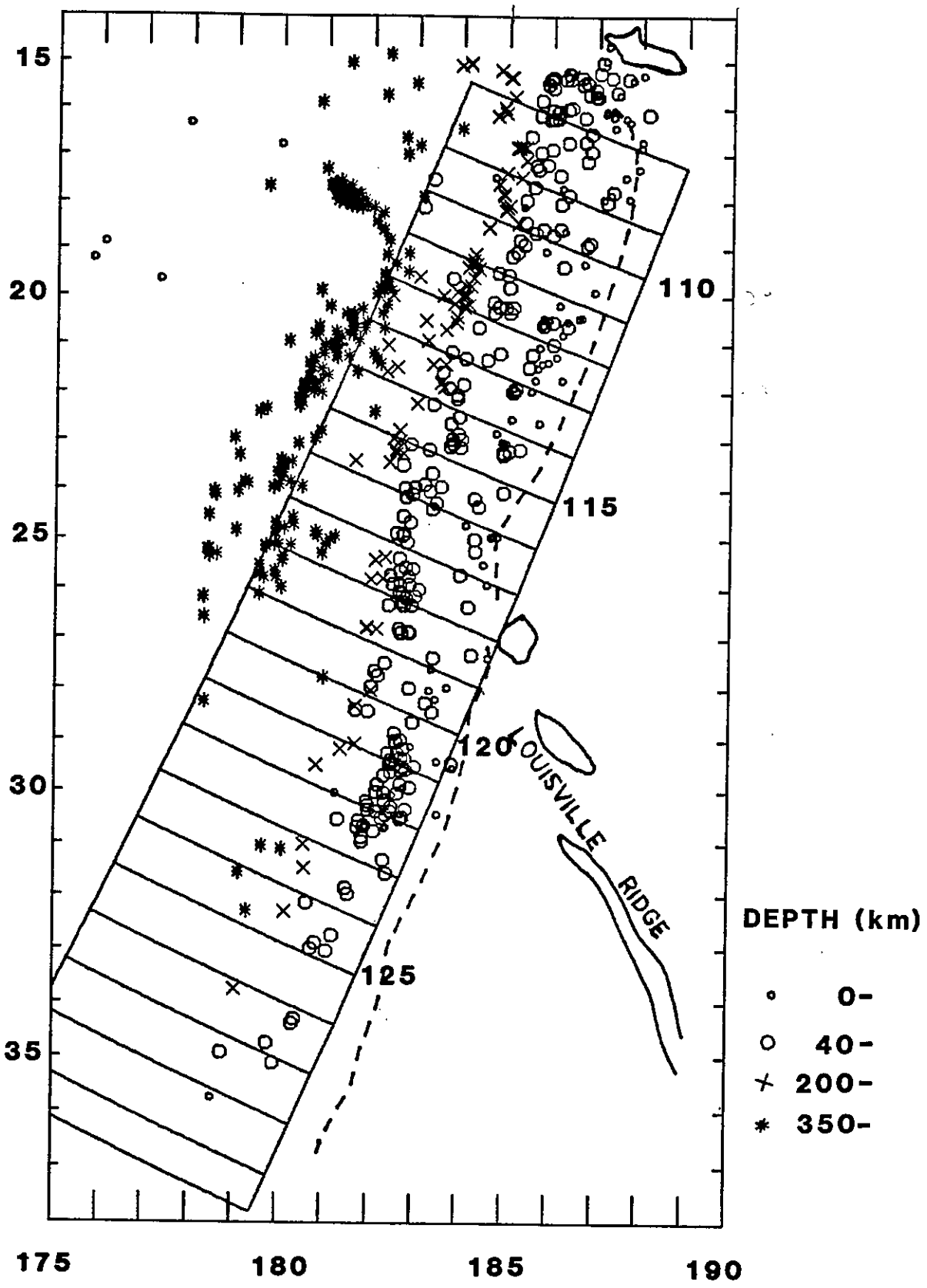

Figure 3.1. Map view of the general seismicity of Tonga-Kermadec area. The depth constrained ISC events are plotted. The broken line represents the trench. The lines perpendicular to the trench are parts of the great circles which pass through the pole of the arc and the numbers denote the azimuth of the great circles. The azimuth of these great circles is measured clockwise from north at the pole of the arc. Two lines parallel to the strike of the trench are at distances of 87.5° and 92.5° from the pole.

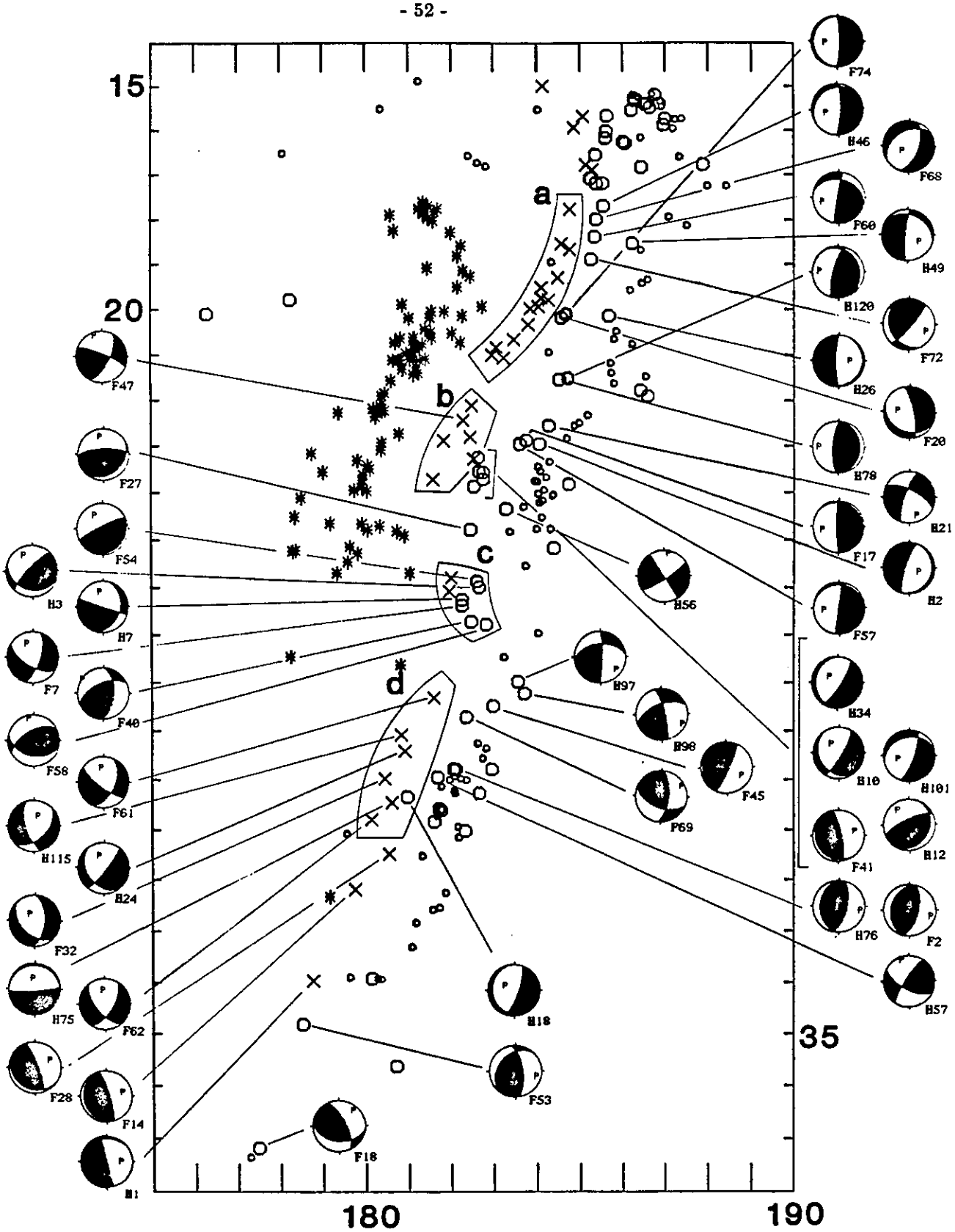

Figure 3.2a. All the events for which focal mechanisms are available are plotted on the map view. The lower hemispheres of the focal spheres are shown for intermediate depth (60 - 200 km) events.

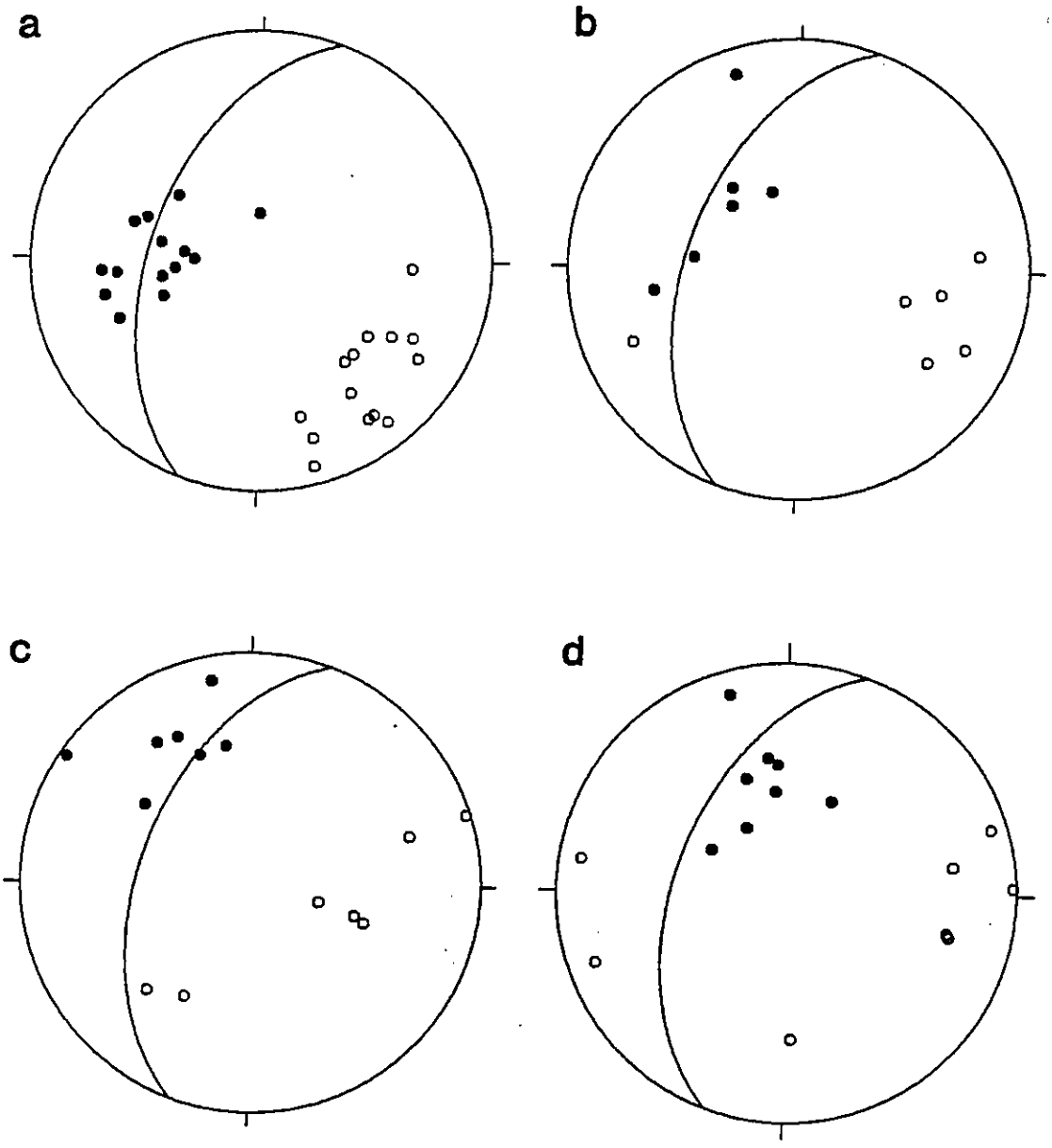

Figure 3.2b. The principal axes of focal mechanisms of the events grouped into 'a', 'b', 'c', and 'd' in Figure 3.2a are shown. The closed circles and open circles denote compressional and tensional axes respectively and the great circles indicate the direction of the dip of the slab.

A similar but more distinctive feature can be found between $17^{\circ}S$ and $22^{\circ}S$. As seen in Figure 3.2, a group of events denoted by 'a' shares very similar focal mechanisms with down dip compression. The depths of these events are between 210 km and 240 km and they clearly line up horizontally, when seen from a direction perpendicular to the strike of the trench (Figure 3.3a). The origin of these earthquakes is not clear, but there seem to be two possible explanations. The first is that there is a large scale shear motion occurring due to the shortening of the slab, as has been observed in the deep seismicity. The second explanation considers the earthquakes are due to the elevated phase change of olivine to spinel within the descending slab. Giardini (1983) showed that the CMT solutions of three of these events deviate from a simple double couple mechanism. Therefore it may be possible that for some unknown reason, the phase change is taking place at a very high rate in this area and causing this group of earthquakes. From observation of P-wave arrival residuals at a local station (AFI), Goto (1984) also suggested an anomalous high velocity feature around this depth range. Solomon and U (1975) also showed a similar feature in the same area, using teleseismic P-wave arrival residuals.

The events of group 'b' show a similar mechanism pattern (i.e., down dip compression) to those of 'a' except event F47, which has a significant strike slip component. In general this region is still highly down dip compressional, which is consistent with the high activity observed below.

The pattern of groups 'c' and 'd' is more complicated, but compression axes stay in a rather small area on the focal sphere while T axes are scattered. These events probably represent a transitional stress state (i.e., down-dip compressional in Tonga to down-dip tensional in Kermadec) of this area. The geometry of the descending plate (Figure 3.1) in this area shows lateral bending, and the deformation in this area appears to be very complicated.

Cross Sections

Figures 3.3 are the cross sections of seismicity plotted parallel to the strike of the subduction zone. In Figure 3.3a, all the events which occurred in the subducting slab and for which focal mechanisms are available, are plotted. For events shallower than 350 km, closed circles, open circles, and crosses denote events which are consistent with down-dip compression, down-dip tension or neither, respectively. In Figure 3.3b, all the depth constrained ISC events

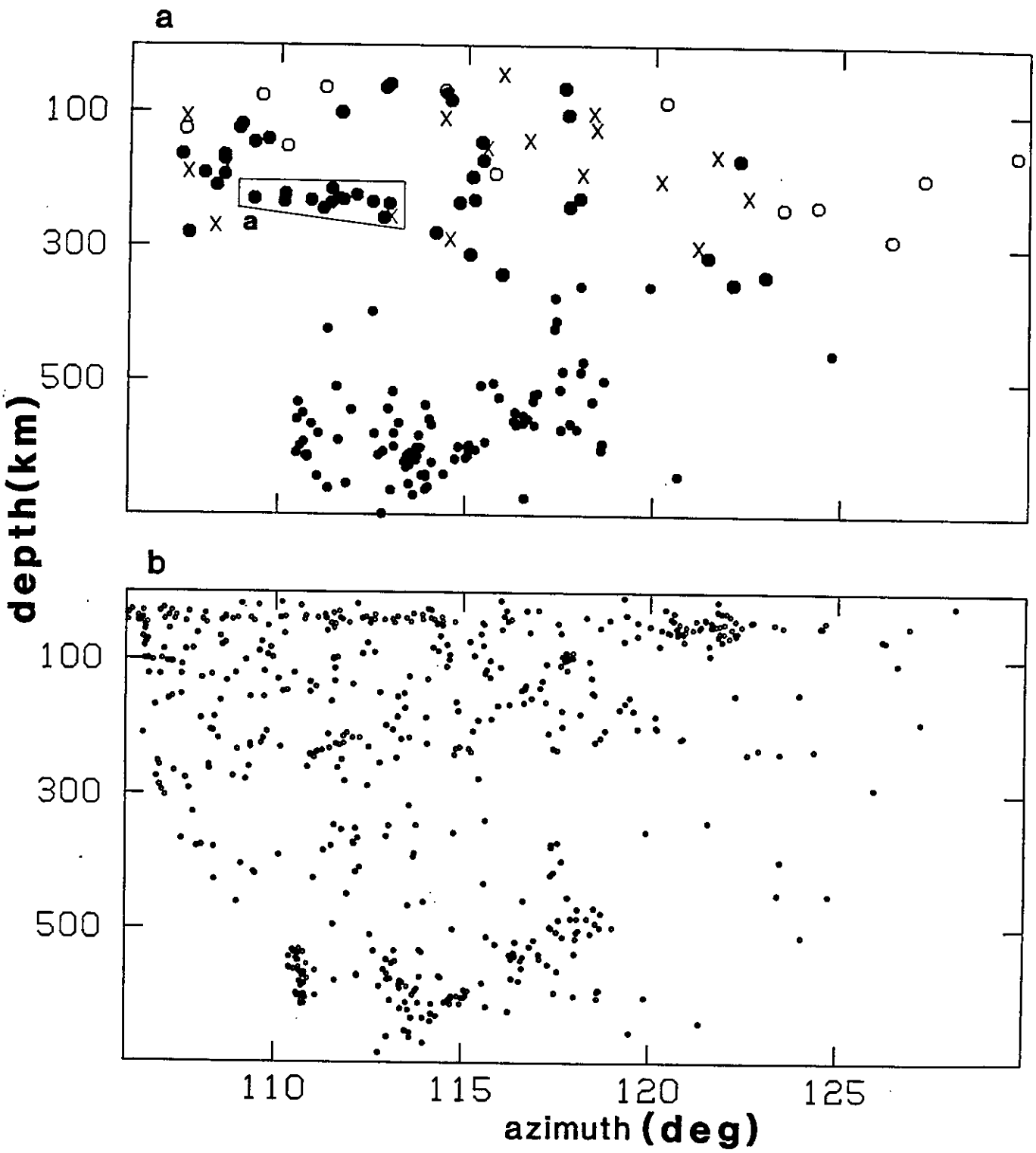

Figure 3.3. Cross sections parallel to the strike of the trench. The vertical exaggeration is 2. (a) All events which occurred within the subducting slab are plotted. For events shallower than 350 km, focal mechanism types are indicated; Open circles and closed circles denote down-dip tensional and down-dip compressional events, respectively. Crosses are the events which show neither of those mechanisms. Note the horizontal line-up of events of group 'a'. (b) Depth constrained ISC events.

are plotted.

The number of events with crosses increases in the region between Tonga and Kermadec, and this manifests the transitional strain feature discussed above. General seismic activity in the intermediate depth range decreases from north to south.

Figures 3.4 show the cross sections of seismicity projected onto planes perpendicular to the strike of the trench. The large circles correspond to the events with focal mechanisms and small ones correspond to the depth constrained ISC events. Focal mechanisms are presented as equal-area projections of the near-side hemisphere of the focal sphere.

Between azimuths 109° and 116°, most events have focal mechanisms of plane strain (or stress) between depth 50 km and 200 km and show either down-dip tension or compression type mechanisms, except event H21. The geometry of the plate (Figure 2 of Isacks and Barazangi, 1977) also shows that this region has a rather simple plane geometry. North of azimuth 109° ($\sim 17.5^{\circ}$ S), the end of the subduction zone results in hinge faulting, introducing more complicated stress and strain structure in the slab. South of azimuth 116° ($\sim 24.5^{\circ}$ S), the lateral bending of the slab near 26° S prevents a simple two dimensional view of the subduction process. In the Kermadec region, seismic activity is too low to further investigate the seismicity in this area using teleseismic data. In the remainder of this chapter, therefore I investigate only the seismicity of the descending slab between azimuths 109° and 116° and assume that the two dimensional view is an appropriate approximation.

Double Seismic Zone in Tonga

It has been believed that the stress state of the intermediate depth range of the subducting slab under the Tonga arc is strongly down-dip compressional (Isacks and Molnar, 1971; Billington 1980; Fujita and Kanamori, 1981). Isacks and Molnar (1971) state *'a compressional stress is transmitted through nearly all parts of the slab'*. Even after the discovery of a clear double seismic zone in Japan (Hasegawa et al., 1978a, b), neither Billington (1980) nor Fujita and Kanamori (1981) suggested the possibility of the presence of a double seismic zone in Tonga, although they identified one event which shows down-dip tension at a depth of 186km (event F41). However, as seen in Figure 3.3a and Figures 3.4, there exist several down-dip tensional events under the Tonga arc and they occur in the lower most portion of each seismic

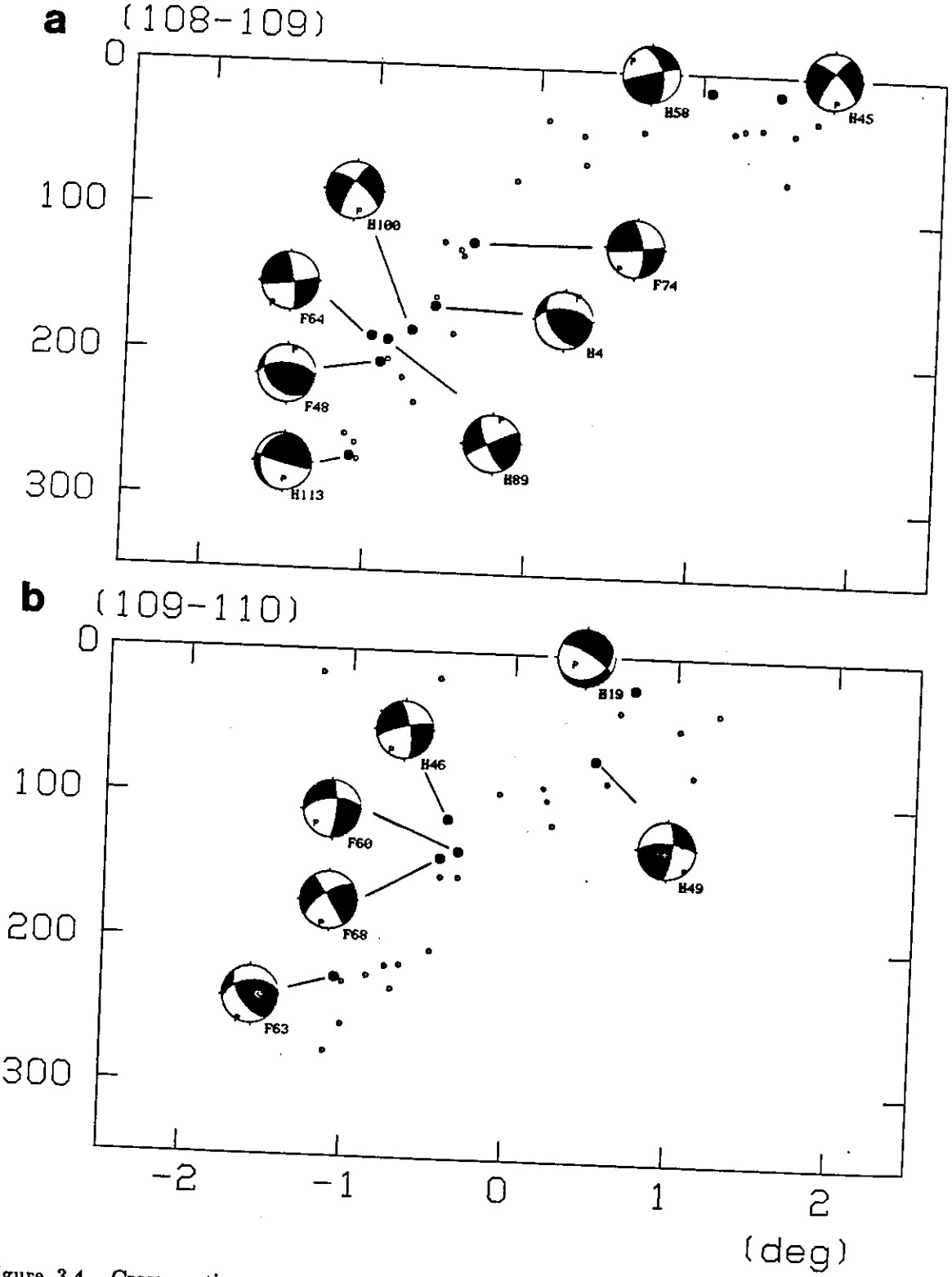

Figure 3.4. Cross sections perpendicular to the trench. Small circles and large closed ones represent depth constrained ISC events and events with focal mechanisms, respectively. The near side of the focal hemisphere is plotted. The numbers on the top of each figure correspond to the azimuth range of each of the cross section. The horizontal scale is a degree along the great circle perpendicular to the strike of the trench. (a) Azimuth between 108° – 109° and (b) 109° – 110°.

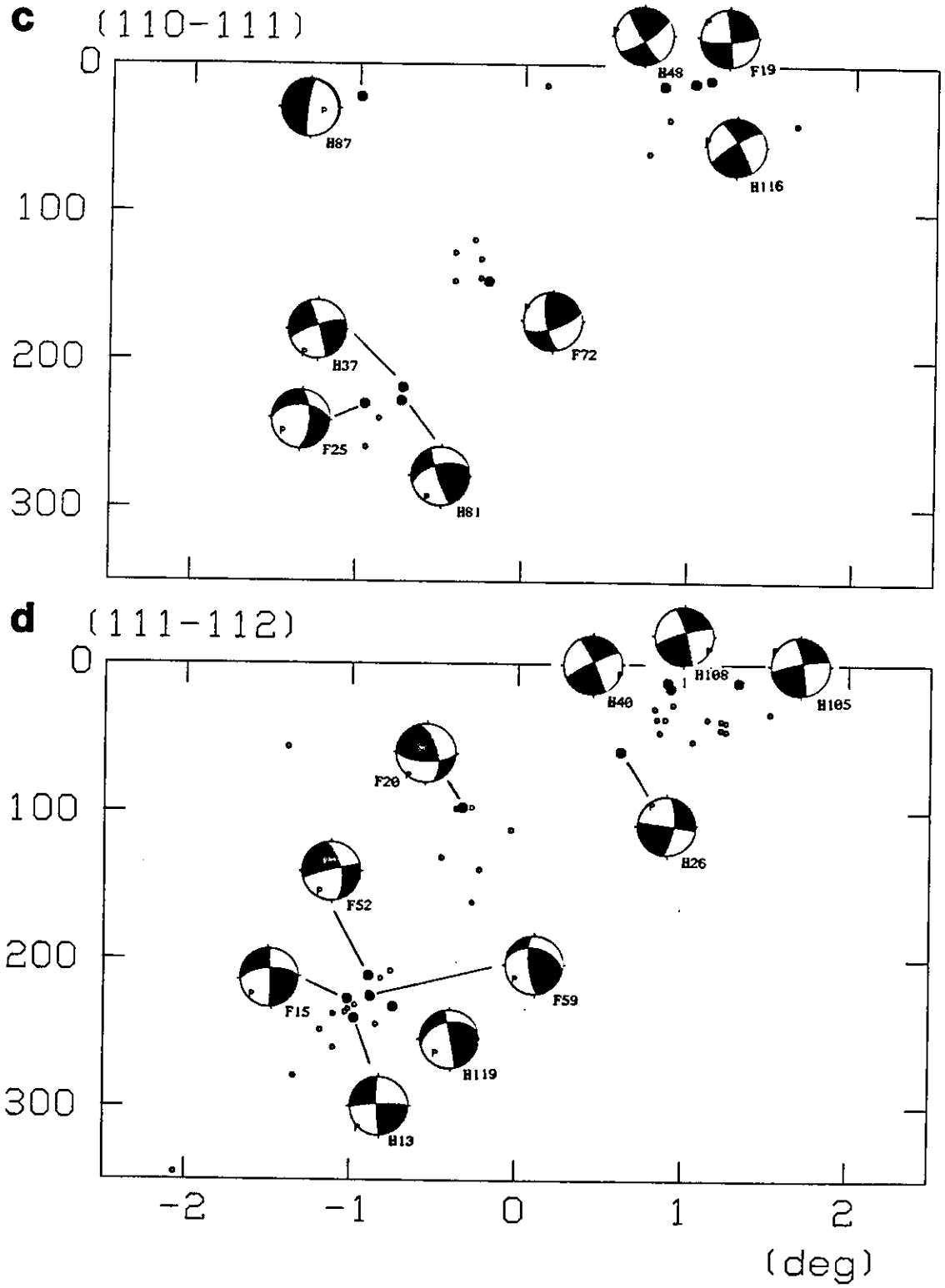

Figure 3.4. Cross sections perpendicular to the trench. (c) Azimuth between 110° – 111° and (d) 111° – 112°.

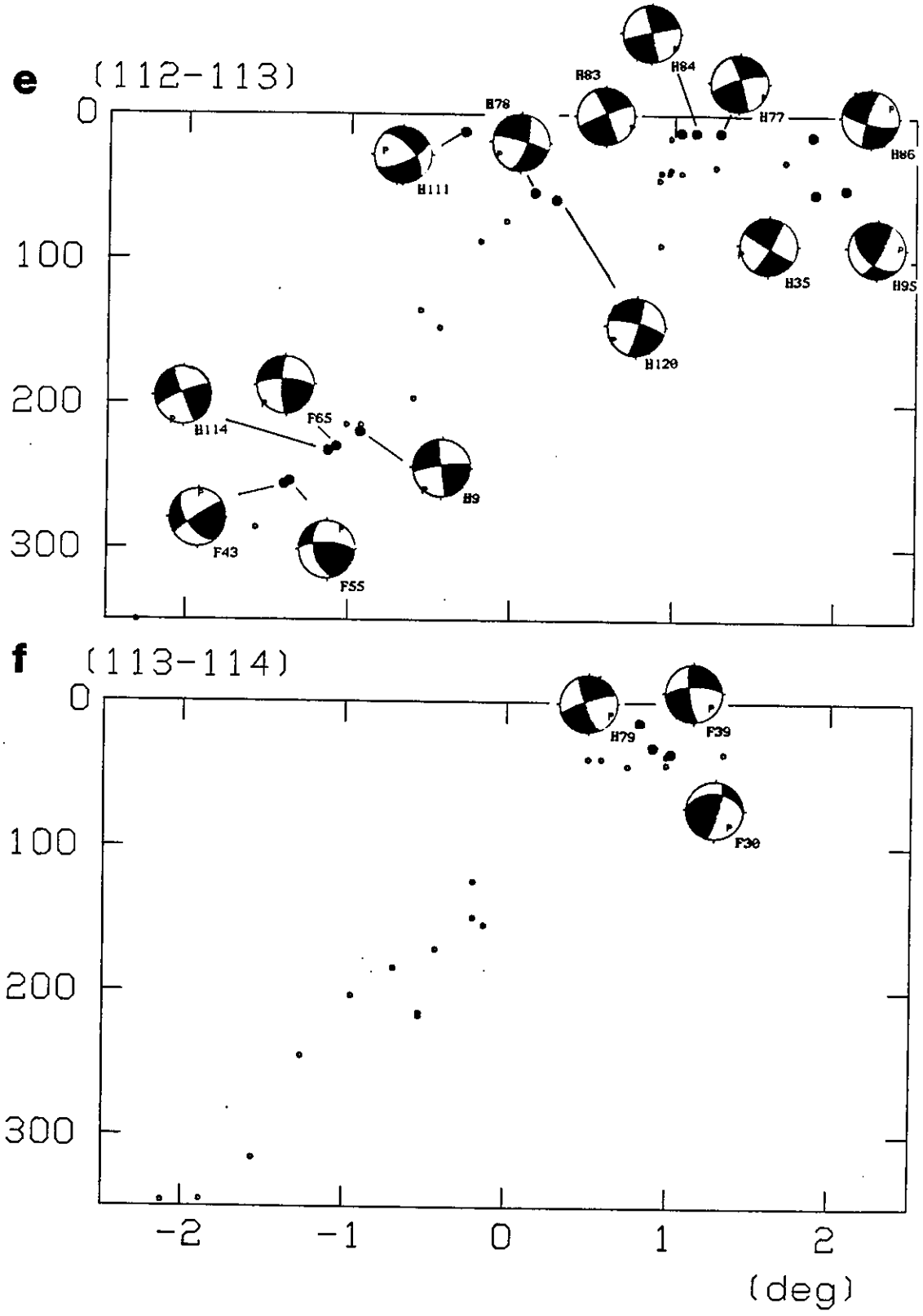

Figure 3.4. Cross sections perpendicular to the trench. (e) Azimuth between 112° – 113° and (f) 113° – 114°.

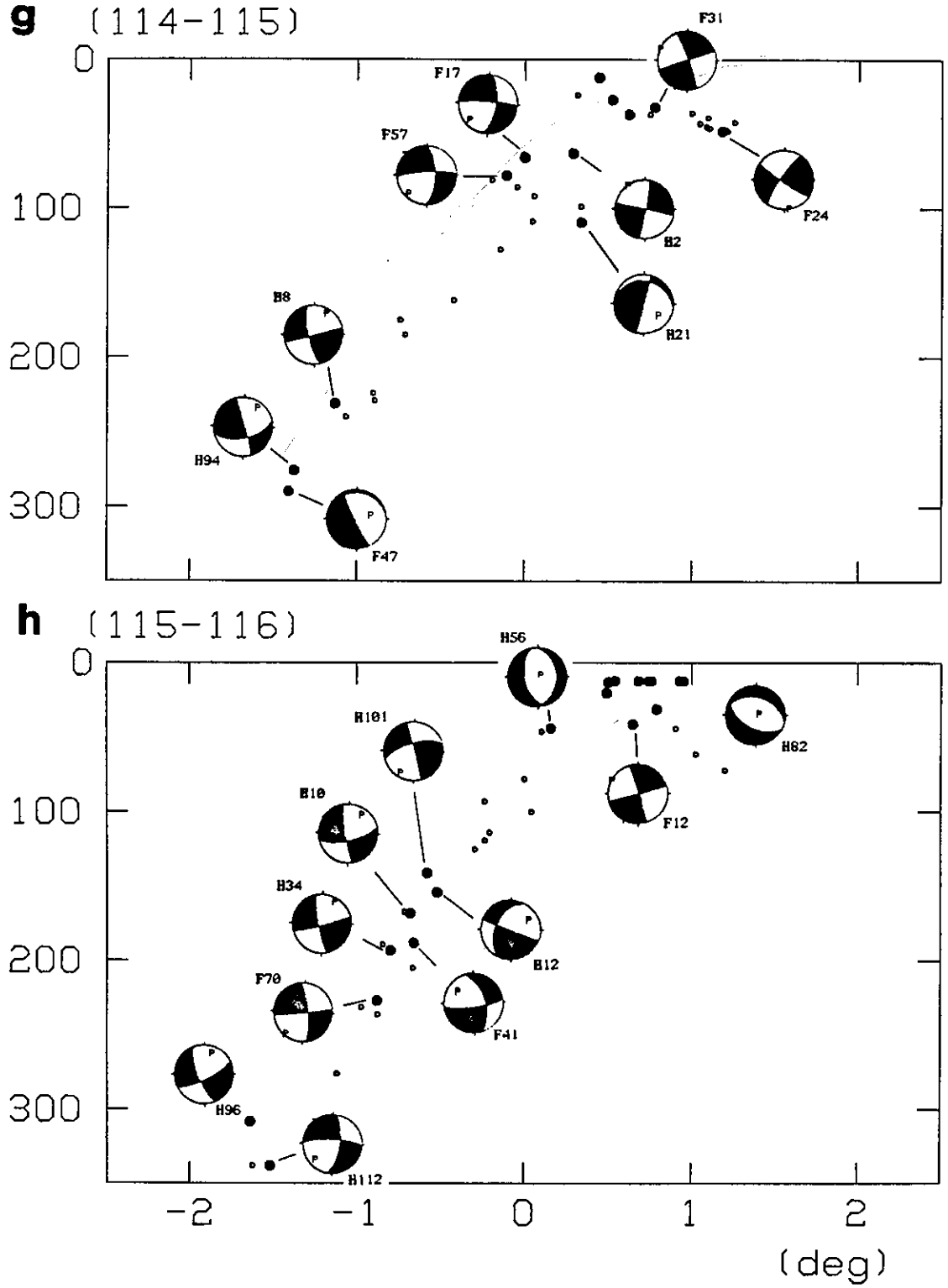

Figure 3.4. Cross sections perpendicular to the trench. (g) Azimuth between 114° – 115° and (h) 115° – 116°.

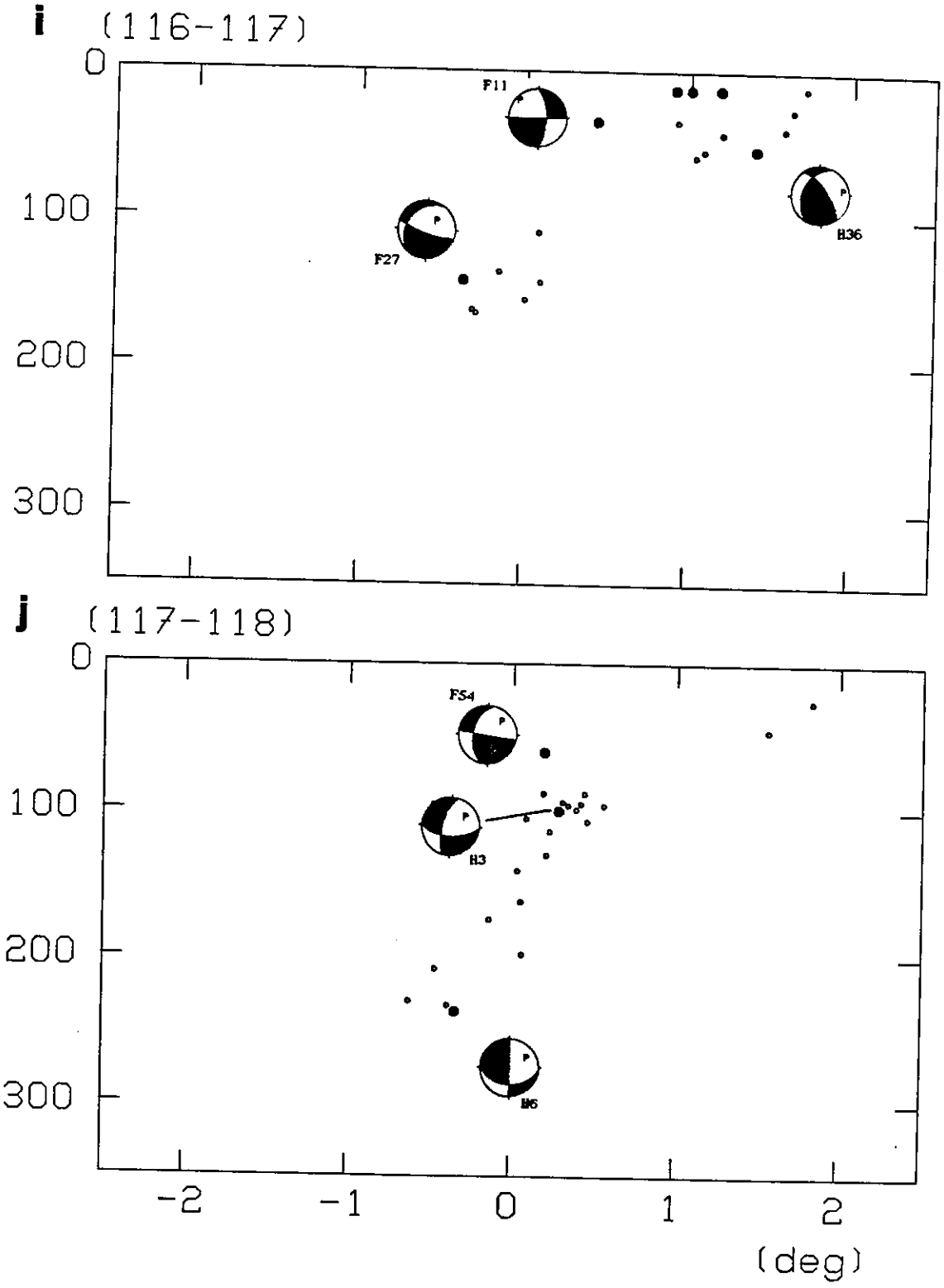

Figure 3.4. Cross sections perpendicular to the trench. (i) Azimuth between 116° – 117° and (j) 117° – 118°.

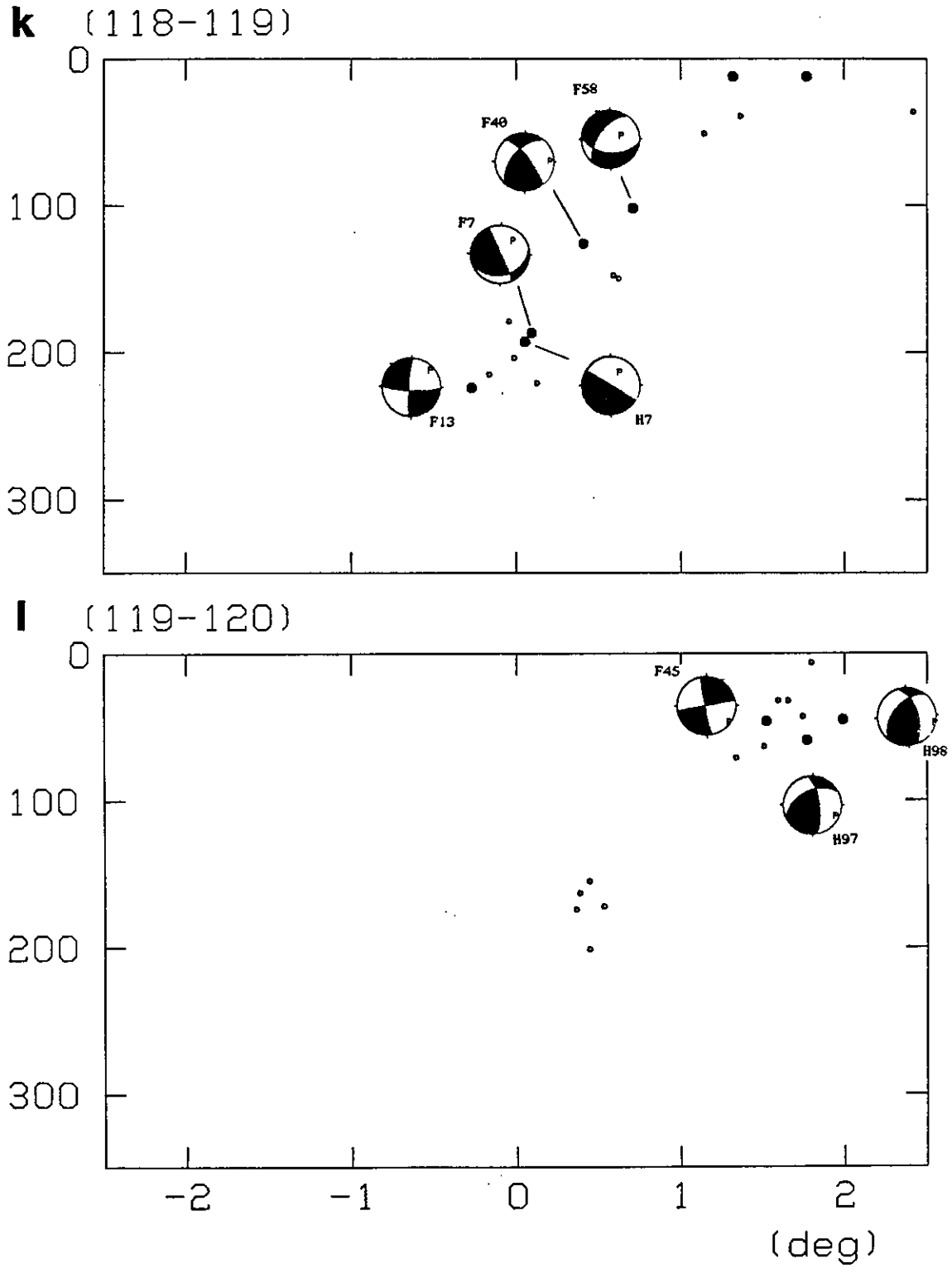

Figure 3.4. Cross sections perpendicular to the trench. (k) Azimuth between 118° – 119° and (l) 119° – 120°.

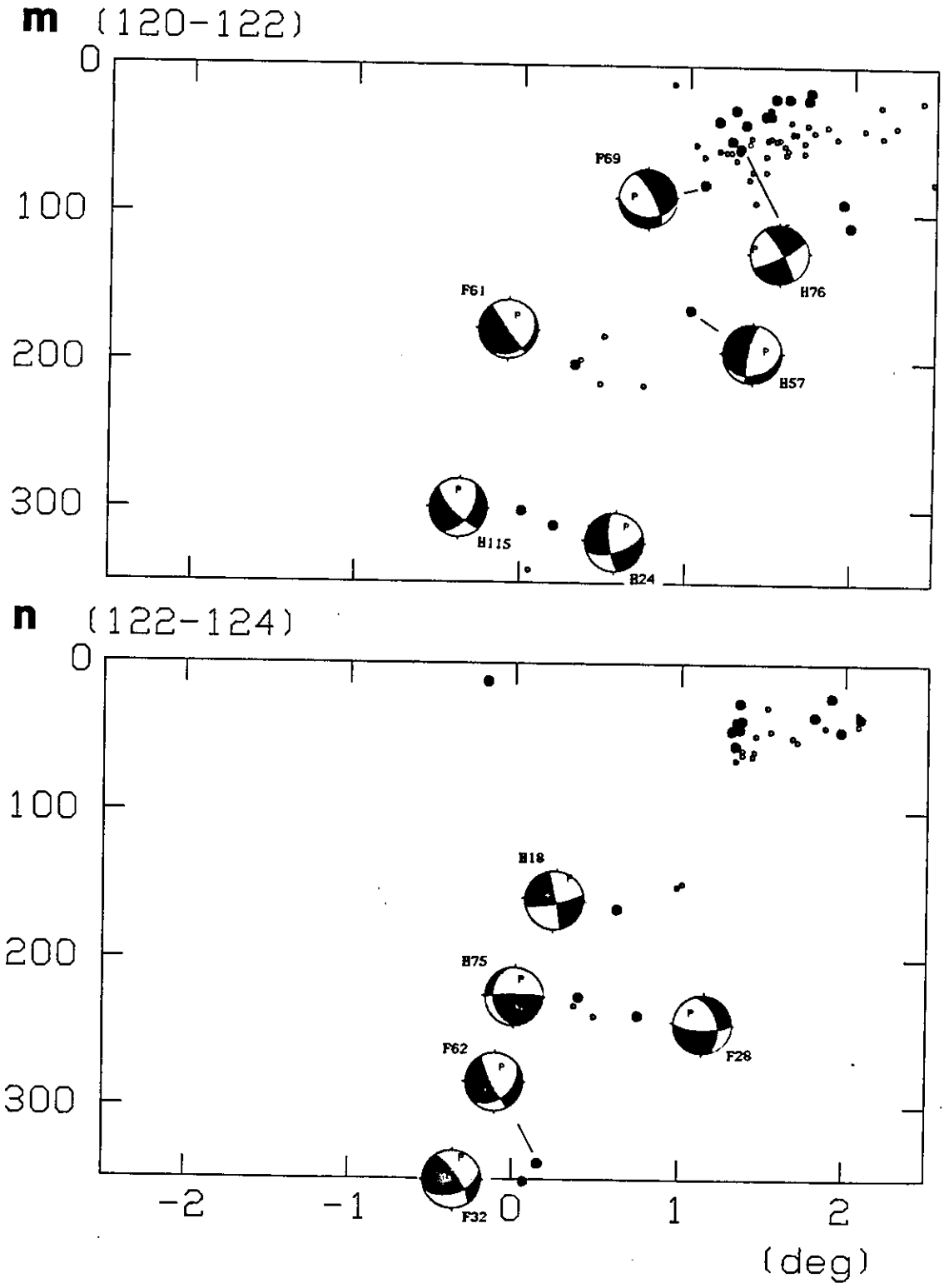

Figure 3.4. Cross sections perpendicular to the trench. (m) Azimuth between 120° - 122° and (n) 122° - 124°.

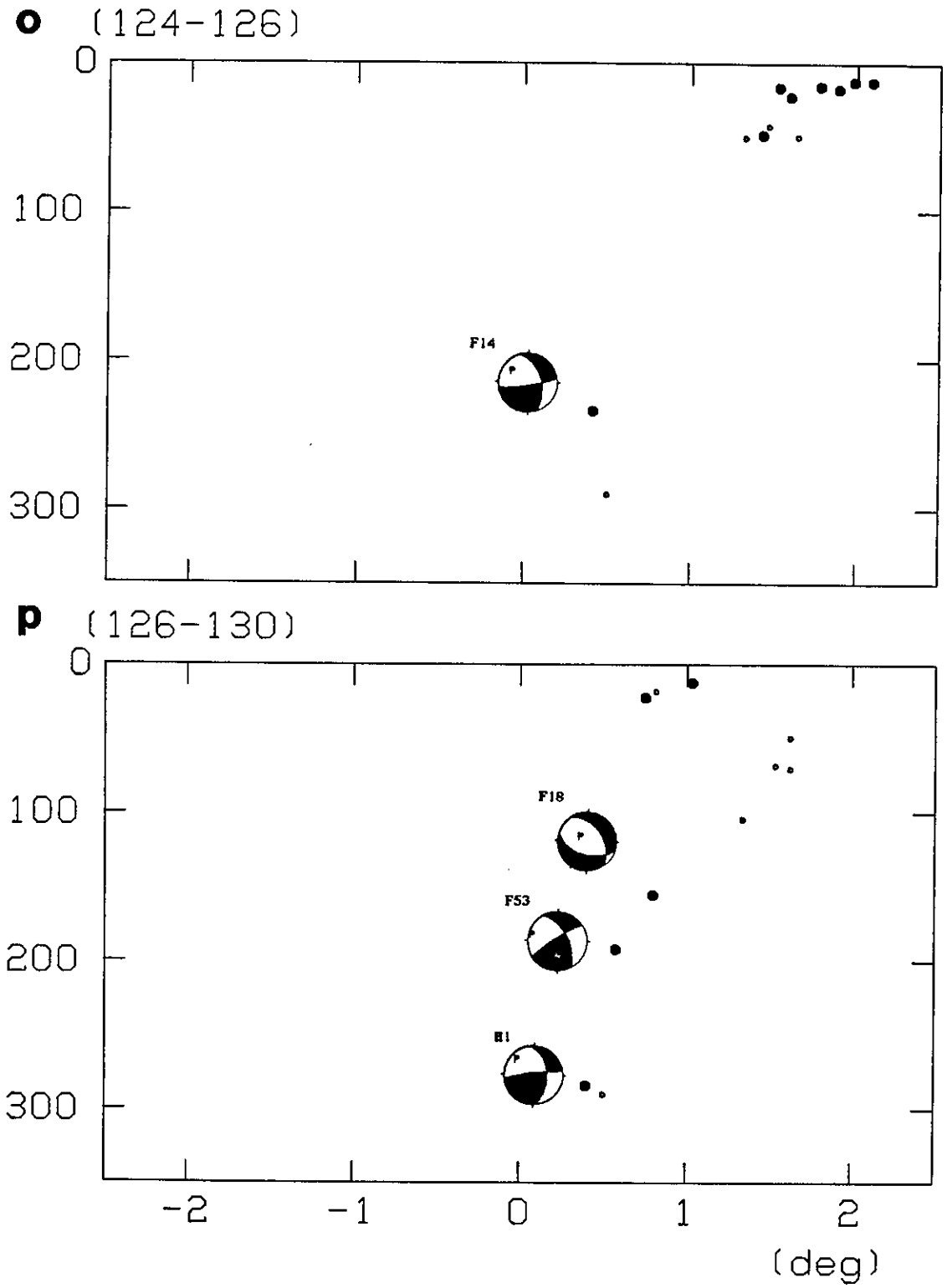

Figure 3.4. Cross sections perpendicular to the trench. (o) Azimuth between 124° – 126° and (p) 126° – 130°.

zone. These features suggest the possibility of a double seismic zone under the Tonga arc. Since finding down-dip tensional events is the key to identifying a double seismic zone in this area, where many down-dip compressional events have already been identified, we first examine these newly identified down-dip tensional events.

Down-dip Tensional Events

The difficulties for identifying shallow (<70 km) down-dip tensional events come from the fact that their focal mechanisms are similar to those of shallow angle thrust faulting events, which are very common in subduction zones, and that the reported depth estimates are not reliable for this depth range. For example, comparing first motion P-wave waveforms, Seno and Kroeger (1983) found that most of the events that were previously thought to be normal faulting between the Japan trench and the double seismic zone, are actually shallow angle thrust events. Therefore it is important to analyze waveforms of those shallow events.

The Harvard catalogue contains three shallow (~ 60km) down-dip tensional events, H2 (depth=61km), H26 (57km), and H49 (70km). Since all the surface reflections are automatically included in the inversion process, their focal depth estimates are reliable except for the shallowest events (Dziewonski et al., 1983). In Figure 3.5, the depth of the event H26 is checked by comparing first motion of WWSSN long period records and synthetic seismograms at some stations. Synthetic seismograms are calculated by using the program developed by Kroeger and Geller (1985). PREM (Dziewonski and Anderson, 1981) was used for the structure and the source was located at a depth of 60km. The early part of the seismogram is best fitted by h=60km and the later part by a slightly greater depth, suggesting that the shear wave velocity structure in this area is slightly slower than the average value. This supports the reliability of the depth estimates of CMT solution (see also Appendix E) and confirms that this event is an intra-plate down-dip tensional event.

The depth of the event H2 (June 22, 1977) is controversial (Giardini, 1984). Although the CMT solution gives the depth of 61km, the solution obtained just from body wave converges to 130 km depth (Giardini, 1984). Aftershock distribution suggests that the rupture extended down to a depth of 166 km (Silver and Jordan, 1983). From pP-P readings, Talandier and Okal (1979) estimated the focal depth to be shallower than 50 km. The generation of tsunamis indicates that the rupture reached the surface and the excitation of overtones of normal modes suggests the source has to be deeper than 100 km (Okal, 1984, personal communication). The rupture process seems to be very complicated, but at least there must be a major rupture

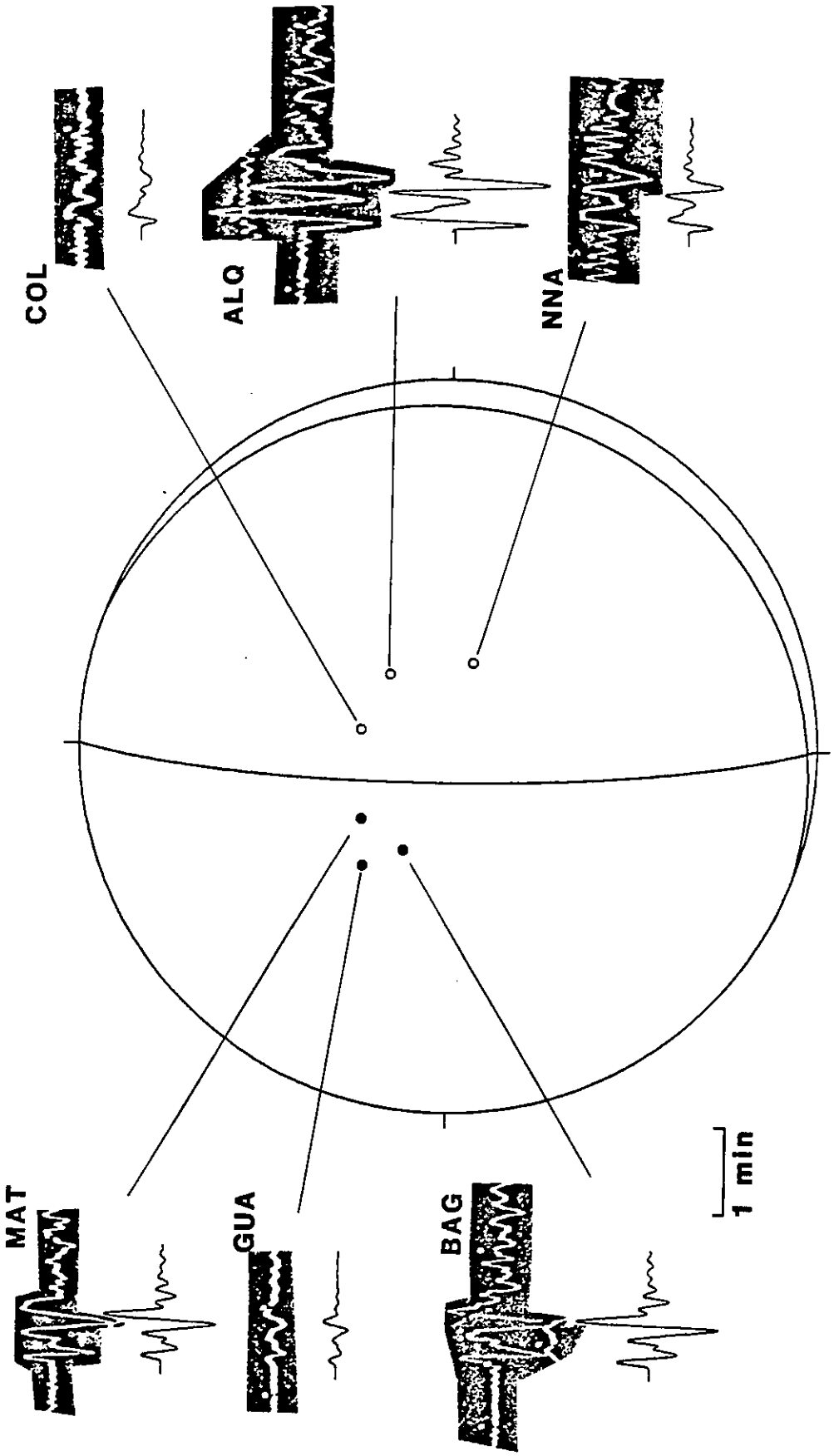

Figure 3.5. Synthetic seismograms are compared with data to check the depth of event H26.

extending deeper than the depth give by the CMT solution. Although the CMT depth is used here, it probably gives the shallowest estimate of this large normal faulting event ($M_o = 1.4 \times 10^{28}$ *dyne* $\cdot$ *cm*).

Search for a Double Seismic Zone

The presence of the above mentioned shallow (~ 60 km) down-dip tensional events and two deeper down-dip tensional events (F41 and F72) shows that there are down-dip tensional events in this region, where down-dip compressional stress had been thought to dominate the whole slab and that more likely these two different kinds of earthquakes make up a double seismic zone. Although all the events for which focal mechanism can be determined have been already studied, there are still several more earthquakes for which, by using P-wave first motion and S-wave polarization of WWSSN records, it is possible to determine focal mechanism types.

Figure 3.6 shows the lower hemisphere of the focal sphere of the events for which the type of mechanism can be determined. Large and small circles represent P-wave first motion data from long and short period WWSSN seismograms, respectively. Events T1, T2, and T3 are classified as down-dip tensional type and events C1, C2, C3, C4, and C5 are classified as down-dip compressional type.

Figure 3.7 summarizes all the results. The closed circle and open circle denote down-dip compressional events and down-dip tensional events, respectively. The smaller circles denote the events for which the type of the focal mechanisms are determined. It is clear that all the compressional events are consistently located above all the tensional events and they constitute a double seismic zone.

Relocation

Relative errors in routine epicentral estimates (e.g., ISC, PDE) are believed to be much smaller than errors in absolute coordinates (e.g., depth). It is, however, not appropriate to use the reported standard deviations as true values of the relative errors in the epicentral parameters. This is because the set of stations used to locate each event is different and because errors due to the differences between the assumed earth structure and the real structure enter

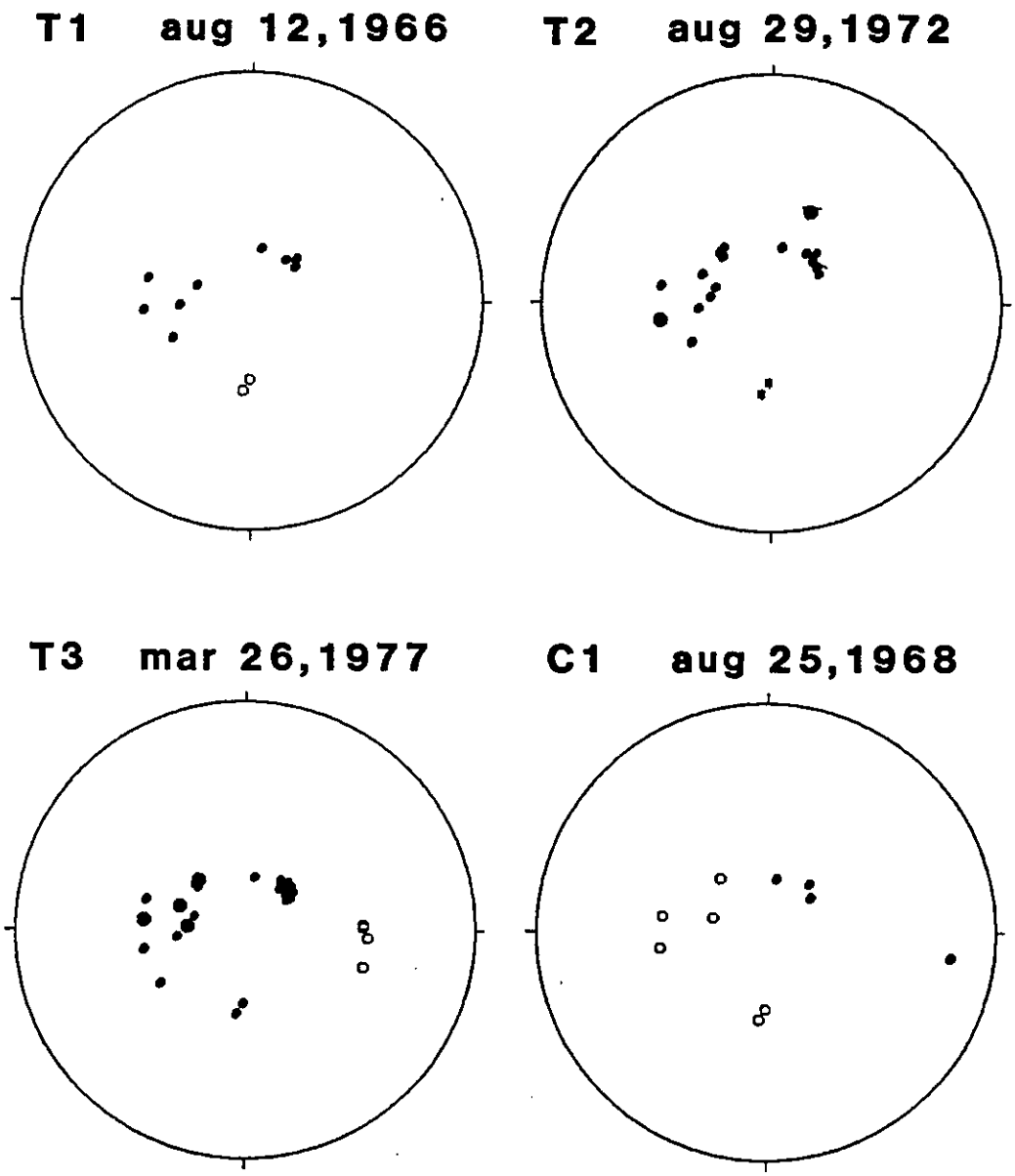

Figure 3.6. Events for which only the type of focal mechanism can be determined (Table C.5). First motion data from long and short period WWSSN records are plotted on the focal sphere. The large and small circles correspond to long and short period data respectively.

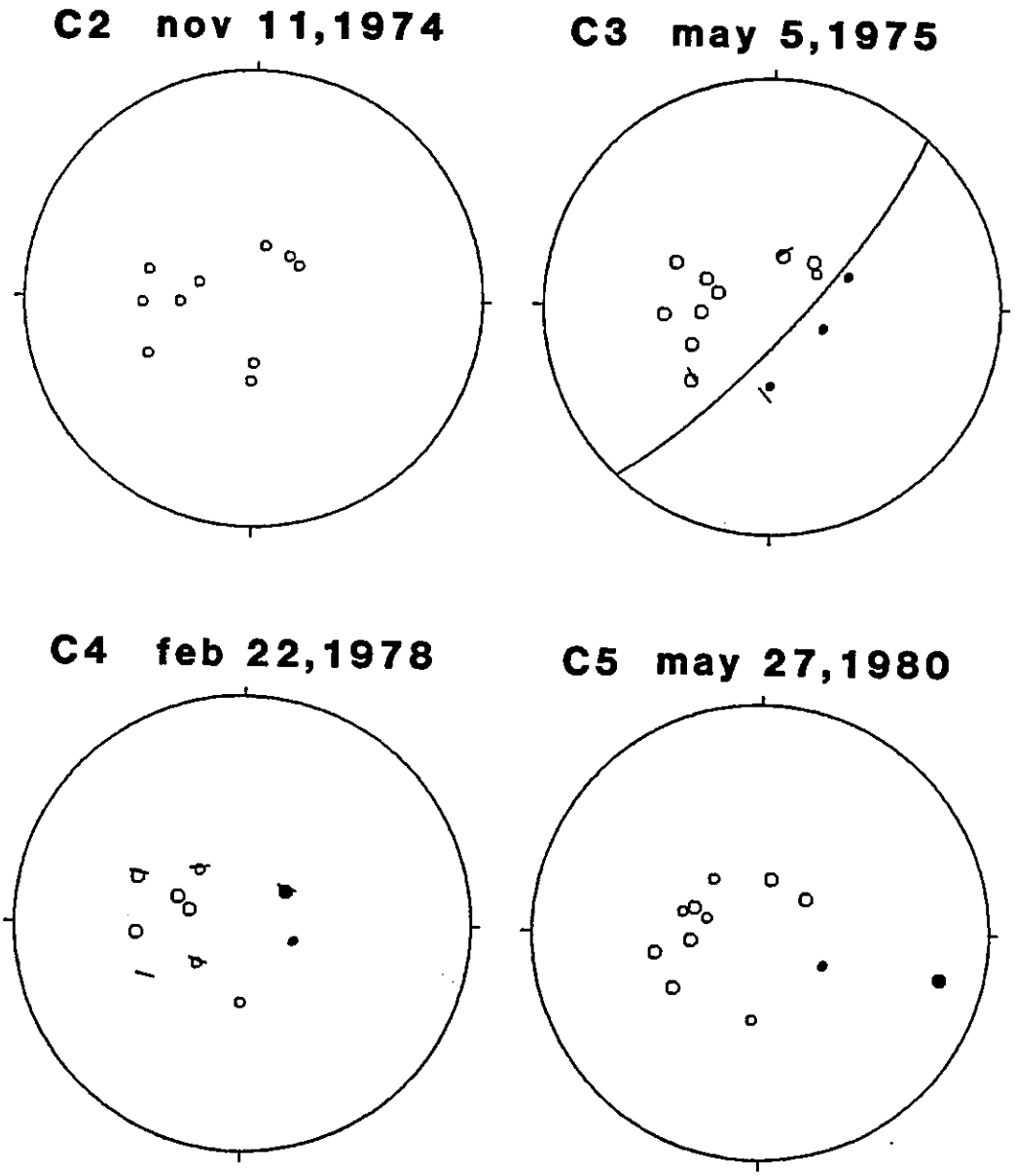

Figure 3.6. continued.

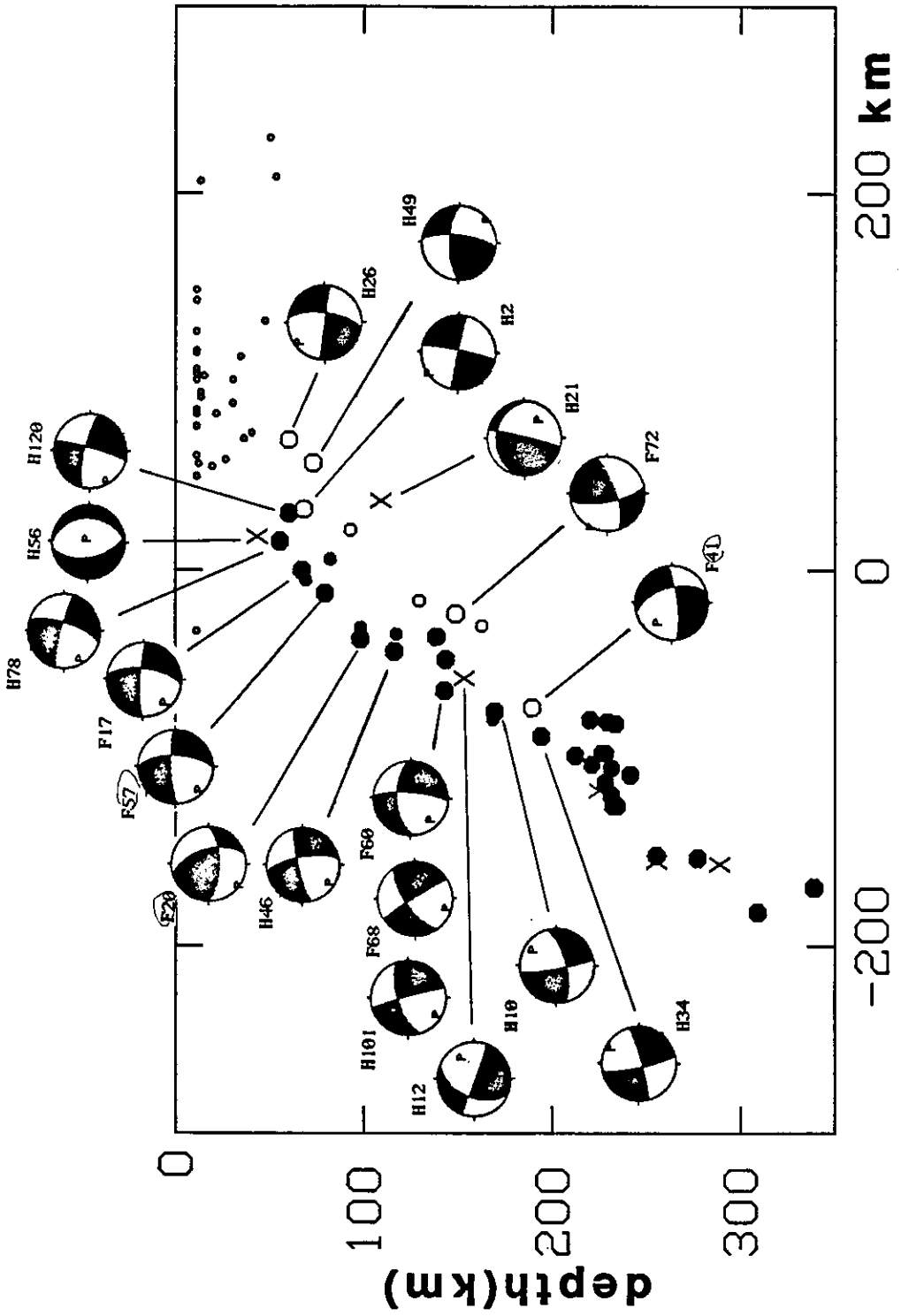

Figure 3.7. All the events between azimuth 109° and 116°, for which either the focal mechanism or type of mechanism is available. Note that events with down-dip compressional type are consistently located above the events of down-dip tensional type, suggesting the existence of a double seismic zone.

into the location process differently from station to station and event to event.

In order to investigate the possibility that the separation of the two seismic zones seen in Figure 3.7 is fortuitous, a relative relocation of the events is performed. The result below supports the presence of the double seismic zone.

Data

Earthquakes are selected from the ISC bulletin from 1971 to 1979 with the following conditions: (1) depths between 60 km and 200 km constrained by pP-P phase; (2) more than 30 P arrival observations; and (3) azimuth between 107° and 117°.

The first condition assures that the least well constrained parameter is constrained by pP-P time. The estimates of station residuals will therefore be more reliable than those obtained without depth constraints. The second criterion is needed to obtain reliable statistical error estimates. In total, 46 earthquakes were selected, including thirteen events for which either focal mechanism or focal mechanism type is determined.

Relocation Procedure

The relocation procedure is similar to those done by Vieth (1974) and Samowitz and Forsyth (1981). The purpose is, however, slightly different. The purpose here, as mentioned above, is to obtain proper relative error estimates of epicentral parameters, so that the apparent separation of the two seismic zones can be tested. Detail of the relocation is given in Appendix D and only a brief description is given here.

Only the P-wave arrival times reported at station distances between 30° and 100° are used for relocation. There are 440 stations in total. For the first step, all 46 events are relocated with the depths fixed by the pP-P depths. ISC locations are used as the starting guesses. After the first step, the stations which have arrivals from more than 10 earthquakes are selected. There are 113 stations left at this stage. The travel time corrections for these stations are determined by least square fit of the residuals to a linear function of distance between the stations and earthquakes. Some of the examples of the station residuals and the travel time correction are shown in Figure 3.8.

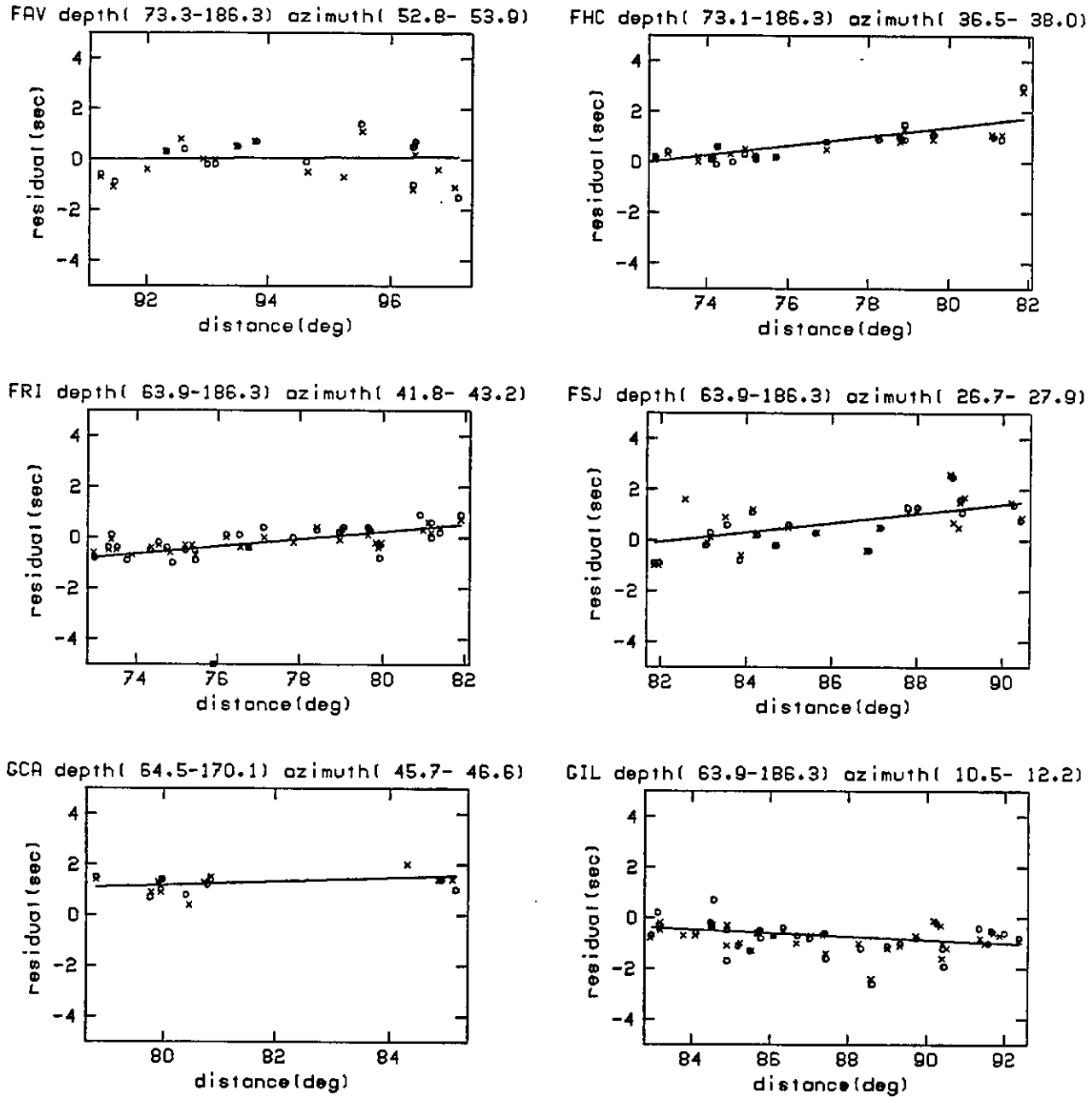

Figure 3.8. Examples of station arrival time residuals and the distance dependent station travel time corrections. Open circles and crosses denote residuals after the first and the second step of the relocation, respectively. Solid straight line is the travel time correction for the station, estimated from the open circles by a least square method.

For the second step, travel times are first adjusted by using the travel time corrections estimated in the first step. Relocation was then performed for each event separately using only the arrivals from those 113 stations. Each station was weighted inversely proportionally to its residual variance estimated in the previous iteration. Although this procedure can be repeated until convergence, it was stopped at the second iteration. Further iteration does not change error estimates significantly.

Result

Figure 3.9 compares the results of relocation at each step. After the second step, Figure 3.9c clearly shows the separation of the two zones. The horizontal bars denote the estimated 90% confidence intervals from student-t statistics and the distance of separation exceeds error bars significantly. In Figure 3.9d, the ten events for which mechanism types are assigned are plotted together with other relocated events. Both down-dip compression and tension events are located consistently on the upper and the lower plane of the double seismic zone, respectively. The error estimate here does not include the error introduced by the fact that all the earthquakes (located in a 700 km long zone parallel to the trench) are plotted on the same cross section. Therefore what is important is that the down-dip compressional events are still located consistently above the down-dip tensional events even after the relocation.

The two zones becomes closer after the relocation, but this is expected for the following reason. The effect of the variation of thermal structure within the slab (e.g., Sleep, 1973) on body wave travel times is not considered in the relocation process (Engdahl and Fujita, 1981; Fujita et al, 1982). As pointed out by Engdahl and Fujita (1981) this effect can be as significant as the station correction itself. However, ignoring this effect tends to move the locations of the events of the lower plane (i.e., down-dip tensional) to the dip direction of the slab relative to the events of the upper plane (see Figure 10 of Fujita et. al., 1982). When the depth is constrained in the location process, this causes the horizontal migration of events in the lower plane toward the upper plane. If the two planes remain separated after the relocation, it indicates the separation of two planes is actually greater than that shown.

In Figures 3.10 a, b, and c, the cross sections of the narrower (~ 300 km wide) section are plotted to show that the apparent separation of the two seismic zones cannot be attributed to the way the data are plotted.

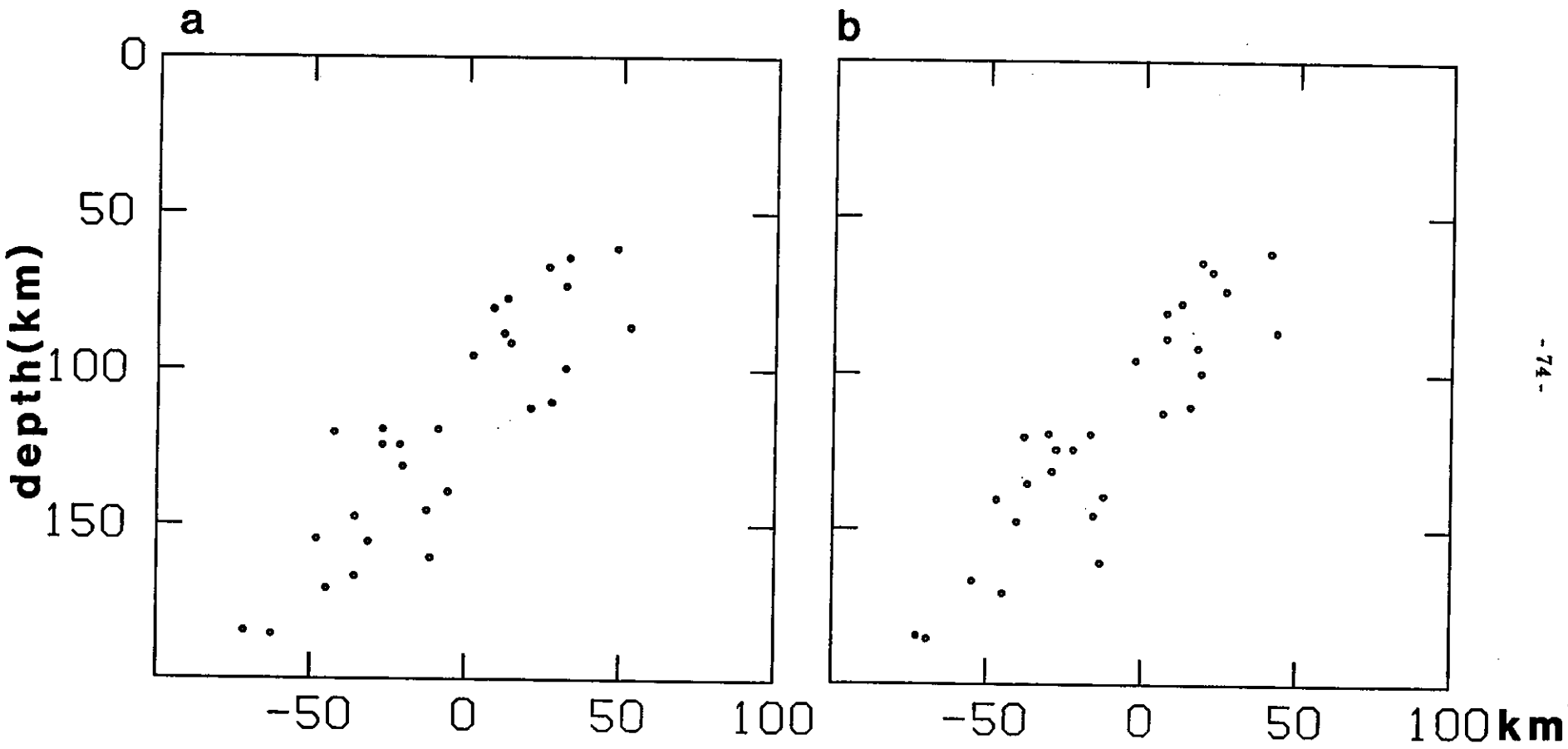

Figure 3.9. Results of relocation. (a) Original ISC location. (b) After the first iteration.

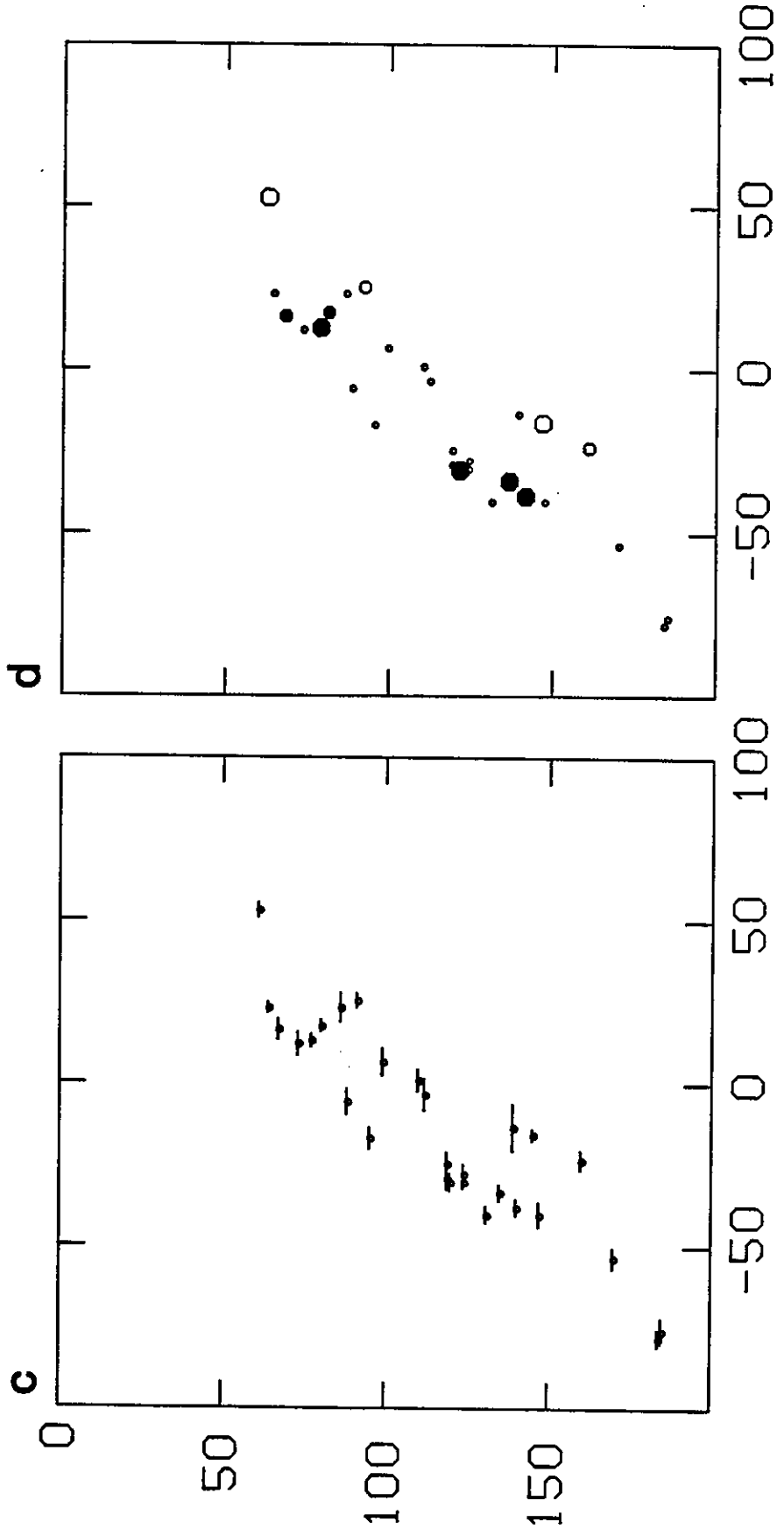

Figure 3.9. (c) After the second iteration. The horizontal bars denote 90% confidence intervals from student-t statistics. (d) The final result with focal mechanism types. Note that the down-dip compressional events are still located above the down-dip tensional type events.

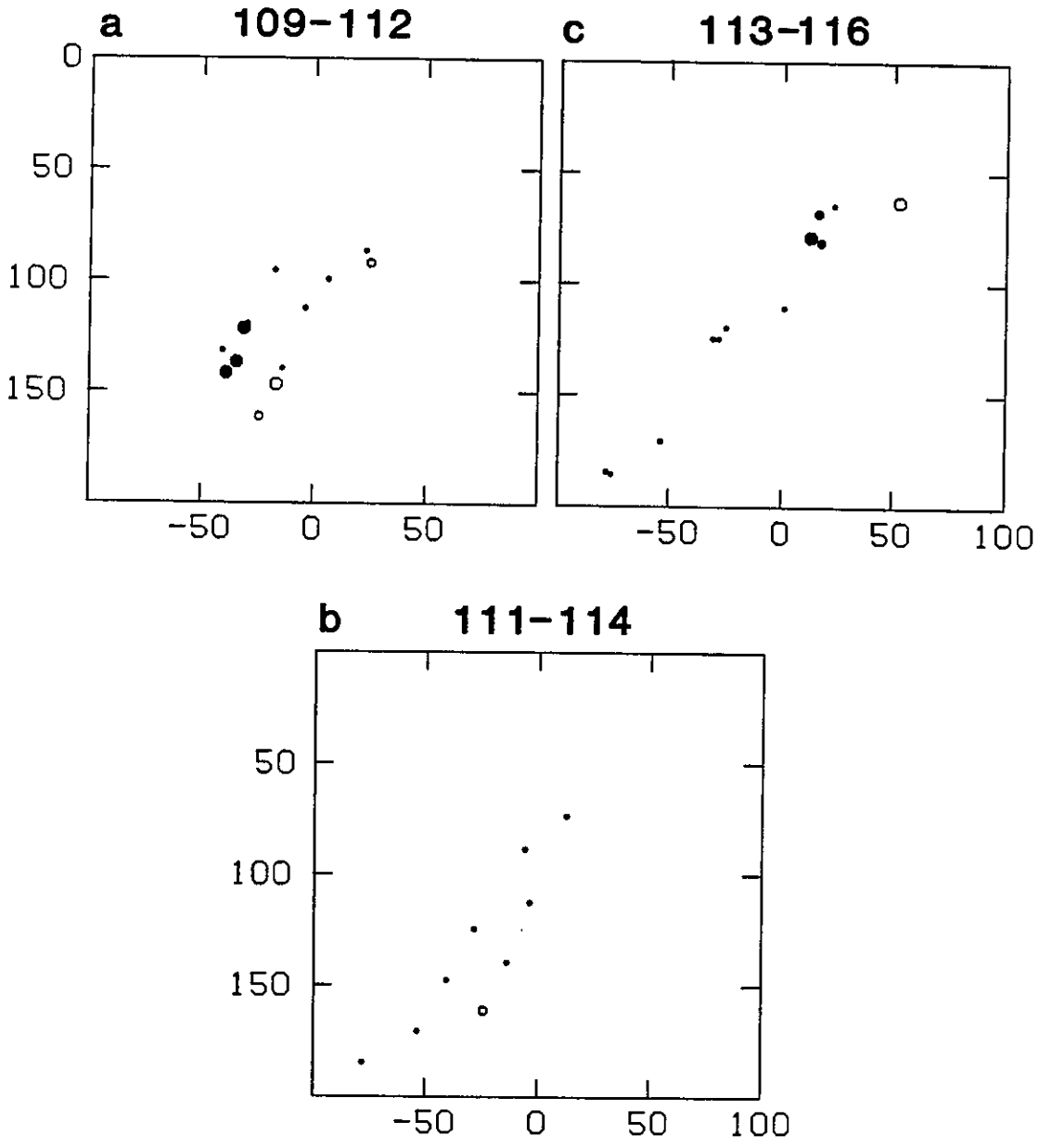

Figure 3.10. More results of the relocation. Cross sections between (a) azimuth 109° to 112°, (b) 111° - 114°, (c) 113°. Note that the down-dip compressional and the down-dip tensional events are still located in the upper and lower edge of the seismic zone in each cross section.

Discussion

Figures 3.11, 3.12, and 3.13 summarize the results of this chapter. Both the earthquake focal mechanisms and the results of the relocation in the previous section support the existence of the double seismic zone. The cross section parallel to the strike of the trench between azimuth 108° and 117° (Figure 3.11) shows some regional variation. Although the double seismic zone between azimuth 114° and 116° is unquestionable, there is a lack of down-dip tensional and down-dip compressional events in the region between azimuth 111.5° and 114°, and in the region between 110° and 111.5°, respectively. It is probably due to the sampling problem. If local network data in this area had been available, with which smaller events could be detected, both zones would probably have been seen. The temporal variation of seismicity due to the state of stress at the thrust zone can also cause similar effects, as shown in the previous chapter. What is important is that both down-dip tensional events and down-dip compressional events occur where they are expected to occur if there is a double seismic zone.

As noted earlier and seen in Figure 3.11, there are many down-dip compressional events directly beneath the double seismic zone. The deeper part of this slab is also known to be the most active of all the subduction zones in the world. (e.g., Giardini and Woodhouse, 1984). Thus, it is reasonable to think that no other slab has stronger support from below 200 km depth than the intermediate depth part of the slab in Tonga. Although there are more down-dip compressional events than down-dip tensional events, the presence of the double seismic zone in Tonga is clear. This suggests that in any currently observed subducting slab, compressional stress or strain (either due to inability of the slab to penetrate into the lower mantle, or the strong viscous resistance to the subduction in the mesosphere) transmitted from below 200 km depth cannot overprint completely and erase the preexisting stress feature of a double seismic zone.

The discovery of this double seismic zone, and the nature of deep earthquake activity beneath it, suggest that double seismic zones are a very common and persistent feature of subducting slabs and that there may be many other undiscovered double seismic zones in the other subduction zones. This will be discussed further in Chapter 5.

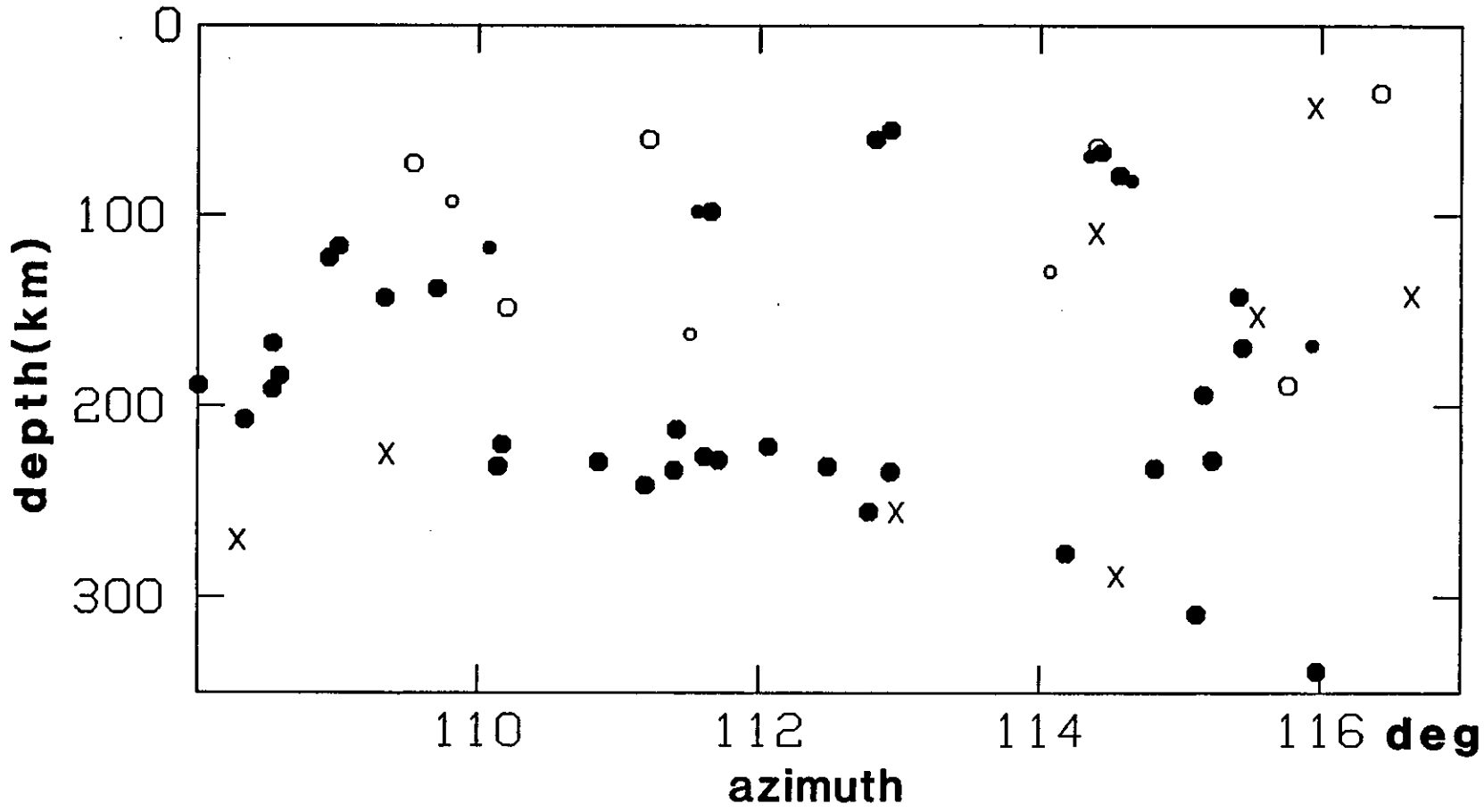

Figure 3.11. Cross section parallel to the strike of the trench. All the events for which either focal mechanisms (large mark) or focal mechanism types (smaller mark) are available are plotted. Earthquake location parameters are listed in Appendix C.

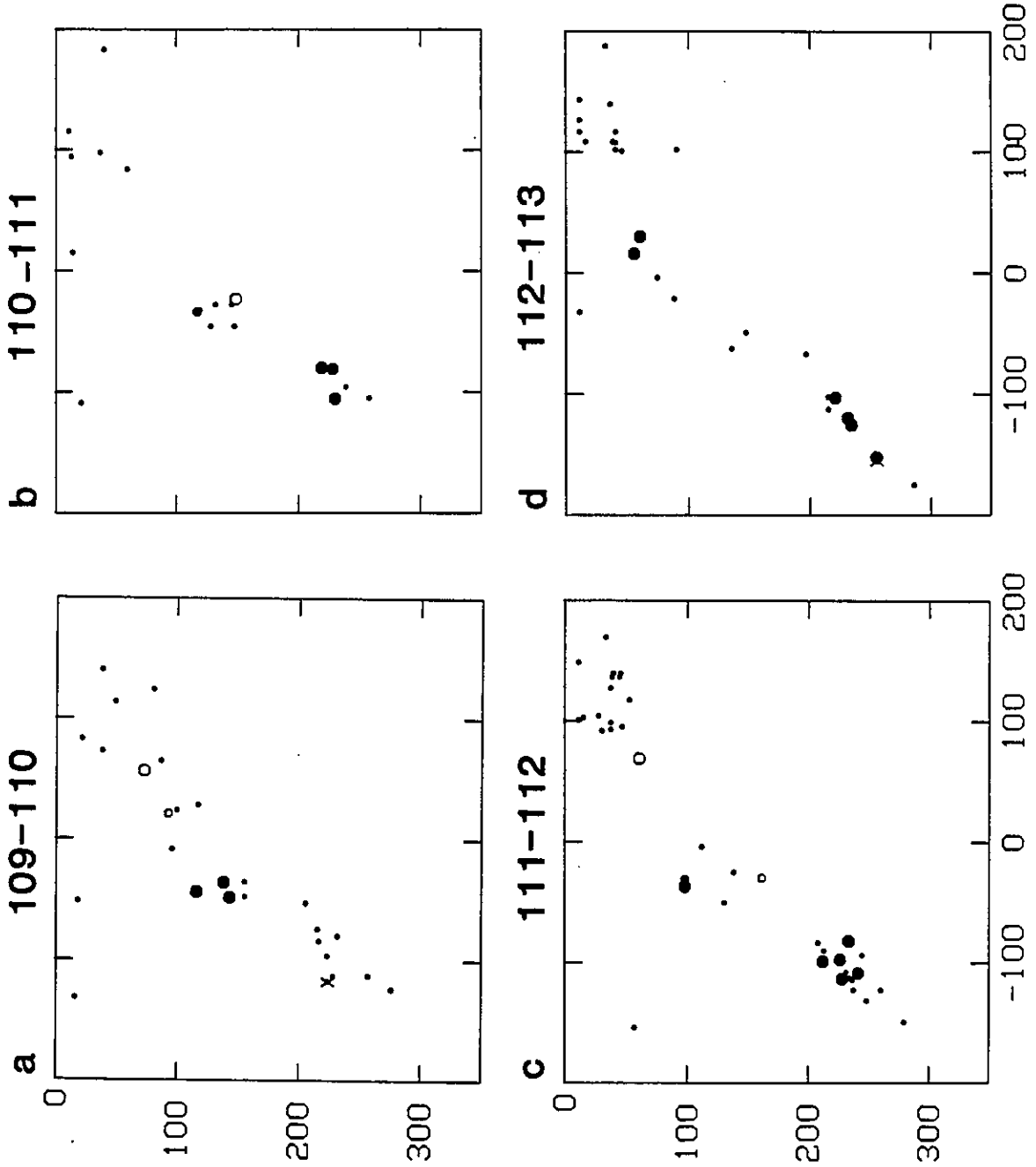

Figure 3.12. Cross sections perpendicular to the trench. The symbols are the same as in Figure 3.11. The dots are the depth constrained ISC events.

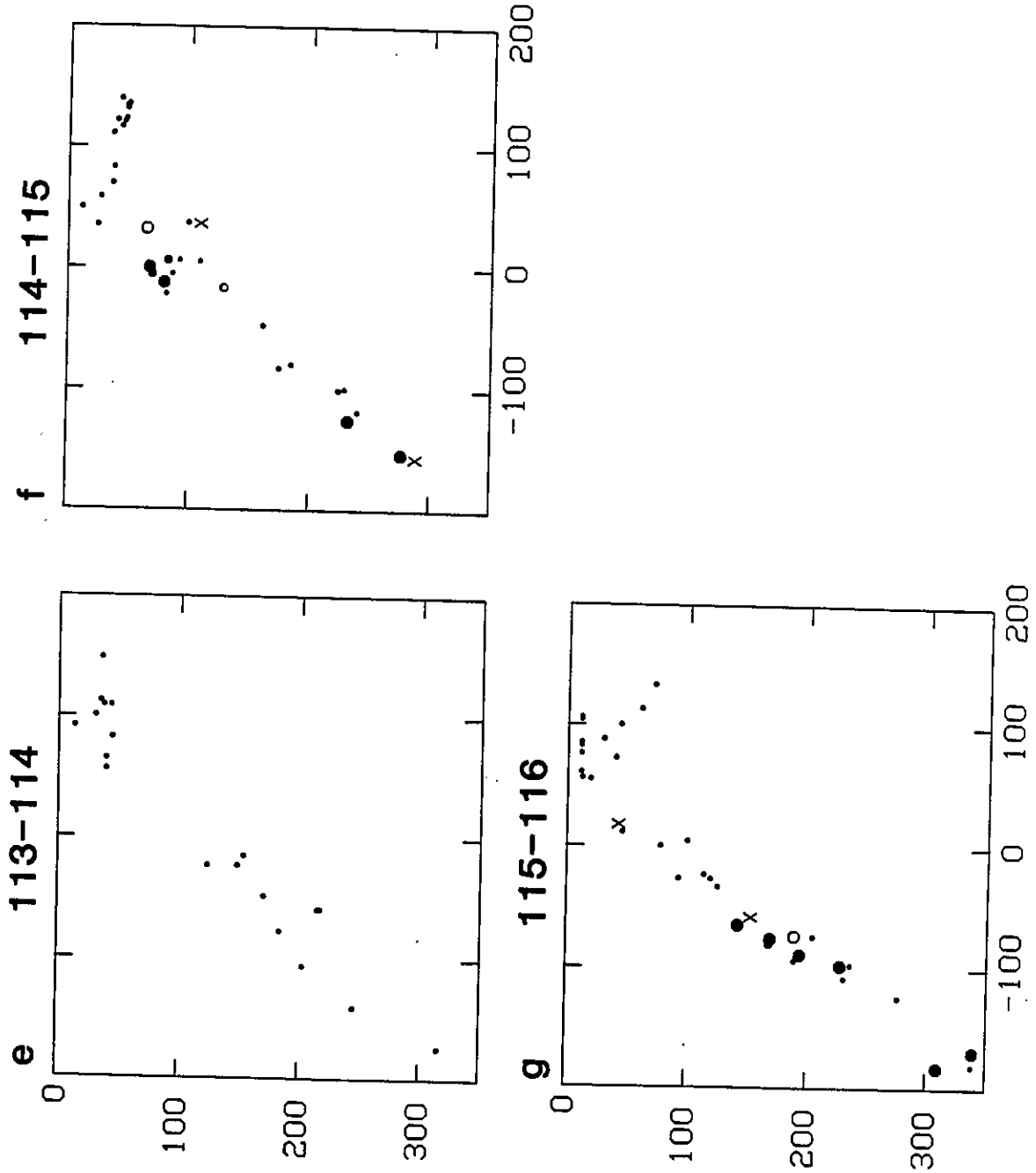

Figure 3.12. continued.

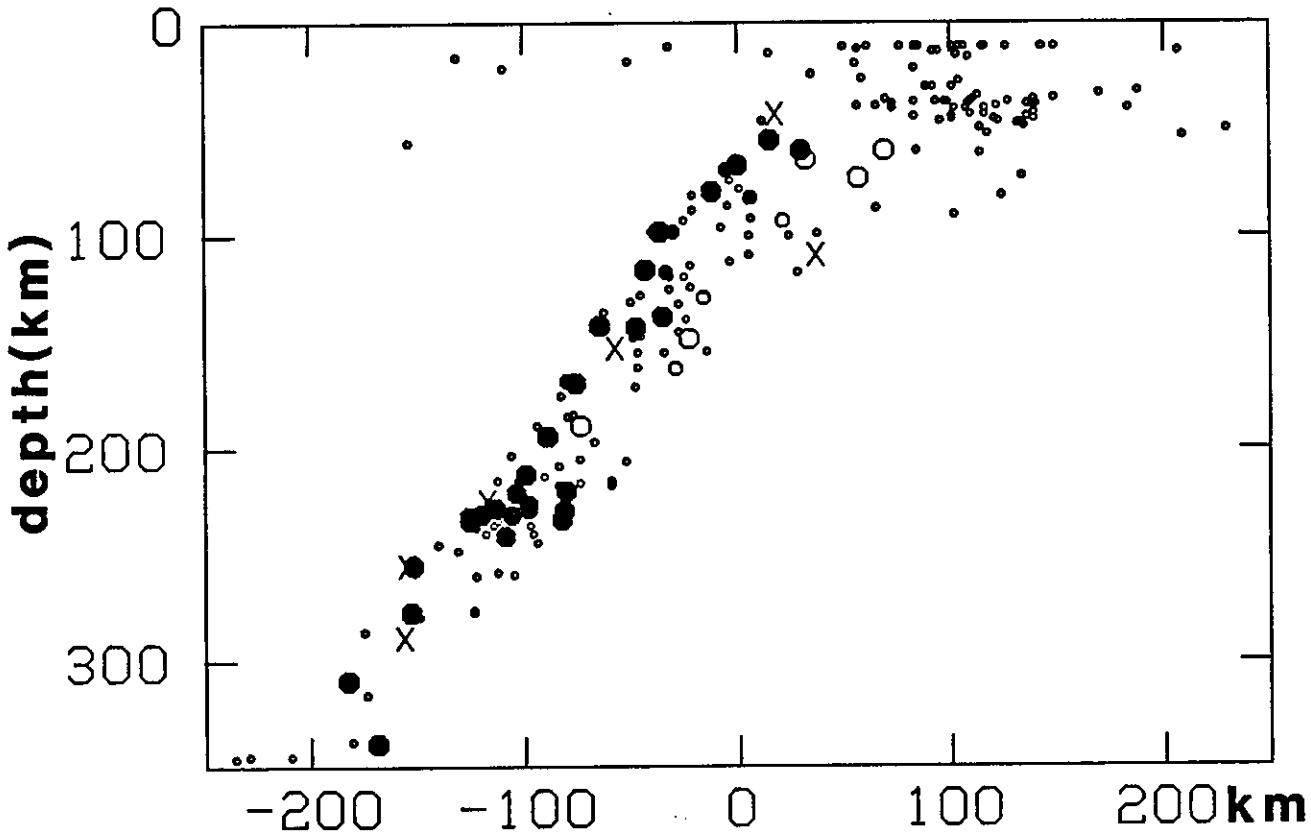

Figure 3.13. Cross section of the all the events between azimuth 109° and 116°. All the data in Figure 3.12 are plotted on a single cross section.

CHAPTER IV

ON THE ORIGIN OF DOUBLE SEISMIC ZONES

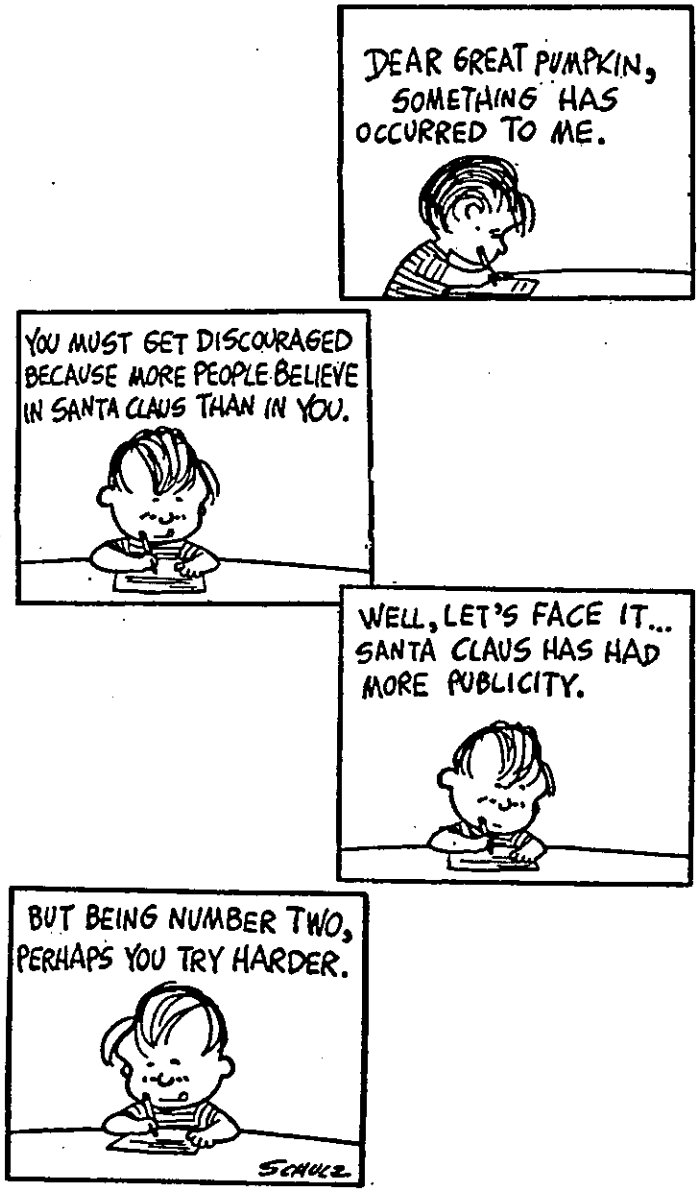

Introduction

Several mechanisms have been proposed for the origin of double seismic zones: stresses associated with phase changes (Veith, 1974), unbending of the slab (Engdahl and Scholz, 1977; Isacks and Barazangi, 1977; Tsukahara, 1977, 1980; Samowitz and Forsyth, 1981), sagging of the plate (Yoshii, 1977; Sleep, 1979), and thermo-elastic stresses (Goto and Hamaguchi, 1978, 1980; House and Jacob, 1982). In this chapter, by estimating the seismic strain rate from intermediate depth earthquakes and the geometrical unbending strain rate of the subducting slabs, I suggest that simple geometrical unbending of subducting slabs with brittle-plastic rheology (Tsukahara, 1980) is sufficient and most appropriate to explain the origin of double seismic zones. Also, by modeling the double seismic zone beneath Tohoku, Japan, I investigate what constraint the presence of a double seismic zone can place on the properties of the descending lithosphere.

Proposed Mechanisms

Phase Change

Veith (1974) rather qualitatively suggested that the olivine-spinel phase transition could cause tensional earthquakes within the slab after the transition. However, he did not particularly specify the cause of the compressional events in the upper plane. It is also hard to believe that the phase transition can be raised as shallow as 60 km depth. Thus, unless our current knowledge about this phase transition or the thermal state of the subducting slabs is completely wrong, it is unlikely that this can be the main cause of the double seismic zones, as suggested by Fujita and Kanamori (1981).

Sagging

Yoshii (1977) and Sleep (1979) proposed the 'sagging' of the subducted slab as a mechanism. In the sagging model, supported by the strength of the lithosphere at the top and by the high viscosity mesosphere from below, the slab sags in the low viscosity asthenosphere. Sleep (1979) further estimated the viscosity of the mesosphere using the presence of the double seismic zone as a constraint. However, the presence of the Tonga double seismic zone described

in this thesis seems to indicate that sagging cannot be the direct cause of the double seismic zone. The compressional strain transmitted from below the double seismic zone inferred from high deep earthquake activity (e.g., Giardini and Woodhouse, 1984) would probably overprint and erase any preexisting strain field solely due to sagging of the slab. As will be discussed later, sagging (or equivalently, the flow pressure normal to the dip of the slab at the base of the low viscosity zone; Yokokura, 1981) is one of the mechanisms that could unbend the subducting lithosphere.

Thermo-Elastic Stress

Goto and Hamaguchi (1978, 1980) and House and Jacob (1982) proposed the stress due to thermo-elasticity as the cause of double seismic zones. Although the stress distribution of their models seems to resemble that of double seismic zones and although they find stresses high enough to cause earthquakes, their treatments are essentially elastic. The strain rate expected from the thermal expansion of the slabs is 10^{-18}~ $10^{-17}s^{-1}$ (House and Jacob, 1982). As I will show later, this strain rate is a few orders of magnitude smaller than the unbending strain rate. It will be shown that even in the apparently straight portion of the slab, the strain rate can easily be on the order of $10^{-17}s^{-1}$~ $10^{-16}s^{-1}$. Therefore the thermo-elastic stress cannot be the main cause of the double seismic zone.

Geometrical Unbending

Engdahl and Scholz (1977), Isacks and Barazangi (1977), Tsukahara (1977, 1980), and Samowitz and Forsyth (1981) proposed unbending of the slab as the cause of double seismic zone. Although some of the earlier models are unrealistic and qualitative, I will show that an unbending model can readily explain the double seismic zone. Further, following Tsukahara's (1980) formulation, I will indicate that studies of mechanical properties of double seismic zones, which have not been seriously investigated compared to those of the bending of the oceanic plate in the outer rise regions (e.g, Goetze and Evans, 1979; Chapple and Forsyth, 1979; Forsyth, 1980), can give some new independent information about the rheological and thermal properties of the oceanic lithosphere. The advantages of studying double seismic zones are that we can better study the seismicity in some areas (e.g., beneath Tohoku, Japan) than in bending regions, and that strain rates are reasonably well constrained.

Strain Rates within the Subducting Slabs

In regions such as subduction zones, where large scale deformation is taking place rapidly, what properly describes the state of the deformation is the strain rate, rather than the stress. In Figure 4.1, the principal stress (and strain) axes of the earthquakes which make up the Tonga double seismic zone are plotted with respect to the direction of the dip of the slab. As expected from the presence of the double seismic zone, except for a few events, either the compression or the tension axis of each earthquake is located near the dip direction of the slab. Furthermore, the second axes are clustered around a direction perpendicular to the slab. This suggests that a plane strain type deformation is occurring within the vertical plane perpendicular to the strike of the trench. A similar conclusion can be drawn from Appendix B of Fujita and Kanamori (1981), for subduction zones where double seismic zones are known to exist.

In this section, assuming that the deformation is occurring in a two dimensional manner, order of magnitude estimate of the seismic strain rates and the geometrical unbending strain rates of the intermediate depth part of the slabs are made.

Seismic Strain Rate

Following Richter (1979), the rate of the seismic moment release of intermediate depth (70 km<depth<150 km) earthquakes is estimated from events with m_b between 5.0 and 5.5, for which the seismic catalog (PDE) is assumed to be relatively complete (see Figure 4.2). The depth range is chosen to avoid possible bias due to errors in depth estimates (particularly for shallow thrusting events). For events smaller than 5.0, there is a detection problem and for the events larger than 5.5, there is a sampling problem (due to the short time window) and a problem due to the saturation of the body-wave magnitude scale (Geller, 1976; Richter, 1979).

As the empirical relation between seismic moment (M_o) and body wave magnitude (m_b) for intermediate depth earthquakes (50 km -200 km), I use the following equation,

$$\log M_{o(m_b)}=11+2.4m_b, \tag{4.1}$$

where M_o is given in units of dyne·cm. This is obtained rather arbitrarily within the error bar of the least square fit to moment-magnitude relation of the CMT solutions and it slightly underestimates moments from magnitudes (Figure 4.3). Abe (1982) obtained

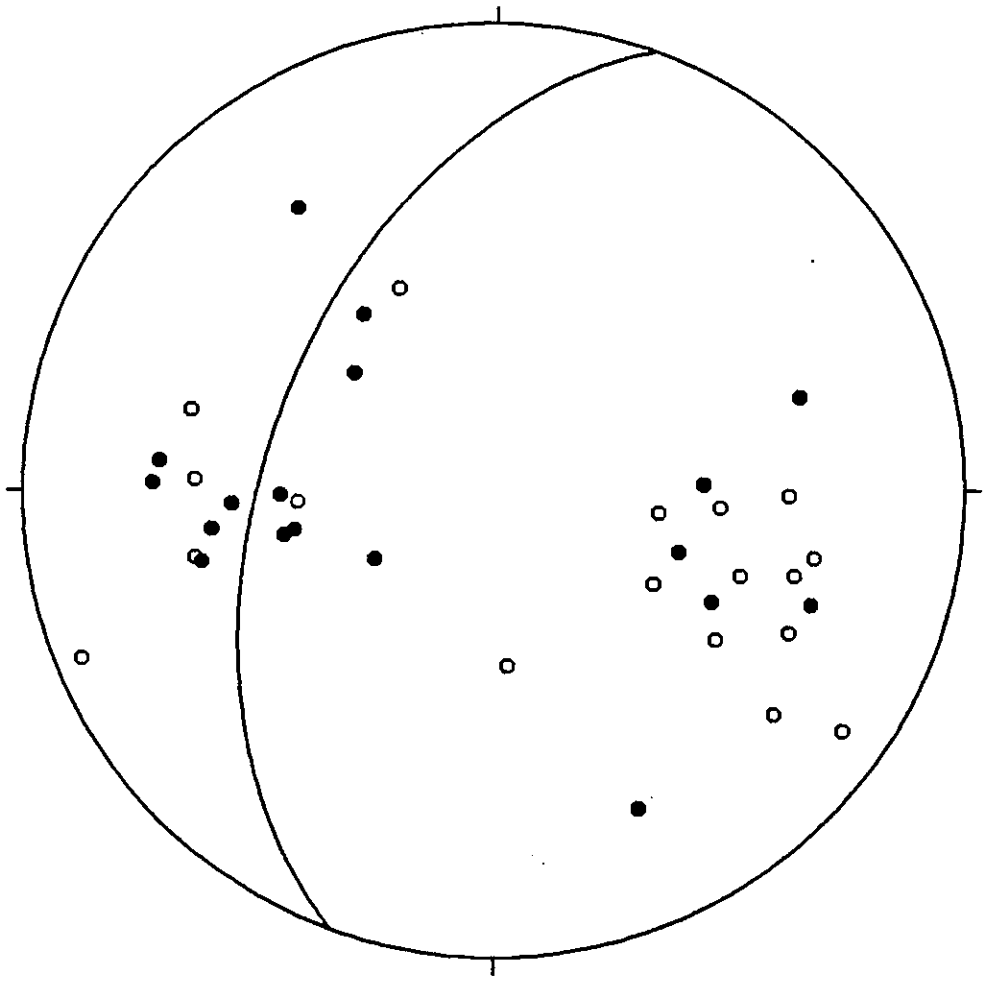

Figure 4.1. The principal stress axes of the events which make up the Tonga double seismic zone are plotted on a lower hemisphere projection. Closed and open circles denote compression and tension axes, respectively. The great circle corresponds to the dip of the slab.

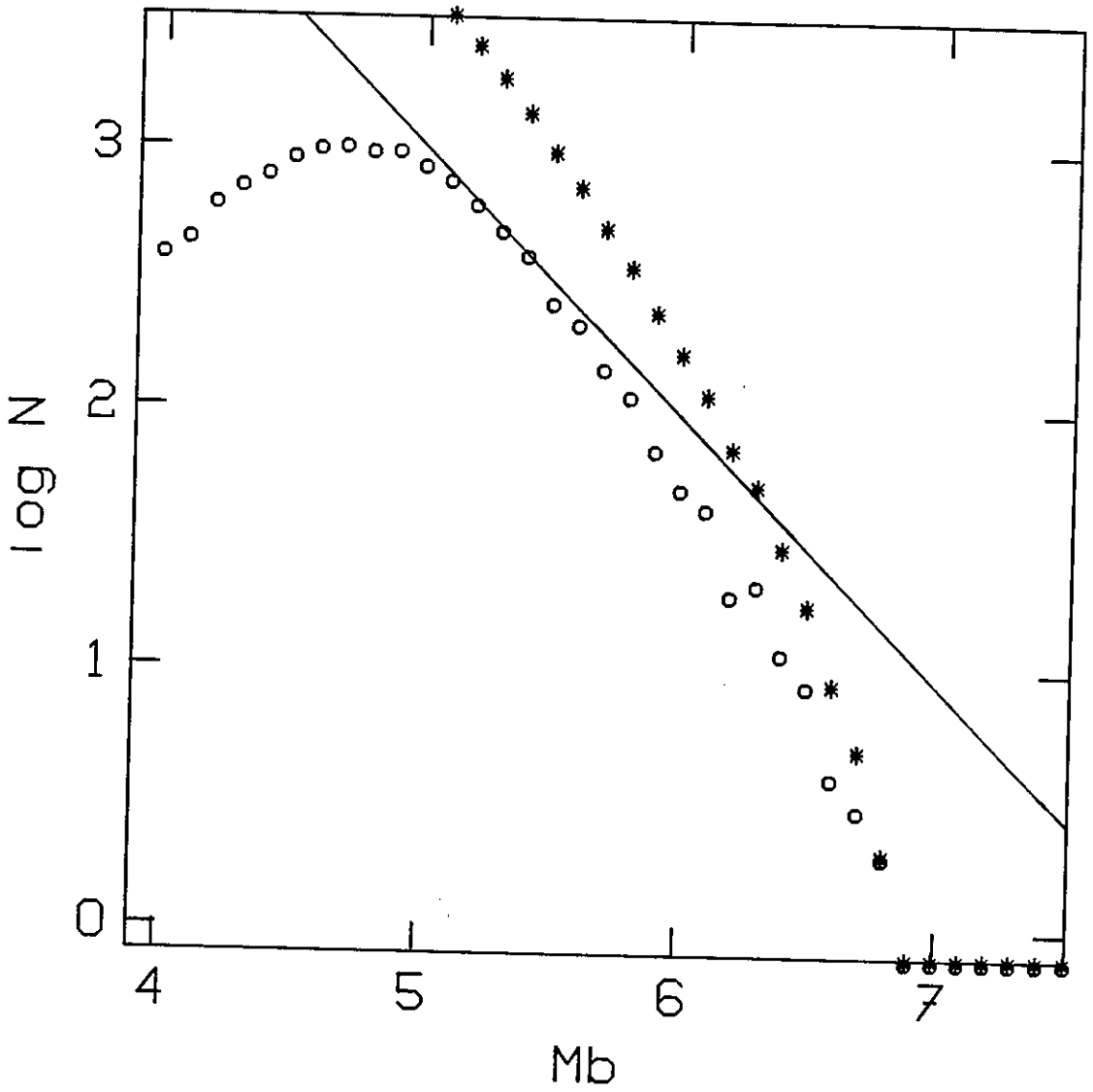

Figure 4.2. Frequency-magnitude relation for all the earthquakes between depths 70 km~ 150 km. Data are from PDE from 1964 to 1983. The circles are the number of events with m_b in 0.1 unit range($N_{(m_b)}$). Asterisks represent total number of earthquakes with m_b greater than the indicated value. The line has a slope of 1. Note the departure from this line above m_b ~ 5.5 and below 5.0, suggesting the saturation of the m_b scale and the incompleteness of data, respectively.

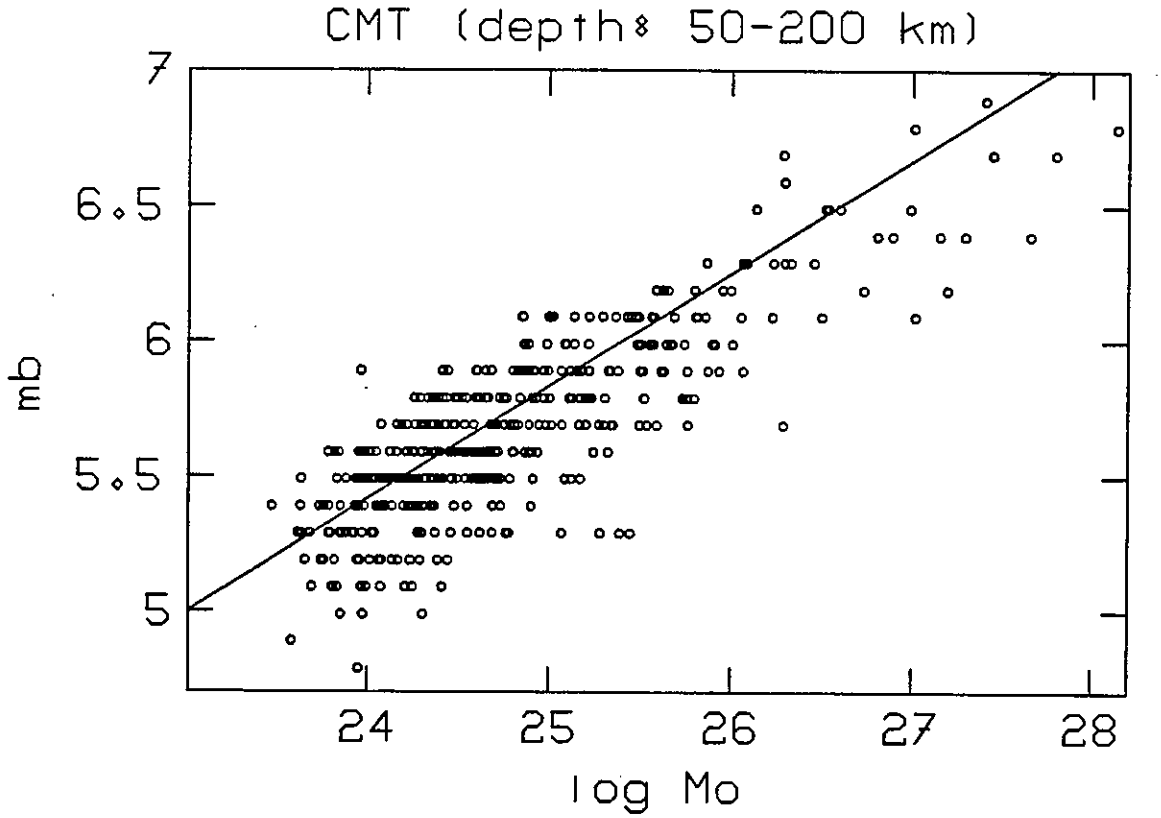

Figure 4.3. Moment versus magnitude relation of CMT solution (depth 50 - 200 km). The line corresponds to equation (4.1). Unit of seismic moment is $dyne \cdot cm$. Magnitude obtained from PDE is converted to a moment using the line.

$\log M_o = 10 + 2.4 m_B$, where m_B is body wave magnitude measured from amplitudes in the period range 3~ 15 sec. On the average, m_B is larger than m_b by ~ 0.7. Therefore, (4.1) underestimates the moment by a factor of 5 compared to Abe's formula, which seems to overestimate the moment slightly . Figure 4.3 compares (4.1) to the CMT solution for the depth range 50 - 200 km. Giardini (1984) obtained a slightly different formula using a similar data set. Using (4.1), the total seismic moment released by earthquakes with m_b between 5.0 and 5.5 is first estimated by using

$$M_{o\,(5.0\text{–}5.5)} = \sum_{m_b=5.0}^{5.5} M_{o\,(m_b)} N_{(m_b)}, \tag{4.2}$$

where $N_{(m_b)}$ is the number of events with magnitude m_b. Assuming the empirical relation between magnitude and frequency,

$$\log N_{(m_b)} = a - b m_b, \tag{4.3}$$

where b = 1, the total seismic moment can be expressed as

$$M_{o\,(5.0\text{–}5.5)} = 10^{11+a} \sum_{5.0}^{5.5} 10^{1.4 m_b}. \tag{4.4}$$

It is then possible to extrapolate the total moment release estimate up to a certain maximum size of earthquakes (Smith, 1976),

$$M_{o\,(5.0\text{–}m_{bmax})} = \sum_{5.0}^{m_{bmax}} M_{o\,(m_b)} N_{(m_b)} = 10^{11+a} \sum_{5.0}^{m_{bmax}} 10^{1.4 m_b}$$

$$= M_{o\,(5.0\text{–}5.5)} \sum_{5.0}^{m_{bmax}} 10^{1.4 m_b} \Big/ \sum_{5.0}^{5.5} 10^{1.4 m_b} \equiv \alpha_{m_{bmax}} M_{o\,(5.0\text{–}5.5)}\,. \tag{4.5}$$

$\alpha_{m_{bmax}}$ is 5.6, 29, 146, and 740 for m_{bmax} = 6, 6.5, 7, and 7.5, respectively. Therefore under all these assumptions, once we know (or assume) a maximum size of earthquake that can occur in a certain area, it is possible to calculate the total seismic moment release for events with $m_b > 5.0$ from the seismic moment release of events with $5.0 \leq m_b \leq 5.5$. The effect of excluding events with $m_b < 5.0$ is negligible, since magnitude enters into (4.4) as a power of 10.

Figures 4.4 show the magnitude distribution of earthquakes in the depth range 70-150 km for each subduction zone. Data are from PDE in the time period 1964-1983. Using the method described above, total seismic moment release within slabs between 70 km and 150 km depth is estimated for each subduction zone. Average seismic moment release rates for the intermediate part of subducting slabs per unit surface area are then estimated by,

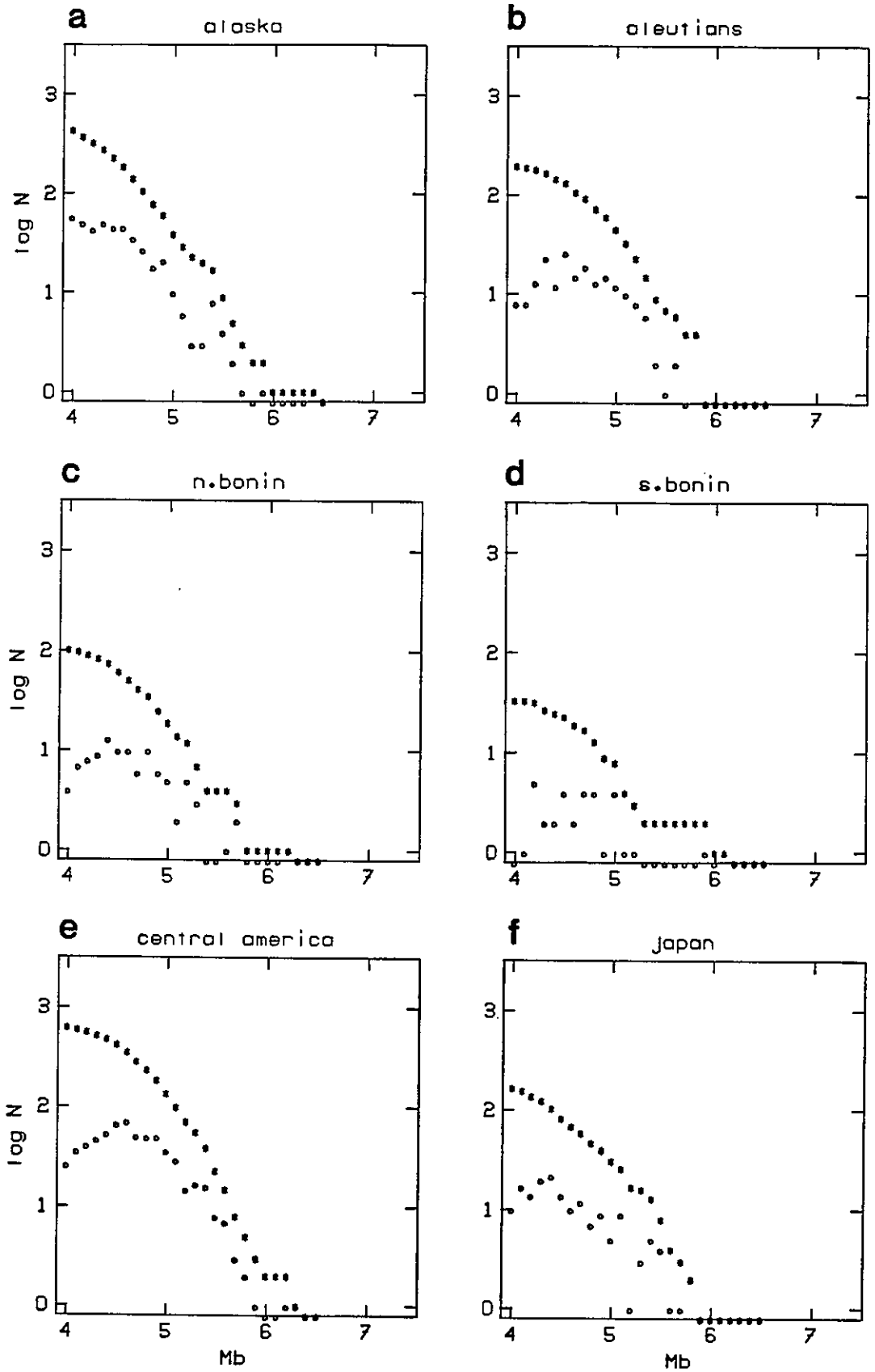

Figure 4.4. Data used to estimate the seismic strain rate for each subduction zone. Arc parameters are in Table 4.1. See caption of Figure 4.2. (a) Alaska, (b) Aleutians, (c) northern Bonin, (d) southern Bonin, (e) central America, and (f) Japan.

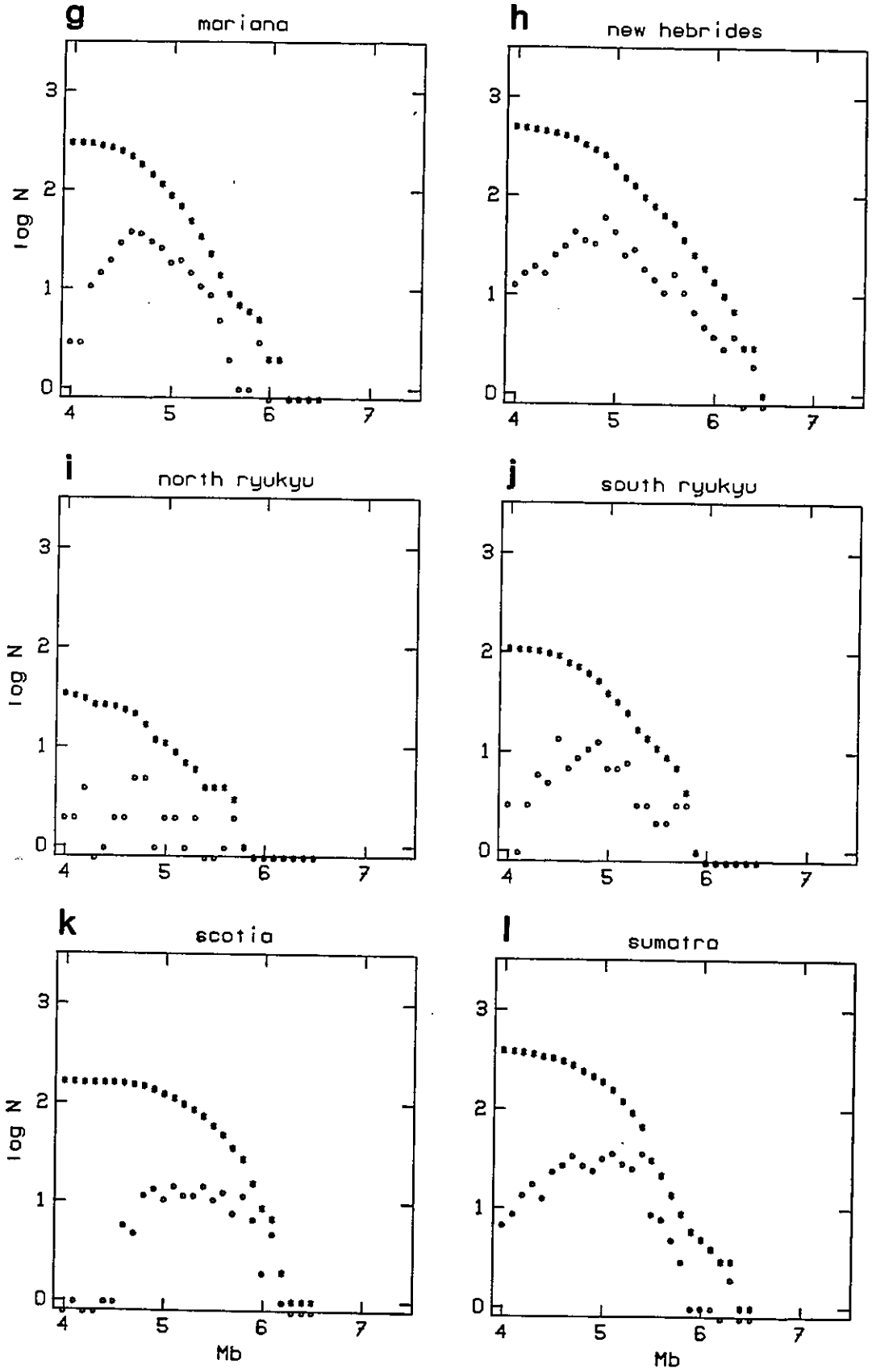

Figure 4.4. (g) Mariana, (h) New Hebrides, (i) northern Ryukyu, (j) southern Ryukyu, (k) Scotia, and (l) Sumatra.

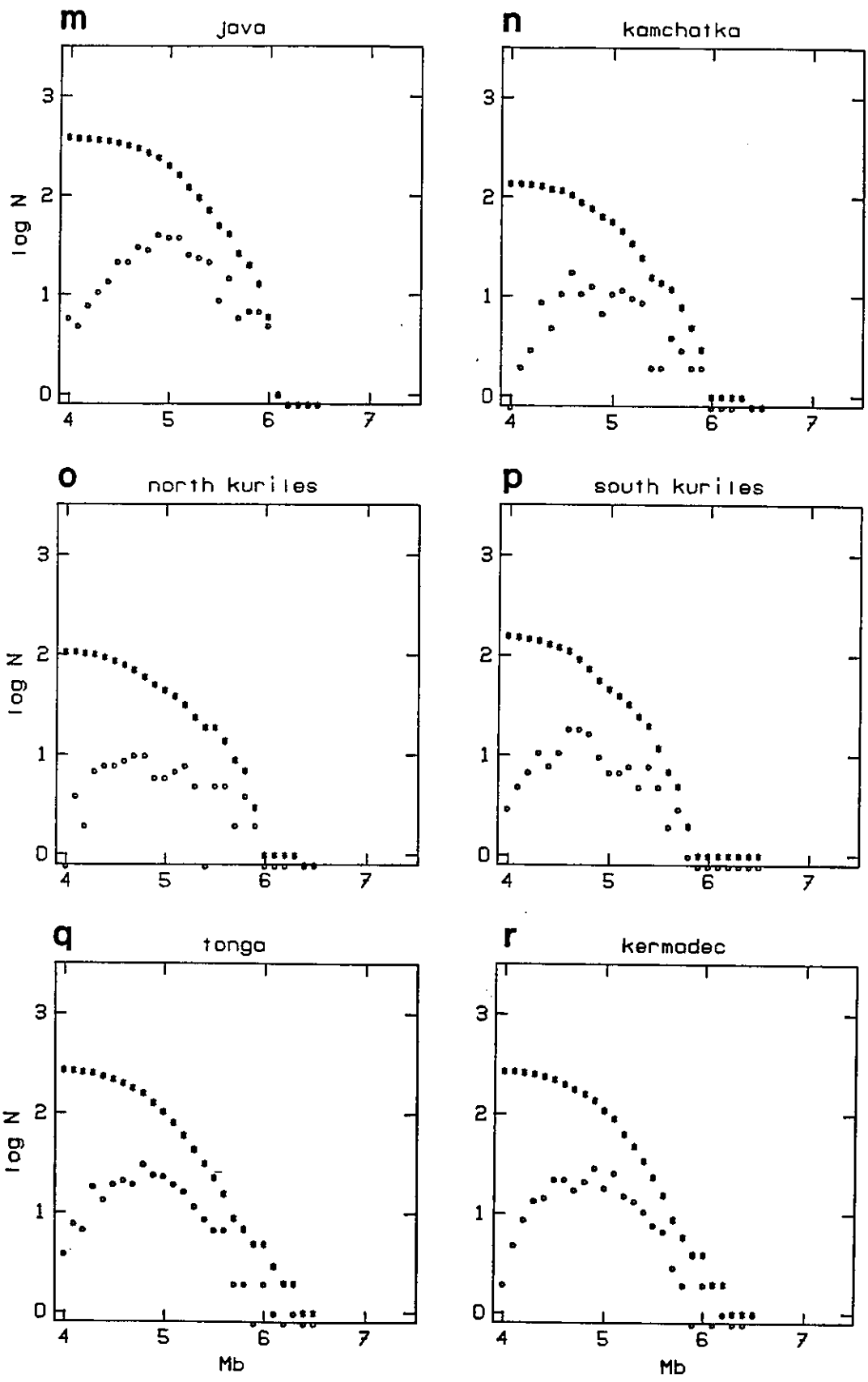

Figure 4.4. (m) Java, (n) Kamchatka, (o) northern Kuriles, (p) southern Kuriles, (q) Tonga, and (r) Kermedec.

$$\dot{M}_{o\,(m_{bmax})}(dyne\cdot cm/km^2yr) = M_{o\,(5.0-m_{bmax})}/(LWT), \tag{4.6}$$

where L, W, and T are the length along the dip between 70 - 150 km depth, the width of trench, and the total time period (20 years in this case) respectively. Corresponding seismic strain rates ($\dot{\epsilon}_s$) are obtained from

$$\dot{\epsilon}_{s\,(m_{bmax})} = \dot{M}_{o\,(m_{bmax})}/(2H_s\,\mu), \tag{4.7}$$

where H_s and μ are the thickness of the seismic zones (~ 40km) and rigidity (~ $7\cdot10^{11} dyne/cm^2$), respectively. Here strain rates are uniaxial along the dip of the slab and earthquakes are assumed to occur on planes dipping 45° to the dip of the slab. Chapple and Forsyth (1979) used a similar approach for bending earthquakes in the outer rise region. Table 4.1 summarizes the parameters used for various subduction zones. The poles of the arcs are estimated from the distribution of the earthquakes between depth 125 km and 175 km by least square fit and the lengths of the trenches are estimated using these poles for each subduction zones.

Table 4.2 summarizes the estimated strain rates. The quantities in the parentheses are the estimated $M_{o\,(5.0-5.5)}$ based on the total number of earthquakes between m_b 5.0 and 5.5,

$$N_{(5.0-5.5)} = \sum_{5.0}^{5.5} N_{(m_b)},$$

instead of (4.2). The differences between the two numbers (before and in parentheses) are the simplest measures of the assumption (4.3) in the magnitude range 5.0 - 5.5.

Quantification of earthquakes is a difficult problem, particularly for small earthquakes. Furthermore, the assumptions which have been made may not hold. The values obtained in Table 4.2 should thus be considered no better than magnitude of order estimates. It is also safe to interpret the variation among the different subduction zones as indicative of the error of this kind of analysis.

For the subduction zones where double seismic zones are observed, average seismic strain rates range from 1.0~ $8.1\times10^{-17}s^{-1}$ and 0.3~ $2.1\times10^{-15}s^{-1}$ for m_{bmax} = 6.0 and 7.0, respectively. m_{bmax} = 6.0 is a fairly small estimate of the maximum size of intermediate depth earthquakes. Therefore, any mechanism which is proposed to explain the presence of double seismic zones must be able to produce strain rates on the order of ~ $10^{-17}s^{-1}$.

The maximum thickness of double seismic zones beneath Tohoku is ~ 40 km (Figure 1.3a). Assuming that both seismic zones are equally active, the maximum thickness of each seismic

TABLE 4.1. ARC PARAMETERS

Arc	Pole (lat.,	long.)	Radius (deg.)	Left End Point		Right End Point		Dip (deg.)	Length (km)
Alaska	65.0,	180.4	12.7	63.3,	209.5	57.0,	201.0	45	855
Aleutians	65.0,	180.4	12.7	57.0,	201.0	52.9,	173.0	55	1990
Northern Bonin	6.4,	75.1	65.4	33.5,	140.0	30.0,	140.5	50	391
Southern Bonin	6.4,	75.1	65.4	30.0,	140.5	25.0,	141.0	60	557
Central America	29.4,	282.3	19.3	11.3,	274.5	17.4,	264.7	50	1238
Japan	37.9,	113.1	21.1	40.5,	141.3	36.2,	140.0	30	476
Java	39.2,	120.8	47.7	-8.0,	124.0	-6.0,	106.0	60	2020
Kamchatka	57.8,	128.9	17.1	57.0,	160.0	48.5,	157.5	50	879
Northern Kurils	57.8,	128.9	17.1	48.5,	157.5	45.0,	152.5	45	485
Southern Kurils	57.8,	128.9	17.1	45.0,	152.5	44.0,	147.0	40	385
Tonga	22.4,	80.1	110.2	-16.0,	185.6	-24.0,	183.6	55	912
Kermadec	-22.4,	159.9	21.1	-25.0,	183.2	-36.0,	178.0	62	1333
Lesser Antilles	13.9,	285.1	13.2	18.0,	298.0	12.0,	299.0	45	669
Marianas	17.3,	139.1	6.3	22.5,	143.0	12.5,	143.0	70	1303
New Hebrides	-1.7,	-157.9	36.8	-21.0,	170.0	-11.0,	166.0	70	1191
Northern Ryukyu	35.5,	116.3	12.3	33.5,	133.5	28.2,	131.0	70	549
Southern Ryukyu	35.5,	116.3	12.3	28.2,	131.0	23.3,	125.0	45	702
Scotia	-58.0,	-31.8	3.0	-55.6,	331.7	-60.6,	332.3	50	598
Sumatra	33.2,	159.9	65.0	-6.0,	106.0	8.0,	94.0	70	2047

TABLE 4.2. SEISMIC STRAIN RATES

Arc	$\dot{M}_{o\,(5.0-5.5)}$ $10^{19} dyne \cdot cm / km^2 yr$	$\dot{\epsilon}_{s\,6.0}$ $10^{-17} s^{-1}$	$\dot{\epsilon}_{s\,7.0}$ $10^{-15} s^{-1}$
Alaska	0.9 (0.7)	2.9	0.7
Aleutians	0.3 (0.3)	1.0	0.3
Northern Bonin	0.5 (0.7)	1.6	0.4
Southern Bonin	0.1 (0.2)	0.3	0.1
Central America	1.7 (1.8)	5.5	1.4
Japan	0.9 (0.7)	2.9	0.8
Java	1.6 (1.6)	5.2	1.4
Kamchatka	0.8 (1.0)	2.6	0.7
Northern Kurils	1.2 (1.1)	3.9	1.0
Southern Kurils	2.1 (1.7)	6.8	1.8
Tonga	2.5 (2.5)	8.1	2.1
Kermadec	1.6 (1.6)	5.2	1.4
Lesser Antilles	0.1 (0.0)	0.3	0.1
Marianas	1.3 (1.4)	4.2	1.1
New Hebrides	2.7 (2.8)	8.8	2.3
Northern Ryukyu	0.2 (0.3)	0.6	0.2
Southern Ryukyu	0.7 (0.7)	2.3	0.6
Scotia	3.3 (2.4)	10.	2.8
Sumatra	2.1 (1.9)	6.8	1.8

zone is ~ 20km. Considering that fault planes dip 45° with respect to the dip of the slab (i.e., one of the principal axes is down-dip, Figure 4.1), the maximum length of the earthquake fault is ~ 30 km. The fault area of $30\times30\ km^2$ corresponds to a seismic moment of $10^{26}\sim10^{27}\ dyne\cdot cm$ for a stress drop of 1 $\sim$ 10 MPa (Kanamori and Anderson, 1975) and to a magnitude of 6.25 ~ 6.67 from (4.1). It is reasonable to think that the maximum magnitude m_{bmax} is ~ 6.5 and that seismic strain rate is ~ $10^{-16}s^{-1}$.

Geometrical Unbending Strain Rate

Oceanic lithosphere bends above a depth of ~ 60 km when it subducts into the mantle. The fact that the subducting lithosphere is almost straight in the mantle below a depth of ~ 200 km indicates that the lithosphere must unbend in a depth range from ~ 60 km to ~ 200 km to become straight. Figure 4.5 schematically shows this effect. Knowing the geometry of the slab, its thickness, and convergent velocity, and assuming a steady state of subduction, it is possible to estimate this unbending strain rate.

The unbending strain rate is proportional to the rate of change of the curvature and thus a function of the third derivatives of the surface geometry of a subducting plate. Thus, it is almost impossible to measure it accurately from the geometry of the slab observed from seismicity. It is, however, still possible to estimate the order of magnitude of an average unbending strain rate.

Figure 4.6 shows a bending-unbending model of subducting lithosphere. The lithosphere starts bending downward at the trench (T) and increases its curvature until it reaches the point of maximum curvature (S_0). Then it starts unbending and the curvature decreases until the point (S_1) beyond which it is straight. Assuming constant unbending, the rate of geometrical unbending (γ), which is the change of curvature, is given by

$$\gamma \equiv \frac{d\kappa}{ds} = 2(\theta_1-\theta_0)/(s_1-s_0)^2, \tag{4.8}$$

where κ is the curvature, s measures distance along the surface of the plate and θ is the dip angle. Since it is impossible to locate points S_0 and S_1 precisely from seismicity, I assume that unbending starts at the depth of 60 km and ends at the depth of 150 km. From a variety of published cross sections of seismicity (mostly from Isacks and Barazangi, 1977), geometrical unbending rates are thus calculated (Table 4.3).

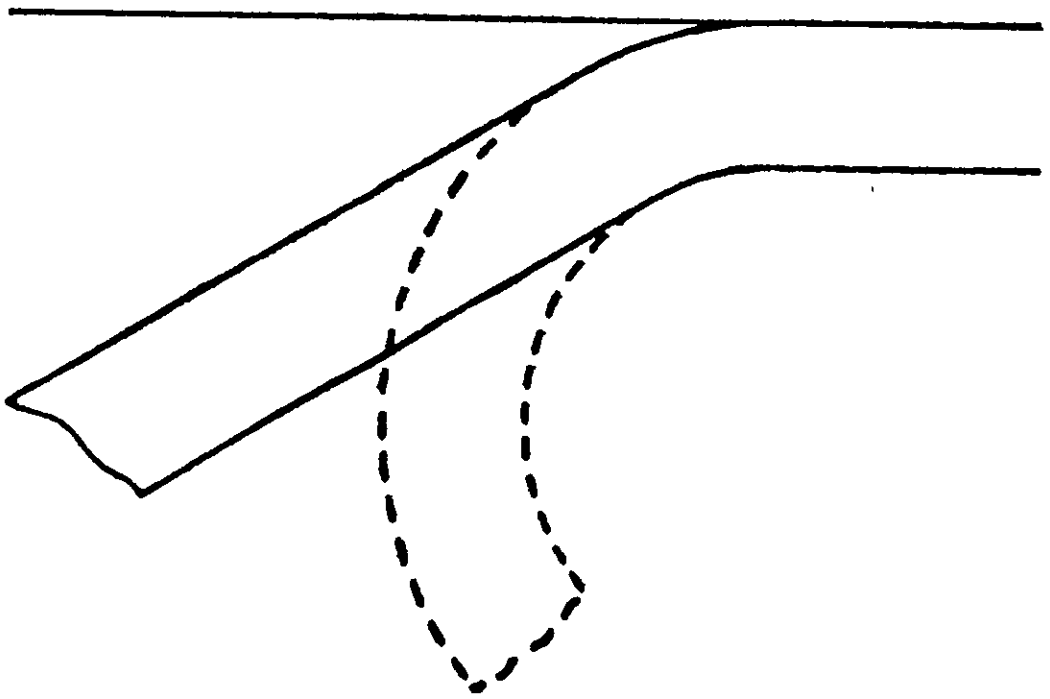

Figure 4.5. Schematic illustration of descending plates with unbending (solid line) and without unbending (dashed line). After Tsukahara (1980).

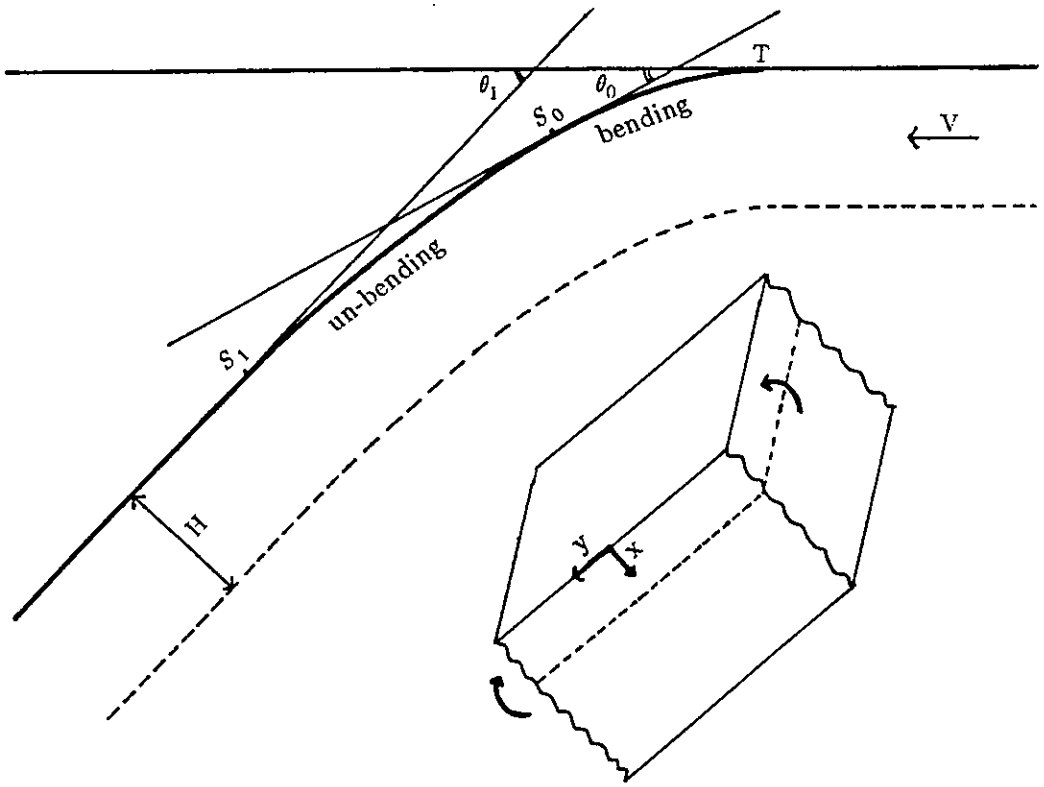

Figure 4.6. Bending and unbending model of a subducting plate.

TABLE 4.3. GEOMETRICAL UNBENDING STRAIN RATES (60 km -150 km depth)

Arc	slab dip (deg.)		$\delta_1 - \delta_0$	unbending rate	strain rate[1]
	60 km	150 km	(km)	(10^{-5} km^{-2})	(10^{-15} sec^{-1})
Aleutians	29	53	134	4.6	2.8
Northern Bonin	39	55	120	4.0	2.6
Southern Bonin	42	65	109	6.6	4.2
Central America	44	74	102	10.0	6.2
Japan	28	32	173	0.41	0.26
Java	30	58	130	5.7	3.6
Kamchatka	37	48	130	2.1	1.3
Northern Kurils	37	46	132	1.8	1.1
Southern Kurils	37	46	143	1.6	1.0
Tonga	37	52	126	3.4	2.2
Kermadec	44	64	110	5.8	3.6
Marianas	40	67	110	7.6	4.8
New Hebrides	58	70	99	4.1	2.6
Northern Ryukyu	44	66	109	6.6	4.2
Southern Ryukyu	38	63	114	6.8	4.2

[1] Convergence rate = 10 cm/yr and plate thickness = 100 km are assumed.

Assuming that the subduction process is steady state, it is possible to convert geometrical unbending rates into strain rates. Following Tsukahara (1980), a rectangular coordinate system is used as shown in Figure 4.6. When the lithosphere is deformed by pure unbending, the distribution of the uniaxial strain rate in the dip direction (i.e., direction of y-axis) is given by

$$\dot{\epsilon}_y(x) = \dot{\Delta\epsilon}(x_n - x)/H, \tag{4.9}$$

where H is the thickness of the lithosphere and x=x_n represents the neutral plane. $\dot{\Delta\epsilon}$ is the difference of the uniaxial strain rate at the upper surface of the plate and that at the lower surface, and related to the unbending rate as follows.

In bending models of a thin plate, the difference between the uniaxial strain at the top surface of the plate and that at the bottom one is

$$\Delta\epsilon = H/R = \kappa H, \tag{4.10}$$

where R and κ are radius of curvature and curvature. It follows that

$$\dot{\Delta\epsilon} = \frac{d(\Delta\epsilon)}{dt} = H\frac{d\kappa}{dt} = \frac{ds}{dt}\cdot\frac{d\kappa}{ds}\cdot H = V\cdot\gamma\cdot H, \tag{4.11}$$

where V is the convergence velocity and γ is the unbending rate. Taking the thickness of the plate (H) as 100 km and the thickness of the seismic portion of the plate as 40 km, the average bending strain rate within the seismic portion of the lithosphere is

$$\dot{\epsilon}_b = \tfrac{1}{2}\,\dot{\Delta\epsilon}\frac{40}{100.} \tag{4.12}$$

Within the seismic portion of the lithosphere, some of this unbending strain is released by earthquakes and the rest is released aseismically. In the lower portion of the plate, the temperature is so high that all the bending strain is released aseismically.

The average strain rates for different subduction zones are listed in the last column of Table 4.3, where the convergence velocity is set equal to 10 cm/yr. They are on the order of $10^{-15}s^{-1}$. These values exceed the seismic strain rate with $m_{bmax} = 6.0$ ($\epsilon_{s(6.0)}$) estimated in the previous section by two orders of magnitude and are comparable to $\epsilon_{s(7.0)}$. Thus the strain rate expected from a simple geometrical unbending is comparable to that of intermediate depth earthquakes and can explain the double seismic zone.

It is often claimed that the geometry of the deeper portion (say, between 100 km - 200 km) of double seismic zone is apparently straight and that the unbending strain rate should be thus small (e.g., House and Jacob, 1982). It is, however, easy to show that even an apparently

straight part of a slab can have an unbending strain rate of $10^{-17}\sim10^{-16}s^{-1}$.

Let us take an average unbending strain rate ($\dot{\epsilon}_b$) equal to $10^{-17}s^{-1}$. From (4.11) and (4.12), the corresponding unbending rate is

$$\gamma = 2\dot{\epsilon}_b / (VH_s) \sim 1.6\times10^{-7}km^{-2} \tag{4.13}$$

where H_s (40 km) is the thickness of the seismic portion of the slab and V = 10 cm/yr. From (4.8), this unbending rate gives a change of the dip to be 0.045° between two points 100 km apart on the slab surface along the dip direction. It is rather obvious that we cannot detect such a small rate of change of the dip angle ($0.045^\circ/100km$) from seismicity. It is even impossible to detect a change of $0.45^\circ/100km$, which corresponds to an unbending strain rate of $10^{-16}s^{-1}$. In other words, even an apparently straight portion of the slab can easily have an unbending strain rate of $10^{-17}\sim10^{-16}s^{-1}$.

The stress distribution expected from this unbending strain is the same as that of double seismic zones (i.e., downdip compressional in the upper layer and downdip tensional in the lower layer). It is shown above that the strain rate due to this unbending is on the order of $10^{-15}s^{-1}$ and is large enough to account for all the strain energy released by earthquakes, while the strain rate due to thermal expansion ($10^{-18}\sim10^{-17}s^{-1}$; House and Jacob, 1982) is too small. Unbending of the subducting plate is required as a natural consequence of the theory of plate tectonics. Therefore, it is quite natural to think that the strain resulted from this unbending, which has to be released somehow, is partly released by earthquakes and causes double seismic zones.

Modeling a Double Seismic Zone

Considering the plastic-brittle property of the material composing the lithosphere, Tsukahara (1980) modeled the essential feature of double seismic zones by a simple geometrical unbending of the subducting plate. In this section, using his formulation I investigate what constraint the presence of a double seismic zone can put on the subduction process.

Brittle-Plastic Rheology

Figure 4.7 (Figure 3 of Tsukahara, 1980) schematically shows the idealized model of brittle-plastic rheology. It should be noted that the term 'brittle' fracture here represents any kind of instantaneous failure that could be detected as an earthquake. When the strain rate is small and the expected steady state stress (σ_p^1) is smaller than the strength of the material (σ_s), deformation occurs aseismically (line A). When the strain rate is so large that the expected steady state stress exceeds the strength of the material, fracture occurs (B). In this case, deformation occurs both seismically and aseismically. The average stress in this case is fixed at the strength of the material.

For the plastic flow law, I use the formula of power law creep of olivine summarized by Kirby (1983),

$$\dot{\epsilon} = A\ \sigma_p^n\ exp\ (-(E^* + PV^*)/(RT)), \tag{4.13}$$

where P, R, and T are pressure, universal gas constant, and absolute temperature, respectively. A, n, E^*, and V^* are material constants and are given by,

$$\log_{10}A = 4.8 \pm 1.2 \qquad A \text{ in } s^{-1}MPa^{-n} \tag{4.14a}$$

$$n = 3.5 \pm 0.6 \tag{4.14b}$$

$$E^* = 533 \pm 60\ \ kJ/mol \tag{4.14c}$$

$$V^* = (17 \pm 4) \times 10^{-6}\ \ m^3/mol. \tag{4.14d}$$

The range of differential stresses over which this power-law constants apply is 10 to 500 MPa.

The average strength of the lithosphere (i.e., apparent stress in the lithosphere) has always been a point of controversy. Tsukahara (1980) chose it to be 5~ 20 MPa and Samowitz and Forsyth (1981) 500 MPa. Here, it is treated as a variable.

Distribution of Strain Rate

Only the strain rates due to pure unbending of a thin plate will be considered. When there is uniform uniaxial additional strain (e.g, strains due to so-called ridge push or slab pull

In the rest of this chapter, stress σ always refers to the uniaxial differential stress $\sigma_1 - \sigma_3$, where σ_1 and σ_3 are the maximum and minimum principal stresses, respectively.

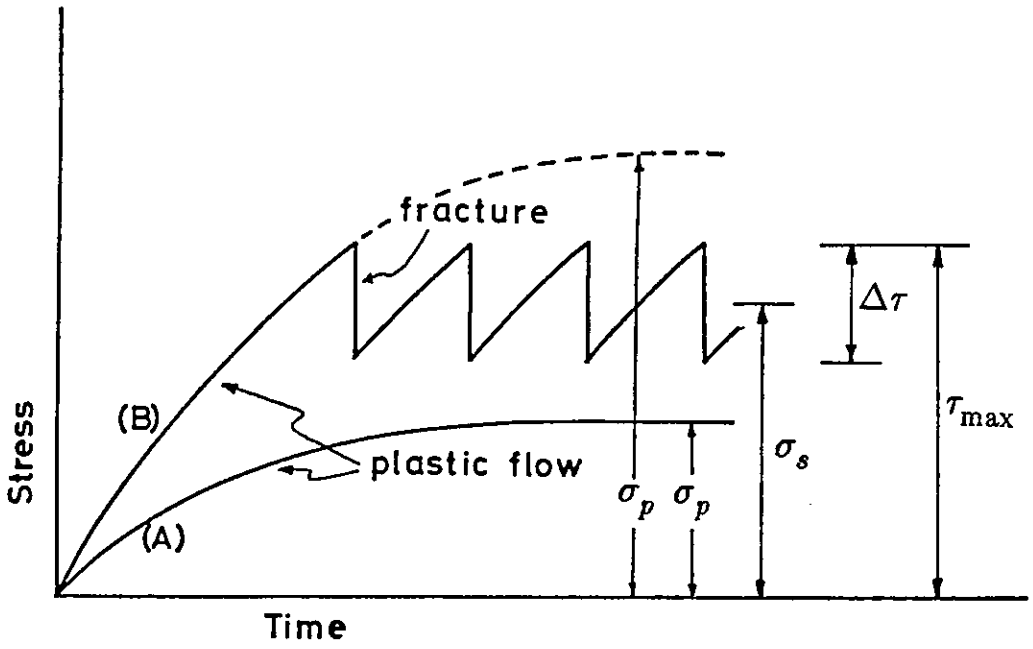

Figure 4.7. Schematic illustration showing the idealized deformation with fracture and plastic flow. σ_s, σ_p, $\Delta\tau$, and τ_{max} denote average strength, stress due to steady state plastic plow, stress drop of earthquakes, and maximum strength, respectively. (A) $\sigma_p \leq \tau_{max}$, (B) $\sigma_p > \tau_{max}$. After Tsukahara (1980).

forces), the reader should refer to the discussion in Tsukahara (1980). The strain rate field is given by (4.9). The neutral plane, $x = x_n$ can be obtained from the balance equation,

$$\int_0^H \sigma(x)\, dx = 0, \tag{4.15}$$

where $\sigma(x)$ is the uniaxial unbending stress and can be calculated from (4.13) as a function of the strain rate. When the value exceeds the strength (σ_s) of the material, it is set equal to σ_s. Thus if $\dot{\Delta\epsilon}$ in (4.12) (or the average unbending strain rate, $\dot{\epsilon}_b$) is specified, and if $T(x)$ and $P(x)$ are known, it is possible to calculate the strain field, $\dot{\epsilon_y}(x)$ and the stress field, $\sigma(x)$ to satisfy (4.9), (4.13), and (4.15).

Model

Figure 4.8 shows the temperature profile of the model of the subducting lithosphere. It is calculated by the finite difference scheme discussed by Minear and Toksoz (1970) and implemented by N. H. Sleep. His program incorporates an induced corner flow in the mantle wedge above the slab and entrained flow in the vicinity of the slab and thus predicts a lower temperature field within the slab than his previous models (e.g., Sleep, 1973; Fujita et al., 1981). The current version has been used by Creager and Jordan (1984) and Nieman et al. (1984) to predict the travel time anomalies due to the slab structure. The thermal constants are chosen to be comparable to those of the sea floor spreading model (Parson and Sclater, 1977) (e.g., the thermal diffusivity is $0.88 \times 10^{-6}\ m^2/s$). The oceanic lithosphere subducts at a thermal age of 100 Ma (calculated by error function with a mantle temperature of $1370^\circ\ C$) with a velocity of 105 km/Ma and a dip angle of 0.5 radian. The computation is terminated ~ 7 Ma after the initiation of subduction. These values are chosen such that the model mimics the subduction zone beneath Tohoku, Japan, where the nature of the double seismic zone is best known.

The stress and strain fields were modeled along the three profiles (depths at the slab surface are 50km, 100km, and 150km) perpendicular to the slab dip (lines A-A′ , B-B′ , and C-C′ in Figure 4.8). Figure 4.9 shows temperature, hydrostatic pressure, and strain rate profiles. The thick, medium, and thin lines correspond to A-A′ , B-B′ and C-C′ , respectively. The difference of strain rate at the top and the bottom of the slab, $\dot{\Delta\epsilon}$ is given by $10^{-15}s^{-1}$, $10^{-16}s^{-1}$, $10^{-17}s^{-1}$ for A-A′ , B-B′ , and C-C′ , respectively. These numbers are chosen because the number of earthquakes beneath Tohoku apparently decreases by one order of magnitude between depth of ~ 60 km and ~ 110 km (Figure 6 of Anderson et al., 1980).

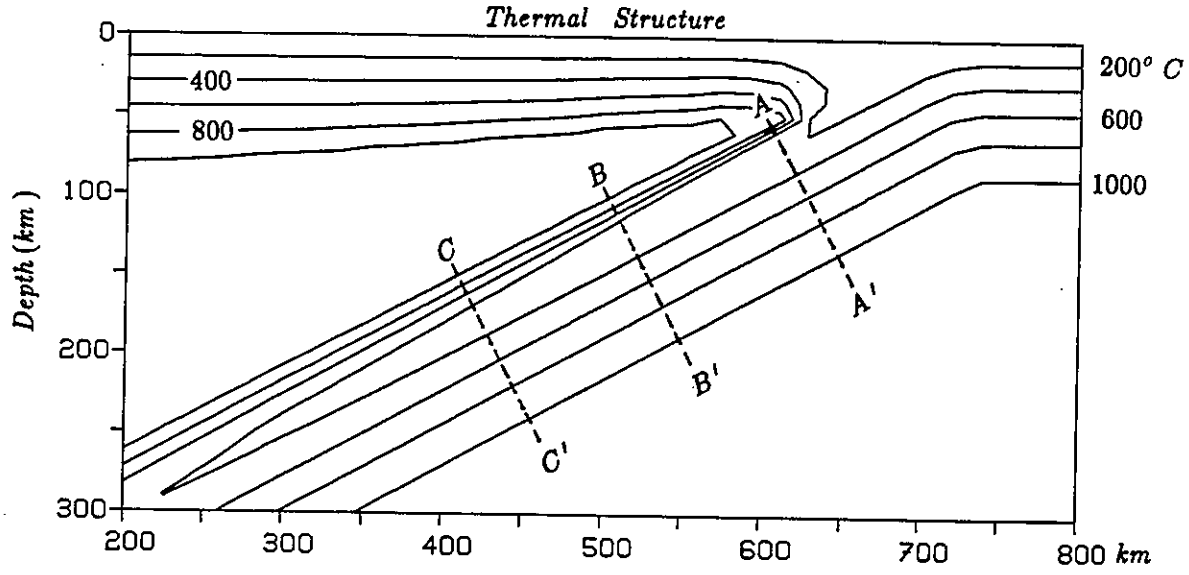

Figure 4.8. Temperature model for the subduction zone beneath Tohoku, Japan. (A-A') slab surface depth 50 km, (B-B') 100 km, (C-C') 150 km.

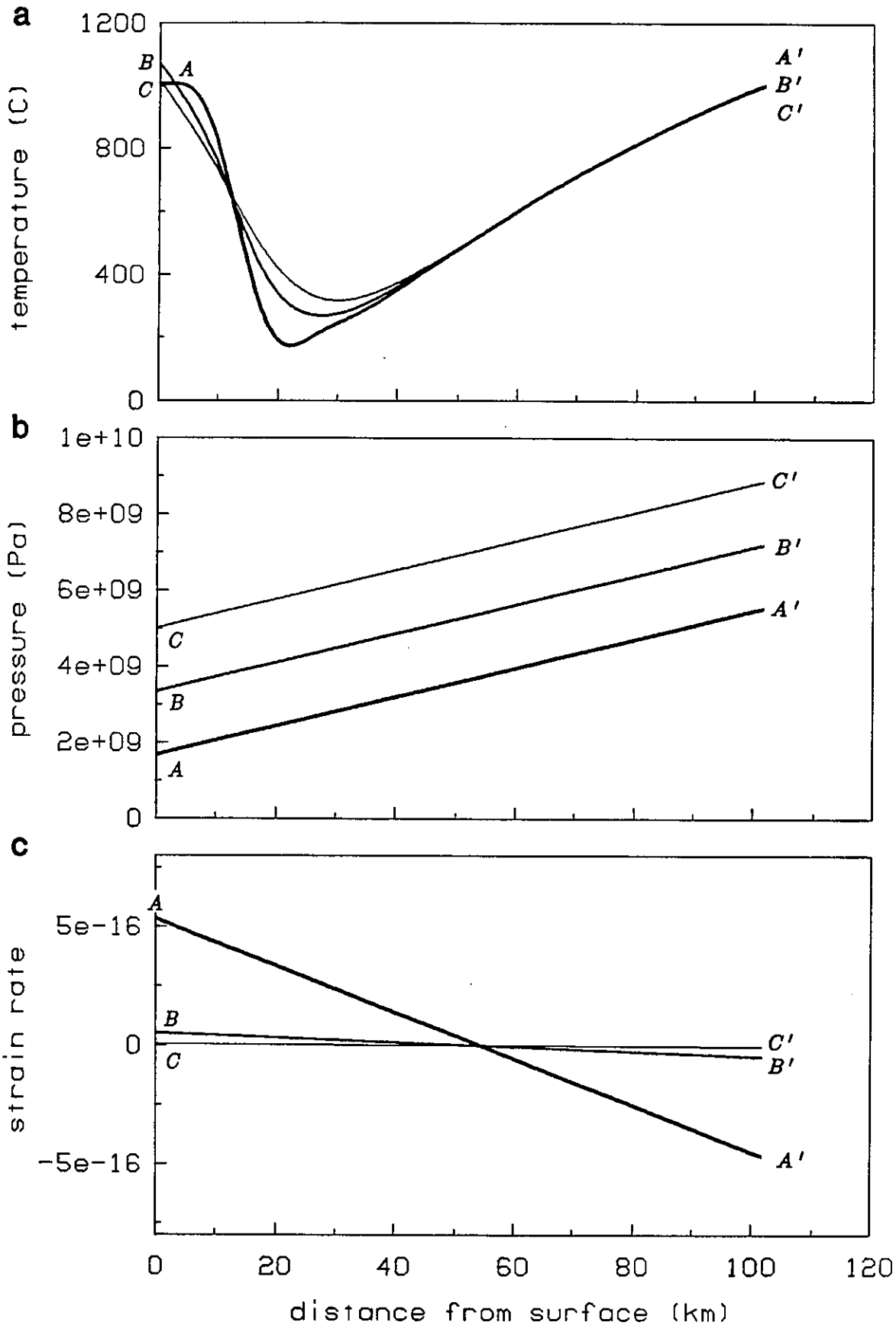

Figure 4.9. Distributions of temperature (a), hydrostatic pressure (b), and uniaxial unbending strain rate (c) perpendicular to the dip of the slab. Thick, medium, and thin lines correspond to lines (A-A′), (B-B′), and (C-C′) in Figure 4.8.

The result is shown in Figure 4.10. Positive stress corresponds to downdip compression, and negative stress corresponds to downdip tension. The first, second, and third rows correspond to the result for A-A′ , B-B′ , and C-C′ , respectively. In the second and third columns, the temperature fields are increased by 100° C and 200° C, respectively. Results of two different sets of parameters for (4.13) are shown. The thinner line in each box represents the stress distribution obtained from parameters in (4.14). The thicker lines are the results from parameters with which the viscosity takes the lowest value within the error given in (4.14). The strength of the slab is set equal to 50 MPa. Parameters which give the highest viscosity within the error in (4.14) apparently gives viscosity so high that the whole slab (~ 100 km thick) becomes seismic.

Although the basic stress distribution of a double seismic zone (i.e, downdip compression in the upper part and downdip tension in the lower part) is consistently reproduced in the models (as expected from the unbending model), the thickness changes from one model to another. This suggests that the careful examination of double seismic zones may put some constraints on the properties of the subducting slab. The temperature distributions in Figure 4.9 do not vary much among the different profiles. The thicknesses of the brittle failure zone (i.e., the thickness of the double seismic zone) in Figure 4.10 does not change in each column because the effect of pressure on viscosity cancels out the effect due to the change of strain rates.

The seismicity beneath Tohoku (e.g., Figure 1.3a; Hasegawa et al., 1978a) shows that the thickness of the double seismic zone stays almost constant down to a surface depth of ~ 100 km, as predicted by the model. The lower plane is almost straight throughout the double seismic zone, which is also consistent with the model (i.e., the temperature profile does not change much along the dip in the lower portion of the slab; Figures 4.8 and 4.9a). The upper plane of the double seismic zone, on the other hand, starts bending (although it does not necessarily mean the plate itself is bending) toward the lower plane at a depth of ~ 100 km and they converge around ~ 180 km. This feature is not represented in the model, and it may mean that the upper portion of the slab tends to get heated faster than the temperature model predicts. Since the mantle temperature is held constant in the numerical modeling, this may suggest that the temperature of the mantle beneath Japan is relatively higher than that of the mantle beneath the Pacific ocean. In the second and the third column of Figure 4.10, in order to see the effect of temperature change, profiles are uniformly increased by 100° C and 200° C, respectively. The thickness of the double seismic zone changes significantly. This suggests that

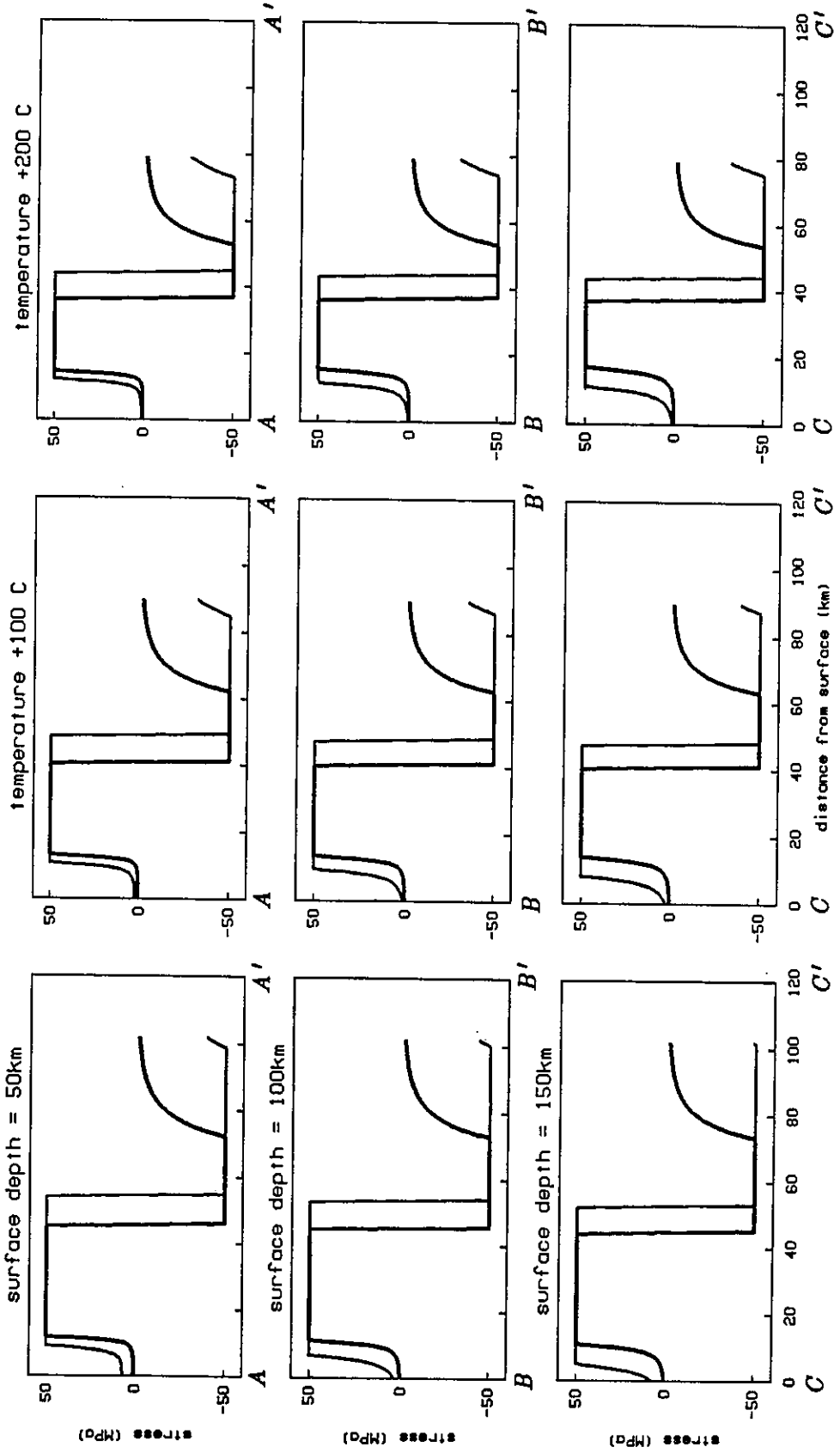

Figure 4.10. Stress field perpendicular to the dip of the slab. Thin lines are the results using the average values in (4.14) and the thicker lines are using the values in (4.14), with which the viscosity is the smallest. First, second and third row are for profile (A-A′), (B-B′), and (C-C′), respectively. For the second and the third column, temperatures are uniformly increased by 100° C and 200° C, respectively.

the temperature is one of the essential factors controlling the double seismic zone.

In the present model, the temperature of the outer edges of the double seismic zone (critical temperature, T_c, above which σ_p with a given strain rate is too small to cause earthquakes) is related to the strength of the slab through (4.13), where $T = T_c$ and $\sigma_p = \sigma_e$. Figure 4.11 shows this critical temperature as a function of depth with give strain rate and the strength. The thick lines are obtained by using the values in (4.14) and thin lines surrounding them represent the possible error given in (4.14). It shows that at the current level of knowledge of the rheology of the lithosphere, even if the strain rate and the strength are known precisely, from observations of the location of the lower edge of the double seismic zone, it is only possible to predict the temperature within an error of $\sim \pm 100^\circ C$. It also shows the significant effect of the strength on the critical temperature and the lesser significance of strain rates. On the other hand, this means that if the temperature structure can be constrained by other means (e.g., petrologically), it is possible to constrain the strength of the lithosphere.

Figure 4.12 shows the relation between the strength and the critical temperature at a depth of 80 km, where the lower plane of the double seismic zone in Tohoku appears to start. Strain rates are the highest around this depth and probably on the order of $10^{-15} \sim 10^{-14}\ s^{-1}$. The thick and thin lines represent the same as in Figure 4.11. The thickness of the double seismic zone beneath Tohoku is ~ 40 km. This corresponds to the isotherm of ~ 600 $^\circ C$ or less in the temperature model in Figure 4.9. A critical temperature of 600$^\circ C$ at a depth of 80 km predicts an unrealistic value for the strength of the lithosphere (not shown in Figure 4.12). At a depth of 80 km, the effect of heat conduction from the surrounding mantle is small and the thermal structure of the inside of the slab is almost static and similar to that of the oceanic lithosphere at the trench. The thermal structure of the oceanic lithosphere is fairly well known (Parsons and Sclater, 1977). Although their estimate of the error bar for each parameter is large, it is primarily due to the coupling among the parameters and does not necessarily mean the thermal structure is uncertain. In fact, the observed data are well predicted by the model and the error appears to be small. Therefore, the temperature model in this depth range should be reliable and probably is not wrong by more than 100$^\circ C$ (N. H. Sleep, personal communication, 1985). From bending earthquakes in the outer rise region in Tonga, Wortel (1982) estimated this critical temperature to be 580$\pm$70$^\circ C$ at a depth of ~ 45 km. Data on earthquakes occurring near oceanic trenches, compiled by Chen and Molnar (1983) also appear to suggest 600° for the critical temperature. Even taking the highest estimate of the critical temperature to be 700$^\circ C$ and the lowest estimate of viscosity, the strength still has to be

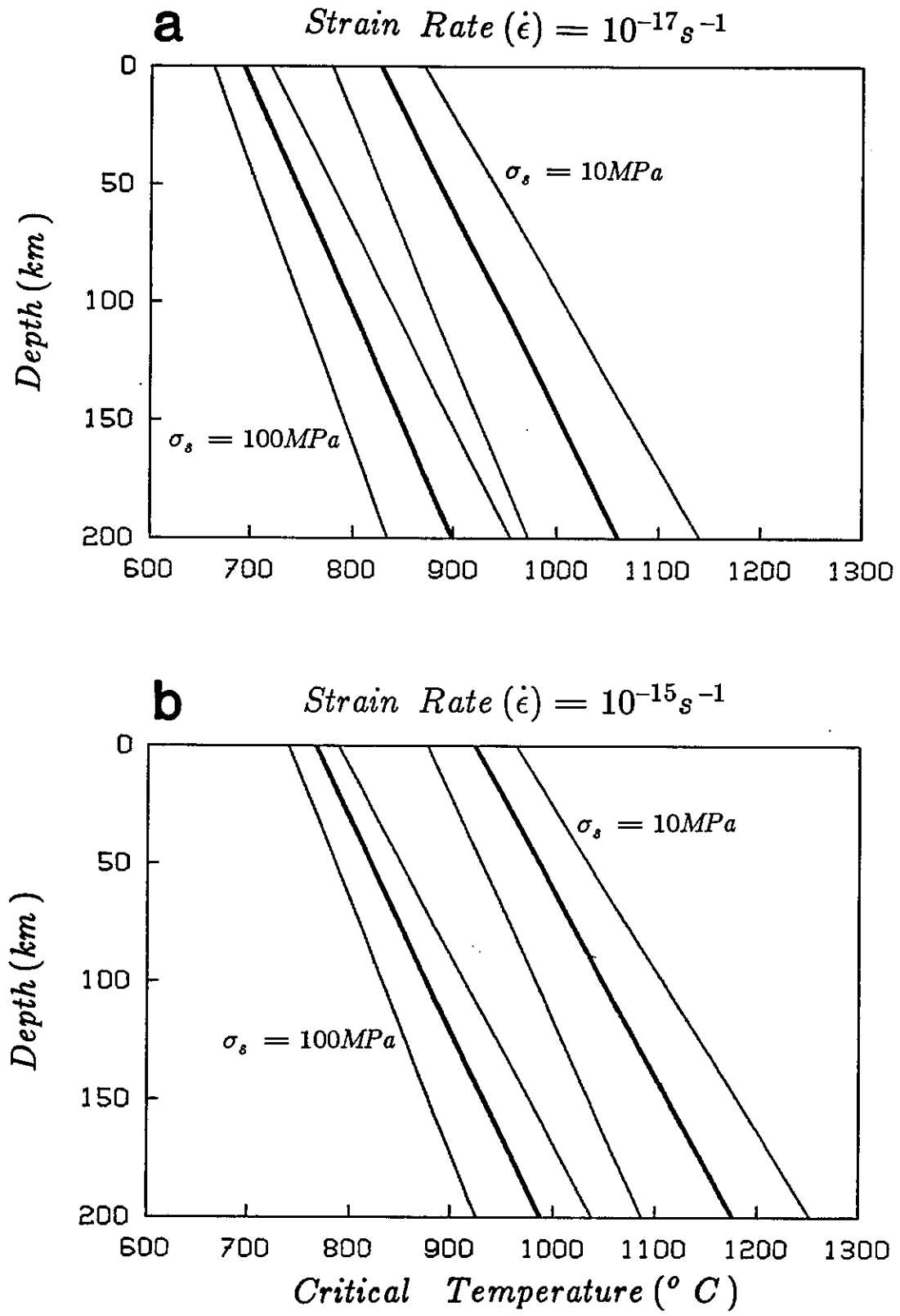

Figure 4.11. Critical temperature as a function of depth with given strain rates and strength. Strain rates are set equal to (a) $10^{-17}s^{-1}$ and (b) $10^{-15}s^{-1}$. Thick lines are for the average values in (4.14) and the thin ones surrounding them show the error bar in (4.14).

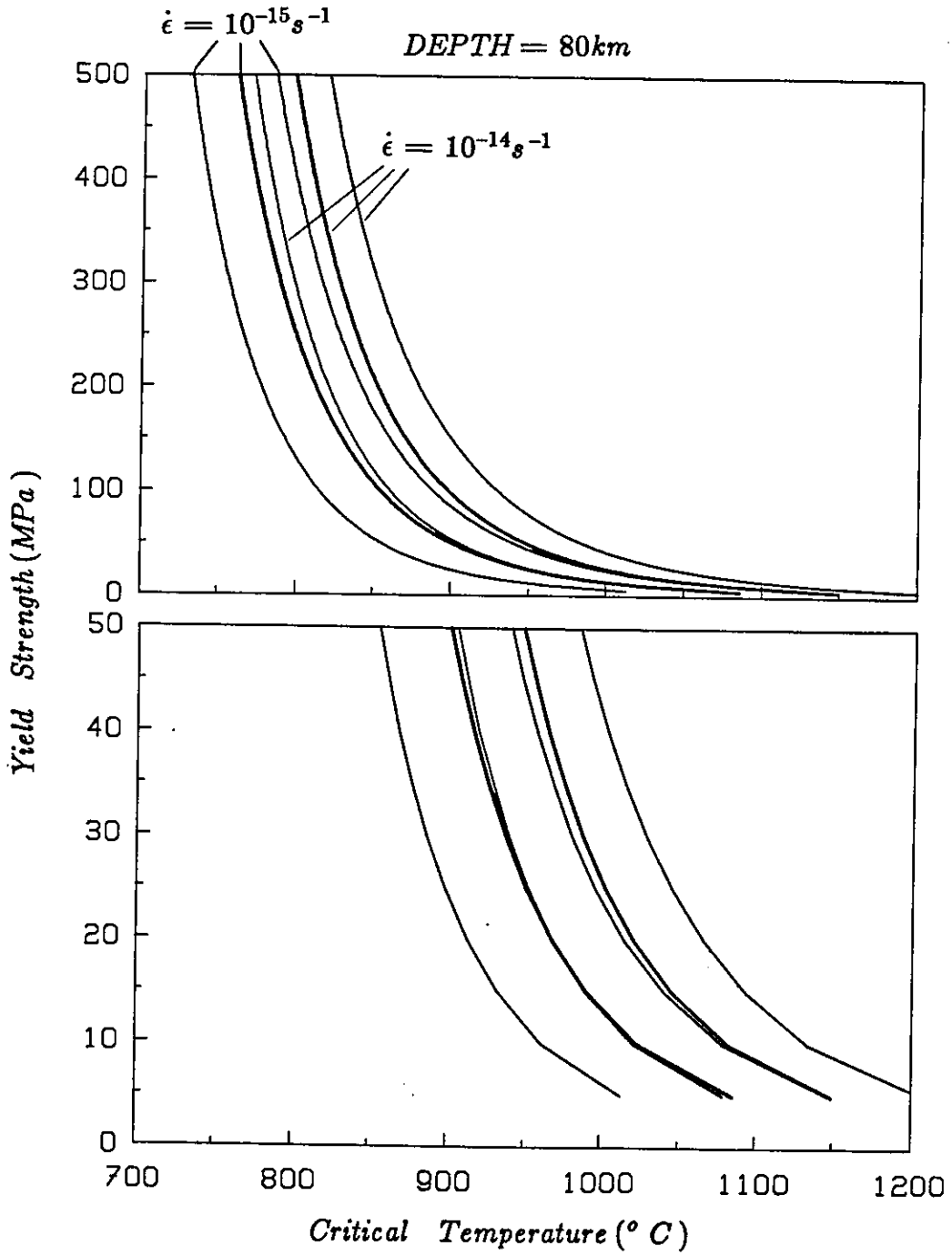

Figure 4.12. Critical temperature as a function of yield strength at a depth of 80 km, where the double seismic zone appears to start. Lines are the same as in Figure 4.11. Strain rates are $10^{-14} s^{-1}$ and $10^{-15} s^{-1}$.

bigger than 500 MPa. This implies either that the lithosphere can sustain a differential stress higher than 500 MPa **without having earthquakes**, or that the olivine flow law of (4.13) and (4.14) is not appropriate for the lithosphere.

Since the olivine flow law of (4.13) and (4.14) is that of 'dry' olivine, it is possible that neglecting the effect of water causes this high computed strength for the lithosphere. Neither the flow law for 'wet' olivine nor the water content in the lithosphere at depths is well known (Kirby, 1983). Thus it is not possible at this stage to determine whether or not the existence of a double seismic zone requires that high stresses exist in the lithosphere.

It is also possible that the flow law obtained on the laboratory scale (both in time and space) is not applicable to geologic scale phenomena (e.g, McNutt and Menard, 1982). Figure 4.13 shows the relation between the yield strength and activation energy, $Q = E^* + PV^*$ for two different critical temperatures. If the strength of the lithosphere is on the same order as the stress drop of earthquakes (~ 10 PMa), Figure 4.13 implies that the activation energy has to be less than ~ 400 kJ/mol. Since the activation energy is expected to be more than 600 kJ/mol in (4.14) at a depth of 80km, this suggests that the flow law obtained in laboratories may be seriously in error when applied to geologic scales. Brittle behavior of rock (or lithosphere) may be scale dependent (due to inhomogeneities) and this would change the flow law for the semi-brittle regime (or brittle-ductile transition; Kirby, 1980). Thus, both strength and activation energy could be much smaller than the values obtained from laboratory experiments for the semi-brittle regime. Estimating the bending moment of oceanic lithosphere following Goetze and Evans' (1979) formulation, McNutt and Menard (1982) suggested that the activation energy was significantly less than 420 kJ/mol (Kirby, 1983; dotted line in Figure 4.13). This value also predicts a relatively low yield strength (<50 MPa) at the lower edge of the double seismic zone.

The stress field calculated here is an instantaneous stress field and neither the variation along the dip of the slab nor that in time is considered. The subducting slab with a strain rate of $10^{-16}s^{-1}$ and a velocity of 100 km/Ma moves 3 km in the dip direction to obtain a strain of 10^{-4}. If the average critical strain of 10^{-5}~10^{-4}, obtained from shallow earthquakes (Tsuboi, 1933; Kanamori and Anderson, 1975; Rikitake, 1976), is applicable for intermediate earthquakes, it is, therefore, not necessary to consider the variation in time and in space.

The stress field model in Figure 4.10 does not show the spatial gap between the upper and the lower plane of the double seismic zone observed in seismicity. Since the unbending strain rate is always largest at the outer edges of both the compressional and the tensional seismic

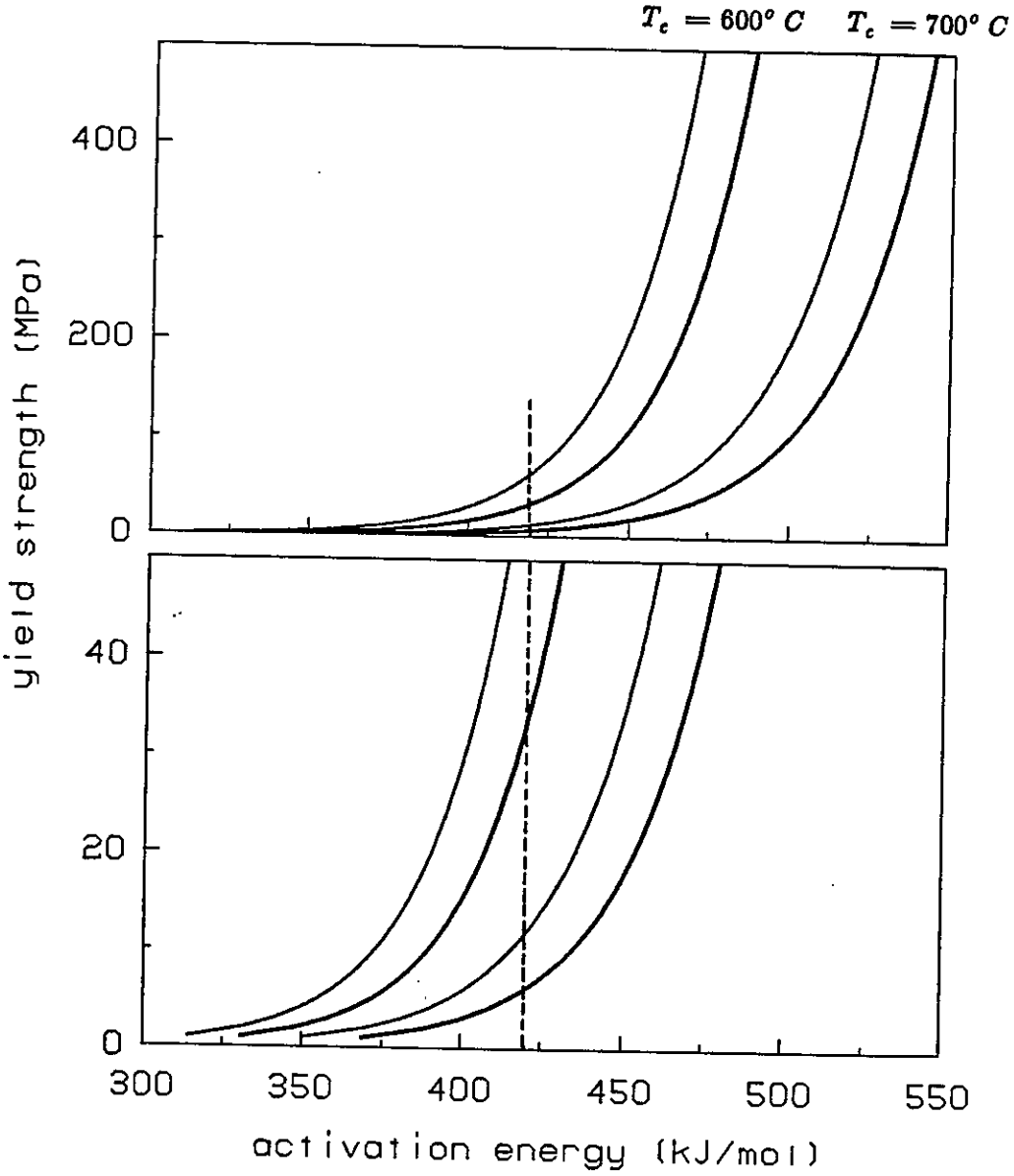

Figure 4.13. Yield strength as a function of activation energy with $T_c = 600° C$ and $700° C$. Thick and thin lines are results with strain rates $10^{-14} s^{-1}$ and $10^{-15} s^{-1}$, respectively.

zones in the model, more earthquakes are expected to occur in the outer regions than inside. Rupture should also tend to initiate at the edges where the strain rate is high. Since hypocentral locations are usually those of the initial point of rupture (as opposed to the centroid), they are expected to be located in the outermost region of both seismic zones. These features should result in further apparent separation of the two seismic zones.

Therefore it is possible to explain a double seismic zone as the result of unbending of the subducting slab. Although the current level of knowledge of the rheology of the lithosphere does not constrain the temperature structure, the possibility of such an approach in the future is shown. The applicability of the 'dry' olivine flow law of (4.13) and (4.14) for the lithosphere is seriously called into question.

What Unbends the Slab ?

I have so far concentrated just on the geometrical (and kinematical) part of the problem and made no dynamical considerations. A question still remains unsolved: what unbends the slabs in the mantle? The answer probably varies from one subduction zone to another and I only list the possible mechanisms. (1) Pressure due to the mantle flow (e.g., Yokokura, 1981; Hager and O'Connell, 1978): Large scale mantle flow exerts forces normal to the slab. As mentioned earlier, sagging (Sleep, 1981) is essentially the same as this, because the normal force due to the mantle flow is, on the first order, proportional to the viscosity and the viscosity increases in the mesosphere. (2) Gravitational forces: Even without the flow pressure, the gravitational force itself unbends the slab when the slab dips too steeply (e.g., Marianas). (3) Overriding plate push: When an overriding plate is moving toward the trench, the slab tends to maintain a shallower dip angle, resulting in unbending.

CHAPTER V

WHERE ARE DOUBLE SEISMIC ZONES ?

After the early suggestions of the possible presence by Sykes (1966) and Tsumura (1973), double seismic zones have been found beneath Tohoku, Japan (e.g., Umino and Hasegawa, 1975; Hasegawa et al., 1978a,b; Yoshii, 1979a), Hokkaido, Japan (Suzuki et al., 1983), Kurile-Kamchatka (Veith, 1974; Stauder and Mualchin, 1976), eastern Aleutians (Reyners and Coles, 1982; Hause and Jacob, 1983), Peru (Isacks and Barazangi, 1977) and Tonga (this thesis). Suggestions of the possibilities beneath the Adak network (Engdahl and Scholz, 1977) and Marianas (Samowitz and Forsyth, 1981) are rather questionable (Topper, 1978; Engdahl and Fujita, 1981; Fujita and Kanamori, 1981).

Considering the results in the previous chapters, I will now discuss and speculate concerning where double seismic zones can exist.

What Controls the Stress States?

Compiling the focal mechanisms of ~ 250 intermediate depth earthquakes in the world, Fujita and Kanamori (1981) suggested that the age of the slab and the arc-normal convergence rate are the two major factors which control the stress state within the slab and the presence of a double seismic zone. Figure 1.4 is taken from Fujita and Kanamori (1981), in which they compared these two factors to the percentage of in-plate compressional events. Although the general effects of these two factors on the intermediate depth stress are as they describe, force balances and the dynamics of the subduction process are probably much more complicated, and it is questionable whether their line of argument can be applied to all of subduction zones in the world. It seems more appropriate to apply it to local problems (Forsyth, 1975; Shiono et al., 1980).

If the stress state of the slab is dominated by downdip compression (or downdip tension) in the intermediate depth range where unbending is taking place, it means that there is an additional uniaxial compressional (or tensional) strain whose magnitude is equal to or more than that of the maximum unbending strain. The average unbending strain rates between depths of 60 km and 150 km are estimated to be on the order of $10^{-15}s^{-1}$. Therefore, a uniaxial strain rate of $10^{-15}s^{-1}$ due to some force other than unbending is required for the slab to be totally compressional (or tensional) and not to have a double seismic zone.

A uniform uniaxial compressional (tensional) strain rate of ~ $10^{-15}s^{-1}$ corresponds to a shortening (elongation) of ~ 5%, when the slab subducts 160 km along dip with a velocity of 10 cm/yr. If this occurs, the slab would probably start either buckling (for compression) or necking (for tension) and would result in highly localized deformation. This is not occurring in most subduction zones, since seismicity shows that most slabs are smoothly continuous (except below Fiji and south America). Therefore neither compressional nor tensile stresses appears to completely dominate the stress state of the slab in the intermediate depth range where unbending is taking place and thus double seismic zones should exist in most subduction zones where deformation is taking place in a two dimensional manner. In other words, unbending strain rates dominate the deformation of slabs and the state of stress in the intermediate depth range and additional uniaxial strains simply shift the neutral stress plane of a double seismic zone higher or lower depending on their sign.

Where are Double Seismic Zones ?

Based on the above discussion, I speculate that double seismic zones should be found in most subduction zones. The observation of double seismic zones has been hampered by the lack of high quality local networks in most subduction zones and the fact that the time span of reliable observations of earthquake focal mechanisms is too short. In this section, utilizing Fujita and Kanamori's (1981) classification of subduction zones, the nature of the seismicity observed at present will be discussed in the light of the preceding argument.

Old and Fast Slabs

It is shown in the previous chapter that the thickness of a double seismic zone is strongly influenced by the thermal structure of the slab. It is well accepted that the thickness of oceanic lithosphere increases with its age (e.g., Parson and Sclater, 1977). Fast subduction also tends to keep the slab colder than the surrounding mantle. Therefore, the seismic zones (defined by some critical temperature) of old and fast slabs are expected to be thick. Most of the subduction zones where the presence of double seismic zones is known (Tohoku, Kuriles, Kamchatka, Tonga) are in this category. This seems to reflect the fact that the seismic zones are thick in these area - the thicker the seismic zones, the easier the double seismic zones can be

found.

Young and Slow Slabs (Stress Segmented ?)

Fujita and Kanamori (1981) pointed out that slabs in in this category (Ryukyu, Aleutians, Scotia) had thin seismic zones and that it became easier for tensile or compressive stresses to dominate short segments of the slab with no single segment exhibiting both. They called these slabs 'stress segmented', because short segments in close proximity show different stress states. Both in Ryukyu and Scotia, earthquakes studied from teleseismic data exhibit tensile and compressional stress features in the northern and southern parts, respectively, without spatial overlapping (Shiono et al., 1980; Forsyth, 1975).

The explanation of Fujita and Kanamori (1981) is certainly attractive and probably true to some extent, but uniaxial strain rates of the order of $10^{-15}s^{-1}$ are still required for either tensile or compressive stresses to completely dominate the stress fields there. Therefore, I suggest that tensional and compressional earthquakes are actually located in the lower and upper edges of seismic zones , respectively, and that if reliable data for smaller earthquakes become available, double seismic zones will be found.

House and Jacob (1983) showed a similar 'stress segmented' feature in the eastern Aleutians from teleseismic data, while Reyners and Coles (1982) and Hauksson et al. (1984) indicate the presence of a double seismic zone beneath the Shumagin Islands, which is located in the eastern edge of the area studied by House and Jacob (1983), from the data of a local network. This seems to support my interpretation of 'stress segmentation'. It should be noted that the composite focal mechanism solutions of the earthquakes of the double seismic zone beneath the Shumagin Islands exhibit a rather puzzling feature; the polarity of the stress state within the upper plane of the double seismic zone reversed within few years (Reyners and Coles, 1982; Hauksson et al., 1984). Since there was no major deformation in this time period, it is quite puzzling and certainly I have no explanation for it.

The seismicity beneath the Adak network (central Aleutians) is also puzzling. Engdahl and Scholz (1977) suggested the presence of a double seismic zone but the detailed study by Topper (1978) seems to deny the possibility and to show a single seismic zone. Since the data are obtained from a local network, a double seismic zone should show up if indeed one exists. Focal mechanism solutions show the predominance of a strike slip component, indicating that

the slab is neither strongly in compression nor tension along the dip (Topper, 1978). The only possible explanation for these features is that lateral deformation is dominating the mode of deformation in the slab, and the simple two dimensional view is not applicable.

Compressional or Tensional Slabs

In the deeper part of a double seismic zone (below ~ 100 km), the unbending strain rate can be lower (10^{-17}~$10^{-16}s^{-1}$). There, it may be possible for either compressional or tensile stresses to dominate the stress field without causing buckling or necking, and to erase the preexisting double seismic zone. The activity of deep (>300 km) earthquakes in Tonga is the highest and the compressional stress (or strain) is expected to be transmitted upward more than anywhere else in the world. The presence of the double seismic zone in Tonga, therefore, seems to indicate that the compressional stresses are not dominating the stress field of the intermediate part of the slab anywhere in the world at present. On this basis, I suggest that a double seismic zone exists beneath the Izu-Bonin arc (Ogasawara in Figure 1.4), where the general seismicity so far known is similar to that of Tonga (Fujita and Kanamori, 1981).

There is no evidence that tensile stress is not dominating the entire slab below ~ 100 km. So, the final question would be whether there are double seismic zones in the slabs where only tensional events are found. It is probably possible for the slabs beneath the Kermadec Islands and the New Hebrides to be tensional, because the slabs appear to be short and no strong resistance from below is expected. In these areas, the gravitational slab pull force may dominate and make slabs totally downdip tensional. Even in these cases, the shallower parts, where the unbending strain rate is higher than $10^{-15}s^{-1}$, would still exhibit double seismic zones, unless the slabs are really starting to break off.

Samowitz and Forsyth (1981) suggested the presence of a double seismic zone beneath the Marianas. Although there may be one, it is difficult to accept their result as evidence. After relocating earthquakes by a similar procedure to that employed in Chapter 3 (but without constraining depths), they found three events for their lower plane of the double seismic zone. They could determine the focal mechanism for only one of those three events, which is downdip tension as expected for the lower plane. ISC, however, reports a pP-P depth of 69 km for the event (event 3 in their Figure 8) and this is 25 km shallower than the depth estimated from their relocation. This suggests that all three events located in the lower plane can actually be

part of the upper plane and there may not be a double seismic zone. Although Fujita and Kanamori (1981) classified the slab beneath the Marianas as tensional, the focal mechanism solutions seem to suggest that lateral deformation may be dominating, reflecting the large curvature of the arc and there may not be a double seismic zone beneath the Marianas.

Fujita and Kanamori (1981) classified slabs beneath the South America continent as tensional. Isacks and Barazangi (1977), however, reported a double seismic zone beneath Peru where unbending of the slab is actually observable. A group of events studied by Malgrange and Madariaga (1983) in north-central Chile also indicates the possibility of the presence of a double seismic zone there. The observable amount of unbending beneath South America is probably due to the fact that the overriding plate (i.e., South American continent) is advancing toward the trench with a high velocity (~ 3cm/yr) as suggested in the previous chapter as one of the cause for unbending. This may be also resulting the dominance of tensional stress generally observed in this area.

From the preceding discussion, I suggest that double seismic zones should be observed in most subduction zones where deformation is mainly taking place in a two dimensional manner.

Concluding Remarks

The unbending strain rate, suggested as the cause of the double seismic zone in this thesis, is large, and it is expected to exist within all subducting slabs, if they are straight at some depth in the mantle. This strain due to unbending has to be released by some mechanism, and if it is released by earthquakes, a double seismic zone results. Throughout this thesis, I have tried to show that this is what is really happening in subducting slabs at intermediate depths.

At the end of this thesis, I would like to mention that the double seismic zone is a first order feature of the theory of plate tectonics. The fact that the oceanic plate subducts into the mantle, keeping its planar shape as indicated by a Wadati-Benioff zone, requires that there is a double seismic zone in the mantle. I hope that readers of this thesis now remember the time when they first learned about plate tectonics and saw the earthquakes in the Wadati-Benioff zone, saying,

'Plate tectonics !

Wadati-Benioff zones !! .....

Oh! There must be a double seismic zone !!!'.

Certainly I did not.


THIS IS HOPELESS!
A BLOODHOUND COULDN'T FIND ANYTHING OUT HERE!
I CAN'T FIND THE BALL!
WADDYA MEAN, PICK IT UP?!
HOW DO YOU EXPECT ANYONE TO FIND A BALL IN WEEDS LIKE THESE? WHAT DID YOU HIT IT OUT HERE FOR?
IT'S IMPOSSIBLE! OF COURSE I'M LOOKING! I SAID I CAN'T FIND IT! IF I COULD FIND IT, WOULD I STILL BE OUT HERE?
THIS IS HOPELESS! NOBODY COULD FIND ANYTHING OUT HERE! YOU COULDN'T FIND A BATTLESHIP OUT HERE IF IT..
..WAIT A MINUTE..
I FOUND IT..

APPENDIX A

LIST OF EARTHQUAKES IN CHAPTER II

Origin time and epicentral locations are from ISC bulletins. pwP denotes a depth corrected for a water depth. Classifications of mechanism types are given in Table 2.3. '?' represents events which could not be classified into any of these categories. Focal mechanism solutions are available for events with '0' and '1'. pwP depths are taken from Seno and Kroeger (1983) for events with '0'. Only focal mechanism types could be determined for events with '2'.

year	mo	day	origin time			lat	long	ISC	depth pP	pwP	m_b	# of stns	mech type	region
1964	1	8	3	45	32.4	37.05	140.54	88.0	0.	0.	0.	29	b	D
1964	1	25	22	48	54.5	36.65	141.04	53.0	0.	0.	4.6	35	a	D
1964	1	26	12	5	51.7	40.70	140.86	122.0	0.	0.	4.8	34	c2	A
1964	1	28	0	2	32.5	40.43	141.61	114.0	0.	0.	4.4	27	b	A
1964	2	5	11	30	16.9	36.47	141.02	54.0	53.0	51.5	5.6	246	d1	D
1964	2	7	12	58	53.1	39.85	142.86	38.0	39.0	35.0	5.7	202	d2	B
1964	2	14	6	56	1.4	36.84	142.04	37.0	25.0	15.8	4.8	91		D
1964	3	3	19	37	3.4	37.07	141.31	62.0	0.	0.	4.4	41	e	D
1964	3	6	2	36	36.3	40.99	142.57	37.0	15.0	9.0	4.9	96	?	A
1964	3	25	2	43	23.0	36.45	141.09	52.0	38.0	36.2	5.1	133	?	D
1964	4	16	1	4	29.5	36.99	142.90	6.0	32.0	12.9	5.2	200		D
1964	4	17	2	58	25.7	36.53	140.74	63.0	0.	0.	4.9	93	e	D
1964	4	29	10	43	2.2	40.93	140.81	125.0	0.	0.	4.2	23	c2	A
1964	5	3	1	54	34.5	40.20	142.03	71.0	66.0	66.0	4.7	101	c2	A
1964	5	8	23	53	21.5	40.19	142.37	54.0	40.0	38.0	4.8	95	?	A
1964	5	21	19	3	13.0	37.19	141.59	54.0	0.	0.	0.	52	a	D
1964	5	24	19	27	8.6	37.50	141.39	75.0	0.	0.	4.2	47	b	D
1964	5	30	14	30	44.9	36.23	141.29	41.0	41.0	37.0	5.7	290	d1	D
1964	6	20	16	59	10.9	40.23	142.31	57.0	41.0	39.0	4.9	92	?	A
1964	8	7	8	5	1.8	37.40	141.54	55.0	0.	0.	4.4	64	a	D
1964	8	19	20	3	19.7	39.14	141.87	109.0	0.	0.	3.9	23	t2	C
1964	8	19	20	3	19.7	39.14	141.87	109.0	0.	0.	3.9	23	t2	C
1964	9	24	17	59	52.5	40.07	142.14	95.0	0.	0.	3.9	39	b	A
1964	10	15	4	49	34.4	36.46	140.75	56.0	0.	0.	0.	20	a	D
1964	10	22	9	54	38.3	36.72	141.20	51.0	43.0	42.3	4.8	129	a	D
1964	10	30	19	34	31.1	38.87	141.72	68.0	0.	0.	4.0	22	c2	C
1964	11	11	19	17	1.0	38.21	140.15	140.0	0.	0.	4.3	35	b	D
1964	11	14	5	56	45.1	36.54	140.62	69.0	0.	0.	4.9	112	d2	D
1964	11	21	7	58	23.1	37.77	141.34	76.0	0.	0.	4.1	30	b	D
1964	11	23	18	55	32.4	36.56	140.94	58.0	0.	0.	4.8	54	e	D
1964	12	20	13	31	55.2	37.38	141.61	48.0	40.0	38.9	5.1	116	a	D
1964	12	20	23	14	44.1	36.50	140.61	67.0	0.	0.	4.6	41	a	D
1965	1	23	21	51	14.0	36.69	140.97	57.0	0.	0.	5.2	111	a	D
1965	2	16	12	24	9.3	38.97	142.01	55.0	0.	0.	5.4	211	d1	C
1965	2	21	22	28	27.4	37.47	139.69	133.0	0.	0.	4.6	61	c2	D
1965	3	13	20	56	7.2	38.51	142.13	54.0	0.	0.	5.0	40	a	C
1965	3	14	12	4	14.3	37.09	141.22	53.0	0.	0.	4.5	38	d2	D
1965	3	16	16	46	16.1	40.75	142.96	36.0	29.0	25.0	5.8	292	d0	A
1965	3	29	10	47	38.4	40.73	142.85	41.0	32.0	26.0	6.1	302	d1	A
1965	4	5	2	13	17.7	39.68	141.08	106.0	0.	0.	4.1	24	c2	B
1965	4	21	22	52	46.5	37.87	141.76	65.0	0.	0.	4.4	45	b	D
1965	4	27	2	18	23.3	38.50	142.21	51.0	0.	0.	4.8	28	a	C
1965	4	28	16	33	7.8	40.41	141.24	96.0	0.	0.	4.3	33	c2	A
1965	5	12	0	28	19.0	37.79	139.05	173.0	0.	0.	4.0	33	c2	D
1965	7	12	11	21	41.1	40.37	141.90	68.0	0.	0.	4.1	29	e	A
1965	7	31	7	36	28.0	36.10	142.42	15.0	34.0	13.4	5.0	130		D
1965	8	14	11	39	29.2	40.81	141.34	98.0	0.	0.	4.7	53	?	A
1965	9	10	19	25	52.6	37.36	141.20	77.0	67.0	66.6	5.1	164	c2	D
1965	9	17	12	59	17.9	36.36	141.42	55.0	35.0	29.5	5.0	135	a	D
1965	9	17	13	20	59.5	36.41	141.36	55.0	36.0	31.6	5.3	174	a	D

year	mo	day	origin time			lat	long	ISC	depth pP	pwP	m_b	# of stns	mech type	region
1965	9	17	14	22	38.8	36.36	141.41	45.0	38.0	32.5	5.4	169	a	D
1965	9	17	15	18	36.5	36.31	141.45	46.0	32.0	26.9	5.4	200	?	D
1965	9	17	16	21	19.3	36.35	141.38	41.0	37.0	31.9	6.1	344	d1	D
1965	9	17	16	59	20.8	36.49	141.28	57.0	0.	0.	4.8	69	a	D
1965	9	17	20	42	38.2	36.35	141.37	47.0	39.0	33.9	4.8	63	a	D
1965	9	22	22	8	1.4	36.44	141.37	45.0	47.0	43.0	5.8	306	d1	D
1965	9	25	14	37	13.3	39.65	143.32	25.0	32.0	24.0	5.3	187		B
1965	9	25	14	53	32.9	39.63	143.33	25.0	30.0	22.0	5.4	182		B
1965	11	14	5	54	14.7	36.61	141.08	55.0	41.0	39.9	5.5	213	d1	D
1965	12	27	4	7	25.1	36.35	142.06	39.0	36.0	22.4	4.7	83		D
1966	1	8	8	0	52.5	36.45	141.08	55.0	0.	0.	4.9	51	d2	D
1966	1	16	23	41	57.8	36.97	141.05	61.0	52.0	51.6	4.6	71	d2	D
1966	1	27	12	0	30.8	39.69	141.04	106.0	0.	0.	4.8	54	c2	B
1966	2	1	11	51	21.1	37.11	139.10	172.0	0.	0.	4.0	28	?	D
1966	2	18	0	27	53.0	36.50	140.63	66.0	0.	0.	5.1	128	d2	D
1966	3	14	6	38	4.5	36.68	141.07	63.0	56.0	55.3	5.0	103	e	D
1966	4	2	22	43	22.3	38.54	142.10	48.0	42.0	40.0	5.1	138	a	C
1966	4	3	4	43	39.2	36.66	141.06	52.0	45.0	44.3	5.6	244	d1	D
1966	4	29	2	25	3.5	36.70	140.27	92.0	83.0	83.0	4.7	86	c2	D
1966	5	2	10	34	38.3	41.01	141.29	127.0	0.	0.	4.2	40	t2	A
1966	5	22	16	43	16.8	36.55	140.93	57.0	0.	0.	4.6	51	e	D
1966	6	9	13	8	12.5	39.82	141.68	81.0	74.0	74.0	4.6	47	?	B
1966	6	23	5	39	17.3	38.22	139.67	153.0	0.	0.	4.2	37	c2	D
1966	6	23	21	51	55.8	38.06	141.69	77.0	71.0	71.0	5.0	117	t2	C
1966	7	18	4	39	21.6	38.37	141.87	55.0	55.0	54.0	4.9	79	d2	C
1966	7	20	11	21	35.8	39.01	142.51	33.0	34.0	30.0	4.7	52	a	C
1966	7	29	22	7	59.5	36.32	141.48	48.0	37.0	31.5	4.7	65	?	D
1966	8	19	12	46	23.8	36.44	141.84	28.0	29.0	20.2	5.2	166		D
1966	8	27	12	58	56.1	39.29	141.29	102.0	94.0	94.0	4.2	64	c2	B
1966	9	18	0	35	19.4	37.09	140.73	95.0	83.0	83.0	4.3	67	t2	D
1966	11	1	2	22	46.3	40.26	140.08	177.0	0.	0.	4.4	46	t2	B
1966	11	2	9	14	8.9	37.60	141.51	86.0	0.	0.	4.1	20	b	D
1966	11	19	5	19	55.3	37.55	141.48	59.0	50.0	49.3	5.3	155	a	D
1966	11	19	7	31	16.4	40.43	142.50	41.0	41.0	37.0	4.7	100	a	A
1966	12	8	14	5	51.6	39.77	141.28	99.0	0.	0.	4.7	43	c2	B
1966	12	17	18	45	49.4	37.25	141.35	74.0	0.	0.	4.3	32	b	D
1966	12	27	1	22	17.7	37.19	141.08	59.0	57.0	57.0	5.5	222	d2	D
1967	1	9	21	58	26.8	36.88	141.05	55.0	0.	0.	4.3	20	t2	D
1967	1	17	11	59	31.5	38.33	142.20	39.0	43.0	40.0	5.9	396	d1	C
1967	1	17	12	26	21.1	38.22	142.26	40.0	41.0	38.0	4.7	68	a	C
1967	2	20	0	35	22.7	41.34	140.12	169.0	0.	0.	4.5	41	c2	A
1967	5	7	21	50	13.2	37.84	141.46	94.0	0.	0.	4.3	33	t2	D
1967	5	17	9	34	43.3	38.17	142.18	43.0	47.0	44.3	4.5	71	?	C
1967	7	2	1	6	15.3	36.48	140.78	60.0	74.0	73.6	4.5	38	?	D
1967	7	8	0	42	17.5	38.30	141.72	62.0	56.0	56.0	4.3	49	d2	C
1967	7	17	12	36	10.0	38.26	142.11	56.0	46.0	44.0	4.8	101	a	C
1967	7	18	16	59	22.0	40.15	142.47	52.0	46.0	43.0	4.7	95	a	A
1967	8	2	13	36	38.5	36.58	140.47	69.0	0.	0.	0.	26	c2	D
1967	8	8	16	5	59.0	37.08	141.23	60.0	0.	0.	4.3	70	d2	D
1967	8	12	4	30	40.5	38.39	142.02	75.0	78.0	77.0	5.3	179	t1	C

year	mo	day	origin time			lat	long	ISC	depth pP	pwP	m_b	# of stns	mech type	region
1967	8	17	14	31	56.2	39.36	142.43	89.0	87.0	84.0	4.6	88	t2	B
1967	8	19	12	14	21.0	40.85	143.58	36.0	41.0	34.0	5.0	94		A
1967	9	19	3	28	56.4	37.38	141.75	40.0	38.0	36.5	4.8	103	a	D
1967	10	10	6	47	0.4	36.65	141.12	50.0	44.0	43.3	4.8	107	a	D
1967	11	1	19	17	22.8	37.17	141.45	54.0	44.0	43.6	4.9	116	a	D
1967	11	4	13	26	47.6	37.39	141.71	43.0	41.0	39.5	5.5	300	d1	D
1967	11	19	12	7	0.4	36.47	141.17	48.0	42.0	39.8	5.7	309	d1	D
1967	12	30	2	27	52.3	38.24	142.06	57.0	0.	0.	4.9	52	c2	C
1968	1	2	11	46	1.3	40.15	141.03	115.0	0.	0.	4.3	37	c2	B
1968	1	5	8	22	40.7	36.75	140.37	93.0	0.	0.	3.9	38	c2	D
1968	1	9	15	38	16.2	36.96	140.05	133.0	0.	0.	4.5	46	t2	D
1968	1	18	23	36	23.5	41.08	142.67	59.0	0.	0.	4.6	65	?	A
1968	1	23	19	16	30.6	40.70	142.83	50.0	41.0	35.0	4.8	77	?	A
1968	2	25	20	0	31.4	37.63	141.51	65.0	63.0	62.3	5.4	225	a	D
1968	3	4	12	7	33.3	36.63	140.91	56.0	0.	0.	4.0	22	d2	D
1968	3	17	0	33	32.4	39.31	141.76	68.0	0.	0.	4.2	35	c2	B
1968	3	22	20	34	44.0	37.49	142.47	8.0	21.0	17.0	5.3	189		D
1968	4	6	18	28	4.2	37.74	141.04	78.0	0.	0.	4.1	31	c2	D
1968	4	7	2	47	42.5	38.39	141.75	58.0	51.0	51.0	4.9	94	e	C
1968	4	7	10	59	32.6	36.49	140.60	61.0	0.	0.	0.	26	d2	D
1968	4	21	8	34	38.6	38.68	142.99	33.0	20.0	20.0	5.4	293	d0	C
1968	4	22	21	40	40.8	36.57	140.90	61.0	68.0	67.6	4.3	53	e	D
1968	4	26	13	21	11.1	37.38	141.63	49.0	45.0	43.9	5.2	164	a	D
1968	5	1	8	43	44.4	38.65	143.22	13.0	24.0	16.0	5.4	243	d1	C
1968	5	1	19	12	53.3	40.87	142.68	15.0	19.0	12.0	4.9	149	d2	A
1968	5	16	0	48	57.0	40.86	143.38	9.0	8.0	1.0	6.1	381	d1	A
1968	5	16	1	4	55.0	41.00	143.22	29.0	34.0	27.0	5.7	66		A
1968	5	16	1	4	55.0	41.00	143.22	29.0	34.0	27.0	5.7	66		A
1968	5	16	4	15	47.0	40.63	142.73	59.0	0.	0.	4.5	71	?	A
1968	5	16	5	44	38.0	40.43	143.75	14.0	30.0	19.0	4.7	107		A
1968	5	16	7	28	3.9	40.22	143.34	36.0	28.0	22.0	4.7	93		A
1968	5	16	8	19	59.0	41.03	142.84	44.0	48.0	41.8	5.0	119	?	A
1968	5	16	8	46	40.8	40.82	143.30	38.0	35.0	28.0	4.9	121		A
1968	5	16	13	52	41.1	40.20	143.58	0.	31.0	23.0	3.1	31		A
1968	5	16	14	3	20.0	39.80	142.70	0.	41.0	37.0	5.3	33	?	B
1968	5	16	16	21	53.0	39.82	143.70	25.0	28.0	18.0	4.9	84		A
1968	5	16	17	21	51.8	41.11	142.57	42.0	39.0	33.5	4.7	80	?	A
1968	5	16	18	43	21.6	40.78	142.15	60.0	55.0	52.0	5.8	309	d2	A
1968	5	16	20	12	34.2	40.70	142.06	87.0	0.	0.	4.2	22	?	A
1968	5	16	21	25	58.1	40.89	143.18	46.0	38.0	31.0	4.9	131		A
1968	5	16	21	28	28.1	40.91	143.44	0.	33.0	26.0	4.7	27		A
1968	5	16	22	56	55.0	39.89	143.57	21.0	26.0	18.0	4.4	35		A
1968	5	16	23	51	36.4	39.60	143.29	40.0	30.0	22.0	4.7	56		B
1968	5	17	0	24	28.3	40.26	142.71	62.0	0.	0.	4.2	68	t2	A
1968	5	17	2	42	51.0	40.57	142.60	50.0	52.0	47.0	4.3	20	?	A
1968	5	17	4	36	30.0	39.32	143.10	49.0	33.0	26.0	4.5	54		B
1968	5	17	5	19	34.8	39.68	143.39	29.0	31.0	23.0	4.7	111		B
1968	5	17	6	24	33.2	39.15	143.58	22.0	29.0	16.0	4.9	149		B
1968	5	17	10	42	44.3	39.69	143.46	18.0	35.0	27.0	5.3	261		B
1968	5	17	13	59	52.9	40.27	143.25	34.0	23.0	17.0	4.5	44		A

year	mo	day	origin time			lat	long	ISC	depth pP	pwP	m_b	# of stns	mech type	region
1968	5	17	14	53	10.3	39.65	143.65	26.0	27.0	17.0	4.9	133		B
1968	5	17	16	2	24.1	40.59	144.08	0.	32.0	15.0	5.1	195		A
1968	5	17	18	3	44.0	39.94	143.30	35.0	26.0	20.0	4.3	32		A
1968	5	17	18	17	7.1	39.68	143.07	26.0	24.0	18.0	5.4	238	d2	B
1968	5	17	19	48	57.0	39.67	143.19	25.0	26.0	19.0	4.8	95		B
1968	5	17	22	36	13.0	40.65	143.80	17.0	30.0	19.0	5.0	165		A
1968	5	17	23	17	12.8	40.28	143.31	34.0	31.0	25.0	5.0	95		A
1968	5	18	15	33	45.7	40.72	143.20	47.0	27.0	20.0	4.9	94		A
1968	5	19	16	19	30.2	36.80	141.70	39.0	35.0	31.3	4.6	85	?	D
1968	5	19	22	16	47.5	40.91	143.21	35.0	44.0	37.0	5.2	233		A
1968	5	20	2	31	45.4	40.20	142.42	54.0	48.0	45.0	4.7	101	a	A
1968	5	20	3	16	19.9	40.09	143.91	0.	28.0	13.0	5.5	238		A
1968	5	20	4	37	23.0	40.22	143.93	4.0	28.0	13.0	4.0	95		A
1968	5	20	5	35	41.8	39.22	143.27	37.0	33.0	24.0	4.6	74		B
1968	5	20	6	15	17.6	40.61	142.78	39.0	42.0	36.0	4.3	31	?	A
1968	5	20	6	53	31.3	40.40	143.84	3.0	31.0	18.0	5.3	119		A
1968	5	20	14	31	50.0	40.61	142.50	36.0	39.0	35.0	4.4	54	?	A
1968	5	22	19	29	26.9	40.27	142.34	50.0	44.0	42.0	5.5	295	a	A
1968	5	23	23	56	20.0	40.25	143.75	5.0	26.0	15.0	4.9	125		A
1968	5	24	14	6	23.4	40.91	143.11	27.0	23.0	22.0	5.7	331	d0	A
1968	5	24	21	34	23.0	40.65	143.94	12.0	28.0	13.0	4.6	80		A
1968	5	25	11	52	56.2	40.16	143.17	26.0	30.0	25.0	5.4	249	d2	A
1968	5	25	14	19	1.2	40.72	143.37	0.	28.0	21.0	5.1	104		A
1968	5	26	17	41	40.8	40.17	142.34	54.0	44.0	42.0	4.9	124	d2	A
1968	5	26	22	59	14.8	40.69	143.43	43.0	39.0	32.0	4.8	84		A
1968	5	27	6	17	55.1	40.40	141.95	55.0	49.0	49.0	4.5	31	?	A
1968	5	28	14	30	19.9	40.98	142.98	38.0	42.0	35.0	4.5	38		A
1968	5	28	20	34	52.0	37.75	141.89	56.0	0.	0.	4.2	26	a	D
1968	5	28	23	0	39.3	40.91	142.00	60.0	64.0	61.0	4.5	35	?	A
1968	5	30	9	4	20.4	40.72	142.25	60.0	66.0	63.0	4.3	32	?	A
1968	6	1	3	58	12.9	38.33	141.84	58.0	56.0	55.0	4.4	34	d2	C
1968	6	1	10	31	49.3	40.22	142.34	48.0	48.0	46.0	5.5	249	d2	A
1968	6	1	19	46	46.1	36.67	140.19	130.0	0.	0.	0.	23	?	D
1968	6	6	18	21	24.6	40.63	142.40	75.0	73.0	69.0	4.7	109	a	A
1968	6	7	22	45	55.6	40.94	142.28	53.0	0.	0.	4.5	26	e	A
1968	6	8	2	44	34.0	40.67	143.76	10.0	30.0	20.0	4.9	138		A
1968	6	10	2	38	42.9	40.17	142.35	52.0	50.0	48.0	4.4	68	?	A
1968	6	12	13	41	49.4	39.47	142.89	31.0	31.0	25.0	6.0	378	d1	B
1968	6	12	14	17	26.0	39.25	142.99	32.0	30.0	23.0	5.2	95		B
1968	6	12	14	38	13.0	39.36	142.86	39.0	32.0	26.0	5.0	97		B
1968	6	12	14	44	7.0	39.40	142.50	0.	29.0	25.0	4.4	30	?	B
1968	6	12	15	8	53.4	39.51	143.04	37.0	29.0	22.0	5.2	111		B
1968	6	12	15	23	52.5	39.50	143.07	26.0	29.0	22.0	5.1	115		B
1968	6	12	15	48	59.7	39.30	143.05	29.0	28.0	21.0	5.1	150		B
1968	6	12	16	23	20.1	39.43	143.08	47.0	27.0	20.0	4.8	66		B
1968	6	12	16	29	12.0	39.20	143.29	20.0	24.0	15.0	4.4	62		B
1968	6	12	17	23	18.8	39.50	143.10	0.	22.0	15.0	0.	48		B
1968	6	12	17	52	0.6	39.20	142.96	23.0	28.0	21.0	5.3	205		B
1968	6	12	18	48	54.1	39.36	142.84	40.0	30.0	24.0	4.7	99		B
											.0	125		B

year	mo	day	origin time			lat	long	ISC	depth pP	pwP	m_b	# of stns	mech type	region
1968	6	12	19	38	43.4	39.23	142.81	38.0	31.0	24.0	4.6	39		B
1968	6	12	19	48	29.1	39.37	142.91	34.0	31.0	25.0	4.3	40		B
1968	6	13	0	4	59.6	39.53	143.07	13.0	25.0	18.0	5.3	203		B
1968	6	13	0	42	15.2	39.29	142.85	35.0	30.0	24.0	4.7	112		B
1968	6	13	1	42	55.7	39.47	143.13	36.0	27.0	20.0	4.6	64		B
1968	6	13	2	5	42.0	39.51	142.94	13.0	22.0	16.0	5.2	246		B
1968	6	13	11	56	21.1	39.24	143.09	15.0	19.0	12.0	5.3	228		B
1968	6	13	14	56	15.1	39.50	143.00	18.0	21.0	15.0	5.1	146		B
1968	6	13	21	10	34.9	39.43	142.97	22.0	32.0	26.0	5.5	275		B
1968	6	14	0	46	10.0	39.54	142.70	59.0	25.0	21.0	4.7	80	b	B
1968	6	14	1	36	38.6	39.48	142.77	40.0	32.0	27.0	4.5	37		B
1968	6	14	3	18	17.2	39.48	142.83	0.	31.0	25.0	5.0	185	d2	B
1968	6	14	6	5	3.5	39.44	142.73	34.0	26.0	20.0	4.6	79		B
1968	6	14	11	52	38.3	39.36	142.93	24.0	28.0	22.0	5.4	224	d2	B
1968	6	15	3	31	16.4	39.43	142.88	8.0	18.0	12.0	5.3	196		B
1968	6	17	16	56	12.5	40.19	143.84	1.0	29.0	16.0	5.4	204		A
1968	6	17	18	57	29.9	38.74	143.60	0.	34.0	22.0	4.9	208		C
1968	6	18	8	56	27.3	39.53	141.82	75.0	0.	0.	4.4	65	c2	B
1968	6	19	1	38	17.1	39.51	143.04	29.0	31.0	24.0	5.3	205		B
1968	6	20	8	15	8.8	40.12	142.33	59.0	45.0	43.0	4.3	66	a	A
1968	6	22	1	12	33.3	40.31	143.68	29.0	19.0	15.0	5.6	283	d0	A
1968	6	25	23	33	15.9	39.60	143.57	2.0	30.0	20.0	5.1	178		B
1968	6	27	17	11	57.6	40.22	142.39	54.0	47.0	44.0	4.7	101	a	A
1968	6	28	14	23	59.7	40.43	143.59	17.0	27.0	18.0	4.8	107		A
1968	6	30	14	48	39.5	38.82	142.70	35.0	22.0	17.0	4.9	126		C
1968	7	5	11	28	13.0	38.54	142.14	44.0	46.0	44.0	6.0	380	d1	C
1968	7	7	13	16	12.3	39.45	142.84	9.0	22.0	16.0	5.0	144		B
1968	7	8	0	18	40.2	40.80	143.28	42.0	34.0	27.0	4.7	95		A
1968	7	8	3	53	34.2	41.03	141.87	72.0	0.	0.	4.5	60	e	A
1968	7	9	8	6	9.0	39.50	142.90	38.0	34.0	28.0	4.5	115		B
1968	7	12	0	44	37.3	39.54	143.20	0.	30.0	22.0	5.8	362		B
1968	7	12	1	30	32.0	39.62	143.10	29.0	28.0	21.0	4.2	30		B
1968	7	12	3	56	24.0	39.59	143.28	1.0	27.0	19.0	5.6	321		B
1968	7	18	11	20	57.8	40.28	143.72	20.0	30.0	20.0	4.6	123		A
1968	7	23	12	5	50.0	39.40	142.90	125.0	23.0	17.0	3.9	22		B
1968	7	23	18	9	18.2	39.93	143.51	23.0	27.0	20.0	4.8	115		A
1968	7	23	23	2	37.1	40.33	143.41	23.0	24.0	17.0	5.3	216		A
1968	7	24	16	25	45.1	40.19	142.45	51.0	46.0	43.0	4.3	35	a	A
1968	7	28	14	3	37.6	40.79	142.47	53.0	51.0	46.0	4.7	74	a	A
1968	8	8	4	55	9.5	36.40	141.50	36.0	37.0	31.1	5.5	276	d1	D
1968	8	16	10	39	16.7	38.57	143.39	0.	229.0	13.0	5.4	265	d1	C
1968	8	25	9	7	29.7	40.09	143.37	14.0	27.0	22.0	5.5	262		A
1968	8	25	9	13	48.1	40.05	143.37	27.0	22.0	17.0	5.4	160		A
1968	8	30	2	44	53.5	40.04	142.81	43.0	36.0	32.0	5.1	176	d2	A
1968	8	31	16	45	26.0	39.83	143.66	3.0	27.0	18.0	4.7	88		A
1968	9	3	7	1	35.3	37.93	141.88	65.0	77.0	76.0	5.2	167	t2	D
1968	9	15	10	50	13.4	40.87	143.30	26.0	32.0	25.0	5.4	268		A
1968	9	20	13	53	36.1	40.69	143.61	28.0	29.0	20.0	4.8	95		A
1968	9	24	3	34	46.0	40.30	143.70	4.0	31.0	21.0	5.2	169		A
1968	9	24	4	46	1.5	40.31	143.80	10.0	27.0	16.0	5.1	120		A

year	mo	day	origin time			lat	long	ISC	depth pP	pwP	m_b	# of stns	mech type	region
1968	10	14	9	11	26.0	38.38	142.22	47.0	42.0	39.0	5.2	170	a	C
1968	10	17	13	28	24.0	39.40	141.98	63.0	58.0	58.0	4.5	84	a	B
1968	11	6	1	28	44.7	40.29	143.76	17.0	28.0	17.0	4.6	75		A
1968	11	7	9	19	6.5	40.18	142.31	55.0	53.0	51.0	5.5	186	d2	A
1968	11	11	14	41	15.1	40.12	143.25	31.0	46.0	41.0	5.5	135		A
1968	11	12	14	4	33.9	40.09	142.70	43.0	41.0	37.0	5.1	146	a	A
1968	11	13	18	41	47.2	40.17	142.65	40.0	46.0	42.0	5.6	300	d2	A
1968	11	17	12	59	9.8	39.71	143.24	36.0	30.0	22.0	4.7	129		B
1968	11	18	6	2	32.1	37.36	141.59	56.0	41.0	39.9	4.9	78	a	D
1968	11	23	5	22	12.8	40.16	142.35	57.0	45.0	43.0	4.5	81	a	A
1968	11	24	21	20	59.9	40.30	142.39	49.0	46.0	43.0	5.9	344	d1	A
1968	11	28	7	0	9.1	40.15	142.47	54.0	45.0	42.0	5.1	169	a	A
1968	11	30	18	13	18.5	40.22	142.31	56.0	48.0	46.0	4.3	41	a	A
1968	12	21	12	58	14.0	40.66	143.82	26.0	30.0	19.0	4.8	107		A
1969	1	1	15	35	17.0	40.12	142.38	60.0	46.0	44.0	4.5	70	?	A
1969	1	14	16	2	0.6	37.53	141.59	58.0	48.0	47.3	5.0	104	a	D
1969	2	14	13	29	12.3	39.43	143.15	0.	32.0	25.0	4.4	45		B
1969	2	17	7	29	8.1	37.50	140.87	96.0	83.0	83.0	4.8	97	c2	D
1969	3	8	10	20	9.9	41.35	139.71	174.0	180.0	178.2	5.5	230	c1	A
1969	3	10	15	52	45.1	36.46	140.69	63.0	0.	0.	4.2	35	?	D
1969	3	16	15	54	16.7	38.57	142.83	33.0	35.0	30.0	5.5	274	t0	C
1969	3	16	15	57	40.5	38.52	142.71	49.0	46.0	41.0	5.2	54		C
1969	3	16	16	57	7.3	40.97	143.14	41.0	29.0	22.0	4.4	65		A
1969	3	21	3	5	9.3	40.37	143.81	14.0	22.0	10.0	5.5	163		A
1969	4	9	12	57	24.8	36.84	139.77	117.0	109.0	109.0	5.5	263	?	D
1969	4	15	17	30	53.0	39.86	143.58	5.0	24.0	16.0	5.4	228		A
1969	4	17	4	56	13.0	39.66	143.56	11.0	16.0	7.0	5.1	163		B
1969	4	19	1	23	21.5	37.93	141.81	59.0	46.0	45.0	4.6	56	a	D
1969	4	19	15	18	9.3	40.74	142.27	62.0	64.0	61.0	4.7	82	a	A
1969	4	25	21	35	22.7	39.81	143.23	36.0	31.0	24.0	4.6	65		B
1969	5	2	20	40	10.5	40.95	143.16	44.0	53.0	46.0	4.8	109		A
1969	5	2	22	45	44.0	40.18	142.45	57.0	48.0	45.0	4.9	117	a	A
1969	5	13	14	19	43.5	36.44	140.72	69.0	0.	0.	5.3	119	a	D
1969	5	16	2	14	15.7	39.75	141.73	88.0	0.	0.	4.0	28	?	B
1969	5	20	6	39	0.	38.37	141.69	71.0	0.	0.	4.3	50	c2	C
1969	5	20	14	21	49.8	40.99	141.88	73.0	0.	0.	4.4	41	e	A
1969	5	22	9	36	41.0	38.26	143.26	22.0	23.0	13.0	4.6	65		C
1969	5	22	11	40	49.7	36.52	140.57	67.0	0.	0.	4.6	53	a	D
1969	5	28	22	25	38.1	40.11	142.02	63.0	0.	0.	4.7	37	e	A
1969	6	6	15	48	8.4	36.55	141.19	62.0	0.	0.	0.	25	e	D
1969	6	10	16	41	39.7	38.70	141.61	73.0	0.	0.	0.	30	b	C
1969	6	12	7	41	21.3	40.37	143.78	4.0	26.0	14.0	5.2	215		A
1969	6	20	6	41	5.8	38.52	142.00	81.0	81.0	80.0	5.3	193	b	C
1969	6	20	15	37	49.6	40.81	142.19	59.0	62.0	59.0	5.5	233	d2	A
1969	6	23	5	57	8.5	37.31	141.62	52.0	40.0	38.9	5.1	154	a	D
1969	7	14	15	55	54.5	39.91	143.56	34.0	32.0	24.0	4.5	55		A
1969	7	21	19	44	12.5	39.50	143.19	22.0	25.0	18.0	5.0	122		B
1969	7	23	13	14	35.0	37.35	141.62	49.0	44.0	42.9	5.4	217	a	D
1969	8	5	18	34	32.5	37.59	140.71	121.0	109.0	109.0	5.1	129	t2	D
1969	8	21	13	21	55.4	36.42	141.03	51.0	51.0	49.2	4.5	69	a	D

year	mo	day	origin time			lat	long	ISC	depth pP	pwP	m_b	# of stns	mech type	region
1969	8	23	6	39	25.0	39.76	144.23	0.	38.0	12.0	5.2	167		A
1969	8	24	4	50	11.1	39.86	144.23	0.	33.0	7.0	4.4	26		A
1969	8	24	22	3	9.6	39.62	144.00	0.	89.0	71.0	5.2	186		B
1969	9	24	1	36	43.2	37.43	140.72	88.0	0.	0.	3.6	20	?	D
1969	10	18	1	14	1.0	39.29	141.46	119.0	114.0	114.0	5.4	258	t1	B
1969	10	30	0	5	39.8	37.54	140.16	158.0	152.0	152.0	5.0	163	?	D
1969	10	31	7	0	13.3	37.10	142.19	39.0	36.0	28.7	5.1	188		D
1969	11	2	3	30	24.6	36.41	140.61	62.0	0.	0.	0.	21	d2	D
1969	11	15	17	50	19.5	36.62	141.17	51.0	0.	0.	4.4	46	a	D
1969	12	12	1	13	14.7	40.19	143.80	0.	30.0	18.0	5.1	178		A
1970	1	4	20	42	13.0	39.01	142.37	61.0	56.0	52.0	4.5	51	b	C
1970	1	8	18	37	33.5	37.08	141.15	67.0	0.	0.	4.0	32	a	D
1970	2	4	10	17	46.5	36.47	140.74	64.0	0.	0.	4.9	96	d2	D
1970	2	15	4	1	35.4	37.41	141.32	69.0	58.0	57.6	4.5	110	c2	D
1970	2	25	7	56	58.2	40.04	142.89	46.0	45.0	41.0	5.0	122		A
1970	3	7	18	52	22.3	37.10	141.54	49.0	43.0	41.9	5.0	113	b	D
1970	3	9	0	50	2.9	39.61	143.45	9.0	17.0	8.0	5.2	217		B
1970	3	23	0	20	55.1	40.18	140.31	147.0	145.0	145.0	5.5	288	c1	B
1970	3	28	7	33	56.5	41.10	141.76	72.0	0.	0.	4.7	32	?	A
1970	4	1	14	23	24.6	39.78	141.91	75.0	67.0	67.0	5.8	303	c1	B
1970	4	12	8	54	17.6	38.87	140.82	137.0	130.0	130.0	4.8	114	?	C
1970	4	14	6	28	51.1	40.48	143.59	17.0	19.0	10.0	4.7	103		A
1970	4	16	15	19	1.0	38.22	141.75	67.0	53.0	53.0	4.2	49	b	C
1970	5	4	22	10	16.3	39.74	142.28	52.0	0.	0.	4.7	84	e	B
1970	5	5	2	37	56.4	40.11	142.35	59.0	46.0	44.0	4.2	53	?	A
1970	5	25	16	15	34.0	37.08	141.20	62.0	0.	0.	4.6	77	c2	D
1970	5	27	19	5	37.9	40.29	142.98	18.0	16.0	11.0	5.7	336		A
1970	5	27	22	35	48.9	40.24	143.08	29.0	30.0	25.0	5.6	268		A
1970	5	27	23	56	38.8	40.33	143.02	25.0	30.0	25.0	5.4	247		A
1970	6	7	17	53	46.7	40.36	142.11	64.0	57.0	56.0	4.4	44	a	A
1970	6	20	2	24	25.3	40.21	143.31	30.0	30.0	24.0	5.1	123		A
1970	7	11	14	28	15.3	36.52	140.62	63.0	0.	0.	5.2	155	d2	D
1970	7	17	9	21	7.0	40.89	141.65	98.0	0.	0.	4.5	38	?	A
1970	7	27	11	4	47.6	36.44	141.26	63.0	0.	0.	0.	30	c2	D
1970	8	1	19	6	30.7	40.07	142.35	54.0	0.	0.	4.3	21	?	A
1970	8	30	12	4	39.5	40.26	142.33	54.0	0.	0.	4.4	49	?	A
1970	8	30	22	55	18.7	39.73	142.17	81.0	0.	0.	0.	27	c2	B
1970	9	14	9	44	54.0	38.77	142.27	46.0	46.0	43.0	5.6	361	d1	C
1970	9	15	5	39	49.0	38.80	142.14	57.0	49.0	47.0	4.5	39	a	C
1970	10	18	3	37	53.2	38.79	142.30	50.0	44.0	41.0	4.2	41	a	C
1970	10	21	1	14	52.3	40.14	142.78	42.0	44.0	40.0	4.7	109	?	A
1970	10	26	19	22	27.8	39.96	141.61	81.0	0.	0.	4.2	39	a	B
1970	11	1	20	21	41.3	39.64	141.20	123.0	117.0	117.0	4.9	112	c2	B
1970	11	26	20	42	38.4	37.58	141.38	63.0	0.	0.	0.	23	b	D
1970	12	18	3	16	11.8	40.21	142.16	58.0	0.	0.	0.	21	?	A
1970	12	20	21	19	56.7	39.29	141.90	71.0	0.	0.	0.	44	c2	B
1971	1	6	6	4	22.7	36.44	141.09	54.0	43.0	41.2	5.4	242	a	D
1971	1	20	21	2	45.7	36.47	141.11	52.0	0.	0.	4.6	58	e	D
1971	1	27	8	31	8.4	37.74	141.69	87.0	0.	0.	0.	23	b	D
1971	1	29	16	42	56.8	40.34	141.60	68.0	61.0	61.0	5.1	156	b	A

year	mo	day	origin time			lat	long	ISC	depth pP	pwP	m_b	# of stns	mech type	region
1971	1	30	5	36	30.3	40.03	141.16	105.0	0.	0.	4.1	24	t2	B
1971	2	17	5	13	1.8	40.18	142.37	57.0	48.0	46.0	5.2	173	a	A
1971	2	27	8	56	35.6	38.35	141.83	62.0	56.0	55.0	5.2	133	d2	C
1971	2	27	16	32	48.4	40.72	143.56	25.0	33.0	25.0	5.2	167		A
1971	3	4	7	48	39.4	40.76	143.53	34.0	36.0	28.0	5.1	133		A
1971	3	6	1	22	35.2	39.79	141.80	68.0	0.	0.	4.4	21	?	B
1971	3	13	2	59	38.8	40.19	142.38	54.0	48.0	45.0	5.1	174	a	A
1971	3	17	16	8	13.6	40.17	142.33	60.0	0.	0.	4.3	52	a	A
1971	3	20	9	34	2.5	40.97	141.84	75.0	0.	0.	4.5	41	?	A
1971	3	22	10	40	4.1	37.23	142.13	43.0	42.0	37.6	5.3	194		D
1971	3	25	16	19	51.6	38.49	142.15	50.0	41.0	39.0	5.6	213	d1	C
1971	4	4	18	39	39.0	38.41	142.18	49.0	42.0	40.0	5.8	350	d1	C
1971	5	15	7	43	15.6	40.65	143.80	20.0	28.0	17.0	0.	82		A
1971	6	3	11	4	11.7	37.07	141.42	65.0	0.	0.	4.1	37	a	D
1971	6	14	10	17	27.7	37.84	140.55	109.0	0.	0.	0.	32	c2	D
1971	6	21	18	23	55.8	40.36	141.43	90.0	0.	0.	4.2	26	c2	A
1971	6	26	8	56	24.7	40.17	142.46	57.0	46.0	43.0	4.9	115	a	A
1971	6	26	13	36	10.2	40.34	142.20	58.0	0.	0.	4.4	26	?	A
1971	7	7	17	41	24.9	36.86	141.26	61.0	0.	0.	4.6	48	c2	D
1971	7	19	12	23	10.2	39.19	143.21	41.0	32.0	24.0	4.8	82		B
1971	9	8	7	25	14.5	37.19	141.41	52.0	44.0	43.6	5.5	238	d2	D
1971	9	14	17	3	8.0	38.18	140.81	102.0	0.	0.	4.1	25	c2	D
1971	9	15	14	55	7.3	39.17	143.39	30.0	12.0	16.0	5.8	317	d0	B
1971	9	16	18	51	42.9	39.22	143.54	0.	27.0	16.0	5.2	146		B
1971	9	20	5	15	19.0	39.34	143.44	31.0	25.0	16.0	4.3	42		B
1971	9	21	8	43	32.0	37.34	138.72	186.0	182.0	182.0	5.4	260	c2	D
1971	9	23	2	53	20.2	40.29	142.69	56.0	58.0	54.0	4.5	88	?	A
1971	9	24	1	9	59.5	39.42	143.28	13.0	20.0	12.0	5.7	333		B
1971	10	12	5	24	55.7	36.81	141.78	57.0	0.	0.	4.8	43		D
1971	10	23	5	38	37.1	36.21	141.71	45.0	37.0	30.4	4.8	101		D
1971	10	29	20	25	47.8	37.36	141.59	54.0	43.0	41.9	4.9	82	a	D
1971	11	3	8	7	32.6	38.96	141.32	86.0	0.	0.	0.	33	b	C
1971	11	15	21	39	5.6	36.47	141.08	53.0	0.	0.	4.6	57	a	D
1972	1	19	17	40	18.4	39.70	143.38	39.0	32.0	24.0	4.5	42		B
1972	2	7	5	7	51.4	39.68	143.45	17.0	44.0	36.0	4.9	137		B
1972	2	8	18	56	46.6	40.07	142.74	43.0	41.0	37.0	5.2	151	a	A
1972	2	11	14	24	27.9	39.82	141.98	71.0	0.	0.	4.3	35	c2	B
1972	2	17	17	30	37.3	36.49	140.68	59.0	0.	0.	3.9	21	d2	D
1972	3	5	12	3	32.3	36.91	140.72	70.0	0.	0.	0.	23	c2	D
1972	3	13	3	20	6.9	41.00	140.09	176.0	0.	0.	4.7	84	t2	A
1972	3	14	11	7	30.3	38.54	141.83	60.0	0.	0.	4.6	67	d2	C
1972	3	19	15	57	50.0	40.84	141.98	72.0	77.0	75.0	5.9	372	c1	A
1972	3	20	2	16	10.0	40.91	141.96	79.0	0.	0.	4.2	50	a	A
1972	3	26	14	26	7.1	40.94	142.84	56.0	57.0	51.0	4.5	59	?	A
1972	4	17	0	37	42.8	37.74	141.83	65.0	59.0	58.0	4.5	60	b	D
1972	5	14	12	1	17.4	40.28	143.47	17.0	27.0	20.0	5.2	226		A
1972	5	17	18	45	12.3	37.84	140.36	115.0	100.0	100.0	4.7	79	b	D
1972	5	18	2	42	18.0	38.60	142.74	37.0	36.0	31.0	5.2	236		C
1972	6	11	21	12	51.2	40.21	141.50	87.0	77.0	77.0	4.5	89	c2	A
1972	6	14	18	27	23.5	36.42	141.43	47.0	38.0	32.9	4.6	96	?	D

year	mo	day	origin time			lat	long	ISC	depth pP	pwP	m_b	# of stns	mech type	region
1972	6	28	1	50	43.8	37.48	141.44	66.0	56.0	55.6	5.2	217	a	D
1972	7	4	1	4	35.8	38.55	142.08	51.0	42.0	40.0	5.4	282	d1	C
1972	8	22	18	9	11.1	39.43	140.28	140.0	0.	0.	4.4	43	c2	B
1972	9	2	6	4	23.6	40.80	142.00	76.0	65.0	63.0	4.3	74	b	A
1972	9	7	5	17	43.6	41.02	141.91	70.0	0.	0.	4.4	51	e	A
1972	9	18	12	14	18.5	40.77	141.24	101.0	0.	0.	4.9	110	b	A
1972	9	25	9	27	33.7	38.49	141.90	60.0	65.0	64.0	5.2	199	c2	C
1972	11	1	6	22	28.0	36.66	141.66	36.0	33.0	27.5	4.4	53	?	D
1972	11	1	14	22	49.4	38.27	141.93	54.0	47.0	46.0	5.0	113	a	C
1972	11	18	0	26	15.1	40.66	141.11	106.0	0.	0.	4.3	29	b	A
1972	11	18	22	55	8.1	37.34	139.77	142.0	0.	0.	4.3	43	c2	D
1972	12	6	23	41	28.1	40.28	143.81	8.0	60.0	49.0	5.1	141		A
1972	12	17	16	24	31.3	37.17	141.50	53.0	42.0	41.3	4.2	64	a	D
1972	12	29	22	8	57.7	40.31	140.02	174.0	0.	0.	4.2	24	?	A
1973	1	9	2	21	14.6	37.78	141.81	53.0	0.	0.	0.	20	a	D
1973	1	16	20	11	33.7	37.77	141.80	56.0	0.	0.	0.	22	a	D
1973	1	24	10	24	14.4	37.37	142.10	59.0	0.	0.	4.2	40		D
1973	2	3	0	35	47.7	36.77	140.97	58.0	0.	0.	0.	21	a	D
1973	2	14	21	45	43.0	39.05	141.48	117.0	110.0	110.0	4.9	159	t1	C
1973	2	14	22	36	14.9	37.05	141.51	59.0	56.0	54.9	5.1	123	a	D
1973	2	15	20	58	9.6	37.75	139.72	141.0	0.	0.	4.2	34	c2	D
1973	3	16	21	50	1.7	37.01	141.66	45.0	48.0	46.2	5.1	195	a	D
1973	3	16	21	53	5.8	36.99	141.65	53.0	0.	0.	4.6	37	?	D
1973	3	19	17	3	8.6	36.65	141.01	63.0	52.0	51.6	4.4	73	e	D
1973	3	26	14	56	11.7	36.67	142.12	39.0	36.0	27.2	5.0	120		D
1973	3	26	17	35	16.8	36.64	142.07	43.0	34.0	25.2	5.0	134		D
1973	4	24	9	49	52.7	40.74	143.54	23.0	28.0	20.0	4.9	164		A
1973	4	30	22	37	47.9	36.29	141.47	46.0	39.0	33.9	4.8	156	?	D
1973	5	5	3	52	27.9	37.13	141.46	54.0	42.0	41.3	5.4	234	a	D
1973	5	15	6	14	11.7	37.83	141.78	56.0	48.0	47.0	4.6	98	a	D
1973	5	26	2	15	35.5	37.14	141.50	55.0	44.0	43.3	5.1	191	a	D
1973	6	4	0	20	8.9	40.17	142.43	59.0	45.0	42.0	4.3	37	?	A
1973	6	5	22	52	26.6	38.36	142.31	45.0	40.0	37.0	4.8	71	a	C
1973	6	19	22	31	19.1	36.48	140.62	68.0	69.0	69.0	5.1	191	a	D
1973	7	6	13	37	54.0	40.23	142.59	49.0	47.0	43.0	5.0	157	a	A
1973	7	10	23	25	32.1	37.64	142.37	42.0	30.0	27.0	5.2	225		D
1973	7	20	8	12	54.0	36.45	141.05	49.0	48.0	46.2	5.8	361	d1	D
1973	7	22	1	37	33.5	36.47	140.63	65.0	0.	0.	4.0	43	d2	D
1973	7	28	3	41	13.1	40.92	143.23	41.0	42.0	35.0	4.5	125		A
1973	7	28	14	28	44.3	40.96	143.14	37.0	34.0	27.0	5.4	259		A
1973	7	31	16	51	17.0	36.44	140.74	66.0	0.	0.	4.4	64	a	D
1973	8	23	19	16	41.0	36.55	139.71	115.0	109.0	109.0	5.1	168	c2	D
1973	8	23	23	50	33.0	37.22	142.18	37.0	37.0	32.2	5.6	321	d1	D
1973	8	27	0	17	21.1	40.16	142.50	41.0	45.0	42.0	4.2	62	a	A
1973	9	5	13	3	14.1	39.57	143.16	35.0	42.0	35.0	5.4	345		B
1973	9	9	5	16	34.6	39.85	143.46	45.0	26.0	19.0	4.5	79		A
1973	9	9	18	25	49.6	39.53	143.24	19.0	21.0	13.0	5.6	366		B
1973	9	9	20	9	12.4	39.44	143.28	28.0	32.0	23.0	5.1	179		B
1973	9	24	9	14	29.4	40.16	142.34	64.0	0.	0.	4.5	93	?	A
1973	9	25	15	35	52.1	40.42	142.11	65.0	0.	0.	4.0	21	?	A

year	mo	day	origin time			lat	long	ISC	depth pP	pwP	m_b	# of stns	mech type	region
1973	10	15	4	4	0.9	40.19	142.42	54.0	47.0	44.0	4.6	49	?	A
1973	10	28	13	56	11.4	37.78	141.58	56.0	0.	0.	0.	21	a	D
1973	11	13	1	12	10.5	38.62	142.26	69.0	67.0	64.0	5.3	231	b	C
1973	11	19	13	1	56.6	38.99	141.93	56.0	49.0	49.0	6.1	438	d1	C
1973	11	19	21	11	17.0	38.90	142.02	58.0	48.0	47.0	5.2	196	d2	C
1973	12	7	21	7	22.2	39.35	142.01	63.0	61.0	61.0	4.9	101	e	B
1974	1	5	10	0	35.3	36.63	140.94	55.0	0.	0.	3.9	21	a	D
1974	1	10	12	44	44.7	36.40	141.72	41.0	34.0	26.7	5.1	140		D
1974	1	28	20	2	30.9	38.37	141.79	58.0	0.	0.	4.8	59	d2	C
1974	2	7	5	28	30.1	38.32	142.22	51.0	0.	0.	4.3	28	a	C
1974	2	7	12	33	38.1	37.41	141.09	89.0	0.	0.	4.6	70	b	D
1974	3	6	20	40	55.3	40.34	142.27	56.0	61.0	59.0	5.0	149	?	A
1974	3	21	5	48	52.8	36.95	141.73	43.0	34.0	31.1	5.2	216	?	D
1974	3	31	15	10	20.7	37.36	141.80	47.0	42.0	40.5	4.4	59	?	D
1974	4	4	7	37	2.7	37.70	140.81	100.0	94.0	94.0	5.2	202	c2	D
1974	4	14	23	22	30.7	40.99	143.67	33.0	40.0	32.0	4.8	77		A
1974	4	22	19	4	27.4	41.05	141.90	74.0	0.	0.	4.5	46	?	A
1974	4	23	11	52	1.1	37.08	141.21	61.0	0.	0.	4.5	67	d2	D
1974	5	5	14	19	12.3	37.78	141.77	50.0	43.0	42.0	5.7	322	d1	D
1974	5	10	6	20	16.1	40.19	141.52	92.0	0.	0.	4.5	60	?	A
1974	6	4	9	26	41.7	36.71	141.15	52.0	45.0	44.6	4.3	36	a	D
1974	6	20	5	25	21.9	38.16	140.83	103.0	0.	0.	4.2	32	c2	D
1974	6	22	10	29	51.9	40.03	142.81	46.0	44.0	40.0	5.1	178		A
1974	6	23	9	36	0.9	39.77	141.39	91.0	77.0	77.0	4.4	79	c2	B
1974	7	2	19	19	43.8	37.75	141.78	86.0	79.0	78.0	4.3	69	b	D
1974	7	8	5	45	38.3	36.44	141.17	45.0	43.0	40.8	6.0	425	d1	D
1974	7	23	14	54	33.9	36.73	142.08	37.0	37.0	28.2	4.6	100		D
1974	8	10	15	2	35.6	40.18	142.45	54.0	45.0	42.0	4.8	127	a	A
1974	8	28	0	50	3.8	36.42	141.24	52.0	45.0	41.7	4.9	119	a	D
1974	9	4	9	20	2.5	40.24	141.76	52.0	49.0	49.0	5.2	241	t2	A
1974	9	5	0	55	57.1	39.49	141.41	85.0	0.	0.	4.6	67	c2	B
1974	9	28	8	9	10.4	38.29	141.80	55.0	0.	0.	4.2	21	a	C
1974	9	28	16	1	8.4	36.44	140.59	69.0	0.	0.	4.5	44	e	D
1974	9	30	0	14	5.6	38.50	142.12	51.0	41.0	39.0	4.7	71	a	C
1974	10	10	6	48	15.5	41.05	143.09	33.0	36.0	29.0	5.7	384		A
1974	10	10	6	56	49.7	40.99	143.15	36.0	43.0	36.0	5.7	340		A
1974	10	12	4	47	30.9	40.52	143.57	20.0	20.0	11.0	5.3	261		A
1974	10	12	6	14	51.0	40.54	143.58	17.0	20.0	11.0	5.5	326		A
1974	10	15	1	16	45.9	40.66	143.78	12.0	17.0	7.0	5.4	278		A
1974	10	16	9	29	46.7	40.35	143.72	8.0	21.0	10.0	5.5	285		A
1974	11	2	21	55	21.4	36.42	141.67	46.0	46.0	40.9	5.1	159		D
1974	11	2	22	45	12.4	36.42	141.70	50.0	0.	0.	4.7	82		D
1974	11	4	1	26	15.3	36.55	140.54	104.0	0.	0.	3.8	33	t2	D
1974	11	9	14	16	37.2	40.10	143.35	26.0	36.0	31.0	5.3	177		A
1974	11	18	22	48	24.2	40.91	141.67	116.0	0.	0.	4.4	45	b	A
1974	12	29	1	49	34.8	38.94	141.60	75.0	0.	0.	4.3	39	c2	C
1974	12	30	23	57	1.4	39.46	143.08	38.0	36.0	29.0	4.6	85		B
1975	1	11	22	12	55.4	40.21	142.40	57.0	45.0	42.0	4.6	68	?	A
1975	1	13	1	19	50.7	40.15	142.42	53.0	46.0	43.0	4.8	121	a	A
1975	1	29	0	35	47.8	38.28	142.00	59.0	0.	0.	0.	20	a	C

year	mo	day	origin time			lat	long	ISC	depth pP	pwP	m_b	# of stns	mech type	region
1975	2	28	21	34	36.0	39.20	142.26	96.0	0.	0.	4.3	53	b	B
1975	3	26	16	32	15.3	37.03	141.74	68.0	63.0	60.4	4.5	64	a	D
1975	4	3	14	34	14.7	40.90	141.93	76.0	70.0	68.0	4.8	142	a	A
1975	4	8	6	27	14.3	37.75	141.75	53.0	44.0	43.0	5.7	361	d1	D
1975	4	13	0	19	10.2	37.67	141.77	55.0	41.0	40.0	4.9	134	a	D
1975	4	21	3	45	15.5	36.49	140.68	65.0	53.0	53.0	4.9	153	e	D
1975	4	25	17	37	33.3	37.91	141.25	97.0	81.0	81.0	4.9	147	t2	D
1975	4	26	3	14	37.9	39.61	141.13	102.0	97.0	97.0	5.2	208	c2	B
1975	5	4	9	31	59.9	37.20	142.09	24.0	20.0	15.6	5.8	399	?	D
1975	5	4	12	58	6.1	40.06	142.13	62.0	0.	0.	4.5	45	?	A
1975	6	14	18	54	32.9	40.22	142.51	43.0	43.0	40.0	5.1	81	?	A
1975	6	15	18	1	56.4	40.20	142.33	60.0	52.0	50.0	4.9	115	?	A
1975	6	17	15	54	47.8	38.26	141.97	55.0	54.0	53.0	4.9	89	a	C
1975	6	17	21	29	37.2	40.18	142.33	63.0	53.0	51.0	5.0	132	e	A
1975	6	18	5	44	5.5	40.97	143.09	44.0	49.0	42.0	5.2	254		A
1975	7	5	2	18	46.9	36.68	140.29	121.0	0.	0.	4.8	69	b	D
1975	8	14	18	9	28.6	37.13	141.11	62.0	60.0	59.6	5.5	281	d1	D
1975	8	24	1	8	14.5	37.09	141.14	64.0	0.	0.	0.	21	?	D
1975	8	26	5	10	43.7	40.98	143.10	44.0	51.0	44.0	5.2	202		A
1975	8	29	10	16	15.5	40.60	143.72	18.0	27.0	17.0	5.1	183		A
1975	9	8	9	28	54.6	40.88	140.76	126.0	123.0	123.0	5.1	132	?	A
1975	9	10	9	26	58.8	40.34	142.73	52.0	56.0	52.0	4.9	136	?	A
1975	10	9	10	17	30.8	38.25	141.92	60.0	41.0	40.0	5.1	147	a	C
1975	11	23	23	2	8.1	41.26	140.21	167.0	163.0	162.6	5.3	258	?	A
1975	11	29	17	45	59.7	37.58	141.48	78.0	0.	0.	4.4	49	b	D
1975	11	30	11	41	5.3	38.86	142.60	30.0	28.0	24.0	4.7	75		C
1975	12	28	16	29	38.1	37.53	141.55	59.0	0.	0.	4.7	68	a	D
1976	1	7	7	50	38.5	39.68	143.48	19.0	24.0	15.0	5.0	117		B
1976	1	7	8	53	5.0	36.21	141.64	49.0	50.1	44.1	4.6	53	?	D
1976	2	18	19	1	28.3	39.35	141.42	127.0	0.	0.	4.4	35	t2	B
1976	2	22	1	12	24.1	36.43	140.62	101.0	0.	0.	4.9	165	t2	D
1976	2	24	17	37	0.2	37.24	141.05	104.0	88.8	88.8	4.9	152	e	D
1976	2	26	16	51	33.5	38.19	140.77	136.0	0.	0.	4.7	96	t2	D
1976	2	29	9	27	15.9	36.75	140.87	59.0	0.	0.	4.8	135	d2	D
1976	3	15	13	48	33.1	40.98	141.80	73.0	0.	0.	4.2	35	c2	A
1976	3	28	6	19	9.5	37.26	141.19	88.0	0.	0.	4.0	45	t2	D
1976	3	28	16	49	30.8	37.74	141.81	58.0	0.	0.	4.2	39	a	D
1976	3	30	3	32	39.0	40.19	143.99	30.0	34.0	19.0	4.3	56		A
1976	3	30	5	53	12.8	39.66	143.26	28.0	28.0	21.0	5.4	252		B
1976	3	30	6	4	13.1	39.59	143.38	23.0	37.0	29.0	5.4	229		B
1976	3	30	9	24	58.3	39.57	143.46	25.0	24.0	16.0	5.1	124		B
1976	4	10	7	25	38.6	39.85	143.66	23.0	25.0	16.0	4.7	84		A
1976	4	19	10	50	55.1	40.29	143.30	25.0	20.0	14.0	5.4	319		A
1976	4	30	22	38	44.2	36.49	140.91	62.0	0.	0.	4.2	36	d2	D
1976	5	2	15	30	16.8	38.06	139.01	206.0	0.	0.	4.3	25	c2	D
1976	5	13	20	28	53.7	36.44	140.75	67.0	0.	0.	4.5	48	e	D
1976	6	4	4	23	33.6	38.35	142.75	28.0	27.0	22.0	5.5	400		C
1976	7	8	11	47	1.6	40.28	142.41	53.0	48.0	45.0	5.4	357	?	A
1976	7	17	19	57	24.8	36.46	140.64	63.0	0.	0.	0.	22	d2	D
1976	7	20	4	59	14.8	37.15	140.37	112.0	0.	0.	0.	24	c2	D

year	mo	day	origin time			lat	long	ISC	depth pP	pwP	m_b	# of stns	mech type	region
1976	7	21	16	59	47.3	39.90	142.05	82.0	0.	0.	0.	38	c2	B
1976	8	6	19	42	36.5	37.38	141.64	48.0	42.0	41.5	5.3	263	a	D
1976	8	24	5	52	47.0	37.50	142.60	0.	29.0	22.0	4.5	31		D
1976	9	15	8	20	7.2	37.29	142.97	32.0	31.0	15.7	5.1	108	?	D
1976	10	6	13	38	42.2	37.12	141.31	82.0	76.0	75.6	5.5	408	t2	D
1976	11	8	8	19	28.1	38.12	142.26	44.0	42.0	39.0	5.9	495	d1	C
1976	11	14	17	10	59.8	37.09	141.57	47.0	41.0	40.0	5.1	110	?	D
1976	11	17	15	2	55.4	38.28	141.24	90.0	0.	0.	0.	23	b	C
1976	12	7	18	57	36.8	41.12	140.19	160.0	0.	0.	0.	27	c2	A
1976	12	13	2	55	58.9	36.73	140.75	107.0	0.	0.	4.5	56	t2	D
1976	12	18	3	5	57.2	38.31	141.88	59.0	0.	0.	4.8	56	d2	C
1976	12	21	15	6	54.7	37.06	141.24	59.0	0.	0.	4.8	74	a	D
1976	12	29	14	36	49.0	36.71	139.15	142.0	145.0	145.0	5.3	393	c2	D
1977	1	3	21	14	57.8	36.44	140.76	62.0	0.	0.	0.	21	e	D
1977	1	21	2	25	5.8	36.71	140.10	56.0	0.	0.	4.5	52	?	D
1977	3	17	5	12	14.3	39.20	141.37	104.0	0.	0.	0.	27	?	C
1977	3	24	1	14	36.1	36.30	141.11	50.0	0.	0.	0.	41	?	D
1977	4	6	13	7	46.8	37.00	141.19	59.0	0.	0.	0.	31	?	D
1977	4	17	19	26	28.0	38.88	141.74	77.0	0.	0.	0.	23	b	C
1977	4	19	6	14	59.5	36.45	140.64	66.0	69.0	69.0	5.2	236	d2	D
1977	4	24	5	32	54.8	39.49	139.85	192.0	0.	0.	0.	28	?	C
1977	4	24	20	42	43.8	40.10	142.72	46.0	43.0	39.0	5.2	177	?	A
1977	5	4	1	18	21.9	37.55	141.42	72.0	0.	0.	0.	23	t2	D
1977	5	13	1	26	43.6	38.31	141.91	54.0	53.0	52.0	5.0	126	d1	C
1977	6	8	14	25	46.0	38.57	141.57	74.0	73.0	73.0	5.4	397	c1	C
1977	7	14	2	46	56.1	36.43	140.45	99.0	0.	0.	0.	26	t2	D
1977	7	26	4	25	17.1	39.89	141.06	103.0	96.0	96.0	4.7	109	c2	B
1977	8	5	7	46	16.6	40.98	141.85	77.0	0.	0.	4.8	30	?	A
1977	8	6	8	29	56.4	39.01	142.32	56.0	0.	0.	4.6	67	c2	C
1977	8	23	12	36	55.9	40.19	143.45	24.0	21.0	14.0	4.9	106		A
1977	9	3	22	27	36.6	39.80	143.07	33.0	30.0	24.0	4.8	92		B
1977	9	6	2	10	6.2	36.85	139.97	138.0	0.	0.	0.	29	t2	D
1977	9	28	8	46	42.9	39.76	142.02	73.0	0.	0.	4.7	69	c2	B
1977	10	4	10	13	3.5	39.73	141.98	72.0	0.	0.	4.6	28	?	B
1977	10	7	21	32	44.2	36.45	140.74	68.0	0.	0.	4.5	40	d2	D
1977	10	22	11	58	46.2	36.74	141.42	52.0	40.0	38.7	4.9	125	?	D
1977	10	25	21	55	8.3	36.26	141.45	46.0	45.0	39.6	5.1	134	?	D
1977	10	26	13	58	41.1	40.52	143.67	28.0	24.0	14.0	4.7	108		A
1977	10	29	19	17	34.4	36.43	140.72	52.0	0.	0.	0.	33	e	D
1977	12	16	15	10	28.8	36.65	141.07	53.0	45.0	44.5	5.6	385	d2	D
1977	12	22	22	18	1.7	39.21	143.16	32.0	32.0	24.0	5.3	213		B
1977	12	23	21	2	8.0	39.19	143.22	20.0	24.0	16.0	5.6	384		B
1977	12	23	21	9	21.9	39.20	143.18	22.0	27.0	19.0	5.3	174		B
1977	12	23	21	14	22.6	39.18	143.20	10.0	38.0	30.0	5.4	273		B
1978	1	20	22	0	30.5	36.89	140.92	87.0	0.	0.	0.	32	t2	D
1978	1	24	10	26	42.5	41.03	140.08	175.0	0.	0.	4.8	119	?	A
1978	2	16	3	59	26.2	37.19	141.20	93.0	0.	0.	0.	29	t2	D
1978	2	18	17	33	15.3	38.19	142.60	44.0	37.0	32.0	5.1	190		C
1978	2	20	4	36	58.4	38.83	142.03	60.0	66.0	65.0	6.0	575	c1	C
1978	2	20	4	53	29.9	38.63	141.95	70.0	0.	0.	4.5	77	c2	C

year	mo	day	origin time			lat	long	ISC	depth pP	pwP	m_b	# of stns	mech type	region
1978	2	20	5	0	30.4	38.77	142.05	65.0	0.	0.	4.3	49	c2	C
1978	2	20	5	39	44.0	38.69	142.03	68.0	77.0	75.0	4.3	37	c2	C
1978	2	23	10	46	42.6	37.91	141.87	70.0	0.	0.	4.1	22	a	D
1978	3	10	22	20	57.8	38.66	143.11	26.0	31.0	24.0	4.8	122		C
1978	3	12	17	59	48.6	38.83	141.97	62.0	55.0	54.0	5.0	185	c2	C
1978	3	21	16	57	3.5	40.12	142.53	59.0	43.0	40.0	4.5	48	a	A
1978	4	6	13	54	50.1	38.75	142.14	63.0	0.	0.	4.5	33	c2	C
1978	4	7	3	29	45.6	36.64	140.93	59.0	0.	0.	4.2	36	e	D
1978	4	10	14	27	37.3	40.14	141.93	113.0	0.	0.	4.1	36	t2	A
1978	4	12	2	0	59.4	38.24	141.92	57.0	0.	0.	4.1	21	?	C
1978	4	19	10	47	52.3	36.44	140.78	60.0	0.	0.	4.6	65	?	D
1978	4	28	2	19	25.2	40.60	139.90	172.0	0.	0.	4.1	46	c2	A
1978	5	9	14	30	45.5	40.38	142.09	66.0	0.	0.	4.1	24	?	A
1978	5	10	15	36	26.8	37.35	141.72	47.0	41.0	40.0	5.5	300	a	D
1978	5	12	22	47	33.5	36.27	141.43	42.0	37.0	32.3	5.3	295	t2	D
1978	5	14	17	41	40.0	40.19	142.41	51.0	46.0	43.0	5.1	186	a	A
1978	5	16	7	35	48.4	41.05	141.40	42.0	52.0	52.0	5.6	445	?	A
1978	5	16	8	24	0.5	41.05	141.41	41.0	46.0	46.0	5.7	466	?	A
1978	5	21	12	8	45.8	40.82	142.44	52.0	54.0	50.0	5.2	220	a	A
1978	5	28	20	27	28.5	36.60	140.69	104.0	0.	0.	0.	22		D
1978	6	4	18	40	8.2	36.44	140.99	53.0	51.0	50.0	4.9	172	e	D
1978	6	12	8	6	11.0	38.23	142.14	45.0	44.0	41.7	5.7	400		C
1978	6	12	8	14	27.3	38.23	142.02	48.0	55.0	53.7	6.7	604		C
1978	6	12	9	12	56.6	38.47	142.36	41.0	42.0	38.6	5.4	292	a	C
1978	6	12	9	40	30.6	38.46	142.14	48.0	45.0	43.0	4.9	181	a	C
1978	6	13	20	45	19.6	38.10	141.98	52.0	0.	0.	4.8	104	b	C
1978	6	14	11	34	20.3	38.38	142.41	39.0	40.0	36.6	5.9	497	a	C
1978	6	14	17	13	46.5	36.74	140.95	96.0	0.	0.	4.0	40	t2	D
1978	6	15	0	45	31.6	38.21	142.05	52.0	0.	0.	4.1	24	?	C
1978	6	15	15	3	40.1	37.96	141.90	54.0	47.0	45.9	5.4	312	a	D
1978	6	16	5	33	32.8	38.24	143.18	0.	38.0	29.3	5.5	349		C
1978	6	16	10	15	16.1	38.18	143.27	20.0	25.0	14.9	5.1	155		C
1978	6	16	23	24	20.6	38.15	143.31	22.0	29.0	18.3	5.0	109		C
1978	6	18	14	59	57.8	38.49	142.77	17.0	22.0	16.6	5.0	167		C
1978	6	21	10	54	22.8	38.34	141.87	54.0	53.0	52.1	5.7	449	a	C
1978	6	21	11	49	4.6	38.20	143.36	7.0	29.0	17.6	5.2	161		C
1978	6	27	19	10	33.3	37.23	142.80	34.0	34.0	18.6	5.7	411		D
1978	7	2	17	1	2.6	38.04	143.53	0.	32.0	15.2	4.6	51		C
1978	7	5	5	8	24.3	36.48	140.68	69.0	0.	0.	4.4	46	t2	D
1978	7	12	11	37	30.0	38.16	142.61	44.0	0.	0.	4.5	40	?	C
1978	7	14	14	4	56.8	37.53	141.47	60.0	49.0	48.5	5.0	170	?	D
1978	7	26	17	13	39.3	39.65	143.55	5.0	35.0	25.6	5.2	179		B
1978	7	26	22	15	52.5	36.20	141.82	38.0	36.0	28.3	4.9	102	?	D
1978	7	27	7	24	8.5	37.93	141.85	58.0	0.	0.	5.1	189	?	D
1978	7	27	13	29	15.1	36.19	141.82	39.0	42.0	34.6	5.0	158	t2	D
1978	7	29	0	25	9.6	37.50	141.46	62.0	0.	0.	4.3	39	a	D
1978	8	11	8	41	9.0	36.31	140.65	78.0	0.	0.	0.	20	c2	D
1978	8	20	21	31	13.1	38.12	142.12	51.0	0.	0.	4.6	51	?	C
1978	8	27	23	30	2.3	38.75	142.34	50.0	41.0	38.0	4.5	47	?	C
1978	9	2	16	43	22.1	38.25	141.95	52.0	0.	0.	4.0	25	a	C

year	mo	day	origin time			lat	long	ISC	depth pP	pwP	m_b	# of stns	mech type	region
1978	9	7	13	4	30.1	38.02	141.16	92.0	0.	0.	4.7	93	c2	D
1978	9	9	2	7	39.6	40.56	142.51	53.0	0.	0.	4.5	45	?	A
1978	9	9	11	59	44.3	37.06	141.50	78.0	0.	0.	4.1	44	b	D
1978	9	19	17	53	23.0	36.84	140.28	121.0	0.	0.	4.3	34	t2	D
1978	9	23	22	43	10.1	38.42	143.15	25.0	28.0	19.9	5.4	264		C
1978	10	8	13	32	52.8	40.99	141.96	72.0	0.	0.	4.1	29		A
1978	10	12	1	20	12.1	37.08	141.16	56.0	0.	0.	3.9	31	d2	D
1978	11	5	16	17	26.6	36.64	141.13	54.0	43.0	42.2	5.1	152	a	D
1978	11	9	2	32	57.8	36.93	141.06	72.0	0.	0.	4.0	22	c2	D
1978	11	13	3	1	42.1	38.77	142.14	55.0	43.0	41.3	5.2	239	?	C
1978	12	1	23	3	39.8	38.42	143.29	27.0	30.0	20.6	4.9	114		C
1978	12	7	5	47	2.6	38.25	142.05	55.0	0.	0.	4.6	37	b	C
1978	12	7	18	37	25.5	37.16	141.47	53.0	43.0	42.3	5.0	148	a	D
1978	12	9	5	30	46.5	38.74	142.20	65.0	0.	0.	4.2	20	b	C
1978	12	21	1	15	4.1	39.65	142.03	108.0	0.	0.	4.5	50	t2	B
1978	12	23	1	39	40.8	38.94	144.26	0.	36.0	12.2	4.6	62		B
1978	12	27	15	42	18.8	36.55	140.57	55.0	0.	0.	0.	23	t2	D
1978	12	29	10	35	2.8	41.05	142.41	44.0	44.0	39.2	4.8	118	b	A
1979	1	2	14	34	51.5	37.13	141.44	50.0	0.	0.	4.3	37	a	D
1979	1	8	8	27	15.6	37.02	141.00	110.0	0.	0.	4.3	36	b	D
1979	1	20	9	1	49.6	36.58	141.04	65.0	0.	0.	4.9	105	e	D
1979	1	22	16	46	36.0	36.38	140.47	92.0	0.	0.	0.	23	t2	D
1979	2	6	0	17	25.3	40.57	144.09	17.0	30.0	13.2	4.8	42		A
1979	2	7	5	28	53.6	36.75	141.41	76.0	0.	0.	0.	26	b	D
1979	2	10	1	56	17.0	37.93	141.45	95.0	0.	0.	0.	29	b	D
1979	2	10	10	28	29.1	38.26	140.63	147.0	0.	0.	4.0	20	t2	D
1979	2	14	1	52	38.1	39.52	140.17	170.0	167.0	167.0	4.8	176	?	B
1979	2	20	6	32	37.3	40.22	143.55	0.	46.0	37.9	5.9	507		A
1979	2	20	7	5	52.6	40.31	143.89	0.	27.0	13.6	5.0	143		A
1979	2	20	14	45	31.6	36.50	140.43	121.0	0.	0.	0.	36	b	D
1979	2	20	15	23	23.3	40.13	144.23	13.0	44.0	19.2	4.7	76		A
1979	2	21	1	8	0.6	38.96	142.38	90.0	0.	0.	4.2	42	t2	C
1979	2	21	13	39	4.8	40.40	143.82	8.0	28.0	15.2	5.5	279		A
1979	2	24	22	1	48.8	40.27	143.84	7.0	33.0	20.9	5.1	188		A
1979	3	7	22	27	18.5	36.38	140.78	61.0	0.	0.	4.7	70	c2	D
1979	3	19	22	40	36.3	36.60	140.74	109.0	0.	0.	4.3	38	b	D
1979	4	1	13	15	21.8	37.10	141.12	91.0	0.	0.	4.4	55	b	D
1979	4	2	17	26	30.6	38.52	142.18	49.0	46.0	43.6	5.1	269	c2	C
1979	4	22	2	39	50.6	40.56	143.79	24.0	29.0	17.6	4.7	124		A
1979	4	23	14	23	9.6	41.02	142.56	88.0	0.	0.	0.	22	?	A
1979	5	3	11	8	40.8	41.17	140.13	162.0	0.	0.	4.3	30	c2	A
1979	5	4	14	40	27.1	36.54	140.63	55.0	0.	0.	0.	22	b	D
1979	5	17	12	56	18.0	36.69	141.26	49.0	42.0	41.0	5.0	210	?	D
1979	5	21	15	0	55.1	39.18	142.86	39.0	36.0	30.0	5.4	268	?	B
1979	5	31	22	9	53.0	38.26	142.05	51.0	0.	0.	4.4	55	a	C
1979	6	7	21	40	34.5	37.60	141.52	92.0	0.	0.	4.4	32	b	D
1979	6	11	7	52	5.3	37.44	139.16	174.0	0.	0.	4.6	135	c2	D
1979	6	21	10	46	1.6	39.63	142.22	56.0	0.	0.	4.0	30	a	B
1979	6	24	8	1	15.1	39.02	142.51	69.0	0.	0.	0.	22	b	C
1979	6	26	8	50	2.3	37.07	141.21	63.0	0.	0.	4.3	58	a	D

year	mo	day	origin time			lat	long	ISC	depth pP	pwP	m_b	# of stns	mech type	region
1979	7	11	1	58	22.3	36.63	141.33	46.0	41.0	39.0	5.6	450	a	D
1979	7	15	17	50	52.3	41.01	141.96	65.0	0.	0.	4.4	33	?	A
1979	7	19	1	29	59.3	39.38	142.05	58.0	69.0	69.0	4.9	151	?	B
1979	7	25	23	11	38.0	40.14	144.95	59.0	57.0	36.3	4.8	155		A
1979	7	29	20	12	15.0	38.41	142.57	0.	31.0	26.6	4.2	79	?	C
1979	8	3	17	11	25.3	38.31	141.98	59.0	0.	0.	0.	23	?	C
1979	8	16	11	55	7.5	38.75	142.86	39.0	33.0	27.8	5.5	367	?	C
1979	8	24	10	55	31.0	39.26	140.90	143.0	0.	0.	4.5	88	?	C
1979	9	3	2	31	6.3	40.14	142.30	64.0	0.	0.	3.9	33	c2	A
1979	9	15	11	45	39.6	36.66	140.76	98.0	0.	0.	3.7	29	t2	D
1979	10	1	23	38	44.8	39.95	141.95	72.0	58.0	58.0	4.7	151	b	B
1979	10	5	21	26	15.1	40.30	143.70	19.0	32.0	21.3	5.0	169		A
1979	10	11	8	46	20.1	40.04	142.22	60.0	0.	0.	4.8	67	a	A
1979	10	28	23	29	22.1	40.12	142.42	53.0	46.0	43.3	5.1	192	a	A
1979	11	1	10	45	52.6	37.62	141.63	96.0	0.	0.	4.2	32	b	D
1979	11	18	18	11	19.6	37.56	141.30	63.0	59.0	58.7	4.8	82	a	D
1979	11	25	10	15	22.0	36.71	141.03	93.0	87.0	86.5	5.2	226	t2	D
1979	12	2	9	45	0.8	36.36	141.39	48.0	35.0	29.6	5.0	119	?	D
1979	12	16	23	23	48.6	36.44	140.66	68.0	0.	0.	4.7	61	d2	D
1979	12	17	5	39	0.1	37.20	140.03	125.0	0.	0.	0.	31	c2	D
1979	12	17	7	20	33.1	38.73	142.11	67.0	0.	0.	0.	28	c2	C
1979	12	19	11	41	43.3	36.45	141.25	52.0	41.0	37.6	4.9	152	a	D
1979	12	31	2	47	46.6	40.29	144.16	6.0	45.0	24.9	5.4	313		A
1980	1	1	22	26	45.3	36.45	140.67	56.0	0.	0.	4.2	35	d2	D
1980	1	7	16	45	29.0	37.50	143.16	27.0	30.0	13.9	4.6	77		D
1980	1	9	5	9	43.4	37.64	140.70	109.0	0.	0.	4.3	28	c2	D
1980	1	22	11	13	17.8	40.58	142.48	66.0	0.	0.	4.1	40	c2	A
1980	1	25	0	51	17.8	36.54	139.89	100.0	0.	0.	3.9	42	c2	D
1980	2	4	10	54	19.4	37.33	141.64	55.0	45.0	44.0	4.8	83	a	D
1980	2	12	15	27	59.7	40.29	142.15	67.0	0.	0.	4.2	38		A
1980	2	12	16	41	3.6	36.54	140.86	65.0	0.	0.	4.2	43	?	D
1980	2	29	17	47	51.0	40.78	141.35	105.0	0.	0.	4.6	34	?	A
1980	3	3	3	51	17.9	36.47	140.62	57.0	0.	0.	0.	32	d2	D
1980	3	16	21	40	36.8	40.17	142.40	53.0	46.0	43.6	5.4	330	?	A
1980	3	22	8	16	38.1	38.71	141.19	101.0	0.	0.	4.3	40	c2	C
1980	3	28	20	43	10.6	40.11	142.00	84.0	0.	0.	4.8	48	c2	A
1980	3	29	9	41	25.7	39.30	142.48	60.0	0.	0.	4.2	36	?	B
1980	4	10	6	55	59.5	40.12	142.36	62.0	0.	0.	4.4	49	?	A
1980	4	14	19	32	51.9	37.91	141.73	71.0	0.	0.	4.1	25	?	D
1980	4	16	13	40	36.4	39.75	141.84	71.0	0.	0.	4.3	31	e	B
1980	4	27	21	59	12.3	38.39	140.68	115.0	0.	0.	4.4	58	t2	C
1980	5	6	19	25	40.7	37.01	141.65	50.0	0.	0.	4.5	52	?	D
1980	5	19	18	56	16.5	36.05	141.89	33.0	31.0	21.9	5.1	194	?	D
1980	5	20	1	9	19.2	36.12	141.90	38.0	33.0	24.9	4.9	144	?	D
1980	5	21	2	17	53.4	40.96	140.70	140.0	0.	0.	4.4	24	?	A
1980	5	24	16	0	7.2	36.48	140.60	63.0	0.	0.	0.	27	b	D
1980	5	26	14	36	17.8	38.08	143.60	10.0	24.0	6.6	4.9	134		C
1980	6	2	11	35	23.3	39.55	140.76	139.0	0.	0.	4.3	22	b	B
1980	6	6	10	5	33.4	38.67	142.24	64.0	0.	0.	4.4	32	b	C
1980	6	9	20	6	35.2	40.85	139.97	167.0	160.0	160.0	5.5	446	c2	A

year	mo	day	origin time			lat	long	ISC	depth pP	pwP	m_b	# of stns	mech type	region
1980	7	3	10	49	18.6	40.98	141.99	68.0	0.	0.	4.4	57	?	A
1980	7	4	5	23	18.9	36.90	140.77	110.0	0.	0.	4.2	27	c2	D
1980	7	16	8	19	29.6	37.35	141.79	47.0	40.0	38.7	5.4	296	a	D
1980	7	27	14	31	59.4	38.72	141.73	87.0	0.	0.	4.0	25	c2	C
1980	7	29	19	53	38.6	38.24	141.79	64.0	0.	0.	4.3	32	?	C
1980	9	23	5	36	30.1	38.51	141.09	102.0	0.	0.	4.1	20	?	C
1980	9	28	21	36	58.0	38.77	141.77	74.0	69.0	68.5	4.8	194	c2	C
1980	10	2	17	47	41.5	37.05	141.24	61.0	59.0	58.5	4.9	106	a	D
1980	10	9	2	7	33.4	36.36	140.94	52.0	45.0	44.3	5.3	252	a	D
1980	10	29	17	49	12.3	36.43	140.79	74.0	0.	0.	4.4	49	?	D
1980	11	1	17	53	1.9	39.35	141.58	106.0	0.	0.	4.1	27	c2	B
1980	11	3	1	6	13.2	38.32	140.61	140.0	137.0	137.0	4.9	235	t2	C
1980	11	4	1	2	9.0	40.29	142.25	61.0	47.0	45.6	5.0	86	?	A
1980	11	26	23	49	2.0	40.44	141.39	96.0	94.0	94.0	5.7	511	c2	A
1980	11	27	1	50	38.4	40.44	141.36	97.0	94.0	94.0	5.3	352	c2	A
1980	12	16	3	21	35.3	40.42	141.43	100.0	0.	0.	3.9	42	b	A
1980	12	19	6	54	11.5	38.67	142.68	48.0	42.0	37.2	4.8	172	?	C

APPENDIX B

NEWLY DETERMINED FOCAL MECHANISM SOLUTIONS IN CHAPTER II

Focal mechanism solutions for the earthquakes in region D newly obtained in Chapter 2 are presented as equal-area projections of the lower hemisphere of the focal sphere. Large circles indicate WWSSN long-period P wave first motion data and small circles WWSSN short-period and JMA data. Polarization angles of long-period S waves are indicated by the dashes. Nodal lines are indicated by the thin lines in this figure and their parameters are listed in Table 2.2. For thrust type mechanisms, it is often difficult to constrain the shallower dipping nodal planes. For such cases, it is assumed that they are pure dip slip mechanisms. The numbers denote earthquake events in Table 2.2.

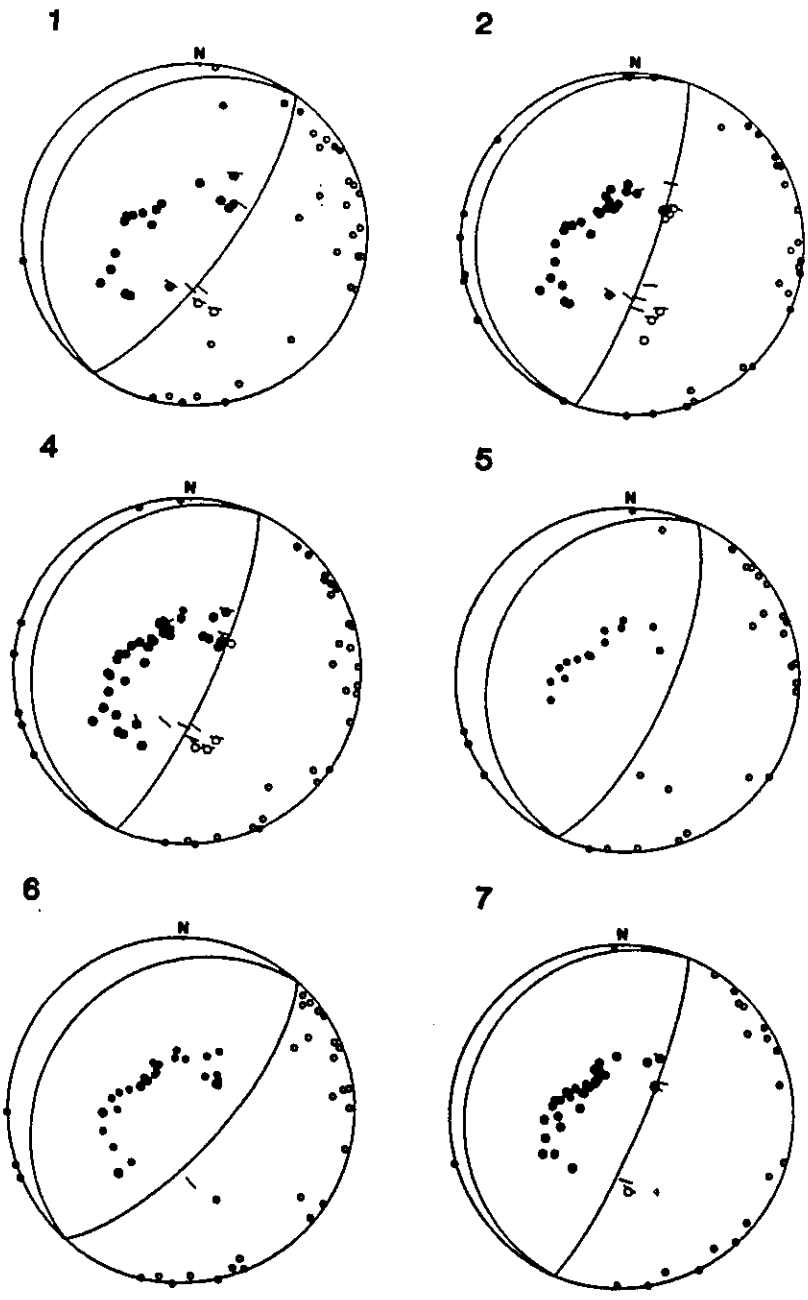
1
N
2
N
4
N
5
N
6
N
7
N

8

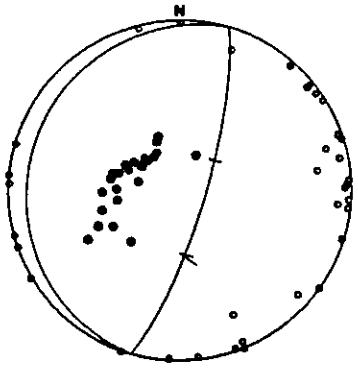

9

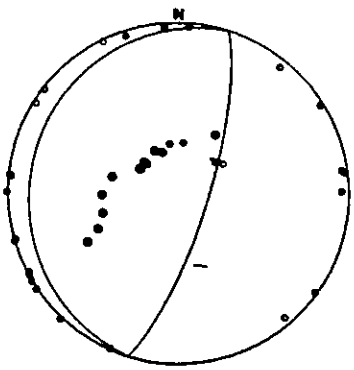

10

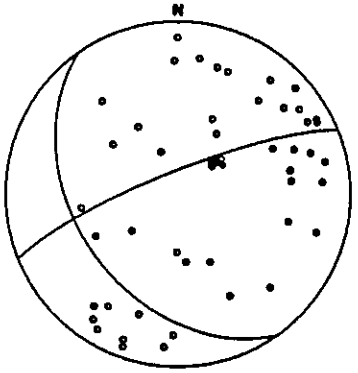

11

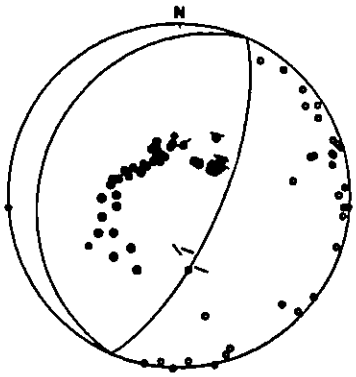

12

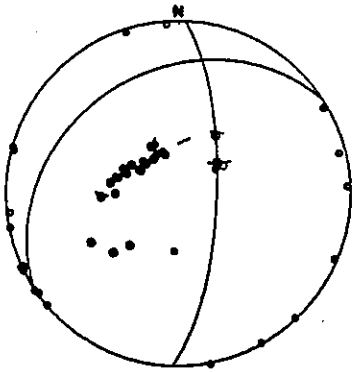

16

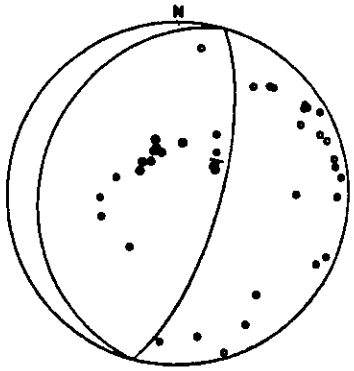

17

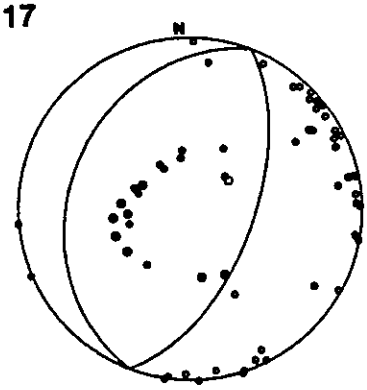

APPENDIX C

LIST OF EARTHQUAKES IN CHAPTER III

In all tables, origin time ,epicentral location and body-wave magnitude are from PDE.

Table C.1: Events for which focal mechanism solutions are determined by P-wave first motions and S-wave polarizations. Depths are obtained from ISC bulletin. Asterisk denotes a depth determined by pP-P time difference by ISC. Depths with superscript 'l' are obtained by comparing the first motion P-wave waveform of long period WWSSN records with synthetic seismograms, calculated by the method of Kroeger and Geller (1985). PREM (Dziewonski and Anderson, 1981) was used for the structure near the sources. For events deeper than 50 km, focal mechanism types are shown in the last column. 'P' and 'T' represent down-dip compression and down-dip tension event. 'X' denotes neither of them.

Table C.2: Focal mechanism solutions for events in Table C.1.

References	NEW	this study
	IM	Isacks and Molnar, 1971
	ISO	Isacks et al., 1969
	JM	Johnson and Molnar, 1972
	SIO	Sykes et al., 1969
	B	Billington, 1980
	R	Richter, 1979

Table C.3: Events for which CMT solutions are available. Depths are centroid depths obtained from CMT solutions.

Table C.4: Focal mechanism solutions for events in Table C.3.

Table C.5: Events for which only focal mechanism types were determined (Figure 3.6). Superscript 's' denotes the depth checked by the author with WWSSN short period seismograms.

TABLE C.1.

F	year	mo	day	hr	min	sec	lat	long	depth	m_b	dist	azimuth	mech
1	1962	5	21	21	15	30.0	-19.92	182.78	351	0.0	1.97	112.15	
2	1963	3	26	9	48	20.3	-29.70	182.10	48	5.9	-1.27	121.40	
3	1963	3	31	5	30	49.8	-29.90	182.10	37	5.7	-1.35	121.59	
4	1963	3	31	19	22	51.5	-30.10	181.80	35	6.0	-1.19	121.87	
5	1963	4	17	2	11	36.7	-19.70	178.30	73	5.9	5.93	113.64	
6	1963	5	20	11	38	5.3	-30.70	181.70	37	6.1	-1.35	122.46	
7	1963	7	4	10	58	13.2	-26.30	182.30	185	6.5	-0.10	118.20	
8	1963	7	29	20	14	7.3	-30.20	182.70	90	5.7	-1.95	121.66	
9	1963	7	29	20	16	36.9	-29.70	183.00	106	5.5	-1.99	121.10	
10	1963	10	8	0	17	1.1	-15.10	186.80	42	5.7	0.23	106.25	
11	1963	12	18	0	30	2.6	-24.80	183.40	32	6.5	-0.44	116.44	
12	1964	7	9	11	22	5.4	-23.30	184.30	35*	5.7	-0.63	114.74	
13	1964	7	21	3	48	59.1	-26.00	182.00	205	5.8	0.26	118.03	P
14	1964	8	5	11	6	2.6	-32.10	179.80	232*	5.8	-0.43	124.39	T
15	1965	3	18	6	22	2.9	-19.90	183.90	225*	5.5	1.01	111.73	P
16	1965	3	22	2	44	47.5	-15.30	186.60	42*	5.9	0.34	106.50	
17	1965	8	20	21	21	51.5	-22.80	183.80	64[1]	6.1	-0.01	114.45	(P)
18	1965	12	8	18	5	25.2	-37.10	177.50	153	6.2	-0.81	129.72	T
19	1966	7	11	22	45	52.0	-19.30	186.60	8	5.3	-1.13	110.23	
20	1966	8	10	5	1	9.3	-20.10	184.60	95[2]	5.8	0.32	111.67	(P)
21	1966	8	20	22	55	0.9	-23.50	184.10	25[1]	5.6	-0.53	114.99	
22	1967	1	1	7	5	50.2	-15.16	186.26	33*	6.0	0.69	106.49	
23	1967	1	19	12	40	15.1	-14.84	181.26	33	6.3	5.28	108.03	
24	1967	2	17	10	10	51.6	-23.74	184.77	46*	6.2	-1.19	114.98	
25	1967	3	4	6	16	22.7	-18.47	184.60	228*	5.5	0.94	110.16	P
26	1967	6	14	5	6	16.3	-15.20	186.40	39*	5.9	0.55	106.48	
27	1967	8	12	9	39	44.3	-24.70	182.50	141*	5.8	0.36	116.66	X
28	1967	9	4	3	51	58.9	-31.40	180.60	236*	5.5	-0.76	123.47	T
29	1967	11	12	10	36	52.0	-17.20	188.00	35*	5.6	-1.61	107.79	
30	1967	12	27	16	22	48.5	-22.30	185.20	33	6.1	-1.02	113.50	
31	1967	12	29	20	29	32.2	-22.80	184.70	30	5.3	-0.78	114.13	
32	1968	1	20	21	21	31.6	-29.90	180.50	349*	5.8	-0.08	122.14	P
33	1968	3	11	8	26	32.8	-16.20	186.10	106*	6.0	0.45	107.52	X
34	1968	4	20	12	25	10.1	-15.70	187.40	37*	5.7	-0.53	106.59	
35	1968	4	26	0	42	34.9	-15.30	186.90	50*	5.3	0.07	106.40	
36	1968	5	28	9	6	29.9	-30.91	182.19	33	5.5	-1.82	122.48	
37	1968	5	30	19	42	25.1	-30.95	182.37	43*	5.5	-1.98	122.46	
38	1968	7	25	7	23	7.8	-30.77	181.65	53*	6.4	-1.34	122.54	
39	1968	7	29	11	11	59.5	-22.46	185.00	29	5.6	-0.91	113.72	
40	1968	8	1	0	14	16.0	-26.65	182.52	124*	5.6	-0.42	118.45	X
41	1968	8	15	6	50	38.7	-23.78	182.58	186[4]	5.5	0.65	115.78	(T)
42	1968	8	28	11	50	30.4	-20.01	176.35	40	5.7	7.46	114.70	
43	1968	9	26	14	37	46.2	-20.92	183.01	254*	5.8	1.39	112.99	X
44	1968	9	26	18	2	50.1	-30.53	181.81	42*	5.8	-1.37	122.26	
45	1969	1	11	4	26	26.8	-28.41	183.04	44*	5.4	-1.53	119.89	
46	1969	1	29	17	44	31.1	-17.20	188.43	35*	6.0	-1.99	107.64	
47	1969	4	28	7	25	29.7	-22.36	182.34	288*	5.9	1.40	114.56	X
48	1969	5	1	19	5	24.7	-16.80	185.33	204*	6.0	0.92	108.35	P
49	1969	5	30	15	55	37.1	-32.22	181.89	34	5.2	-2.10	123.79	
50	1969	6	29	10	34	6.5	-30.51	181.76	43*	5.6	-1.32	122.26	

TABLE C.1.

F	year	mo	day	hr	min	sec	lat	long	depth	m_b	dist	azimuth	mech
51	1969	10	26	6	38	3.4	-16.17	186.05	120*	5.8	0.51	107.51	T
52	1969	11	14	7	37	45.7	-19.67	184.15	209*	5.5	0.88	111.43	P
53	1970	1	8	17	12	39.1	-34.74	178.57	190*	6.1	-0.59	127.22	T
54	1970	1	20	7	19	51.2	-25.80	182.65	58*	6.5	-0.20	117.62	P
55	1970	2	18	15	23	33.7	-20.75	183.12	252*	5.8	1.36	112.80	P
56	1970	8	28	10	6	8.8	-33.86	180.18	46*	5.6	-1.44	125.87	
57	1971	3	23	2	15	26.9	-22.88	183.64	76	6.0	0.10	114.58	(P)
58	1971	9	12	8	6	54.1	-26.70	182.86	100*	5.8	-0.72	118.38	X
59	1971	12	27	11	0	56.8	-19.86	184.08	223*	5.4	0.87	111.63	P
60	1972	1	15	3	39	17.0	-18.30	185.38	135l	5.6	0.31	109.72	(P)
61	1972	3	7	7	45	21.9	-28.23	181.65	200*	6.2	-0.33	120.20	X
62	1972	3	28	13	58	21.9	-30.72	180.18	337	5.7	-0.16	123.00	P
63	1972	5	22	20	45	57.3	-17.69	184.81	224*	6.2	1.05	109.36	P
64	1972	9	22	11	45	14.8	-16.47	185.40	186*	5.5	0.98	108.02	P
65	1973	12	19	12	55	57.1	-20.59	183.52	228*	5.8	1.07	112.50	P
66	1974	5	7	2	25	10.8	-16.69	182.66	33	5.5	3.33	109.21	
67	1974	6	4	4	14	15.9	-15.85	184.90	275*	6.0	1.65	107.62	P
68	1975	1	17	9	30	42.3	-17.91	185.42	140l	5.8	0.42	109.35	(P)
69	1976	1	24	21	48	25.9	-28.64	182.41	78	6.2	-1.11	120.32	T
70	1976	2	14	11	22	17.4	-23.19	182.59	235*	5.9	0.87	115.24	P
71	1976	5	19	19	10	41.7	-31.12	182.21	30l	5.8	-1.92	122.67	
72	1971	8	28	4	9	7.4	-18.81	185.30	145*l	5.4	0.20	110.22	(T)
73	1972	8	29	5	59	1.7	-19.99	184.72	160*s	5.4	0.26	111.52	(t)
74	1977	8	11	1	42	47.5	-17.56	185.63	119*l	6.3	0.37	108.95	P

TABLE C.2. First Motion Solution

F	year	mo	day	hr	min	sec	P-axis pl	P-axis az	T-axis pl	T-axis az	nodal planes dip	nodal planes str	nodal planes dip	nodal planes str	ref
1	1962	5	21	21	15	30.0	50	294	38	98	10	141	84	15	IM53
2	1963	3	26	9	48	20.3	15	104	75	284	60	14	30	194	ISO10
3	1963	3	31	5	30	49.8	16	92	74	288	60	5	30	175	ISO12
4	1963	3	31	19	22	51.5	18	81	68	302	64	2	30	148	ISO13
5	1963	4	17	2	11	36.7	12	211	77	306	48	107	45	312	SIO
6	1963	5	20	11	38	5.3	0	116	78	25	46	36	46	194	ISO17
7	1963	7	4	10	58	13.2	39	339	1	71	65	18	62	121	ISO22
8	1963	7	29	20	14	7.3	32	114	56	273	78	16	16	237	ISO15
9	1963	7	29	20	16	36.9	32	114	56	273	78	16	16	237	ISO16
10	1963	10	8	0	17	1.1	57	343	30	194	76	93	19	320	ISO3
11	1963	12	18	0	30	2.6	45	92	45	272	90	2	0	182	ISO9
12	1964	7	9	11	22	5.4	29	108	61	288	74	18	16	198	ISO7
13	1964	7	21	3	48	59.1	42	308	47	107	87	208	10	102	ISO21
14	1964	8	5	11	6	2.6	32	74	58	254	77	344	13	164	ISO23
15	1965	3	18	6	22	2.9	38	266	43	133	87	199	26	292	ISO18
16	1965	3	22	2	44	47.5	34	339	40	212	87	275	30	10	ISO4
17	1965	8	20	21	21	51.5	40	263	50	93	85	178	8	310	ISO20
18	1965	12	8	18	5	25.2	15	42	57	288	66	335	40	98	IM62
19	1966	7	11	22	45	52.0	38	99	50	300	84	18	12	136	ISO5
20	1966	8	10	5	1	9.3	54	282	29	62	76	348	24	111	ISO19
21	1966	8	20	22	55	0.9	28	98	59	304	74	18	20	160	ISO8
22	1967	1	1	7	5	50.2	32	354	54	203	79	275	18	41	ISO1
23	1967	1	19	12	40	15.1	8	230	14	322	87	97	75	2	ISO39
24	1967	2	17	10	10	51.6	79	124	11	304	56	214	34	34	JM98
25	1967	3	4	6	16	22.7	32	258	32	144	90	202	40	292	B24
26	1967	6	14	5	6	16.3	18	344	40	240	76	288	50	30	JM83
27	1967	8	12	9	39	44.3	27	350	61	193	72	267	20	54	IM56
28	1967	9	4	3	51	58.9	32	61	56	263	16	119	78	340	IM60
29	1967	11	12	10	36	52.0	0	94	90	0	45	184	45	4	JM88
30	1967	12	27	16	22	48.5	40	143	16	247	50	292	76	189	JM94
31	1967	12	29	20	29	32.2	24	108	65	280	70	16	20	204	JM95
32	1968	1	20	21	21	31.6	62	330	7	71	45	134	57	3	IM59
33	1968	3	11	8	26	32.8	48	339	12	234	67	115	48	2	IM50
34	1968	4	20	12	25	10.1	20	8	70	188	64	278	26	98	JM86
35	1968	4	26	0	42	34.9	10	347	48	237	68	276	50	30	JM85
36	1968	5	28	9	6	29.9	15	104	75	284	60	14	30	194	JM111
37	1968	5	30	19	42	25.1	25	90	65	270	70	0	20	180	JM114
38	1968	7	25	7	23	7.8	15	102	75	282	60	12	30	192	JM112
39	1968	7	29	11	11	59.5	34	138	50	282	82	33	20	283	JM93
40	1968	8	1	0	14	16.0	3	305	44	210	53	3	58	245	R13
41	1968	8	15	6	50	38.7	32	72	56	268	78	348	14	141	B42
42	1968	8	28	11	50	30.4	1	190	4	100	86	235	88	145	JM75
43	1968	9	26	14	37	46.2	72	0	13	140	60	61	34	212	WM1
44	1968	9	26	18	2	50.1	22	80	59	308	70	6	30	136	JM109
45	1969	1	11	4	26	26.8	35	116	55	296	80	26	10	206	JM100
46	1969	1	29	17	44	31.1	27	272	63	92	72	182	18	2	JM87
47	1969	4	28	7	25	29.7	11	342	24	246	80	292	64	27	R34
48	1969	5	1	19	5	24.7	69	326	17	186	30	296	64	85	WM3
49	1969	5	30	15	55	37.1	35	90	45	270	80	0	10	180	JM115
50	1969	6	29	10	34	6.5	25	90	65	270	70	0	20	180	JM110

TABLE C.2. First Motion Solution

							P-axis		T-axis		nodal planes				
F	year	mo	day	hr	min	sec	pl	az	pl	az	dip	str	dip	str	ref
51	1969	10	26	6	38	3.4	2	334	72	239	50	261	46	47	B15
52	1969	11	14	7	37	45.7	54	251	34	91	80	353	14	218	B26
53	1970	1	8	17	12	39.1	16	101	62	225	65	352	35	220	B68
54	1970	1	20	7	19	51.2	37	331	53	159	9	38	82	244	R16
55	1970	2	18	15	23	33.7	52	310	32	164	79	60	20	300	B30
56	1970	8	28	10	6	8.8	8	248	8	339	78	24	90	114	R3
57	1971	3	23	2	15	26.9	44	268	44	108	90	8	10	278	B38
58	1971	9	12	8	6	54.1	10	349	65	102	59	241	40	104	R12
59	1971	12	27	11	0	56.8	32	267	22	162	84	37	50	302	B27
60	1972	1	15	3	39	17.0	37	257	43	123	87	189	30	285	B23
61	1972	3	7	7	45	21.9	39	352	14	250	74	126	52	24	B48
62	1972	3	28	13	58	21.9	42	356	1	87	61	141	62	33	R6
63	1972	5	22	20	45	57.3	63	279	10	164	60	56	40	284	B22
64	1972	9	22	11	45	14.8	53	284	37	96	82	10	9	169	B17
65	1973	12	19	12	55	57.1	42	288	43	138	89	212	17	304	R52
66	1974	5	7	2	25	10.8	3	350	12	259	83	304	80	35	B6
67	1974	6	4	4	14	15.9	40	285	44	137	88	209	18	305	R69
68	1975	1	17	9	30	42.3	67	241	11	124	39	237	58	18	R63
69	1976	1	24	21	48	25.9	8	61	48	327	64	5	54	111	R9
70	1976	2	14	11	22	17.4	53	278	37	98	82	8	8	188	NEW
71	1976	5	19	19	10	41.7	0	197	8	287	84	331	84	62	NEW
72	1971	8	28	4	9	7.4	29	109	50	336	80	40	27	153	NEW
73	1972	8	29	5	59	1.7	31	111	59	291	76	21	14	201	NEW
74	1977	8	11	1	42	47.5	53	270	37	90	8	180	82	0	NEW

TABLE C.3. Harvard Centroid Moment Tensor earthquake

H	year	mo	day	hr	min	sec	lat	long	depth	m_b	dist	azimuth	mech
1	1977	3	22	2	23	20.0	-33.89	178.81	282	5.6	-0.41	126.36	T
2	1977	6	22	12	8	33.4	-22.88	184.10	61	6.8	-0.30	114.42	T
3	1978	1	28	19	36	38.6	-25.92	182.70	98	6.0	-0.29	117.71	P
4	1978	6	25	10	21	45.0	-17.11	185.57	164	5.5	0.59	108.55	P
5	1978	7	17	13	26	14.9	-14.89	184.18	322	6.0	2.66	106.99	
6	1978	9	16	23	38	8.9	-25.73	182.05	235	5.7	0.33	117.77	P
7	1978	11	23	4	41	39.3	-26.18	182.31	191	5.5	-0.06	118.09	X
8	1979	8	5	0	53	45.9	-22.72	182.51	229	6.4	1.12	114.83	P
9	1979	11	11	16	31	22.1	-20.26	183.85	218	5.5	0.92	112.08	P
10	1980	4	13	18	4	31.9	-23.47	182.70	166	6.7	0.67	115.46	P
11	1980	4	26	2	35	0.0	-15.59	185.66	185	5.5	1.07	107.11	
12	1980	5	12	14	23	45.6	-23.63	182.81	152	5.5	0.51	115.56	X
13	1980	11	30	12	24	39.8	-19.43	184.15	238	6.0	0.97	111.21	P
14	1981	2	20	9	40	55.7	-33.28	181.09	15	5.6	-1.90	125.03	
15	1981	3	5	12	53	29.5	-37.31	177.30	20	5.7	-0.76	129.98	
16	1981	3	7	23	30	8.4	-30.57	181.79	24	5.7	-1.37	122.31	
17	1981	6	1	14	7	1.8	-16.13	186.44	15	5.1	0.18	107.33	
18	1981	6	26	0	51	6.0	-30.27	181.01	164	5.7	-0.63	122.30	P
19	1981	8	1	6	10	9.6	-18.64	186.45	20	5.7	-0.75	109.66	
20	1981	8	13	2	57	4.4	-16.09	185.63	188	5.4	0.91	107.58	X
21	1981	8	25	7	16	58.4	-22.89	184.15	108	5.8	-0.34	114.41	X
22	1981	9	1	7	23	2.1	-15.14	186.71	20	5.8	0.30	106.32	
23	1981	9	25	14	30	53.4	-29.97	181.99	27	5.9	-1.29	121.69	
24	1981	9	28	17	56	18.0	-29.33	180.96	309	6.0	-0.21	121.45	P
25	1981	10	1	16	2	51.6	-33.91	180.38	20	5.6	-1.61	125.85	
26	1981	11	4	14	38	10.7	-20.05	185.72	57	6.3	-0.63	111.23	T
27	1981	11	16	19	42	38.2	-33.89	180.30	14	5.5	-1.54	125.85	
28	1981	11	18	17	37	48.7	-29.52	182.77	15	5.6	-1.74	121.01	
29	1981	11	25	19	1	47.9	-15.25	186.69	22	5.6	0.27	106.42	
30	1981	12	23	18	47	18.3	-15.45	186.25	120	5.6	0.59	106.77	
31	1981	12	24	5	33	20.7	-29.97	182.39	19	6.0	-1.61	121.55	
32	1981	12	26	17	5	32.5	-29.93	182.26	31	6.1	-1.49	121.56	
33	1981	12	29	19	6	31.6	-30.24	182.12	31	5.5	-1.50	121.89	
34	1982	1	4	22	20	53.6	-23.17	182.69	191	6.0	0.79	115.18	P
35	1982	2	28	17	0	24.2	-21.70	186.46	52	5.6	-1.88	112.51	
36	1982	3	7	15	41	57.1	-25.10	184.43	51	5.9	-1.41	116.36	
37	1982	3	21	13	35	3.1	-18.59	184.81	217	5.9	0.71	110.19	P
38	1982	3	28	3	52	34.6	-31.49	181.34	36	6.0	-1.38	123.30	
39	1982	3	29	12	20	26.7	-15.47	180.39	12	5.8	5.81	108.94	
40	1982	4	8	11	40	30.5	-20.61	185.82	14	5.5	-0.93	111.71	
41	1982	4	12	0	34	44.3	-30.18	182.11	31	5.7	-1.47	121.84	
42	1982	4	16	14	4	51.2	-15.79	187.01	59	6.0	-0.21	106.82	
43	1982	5	1	10	27	52.8	-29.22	182.65	19	5.4	-1.53	120.77	
44	1982	5	2	11	19	38.0	-29.32	182.85	20	6.0	-1.73	120.80	
45	1982	6	2	12	37	34.5	-18.08	187.51	11	6.4	-1.49	108.78	
46	1982	6	11	0	38	9.8	-17.62	185.59	113	6.3	0.38	109.02	P
47	1982	6	17	11	46	4.8	-15.32	186.55	50	5.3	0.37	106.54	
48	1982	7	4	21	26	38.8	-19.53	186.19	12	5.6	-0.85	110.58	
49	1982	7	30	3	41	1.9	-18.45	186.26	70	5.5	-0.52	109.55	T
50	1982	8	7	18	20	22.1	-16.55	187.36	15	5.5	-0.80	107.40	

TABLE C.3. (continued)

H	year	mo	day	hr	min	sec	lat	long	depth	m_b	dist	azimuth	mech
51	1982	9	3	23	39	39.0	-15.30	186.91	10	5.9	0.06	106.39	
52	1982	9	4	2	8	9.0	-15.43	186.94	10	5.7	-0.02	106.50	
53	1982	9	4	13	31	14.9	-25.52	183.76	10	6.0	-1.01	116.98	
54	1982	9	16	8	23	12.4	-15.71	187.26	11	5.6	-0.41	106.65	
55	1982	9	20	12	57	45.3	-26.93	184.04	10	5.4	-1.78	118.19	
56	1982	9	28	15	14	36.7	-24.27	183.33	42	6.0	-0.17	115.97	X
57	1982	10	5	10	15	29.2	-29.86	181.72	163	5.5	-1.03	121.68	X
58	1982	10	19	3	34	32.1	-17.89	187.11	10	5.5	-1.06	108.74	
59	1982	11	10	21	20	45.8	-15.49	184.04	10	5.5	2.56	107.60	
60	1982	11	11	21	21	30.8	-27.43	183.26	10	5.3	-1.33	118.91	
61	1982	11	22	5	32	45.3	-23.91	184.18	10	5.5	-0.75	115.34	
62	1982	11	27	2	19	10.1	-32.51	181.75	10	5.4	-2.10	124.10	
63	1982	12	3	1	38	46.4	-23.63	184.23	10	5.3	-0.69	115.07	
64	1982	12	5	15	52	24.8	-23.41	184.05	10	5.6	-0.45	114.92	
65	1982	12	14	12	2	6.1	-24.02	184.37	10	5.4	-0.96	115.38	
66	1982	12	19	0	6	19.7	-32.55	181.59	10	5.8	-1.99	124.19	
67	1982	12	19	13	0	15.8	-24.18	184.08	10	5.4	-0.77	115.63	
68	1982	12	19	17	43	54.8	-24.13	184.14	29	5.9	-0.80	115.56	
69	1982	12	20	2	58	10.5	-23.72	184.02	10	5.6	-0.55	115.22	
70	1982	12	20	5	54	37.3	-24.50	184.13	10	5.8	-0.94	115.91	
71	1982	12	20	14	35	45.0	-24.74	184.32	10	5.6	-1.19	116.06	
72	1982	12	21	16	12	18.0	-24.73	184.01	10	5.4	-0.92	116.16	
73	1983	1	8	11	21	29.5	-15.39	186.67	53	6.1	0.24	106.56	
74	1983	1	16	13	10	45.4	-16.78	182.85	12	5.7	3.12	109.23	
75	1983	1	26	16	2	21.3	-30.38	180.66	224	6.0	-0.40	122.52	X
76	1983	2	7	18	23	16.6	-29.71	182.16	53	6.0	-1.32	121.39	
77	1983	2	17	16	10	39.1	-21.59	185.82	10	5.8	-1.29	112.62	
78	1983	3	21	7	44	17.7	-21.47	184.55	52	6.3	-0.15	112.95	P
79	1983	4	7	15	38	36.0	-22.53	184.88	12	5.5	-0.83	113.82	
80	1983	4	11	17	3	41.7	-35.55	180.75	48	5.7	-2.55	127.23	
81	1983	4	15	0	9	33.3	-19.22	184.53	226	5.7	0.72	110.88	P
82	1983	4	24	3	29	17.5	-23.98	184.04	39	5.9	-0.66	115.46	
83	1983	4	27	17	20	35.2	-21.14	185.73	10	5.5	-1.05	112.24	
84	1983	4	30	2	51	43.3	-21.35	185.75	10	5.8	-1.14	112.43	
85	1983	5	5	4	43	50.4	-33.87	179.65	10	5.8	-1.04	126.06	
86	1983	5	11	21	48	15.4	-21.43	186.55	12	5.7	-1.86	112.23	
87	1983	5	15	0	24	0.6	-18.91	184.36	20	5.7	0.98	110.65	
88	1983	5	29	22	7	57.4	-15.60	185.12	276	5.4	1.55	107.31	
89	1983	6	1	2	0	1.9	-17.00	185.29	188	6.1	0.88	108.55	P
90	1983	6	1	10	58	45.7	-15.92	187.20	10	5.6	-0.43	106.87	
91	1983	6	10	22	39	11.6	-24.27	183.72	18	5.7	-0.50	115.83	
92	1983	6	15	6	8	0.5	-15.19	186.31	54	5.5	0.64	106.50	
93	1983	6	25	10	3	12.6	-32.80	181.20	13	5.6	-1.79	124.55	
94	1983	6	25	15	4	14.3	-22.04	182.53	274	5.5	1.37	114.20	P
95	1983	7	8	10	4	53.1	-21.82	186.62	49	5.5	-2.07	112.57	
96	1983	7	17	23	2	45.9	-22.79	181.87	306	5.2	1.63	115.13	P
97	1983	7	24	0	52	23.8	-27.90	183.59	57	5.3	-1.78	119.24	
98	1983	7	28	1	40	36.2	-28.15	183.74	43	5.6	-2.00	119.42	
99	1983	8	10	20	5	49.4	-23.71	183.98	11	5.5	-0.51	115.23	
100	1983	8	15	19	44	44.6	-17.10	185.41	181	5.5	0.73	108.60	X

TABLE C.3. (continued)

H	year	mo	day	hr	min	sec	lat	long	depth	m_b	dist	azimuth	mech
101	1983	8	21	22	57	34.3	-23.48	182.81	139	5.5	0.57	115.43	P
102	1983	8	30	8	50	17.9	-16.68	187.92	40	6.1	-1.35	107.33	
103	1983	9	13	19	30	57.9	-23.99	184.39	10	5.3	-0.96	115.34	
104	1983	9	17	12	11	43.1	-16.54	182.44	16	6.1	3.58	109.16	
105	1983	10	17	13	25	24.8	-20.44	185.87	10	5.8	-0.91	111.54	
106	1983	10	28	5	56	55.2	-31.05	179.60	10	5.6	0.16	123.50	
107	1983	12	3	1	24	0.2	-15.65	187.04	41	6.1	-0.19	106.67	
108	1983	12	4	19	30	43.0	-20.72	186.25	10	5.4	-1.34	111.67	
109	1983	12	9	13	48	11.8	-16.74	186.47	63	5.3	-0.08	107.89	
110	1983	12	20	16	6	10.3	-16.47	178.10	10	5.5	7.42	110.75	
111	1983	12	23	14	35	52.3	-20.91	184.29	10	5.2	0.29	112.53	
112	1984	1	19	16	15	21.5	-23.63	181.63	336	5.9	1.51	115.99	P
113	1984	2	25	15	29	20.1	-16.69	185.18	269	5.7	1.09	108.30	X
114	1984	3	2	0	0	42.9	-20.98	183.29	231	5.4	1.12	112.95	P
115	1984	3	6	0	25	27.2	-29.00	180.88	299	5.2	-0.02	121.18	X
116	1984	3	21	10	10	49.9	-19.37	186.47	10	5.3	-1.04	110.34	
117	1984	3	23	20	31	40.2	-15.24	186.33	43	5.6	0.60	106.54	
118	1984	4	18	6	49	13.9	-15.93	185.65	158	5.9	0.95	107.43	P
119	1984	4	29	17	20	14.9	-19.71	184.30	230	5.4	0.73	111.41	P
120	1984	8	17	10	42	20.1	-21.42	184.73	57	5.6	-0.28	112.84	P

TABLE C.4. Harvard Centroid Moment Tensor Solution

							P-axis		T-axis		nodal planes				
H	year	mo	day	hr	min	sec	pl	az	pl	az	dip	str	dip	str	moment
1	1977	3	22	2	23	20.0	41	85	47	245	10	237	87	346	1.1e25
2	1977	6	22	12	8	33.4	56	107	34	286	11	14	79	197	1.4e28
3	1978	1	28	19	36	38.6	29	334	51	105	28	110	78	224	4.7e25
4	1978	6	25	10	21	45.0	61	300	18	175	34	296	66	67	4.3e24
5	1978	7	17	13	26	14.9	37	168	45	29	22	198	86	97	7.1e25
6	1978	9	16	23	38	8.9	27	327	28	72	50	109	89	200	6.3e24
7	1978	11	23	4	41	39.3	38	350	37	224	31	16	89	108	3.7e24
8	1979	8	5	0	53	45.9	57	315	32	124	14	195	77	38	6.7e25
9	1979	11	11	16	31	22.1	54	282	35	118	12	242	81	21	1.3e24
10	1980	4	13	18	4	31.9	51	325	31	101	25	144	79	30	2.8e27
11	1980	4	26	2	35	0.0	58	103	29	256	19	316	75	177	1.6e24
12	1980	5	12	14	23	45.6	27	326	60	175	21	29	73	246	2.3e24
13	1980	11	30	12	24	39.8	46	292	43	123	6	281	88	27	3.4e25
14	1981	2	20	9	40	55.7	43	105	47	292	4	135	88	18	8.0e24
15	1981	3	5	12	53	29.5	38	205	21	313	46	355	80	255	7.8e24
16	1981	3	7	23	30	8.4	20	96	70	270	25	190	65	4	5.5e24
17	1981	6	1	14	7	1.8	85	64	4	224	41	312	49	135	7.6e23
18	1981	6	26	0	51	6.0	59	302	29	102	18	169	75	19	2.0e25
19	1981	8	1	6	10	9.6	17	232	63	358	34	350	65	125	3.1e24
20	1981	8	13	2	57	4.4	26	358	64	190	20	77	71	272	2.2e24
21	1981	8	25	7	16	58.4	27	155	7	248	66	295	76	199	4.1e24
22	1981	9	1	7	23	2.1	46	61	17	169	44	218	72	108	6.4e24
23	1981	9	25	14	30	53.4	12	106	78	302	33	191	57	19	1.2e25
24	1981	9	28	17	56	18.0	45	341	28	103	34	143	81	38	7.6e25
25	1981	10	1	16	2	51.6	27	105	59	252	23	226	73	3	9.4e24
26	1981	11	4	14	38	10.7	53	87	37	273	8	19	82	180	7.4e25
27	1981	11	16	19	42	38.2	18	102	64	233	32	218	65	357	1.4e25
28	1981	11	18	17	37	48.7	22	97	68	285	23	182	67	9	1.0e25
29	1981	11	25	19	1	47.9	61	344	27	187	20	300	73	89	8.8e00
30	1981	12	23	18	47	18.3	41	61	48	232	6	200	87	327	8.7e24
31	1981	12	24	5	33	20.7	23	100	65	259	23	206	69	3	2.1e26
32	1981	12	26	17	5	32.5	18	103	71	261	28	203	63	7	4.6e26
33	1981	12	29	19	6	31.6	21	86	68	258	24	181	66	354	9.5e23
34	1982	1	4	22	20	53.6	58	312	31	115	16	181	77	32	4.4e25
35	1982	2	28	17	0	24.2	16	289	73	85	30	29	61	193	3.0e24
36	1982	3	7	15	41	57.1	9	309	34	213	60	356	73	256	7.8e24
37	1982	3	21	13	35	3.1	60	267	27	115	21	232	73	15	6.2e24
38	1982	3	28	3	52	34.6	17	102	70	248	30	208	62	4	4.1e25
39	1982	3	29	12	20	26.7	7	199	9	107	78	243	89	153	5.0e25
40	1982	4	8	11	40	30.5	19	112	69	264	27	217	65	15	1.5e24
41	1982	4	12	0	34	44.3	17	104	67	240	31	215	63	2	2.4e25
42	1982	4	16	14	4	51.2	34	82	50	228	19	223	82	337	2.0e25
43	1982	5	1	10	27	52.8	15	105	74	270	30	200	60	11	2.3e24
44	1982	5	2	11	19	38.0	13	104	74	247	33	206	58	6	4.5e25
45	1982	6	2	12	37	34.5	66	182	6	285	44	352	55	215	4.0e25
46	1982	6	11	0	38	9.8	53	259	34	105	16	237	80	4	2.0e26
47	1982	6	17	11	46	4.8	29	43	45	166	33	183	81	288	6.8e23
48	1982	7	4	21	26	38.8	12	108	71	341	36	179	59	31	2.0e24
49	1982	7	30	3	41	1.9	47	116	36	258	21	291	84	185	2.5e24
50	1982	8	7	18	20	22.1	33	108	56	274	13	223	79	13	7.6e24

TABLE C.4. (continued)

H	year	mo	day	hr	min	sec	P-axis pl	P-axis az	T-axis pl	T-axis az	nodal planes dip	nodal planes str	nodal planes dip	nodal planes str	moment
51	1982	9	3	23	39	39.0	33	78	56	262	12	160	79	349	5.5e25
52	1982	9	4	2	8	9.0	15	131	47	237	46	261	70	11	2.6e25
53	1982	9	4	13	31	14.9	26	88	64	262	19	185	71	356	1.5e25
54	1982	9	16	8	23	12.4	7	320	6	229	81	5	90	95	3.4e24
55	1982	9	20	12	57	45.3	16	87	72	241	30	187	62	351	1.1e25
56	1982	9	28	15	14	36.7	7	13	7	282	80	58	90	148	4.4e25
57	1982	10	5	10	15	29.2	10	344	27	79	64	119	79	214	1.6e24
58	1982	10	19	3	34	32.1	33	85	54	242	15	212	79	346	4.4e24
59	1982	11	10	21	20	45.8	23	243	12	148	65	283	83	17	1.4e25
60	1982	11	11	21	21	30.8	22	103	68	284	23	192	67	13	4.7e24
61	1982	11	22	5	32	45.3	25	102	65	269	21	203	70	8	1.7e24
62	1982	11	27	2	19	10.1	25	109	64	269	21	217	70	13	3.3e24
63	1982	12	3	1	38	46.4	26	111	63	280	19	211	71	17	3.3e24
64	1982	12	5	15	52	24.8	17	112	72	303	28	197	62	25	7.7e24
65	1982	12	14	12	2	6.1	21	103	63	241	28	221	68	0	2.4e24
66	1982	12	19	0	6	19.7	18	106	71	265	27	207	64	11	2.3e24
67	1982	12	19	13	0	15.8	20	95	68	247	26	201	66	357	3.7e24
68	1982	12	19	17	43	54.8	23	100	66	269	22	198	68	6	2.0e27
69	1982	12	20	2	58	10.5	27	95	62	254	20	206	72	358	3.3e25
70	1982	12	20	5	54	37.3	23	102	66	259	24	209	68	5	6.4e24
71	1982	12	20	14	35	45.0	11	99	75	237	35	201	57	1	5.8e24
72	1982	12	21	16	12	18.0	29	99	61	276	16	192	74	8	7.9e24
73	1983	1	8	11	21	29.5	50	15	39	176	11	214	85	94	3.0e25
74	1983	1	16	13	10	45.4	7	357	2	266	84	41	87	132	3.7e24
75	1983	1	26	16	2	21.3	52	354	38	177	7	278	83	86	3.7e26
76	1983	2	7	18	23	16.6	16	98	73	295	29	181	62	12	1.6e25
77	1983	2	17	16	10	39.1	26	115	61	264	22	232	72	14	2.6e24
78	1983	3	21	7	44	17.7	29	272	61	96	16	357	74	183	1.2e26
79	1983	4	7	15	38	36.0	25	126	65	292	21	227	70	31	7.2e23
80	1983	4	11	17	3	41.7	21	115	56	240	33	241	71	5	2.2e24
81	1983	4	15	0	9	33.3	55	262	19	142	36	269	70	30	8.1e24
82	1983	4	24	3	29	17.5	5	12	66	271	45	79	54	303	3.9e24
83	1983	4	27	17	20	35.2	22	112	66	269	24	217	67	15	5.1e24
84	1983	4	30	2	51	43.3	31	112	59	285	14	213	76	20	3.1e24
85	1983	5	5	4	43	50.4	46	194	25	314	36	357	78	250	6.4e24
86	1983	5	11	21	48	15.4	28	310	59	101	20	71	74	210	3.5e24
87	1983	5	15	0	24	0.6	9	163	3	72	82	207	86	298	1.1e26
88	1983	5	29	22	7	57.4	72	305	17	111	28	195	62	25	2.3e24
89	1983	6	1	2	0	1.9	68	313	21	126	24	211	66	38	7.2e25
90	1983	6	1	10	58	45.7	2	127	7	217	84	262	86	352	2.2e25
91	1983	6	10	22	39	11.6	21	105	69	282	24	196	66	14	3.5e24
92	1983	6	15	6	8	0.5	45	32	40	183	16	206	87	107	4.3e24
93	1983	6	25	10	3	12.6	82	169	5	302	40	26	51	217	2.6e24
94	1983	6	25	15	4	14.3	52	322	22	84	34	134	73	17	5.7e24
95	1983	7	8	10	4	53.1	5	307	48	42	54	73	62	185	7.0e23
96	1983	7	17	23	2	45.9	60	342	21	114	30	172	69	41	6.1e23
97	1983	7	24	0	52	23.8	22	125	35	232	48	264	82	1	6.0e24
98	1983	7	28	1	40	36.2	13	114	32	213	58	249	78	347	4.5e24
99	1983	8	10	20	5	49.4	25	96	63	255	21	205	71	359	2.5e24
100	1983	8	15	19	44	44.6	73	320	16	117	30	197	61	32	2.1e24

TABLE C.4. (continued)

							P-axis		T-axis		nodal planes				
H	year	mo	day	hr	min	sec	pl	az	pl	az	dip	str	dip	str	moment
101	1983	8	21	22	57	34.3	55	260	25	128	28	257	74	19	9.3e23
102	1983	8	30	8	50	17.9	4	246	63	150	48	311	54	180	1.1e25
103	1983	9	13	19	30	57.9	25	112	65	283	20	210	70	19	2.7e24
104	1983	9	17	12	11	43.1	1	4	0	274	89	49	89	139	7.8e25
105	1983	10	17	13	25	24.8	34	110	54	271	14	235	80	12	1.9e25
106	1983	10	28	5	56	55.2	9	227	5	317	80	2	87	272	1.2e25
107	1983	12	3	1	24	0.2	57	10	31	211	17	330	76	113	1.7e25
108	1983	12	4	19	30	43.0	27	112	60	266	20	229	73	12	1.9e24
109	1983	12	9	13	48	11.8	13	123	62	237	39	242	62	12	8.7e23
110	1983	12	20	16	6	10.3	60	174	14	289	39	348	63	220	1.9e24
111	1983	12	23	14	35	52.3	11	73	78	268	34	159	56	345	2.4e24
112	1984	1	19	16	15	21.5	38	262	50	104	13	301	84	181	2.3e25
113	1984	2	25	15	29	20.1	52	195	36	351	14	36	82	271	5.2e24
114	1984	3	2	0	0	42.9	67	274	21	120	25	227	67	22	1.7e24
115	1984	3	6	0	25	27.2	52	25	11	280	46	46	65	162	1.1e24
116	1984	3	21	10	10	49.9	13	111	71	241	35	220	59	9	3.9e24
117	1984	3	23	20	31	40.2	49	8	41	180	6	226	86	93	1.1e25
118	1984	4	18	6	49	13.9	65	264	24	97	21	198	70	3	5.7e25
119	1984	4	29	17	20	14.9	35	248	19	144	50	281	80	19	3.3e24
120	1984	8	17	10	42	20.1	30	276	58	119	18	337	76	195	3.0e23

TABLE C.5. Events with Mechanism Type (Figure 3.6)

event	year	mo	day	hr	min	sec	lat	long	depth	m_b	distance	azimuth
T1	1966	8	12	3	59	49.7	-22.40	183.80	127[*s]	5.4	0.14	114.08
C1	1968	8	25	11	15	46.3	-20.03	184.69	96[*s]	5.5	0.27	111.57
T2	1972	8	29	5	59	1.7	-19.99	184.72	160[*s]	5.4	0.26	111.52
C2	1974	11	11	6	29	21.1	-23.91	182.44	166[*s]	5.6	0.71	115.95
C3	1975	5	5	20	28	8.3	-23.01	183.76	80[l]	5.6	-0.06	114.66
T3	1977	3	26	8	19	18.5	-18.58	185.85	91[*sl]	5.6	-0.20	109.82
C4	1978	2	22	19	37	17.0	-22.70	183.79	67[l]	5.6	0.04	114.36
C5	1980	5	27	13	1	34.8	-18.65	185.25	115[l]	6.1	0.30	110.09

APPENDIX D

RELOCATION METHOD OF CHAPTER III

The relocation procedure employed in Chapter 3 is similar to that of Veith (1974) and Samowitz and Forsyth (1981), and it tries to locate a group of earthquakes relative to each other. The basic assumption is that the ray paths from earthquakes in some small region to a particular station at teleseismic distance ($>30^{o}$) are similar and thus the travel time residuals due to Earth model error are similar for each station. Under these assumptions, the master event technique and joint hypocenter determination technique (JHD; Douglas, 1967; Dewey, 1972) have been introduced. The region of interest in Chapter 3 is large (800 km along the strike of trench) and the above conditions may not be fulfilled. Following Samowitz and Forsyth (1981), I assume that the travel time residuals to a given station (due to the Earth model error) vary smoothly as a function of distance between the station and earthquakes, and can be modeled linearly to the first order.

There are two steps in the relocation procedure. For each step, the earthquake location program originally written by Dewey (JHD77; Dewey, 1972) was used with some modification. Although JHD77 is a program for the joint hypocenter determination it is used simply as an epicenter estimation program (depths are determined by pP-P time difference). The detailed procedure can be found in Dewey (1972) and only the weighting scheme will be repeated here.

The procedure of earthquake location is a classical non-linear inverse problem and it is solved by the method of successive least squares. For the first three iterations, a weighting scheme developed by Bolt (1960) is used to minimize the effects of extreme residuals. The stations are grouped into four depending on which quadrant of the Earth's surface (with respect to the earthquake) they are located. The residuals r_j are weighted according to the extent to which they deviate from the mean residual of the quadrant in which the station j is located. Figure D.1a shows the weighting function. After three iterations, the residual variance of the earthquake, σ_0^2, is estimated and this value is used in the weighting scheme for the rest of the iterations. The weight for a given iteration for a given station is set by

$$w_j = \left\{ \frac{1.0}{1+0.02exp\,[r_j^2/2\sigma_0^2]} \right\}^{1/2} \qquad (D.1)$$

(Figure D.1b). In total, seven depth-fixed iterations are preformed for each earthquake to determine the epicenter.

Data are selected from the ISC bulletin from 1970 to 1979 with the following conditions; (1) pP-P constrained depths between 60 km and 200 km, (2) more than 30 P arrival observations, (3) azimuth (measured from the north Pole at the pole of the arc) between 107^o and 117^o. In total, 46 earthquakes are selected, including thirteen events for which either focal mechanisms or focal mechanism types are known.

For the first step, the earthquakes are relocated using the P-wave arrival times reported at station distances between 30^o and 100^o in order to estimate the station correction term in the residuals. After the earthquakes are relocated, the stations which have arrivals from more than 10 earthquakes are selected for the next step. There are 113 stations left at this stage. The travel time corrections for these stations are determined by least square fit of the residuals to a linear function of distance between the stations and earthquakes. Figures D.2 show residuals by open circles and the travel time corrections by solid lines.

In the second step, the travel times are first subtracted by the amount estimated from the linear function obtained in the first step. Relocation was then performed for each event separately using only the arrivals from those 113 stations. Each station was weighted inversely proportionally to its residual variance estimated in the first step. Crosses in Figures D.2 denote the residuals after the second step. They are distributed around the solid lines and thus further steps (i.e., reestimating the station correction terms and repeating the second step) will not affect the result significantly.

Table D.1 compares the original ISC locations to the relocated ones. For each earthquake, the first row is the ISC estimate and the second row is the relocated one. 90 % confidence intervals for the latitude and the longitude are given in units of km for the relocated location.

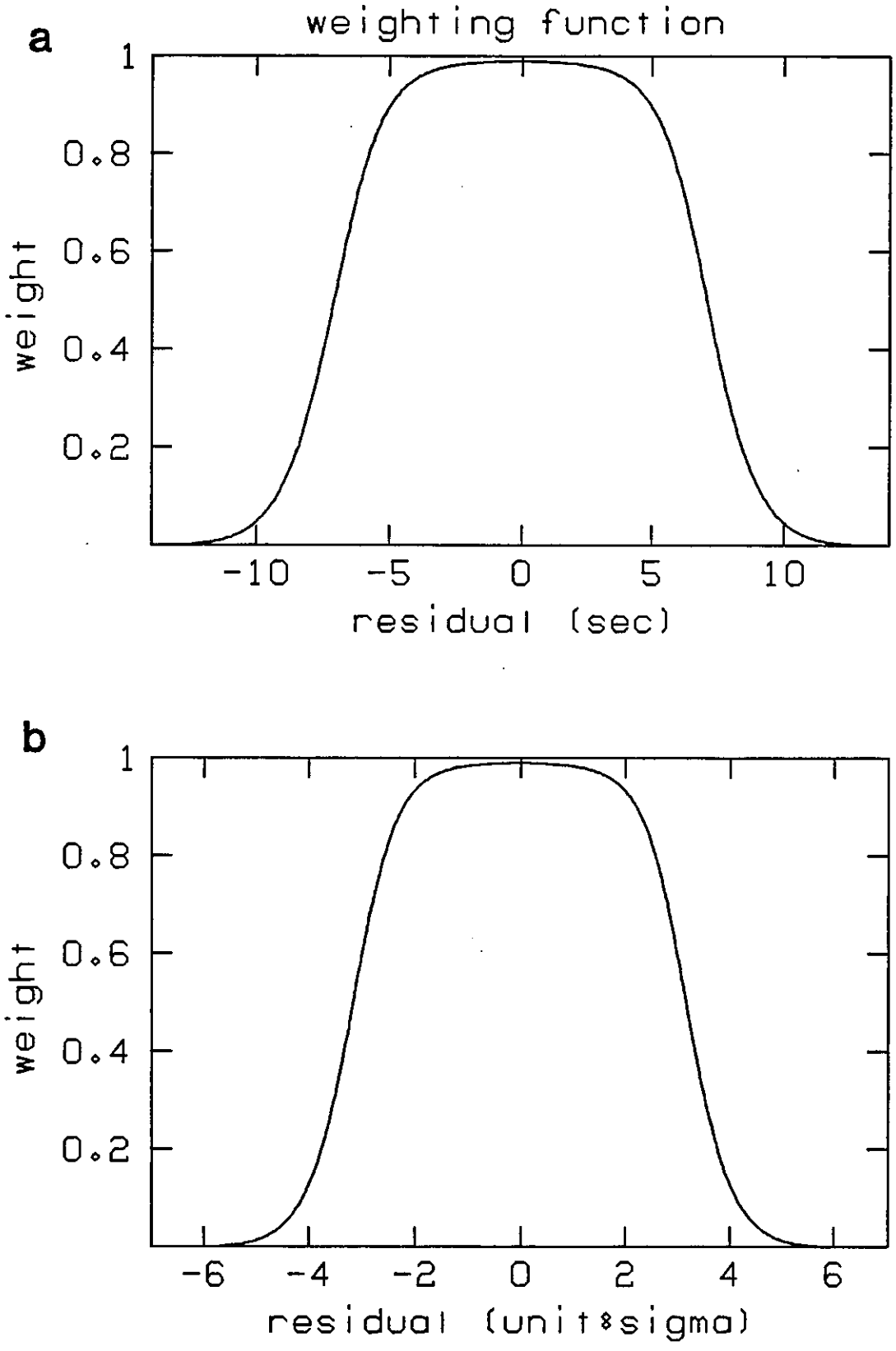

Figure D.1. Weighting function in the location program. (a) For the first three iterations. (b) After the third iteration.

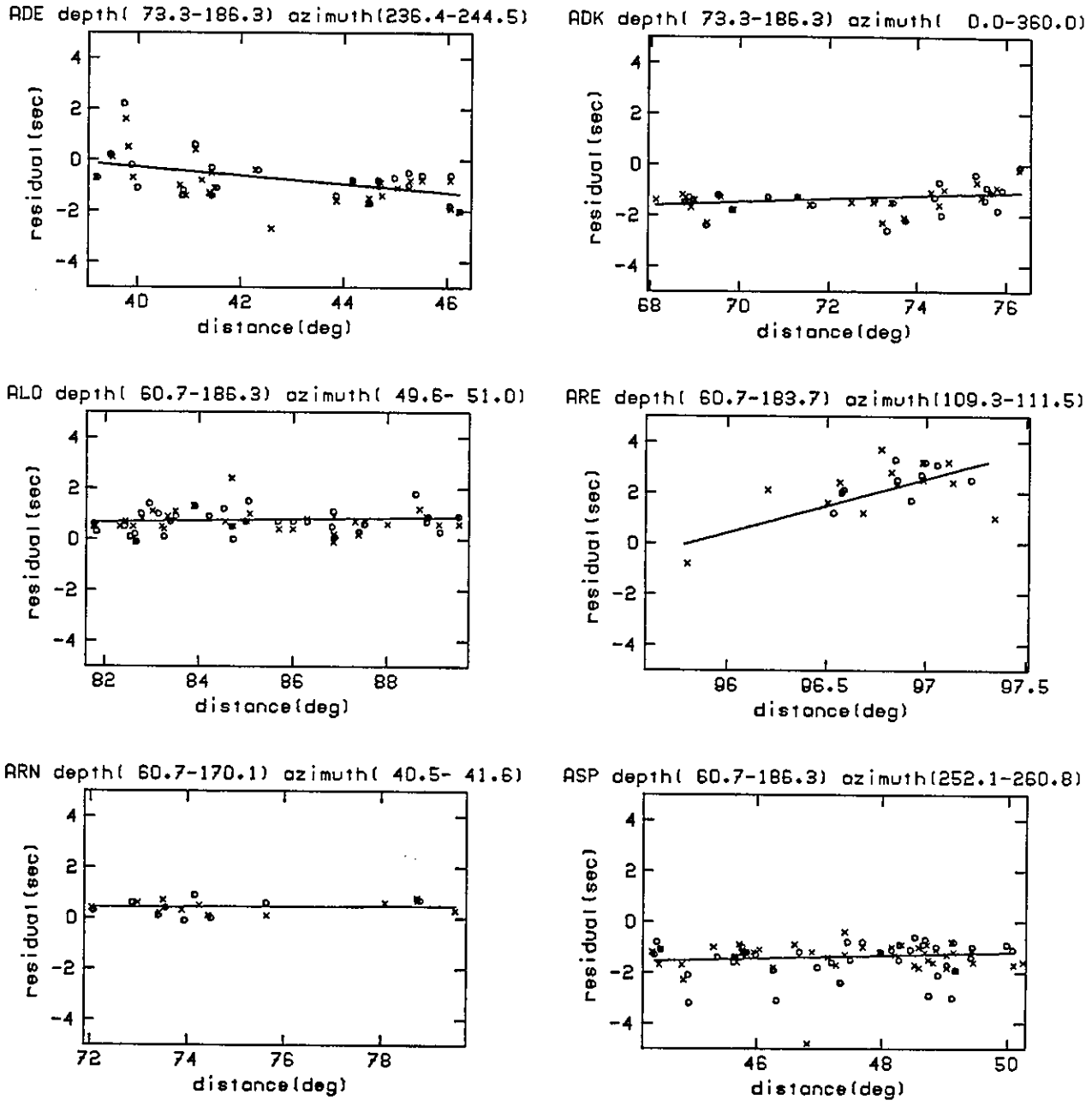

Figure D.2. Residuals and the travel time correction for all the stations used in the second step of the relocation. Open circles and crosses denote residuals after the first and the second step of the relocation. Solid straight line is the travel time correction for the station, estimated from the open circles by least square method. Each point on plot corresponds to the residual for one earthquake at the give station. The horizontal axis is a station-event distance. The three letters code for the station and the depth and azimuth ranges of earthquakes, which have arrivals at the station, are shown on the top of each figure.

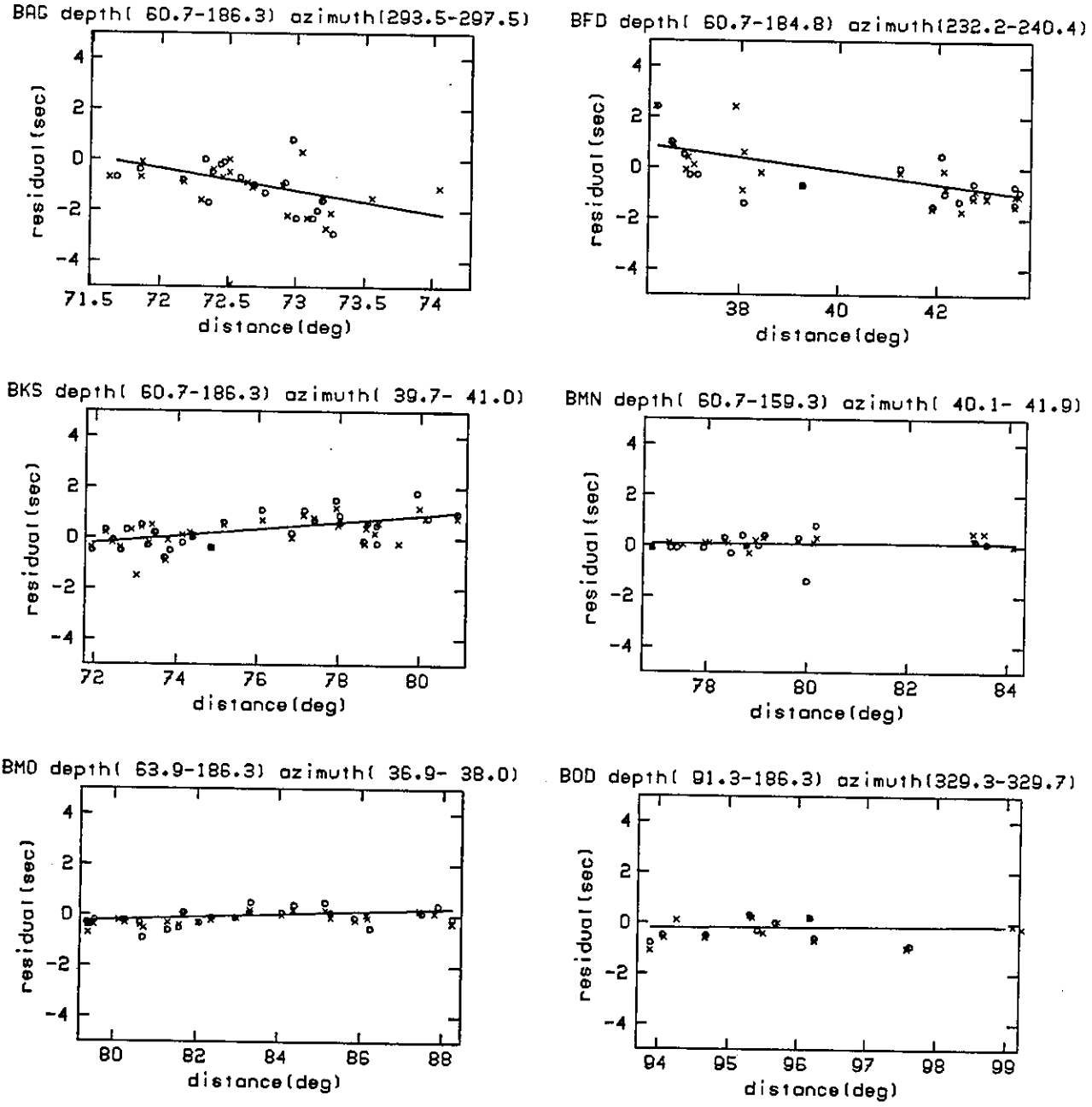

Figure D.2. Residuals and the travel time correction.

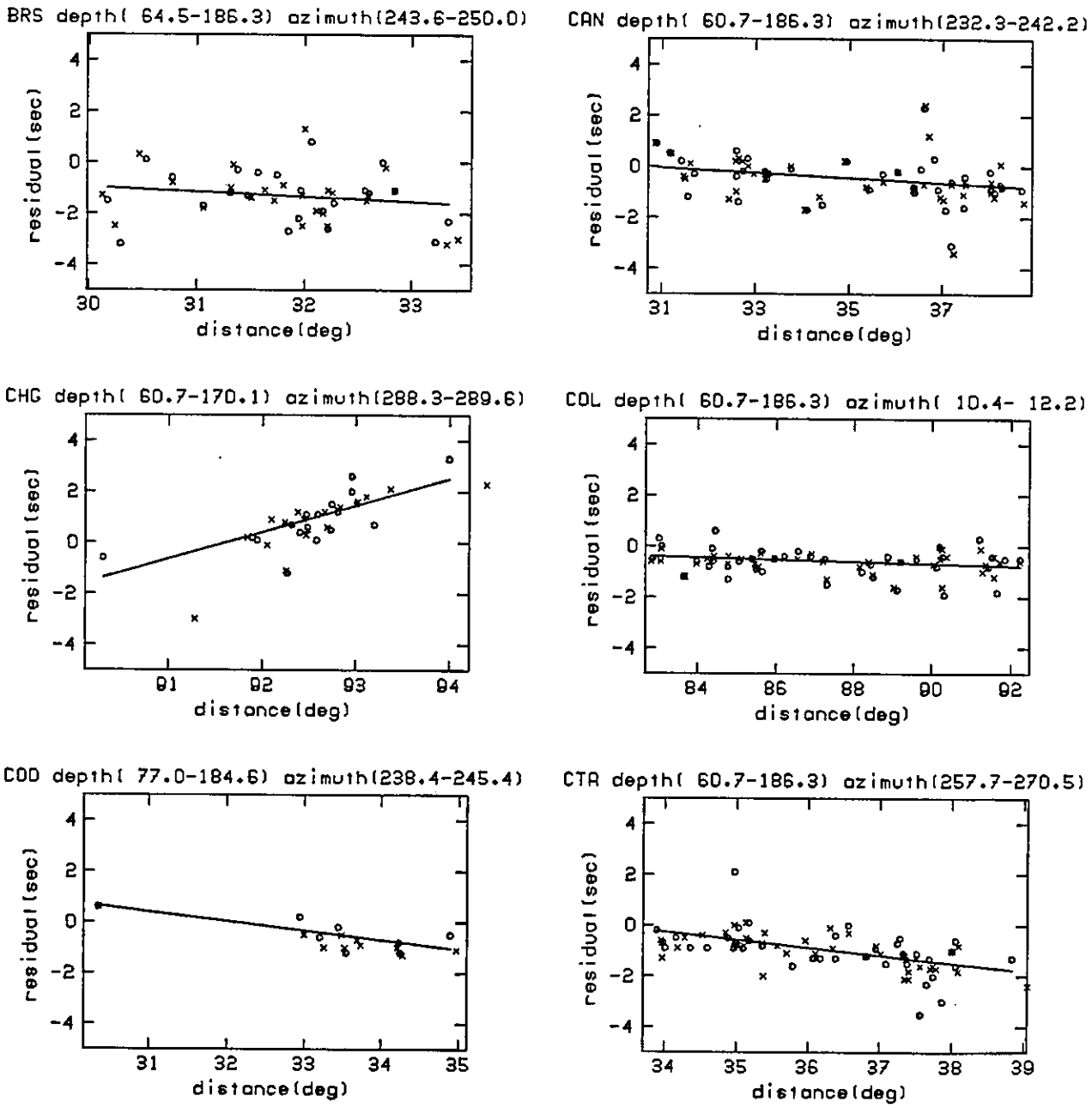

Figure D.2. Residuals and the travel time correction.

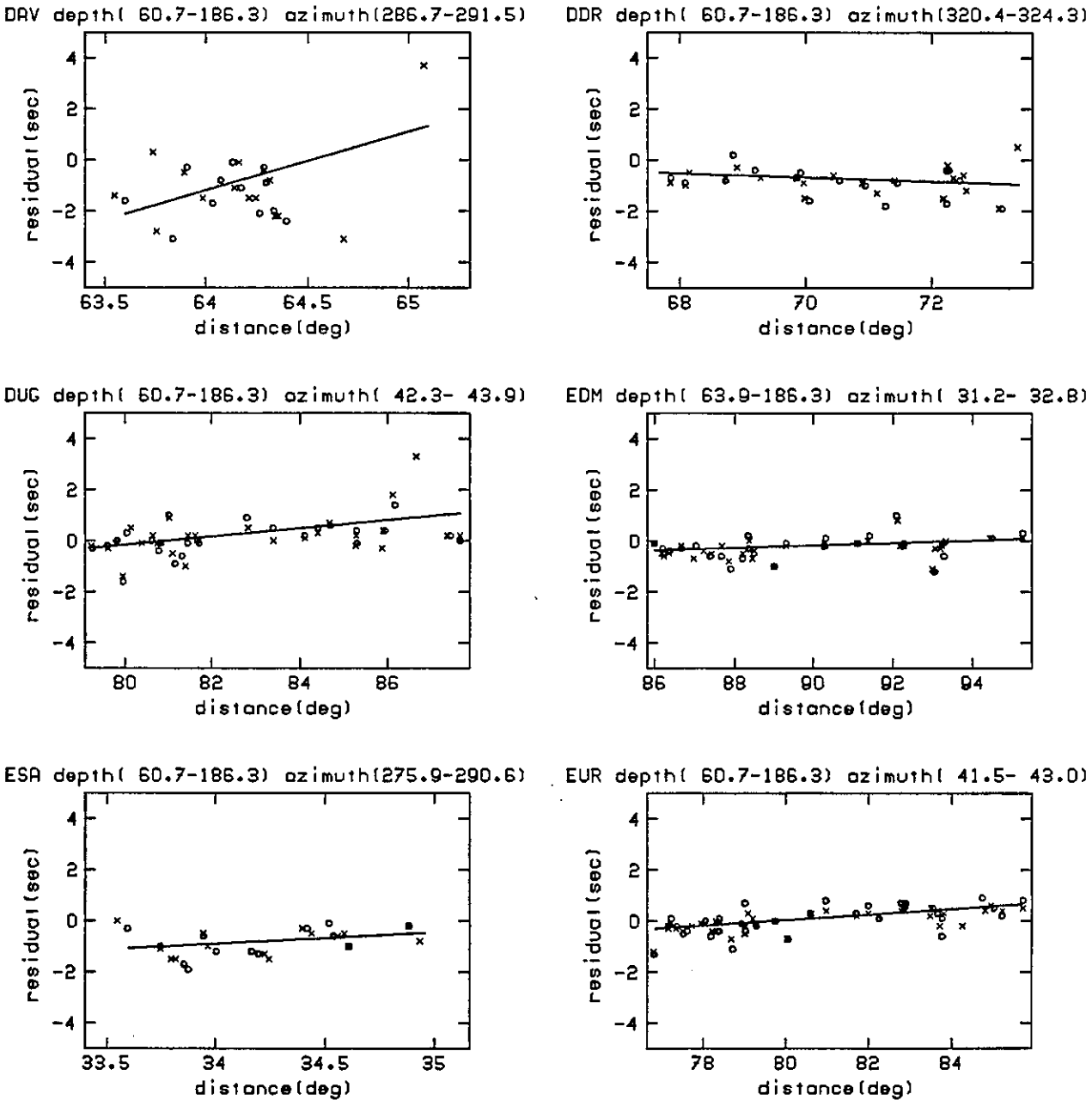

Figure D.2. Residuals and the travel time correction.

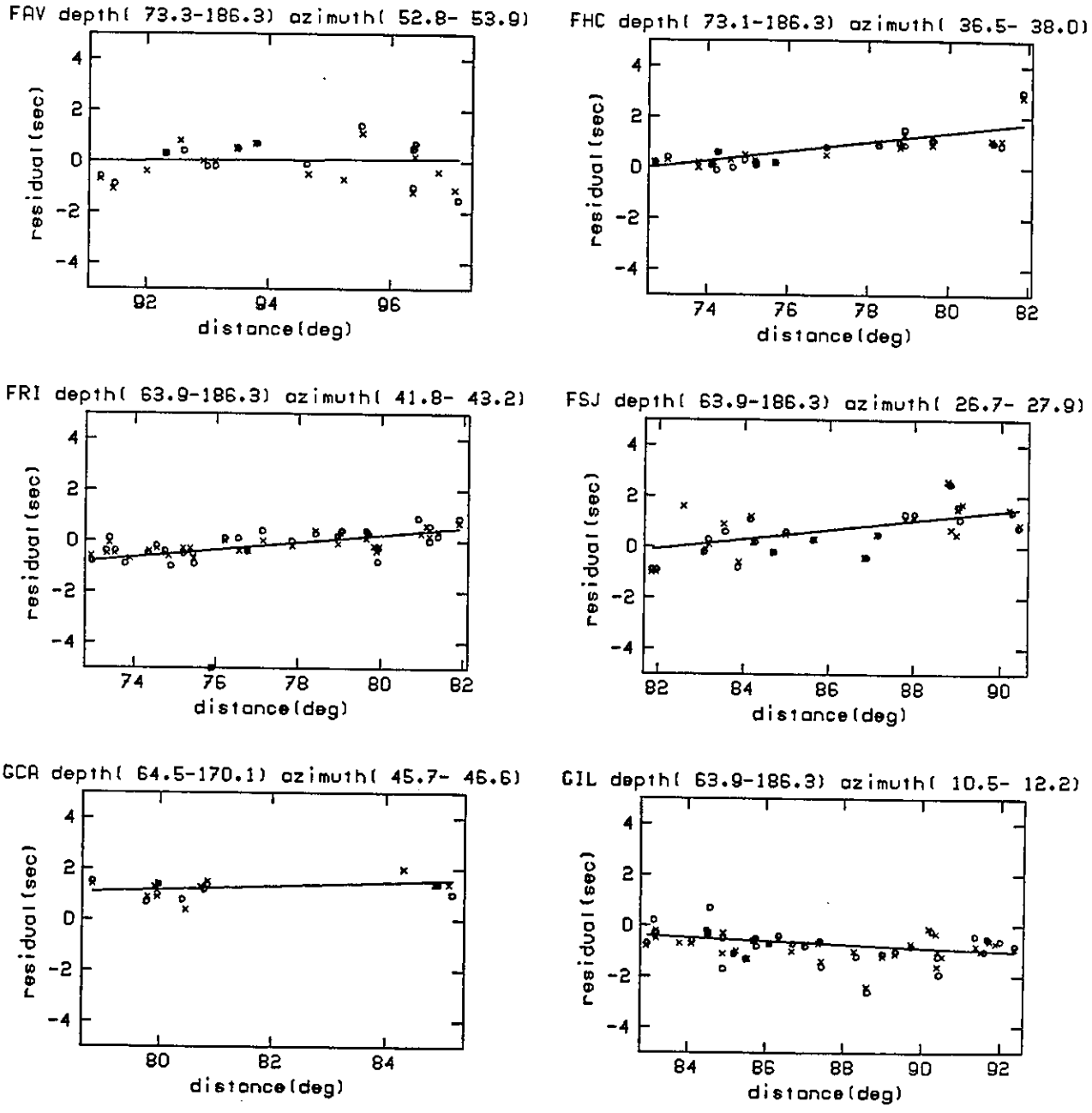

Figure D.2. Residuals and the travel time correction.

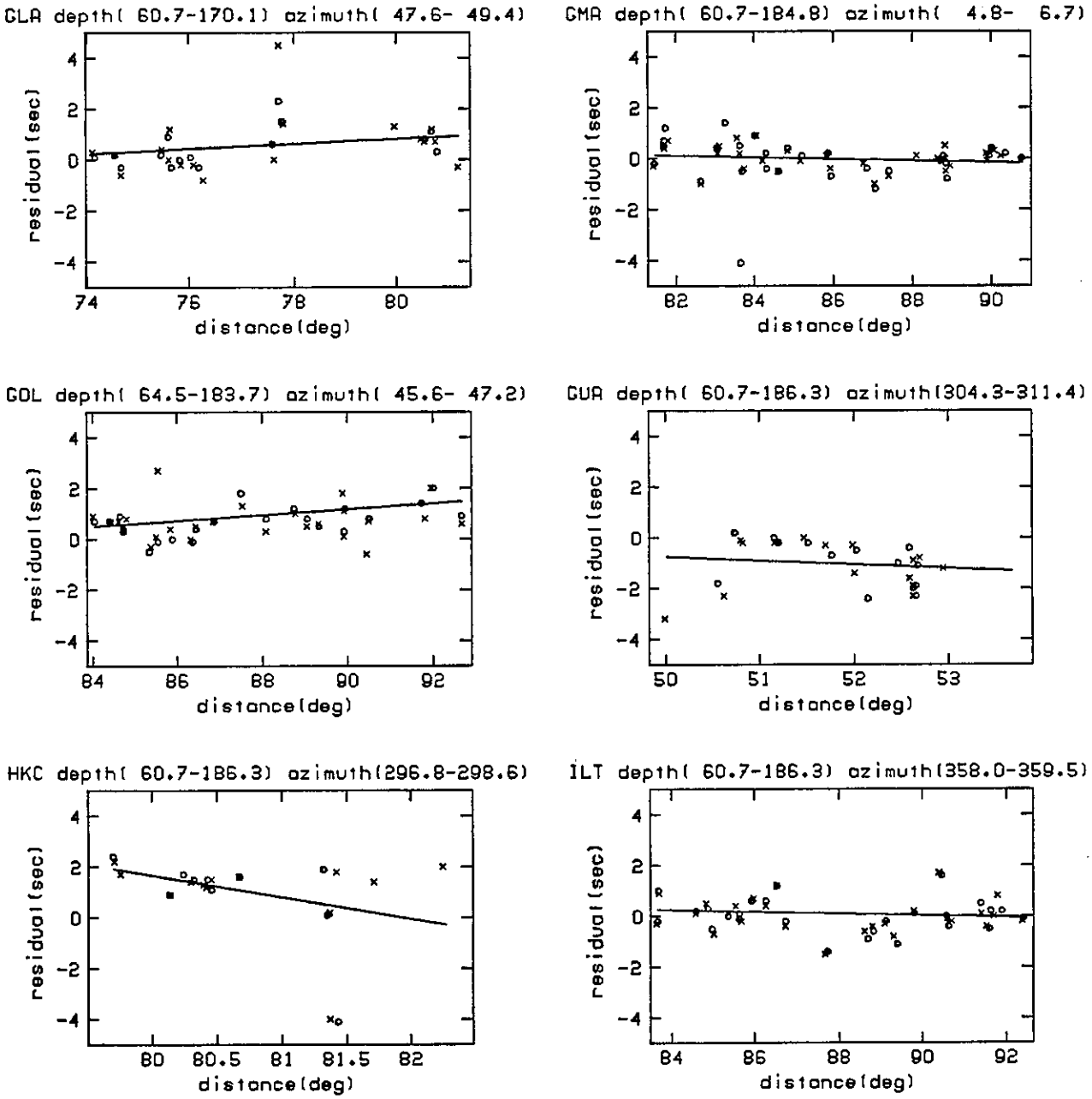

Figure D.2. Residuals and the travel time correction.

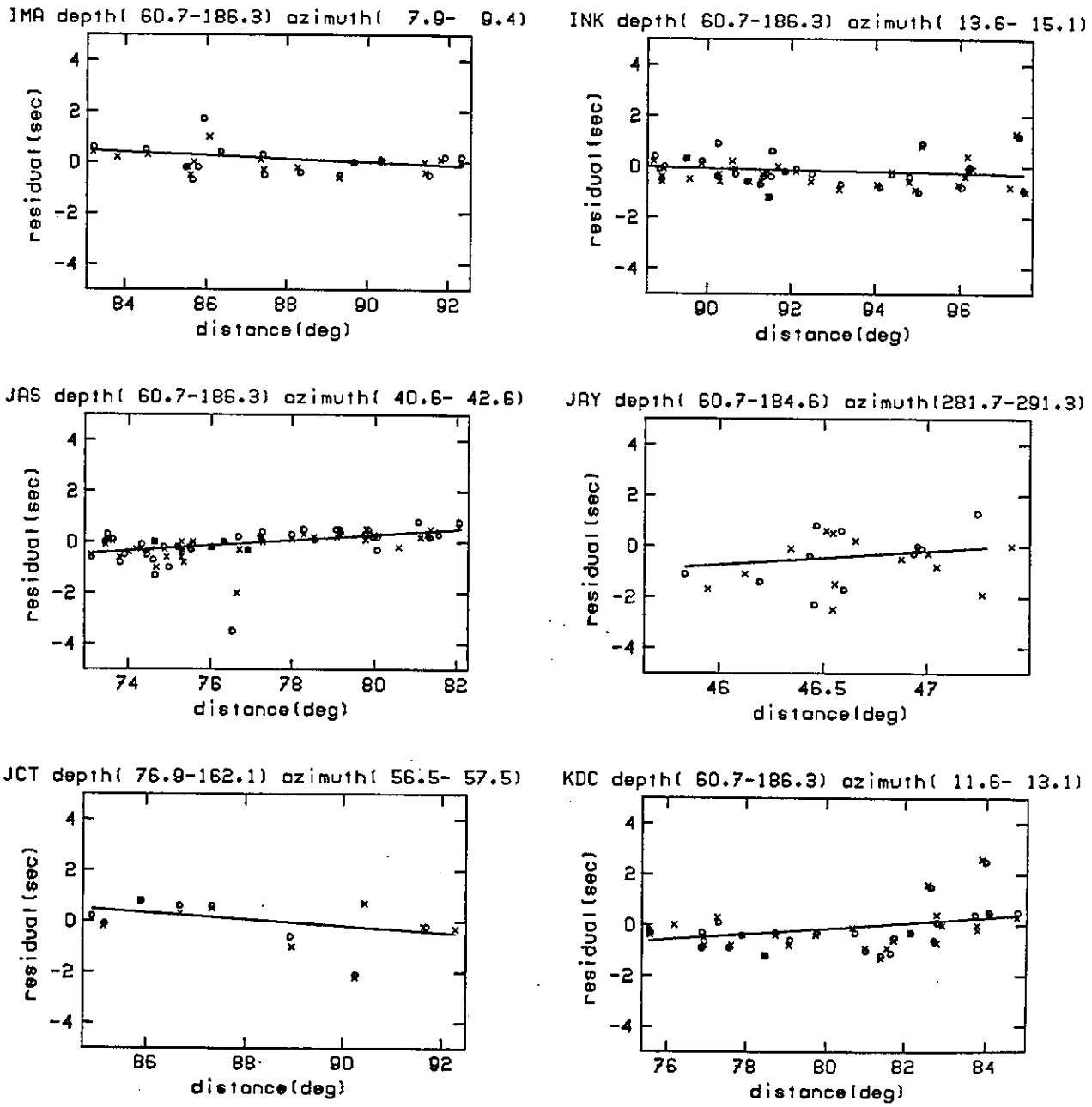

Figure D.2. Residuals and the travel time correction.

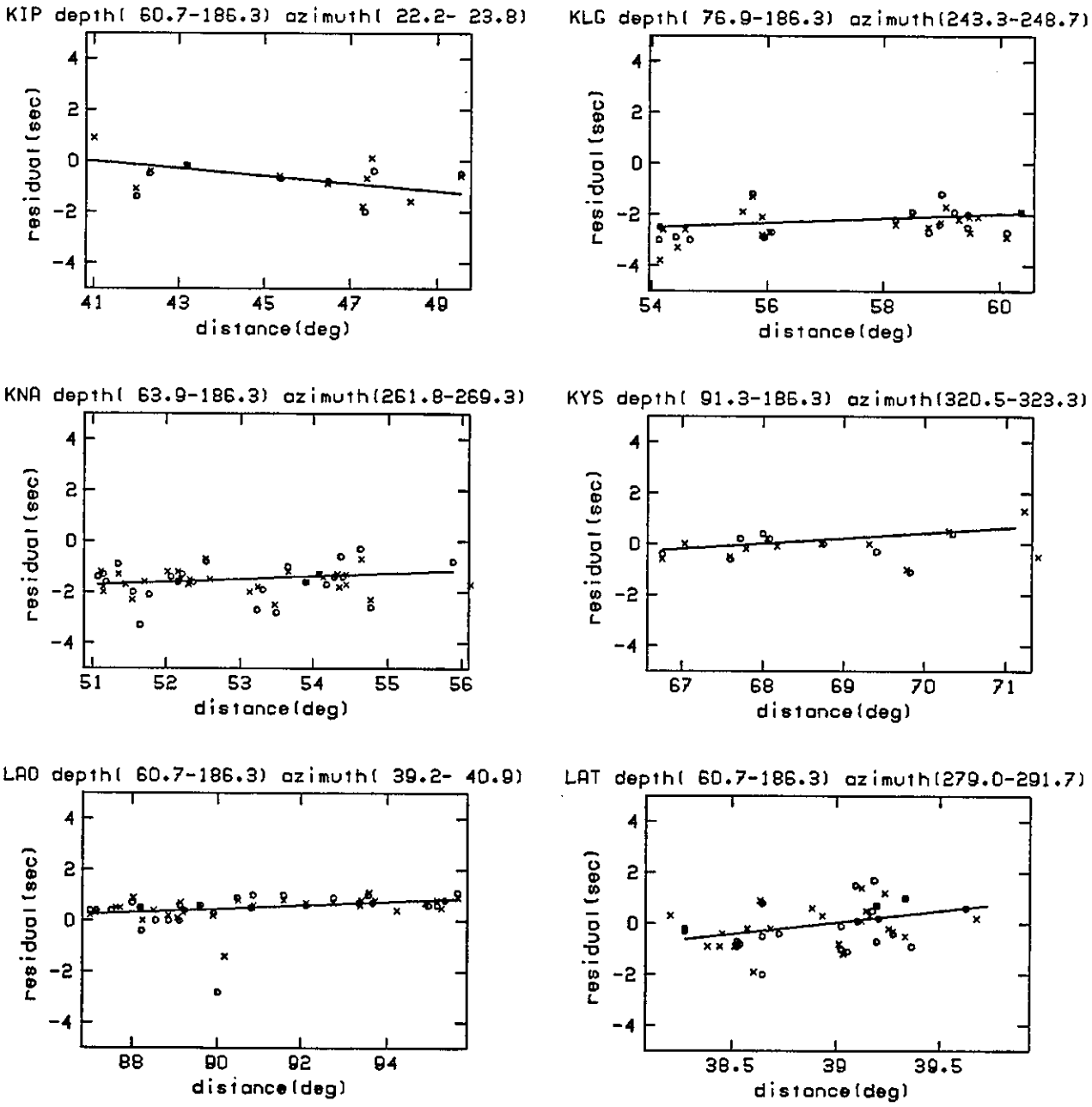

Figure D.2. Residuals and the travel time correction.

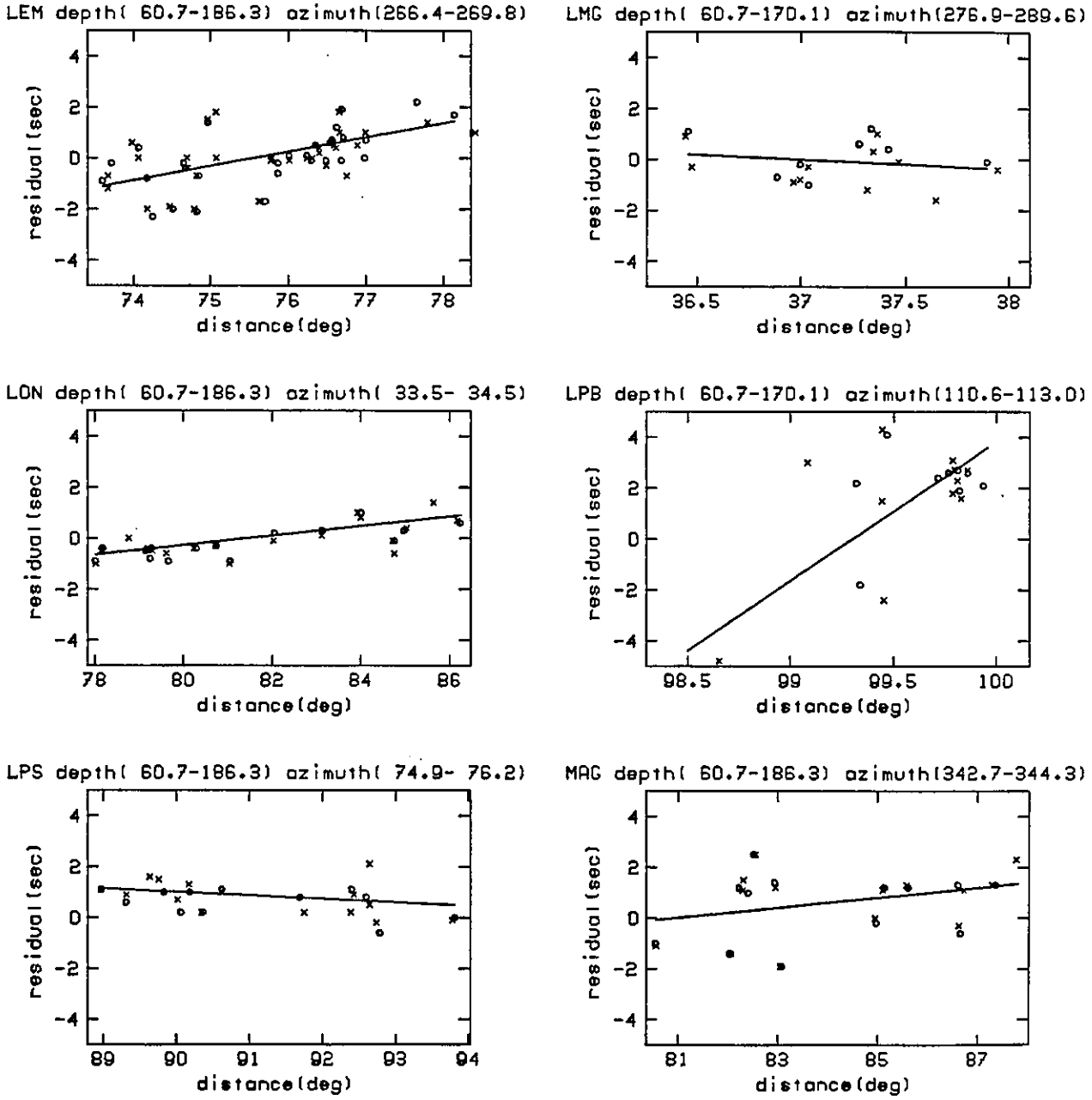

Figure D.2. Residuals and the travel time correction.

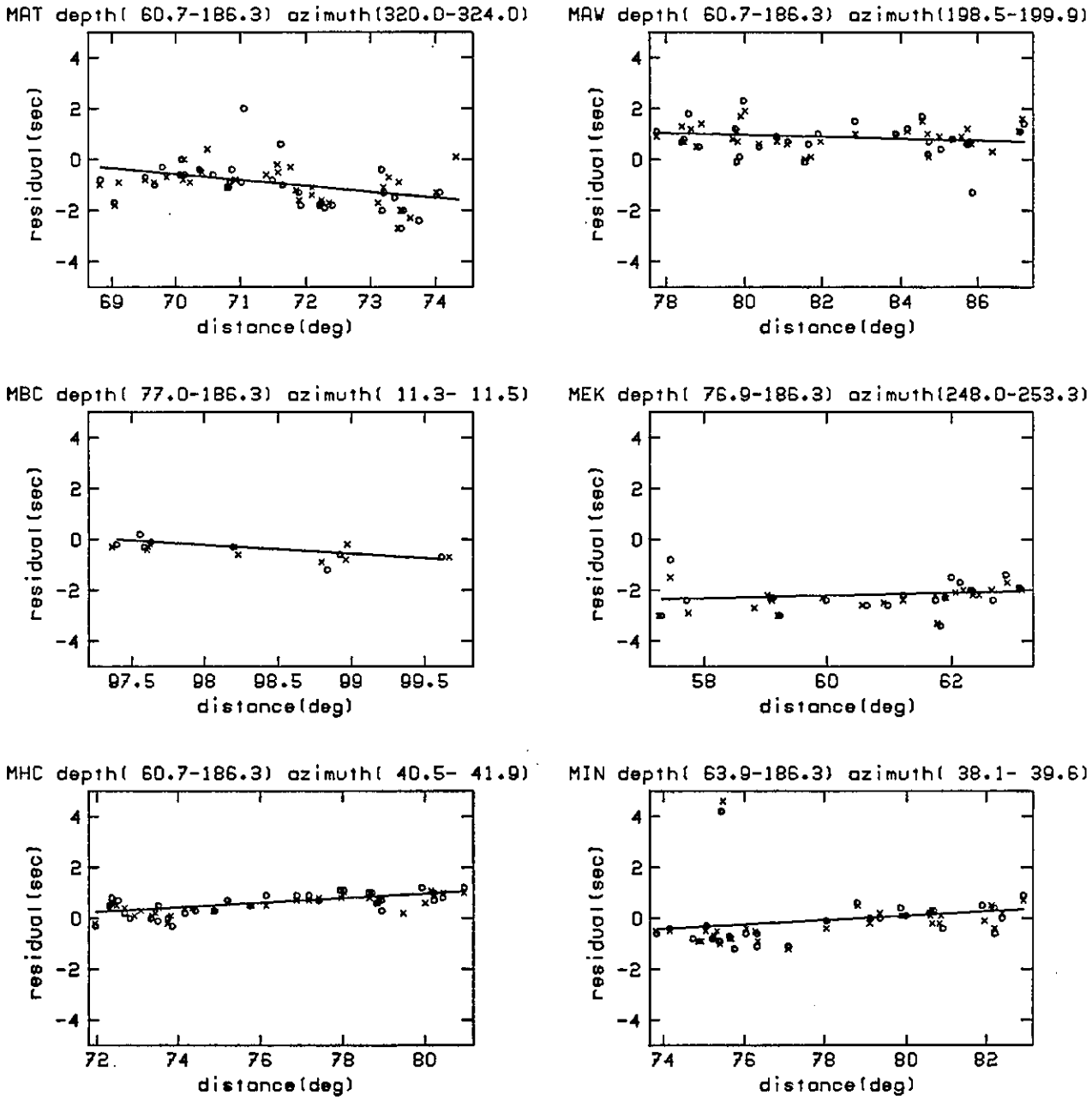

Figure D.2. Residuals and the travel time correction.

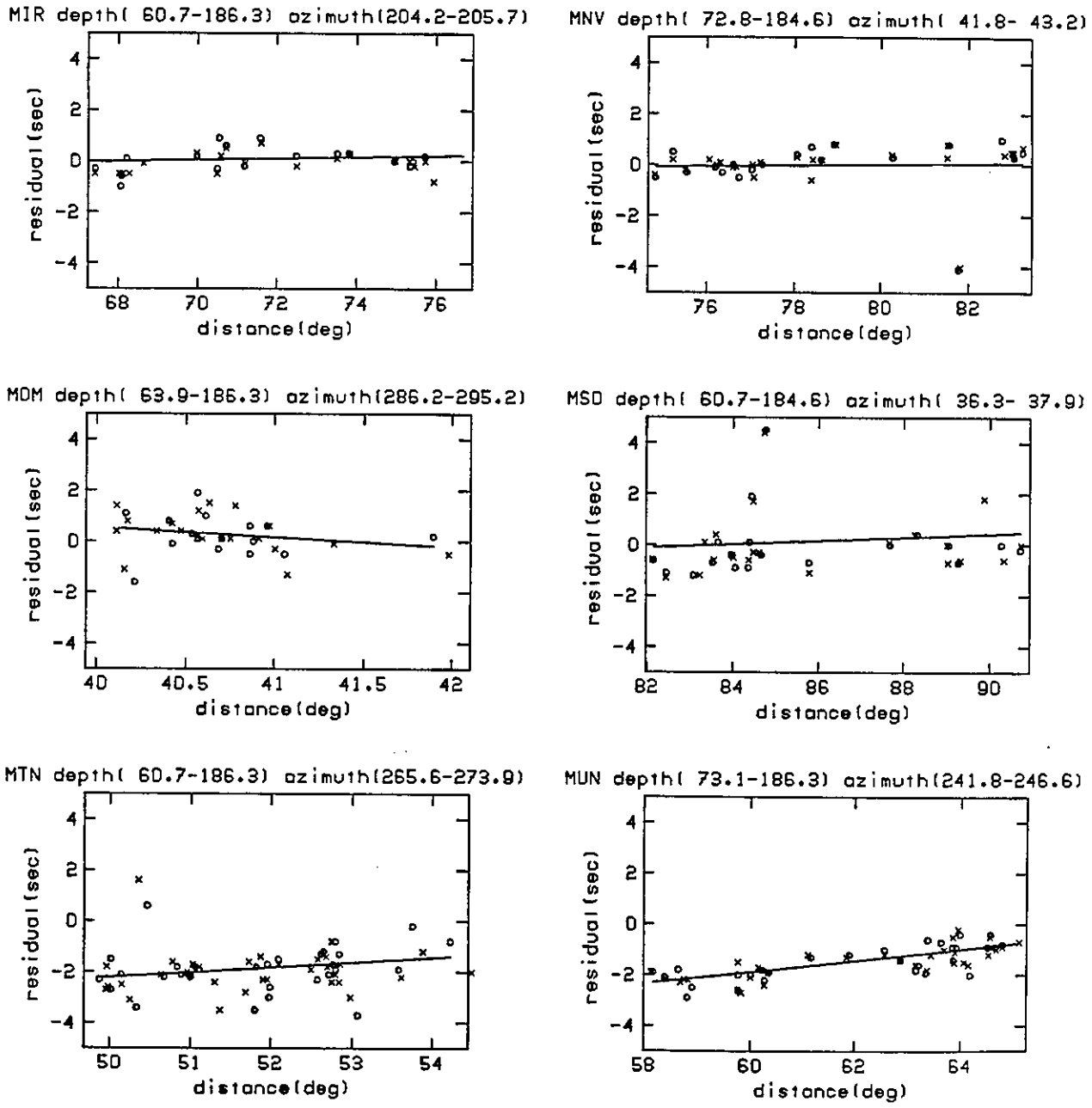

Figure D.2. Residuals and the travel time correction.

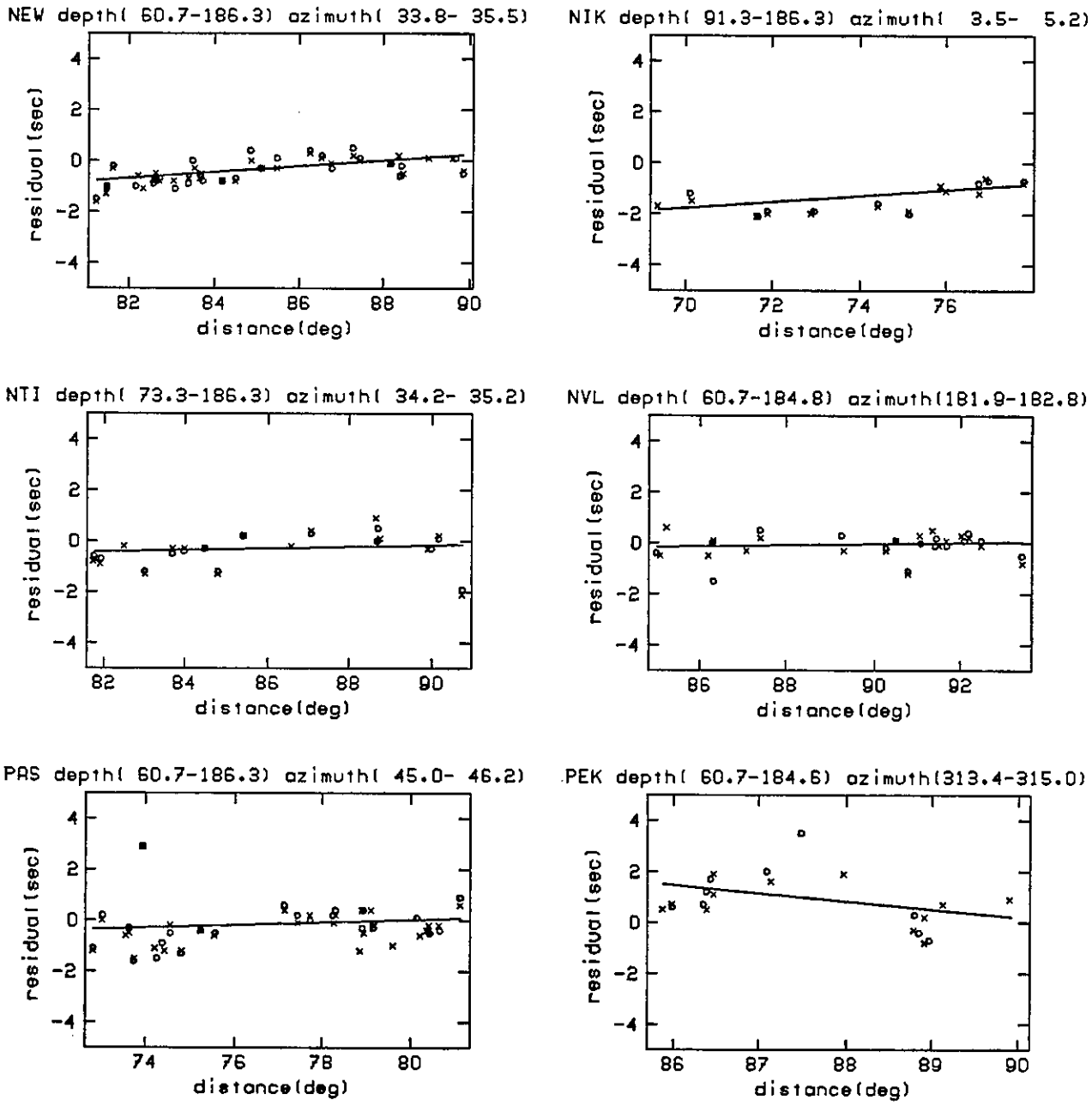

Figure D.2. Residuals and the travel time correction.

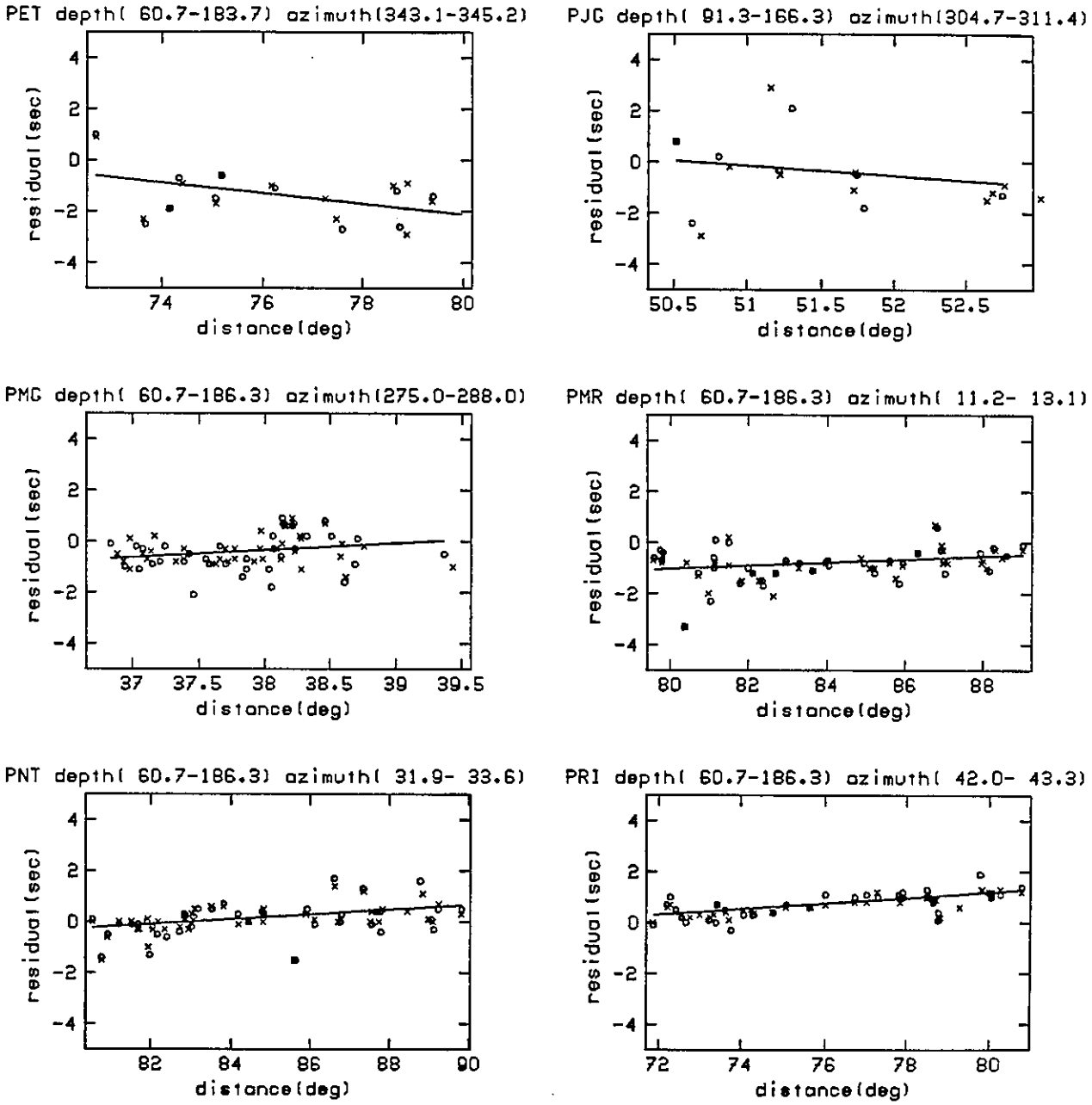

Figure D.2. Residuals and the travel time correction.

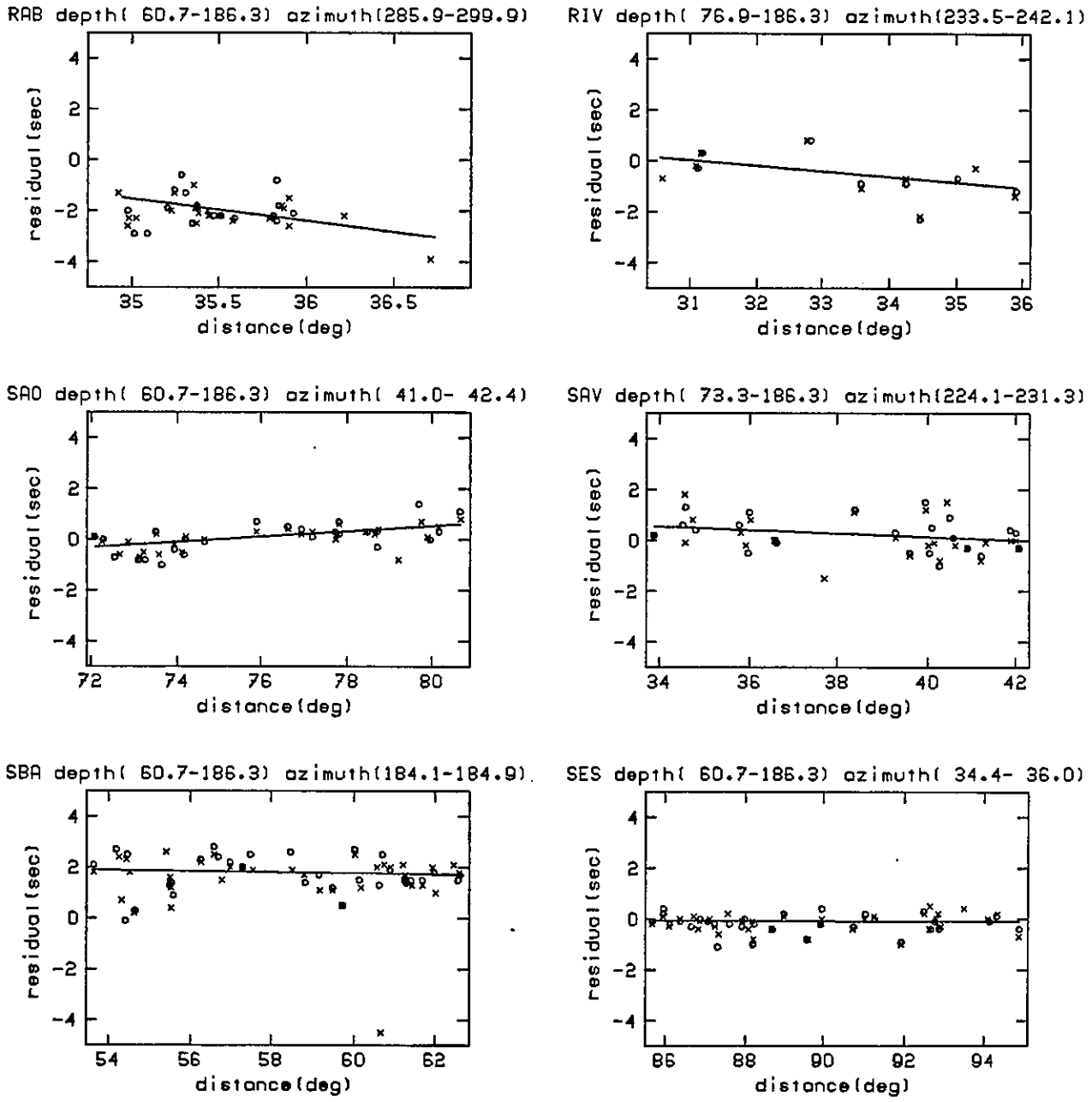

Figure D.2. Residuals and the travel time correction.

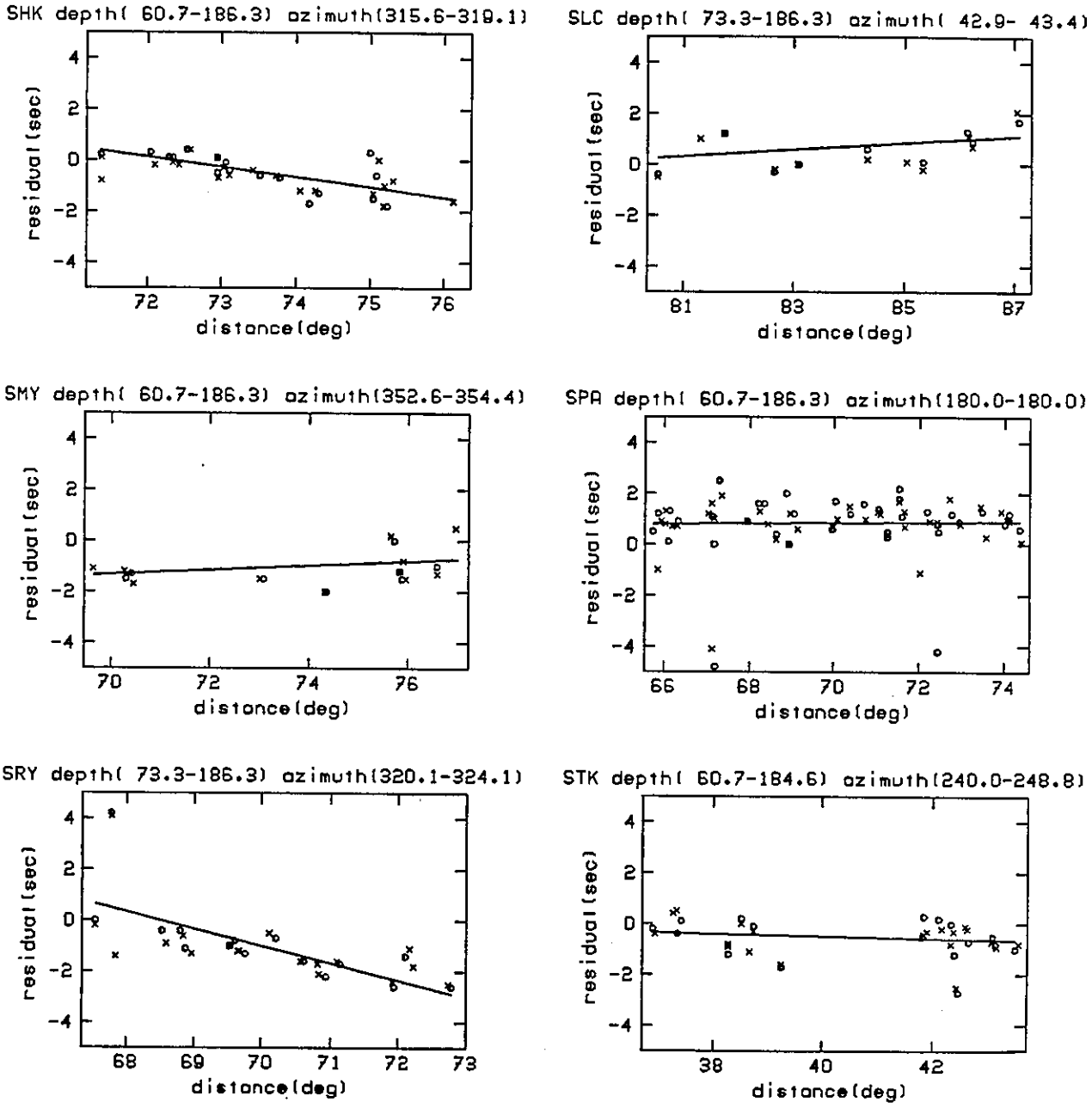

Figure D.2. Residuals and the travel time correction.

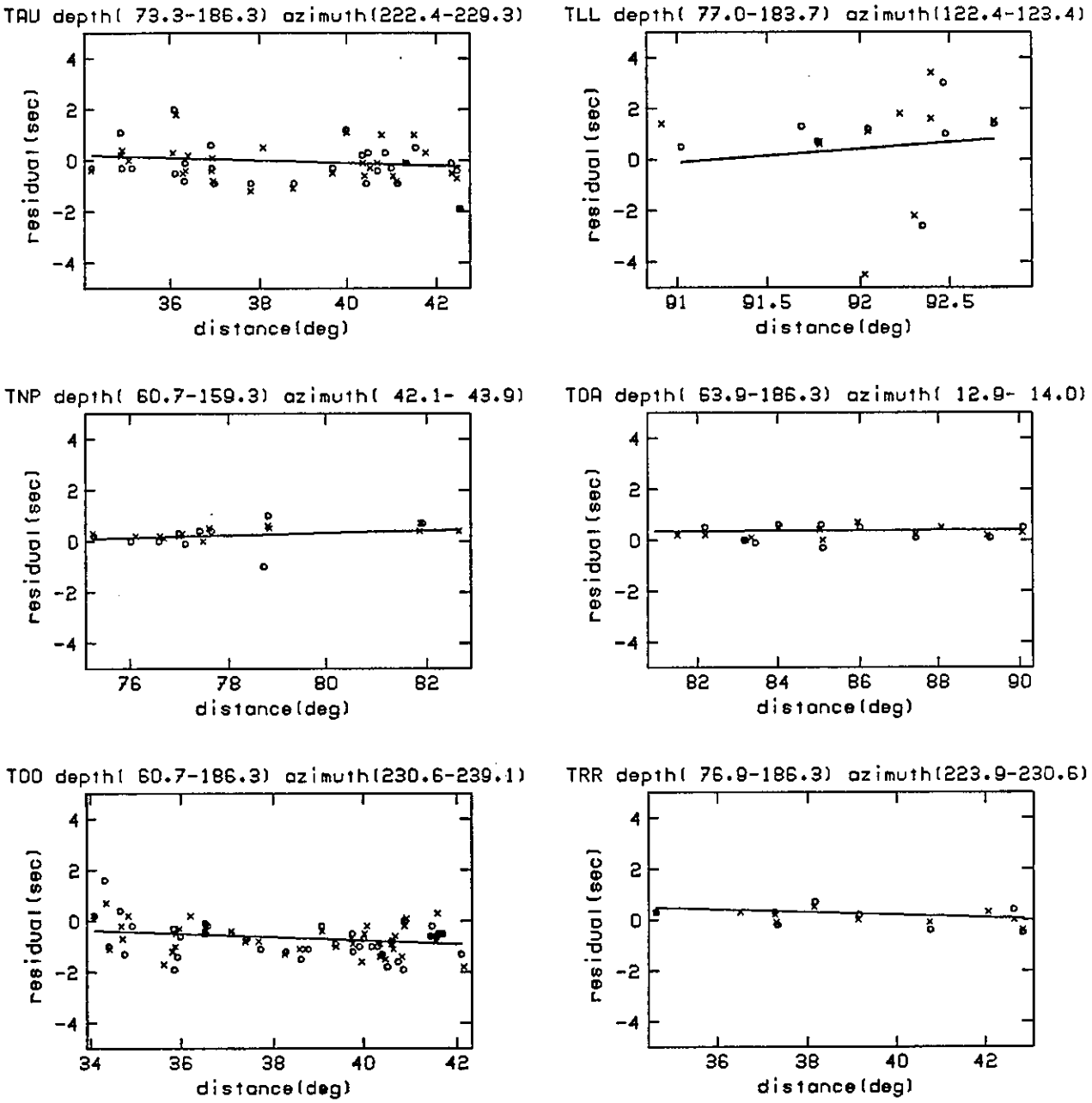

Figure D.2. Residuals and the travel time correction.

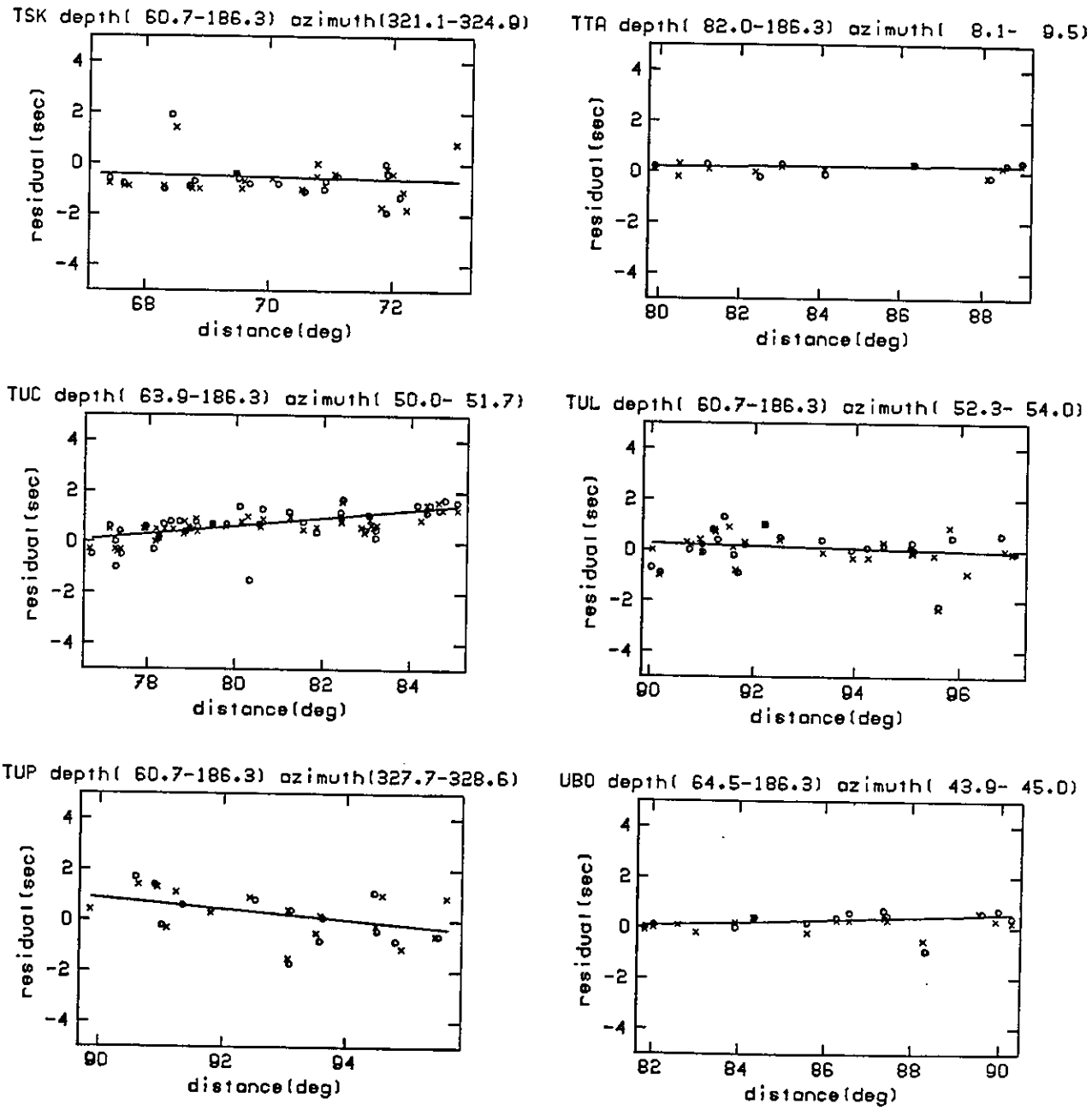

Figure D.2. Residuals and the travel time correction.

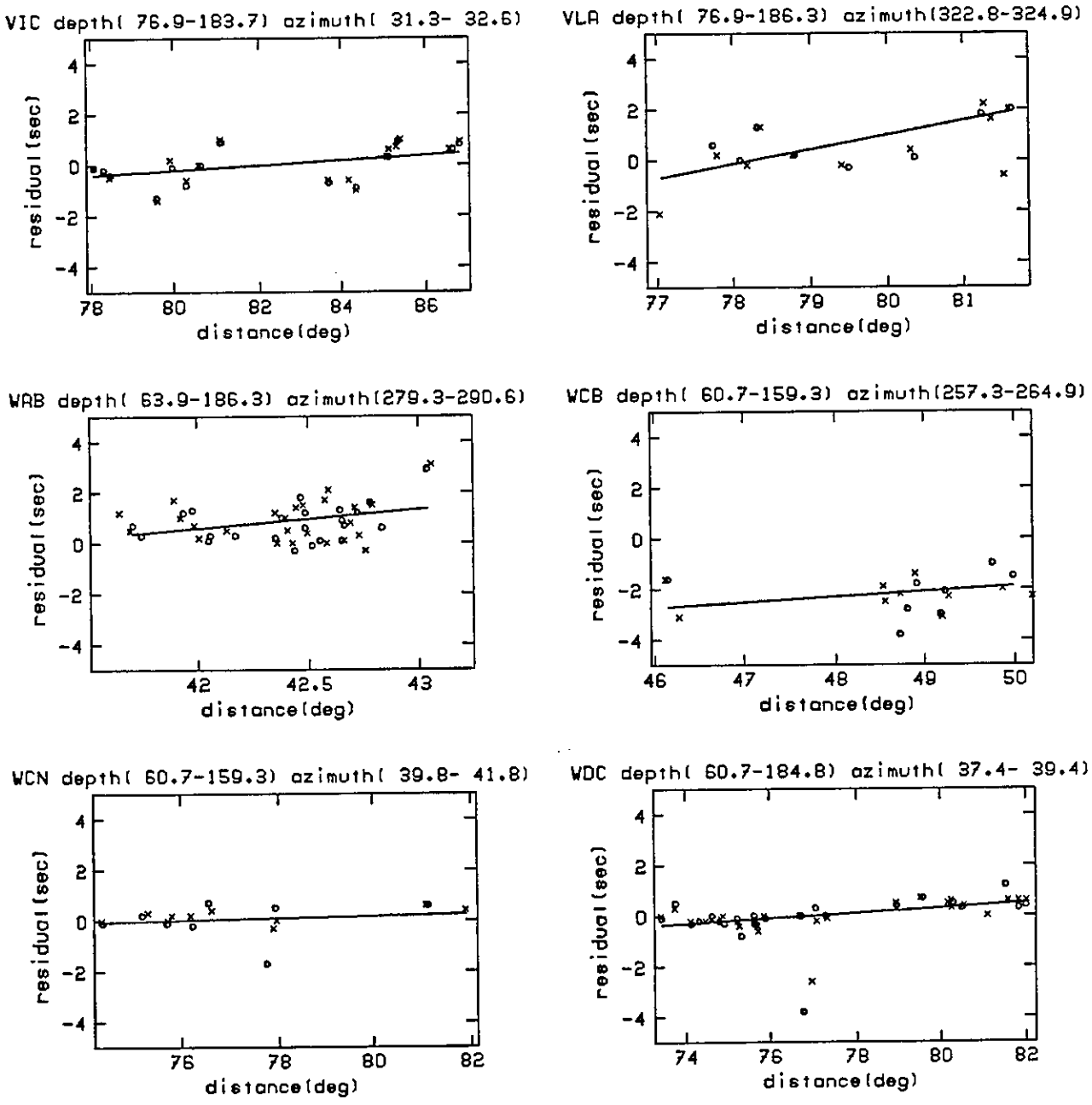

Figure D.2. Residuals and the travel time correction.

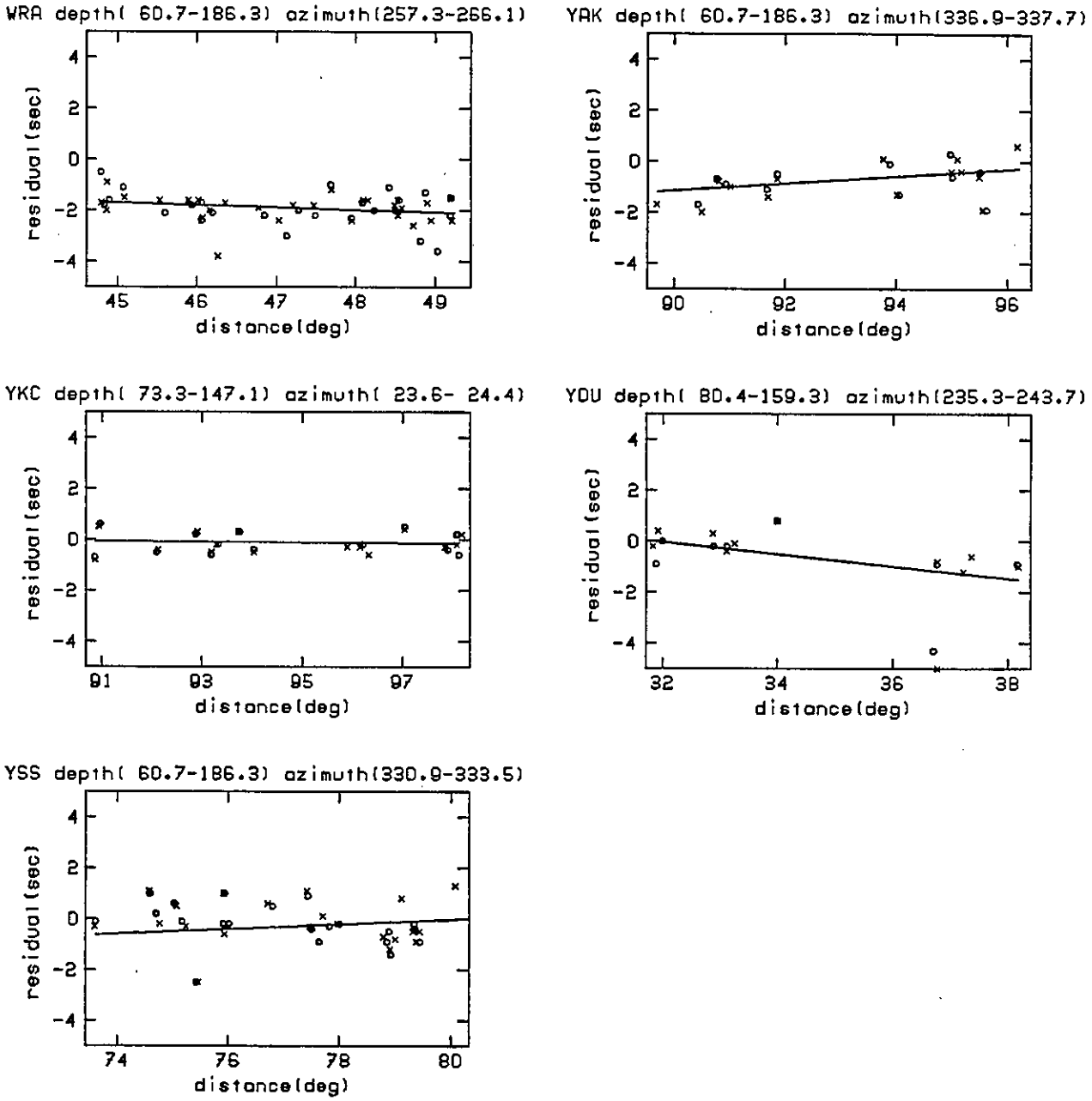

Figure D.2. Residuals and the travel time correction.

TABLE D.1. ISC *vs.* Relocation

year	mo	day	hr	min	sec	lat	long	depth $\Delta lat\,(km)$	m_b $\Delta long\,(km)$	# of stns	dist (deg)	azimuth (deg)	event
1971	2	2	15	18	21.1	-21.24	184.61	88.00	5.30	90	-0.11	112.72	
1971	2	2	15	18	21.5	-21.14	184.46	5.45	4.00	51	0.05	112.68	
1971	3	23	2	15	23.7	-22.96	183.86	77.00	6.10	166	-0.12	114.57	
1971	3	23	2	15	26.6	-22.97	183.85	2.57	2.04	81	-0.12	114.59	F57
1971	4	13	5	57	37.5	-15.98	186.11	102.00	5.40	123	0.53	107.31	
1971	4	13	5	57	37.8	-15.99	186.07	2.30	1.88	70	0.56	107.33	
1971	8	28	4	9	4.1	-18.80	185.40	145.00	5.50	121	0.11	110.18	
1971	8	28	4	9	6.6	-18.84	185.35	2.35	1.85	79	0.14	110.23	F72
1971	10	6	10	26	50.7	-17.75	186.38	65.00	4.80	39	-0.37	108.86	
1971	10	6	10	26	50.6	-17.78	186.20	7.26	4.60	23	-0.22	108.95	
1972	1	15	3	39	21.5	-18.33	185.41	~~155.66~~	5.60	132	0.28	109.74	
1972	1	15	3	39	17.6	-18.28	185.40	3.20	2.55	72	0.30	109.70	F60
1972	6	11	14	29	57.8	-21.09	184.88	73.00	5.30	89	-0.29	112.49	
1972	6	11	14	29	56.9	-20.97	184.72	4.56	3.71	63	-0.11	112.43	
1972	7	10	6	30	8.0	-23.04	184.03	64.00	5.10	54	-0.30	114.59	
1972	7	10	6	30	5.9	-23.00	183.95	2.42	1.68	37	-0.21	114.58	
1972	7	21	8	37	15.0	-21.96	183.94	124.00	5.40	138	0.19	113.62	
1972	7	21	8	37	12.5	-21.88	183.91	3.97	3.21	76	0.25	113.56	
1972	7	25	9	20	29.9	-21.50	183.62	184.00	5.40	137	0.64	113.31	
1972	7	25	9	20	28.8	-21.47	183.56	3.23	2.60	78	0.70	113.30	
1972	8	29	5	59	2.8	-20.12	184.85	160.00	5.40	113	0.10	111.60	
1972	8	29	5	59	2.4	-20.02	184.76	3.36	3.03	71	0.21	111.54	T2
1972	9	22	11	45	10.5	-16.50	185.54	186.00	5.60	149	0.84	107.99	
1972	9	22	11	45	11.0	-16.53	185.49	1.83	1.56	84	0.87	108.04	F64
1972	11	20	13	6	50.3	-24.84	182.76	162.00	5.20	116	0.08	116.70	
1972	11	20	13	6	48.5	-24.77	182.71	4.08	3.30	63	0.15	116.65	
1972	11	30	2	45	52.7	-16.05	185.74	145.00	5.20	99	0.83	107.51	
1972	11	30	2	45	47.1	-15.94	185.74	4.43	3.70	67	0.87	107.40	
1973	1	8	21	10	13.7	-24.45	182.77	164.00	4.70	36	0.23	116.33	
1973	1	8	21	10	13.1	-24.26	182.74	8.08	5.19	26	0.33	116.17	
1973	4	8	20	48	46.3	-24.00	182.96	124.00	5.50	119	0.24	115.85	
1973	4	8	20	48	46.1	-23.93	182.96	2.71	2.06	79	0.27	115.79	
1973	6	7	18	55	38.1	-22.16	183.42	185.00	5.20	71	0.56	113.99	
1973	6	7	18	55	39.6	-22.17	183.27	4.19	3.86	51	0.68	114.05	
1973	7	19	21	22	14.1	-19.71	185.08	139.00	4.90	40	0.05	111.14	
1973	7	19	21	22	16.8	-19.74	184.99	9.37	7.20	28	0.12	111.20	
1973	9	17	7	21	44.9	-17.21	185.70	131.00	5.40	128	0.44	108.60	
1973	9	17	7	21	47.1	-17.32	185.72	2.56	2.23	81	0.38	108.69	
1973	12	24	8	14	24.6	-19.06	185.14	119.00	5.70	118	0.24	110.51	
1973	12	24	8	14	25.1	-19.06	185.12	3.99	3.45	75	0.26	110.52	

TABLE D.1. (continued)

year	mo	day	hr	min	sec	lat	long	depth $\Delta lat\,(km)$	m_b $\Delta long\,(km)$	# of stns	dist (deg)	azimuth (deg)	event
1974	2	1	11	48	31.8	-20.14	185.17	112.00	4.90	45	-0.19	111.50	
1974	2	1	11	48	33.4	-20.13	184.93	10.17	4.94	27	0.03	111.58	
1974	2	28	16	6	14.3	-18.55	185.65	95.00	5.30	54	-0.02	109.86	
1974	2	28	16	6	15.0	-18.46	185.50	3.98	3.36	35	0.15	109.83	
1974	11	11	6	29	16.7	-24.06	182.84	166.00	5.60	88	0.32	115.95	
1974	11	11	6	29	17.3	-24.10	182.74	5.00	3.78	64	0.39	116.02	C2
1974	11	17	1	0	34.5	-16.84	185.75	185.00	4.90	61	0.53	108.24	
1974	11	17	1	0	36.3	-16.88	185.73	4.90	4.46	40	0.53	108.28	
1975	1	17	9	30	36.6	-17.86	185.43	140.00	5.80	161	0.43	109.30	
1975	1	17	9	30	40.7	-17.99	185.48	3.05	2.42	86	0.34	109.40	F68
1975	2	10	5	51	45.0	-15.73	185.76	158.00	4.90	59	0.93	107.20	
1975	2	10	5	51	45.4	-15.66	185.61	9.14	8.00	40	1.09	107.19	
1975	5	5	20	28	4.2	-22.87	183.85	80.00	5.60	135	-0.08	114.50	
1975	5	5	20	28	8.4	-23.09	183.85	2.48	1.87	79	-0.16	114.70	C3
1975	5	27	9	11	35.9	-21.20	184.12	147.00	5.10	85	0.32	112.86	
1975	5	27	9	11	35.5	-21.17	184.09	5.21	3.91	58	0.36	112.84	
1975	8	24	13	48	48.4	-24.30	183.41	110.00	5.00	57	-0.25	115.97	
1975	8	24	13	48	50.1	-24.19	183.17	4.01	3.43	36	-0.01	115.95	
1975	8	26	12	19	33.2	-23.80	183.24	119.00	5.30	99	0.08	115.57	
1975	8	26	12	19	33.5	-23.81	183.07	4.83	3.53	63	0.22	115.64	
1976	8	28	16	13	41.6	-16.10	186.72	102.00	5.00	63	-0.06	107.21	
1976	8	28	16	13	39.6	-16.16	186.84	8.01	6.93	42	-0.19	107.22	
1976	12	5	17	11	15.8	-17.69	187.37	73.00	5.10	71	-1.22	108.46	
1976	12	5	17	11	15.9	-18.06	187.60	5.11	3.78	46	-1.56	108.73	
1976	12	15	7	10	27.3	-17.33	186.17	77.00	5.50	120	-0.03	108.54	
1976	12	15	7	10	27.6	-17.40	186.08	4.86	3.80	65	0.03	108.64	
1977	2	26	14	7	46.2	-18.03	183.16	73.00	4.90	43	2.37	110.27	
1977	2	26	14	7	41.1	-18.51	183.97	19.61	10.97	25	1.48	110.42	
1977	3	26	8	19	12.7	-18.48	185.81	91.00	5.70	150	-0.13	109.74	
1977	3	26	8	19	18.4	-18.57	185.88	2.99	2.36	75	-0.23	109.80	T3
1977	6	22	12	8	33.7	-22.91	184.26	61.00	6.30	270	-0.44	114.39	
1977	6	22	12	8	32.7	-23.00	184.26	3.19	2.26	91	-0.48	114.47	H2
1977	7	29	16	51	7.6	-19.45	185.05	131.00	5.10	83	0.18	110.91	
1977	7	29	16	51	6.8	-19.36	184.88	3.83	2.52	44	0.36	110.88	
1977	8	11	1	42	47.1	-17.58	185.61	120.00	6.20	224	0.38	108.97	
1977	8	11	1	42	54.3	-17.68	185.69	3.41	2.81	84	0.27	109.04	F74
1977	12	8	6	15	17.2	-24.09	184.35	61.00	5.50	127	-0.97	115.45	
1977	12	8	6	15	19.4	-24.09	184.28	3.87	2.89	72	-0.91	115.47	
1977	12	29	10	19	42.9	-17.94	186.21	99.00	5.30	56	-0.29	109.10	
1977	12	29	10	19	42.9	-17.85	185.99	5.26	4.19	36	-0.06	109.09	

TABLE D.1. (continued)

year	mo	day	hr	min	sec	lat	long	depth $\Delta lat\,(km)$	m_b $\Delta long\,(km)$	# of stns	dist (deg)	azimuth (deg)	event
1978	2	22	19	37	17.1	-22.88	184.04	67.00	5.60	154	-0.24	114.44	
1978	2	22	19	37	16.7	-22.78	183.97	5.09	3.26	79	-0.15	114.37	C4
1978	6	25	10	21	42.7	-17.13	185.65	159.00	5.50	152	0.51	108.54	
1978	6	25	10	21	44.7	-17.13	185.63	3.26	2.60	70	0.53	108.55	H4
1978	10	22	11	0	19.6	-18.48	186.20	86.00	5.10	57	-0.48	109.60	
1978	10	22	11	0	21.5	-18.43	185.92	5.06	4.45	29	-0.21	109.65	
1979	2	5	18	58	23.0	-16.64	186.36	82.00	5.30	95	0.06	107.83	
1979	2	5	18	58	22.7	-16.66	186.31	3.80	3.07	42	0.10	107.87	
1979	3	10	9	1	47.0	-18.84	186.79	80.00	5.10	77	-1.13	109.73	
1979	3	10	9	1	52.8	-19.00	186.72	4.13	2.95	38	-1.12	109.91	
1979	8	27	3	8	35.9	-21.82	183.76	170.00	5.40	125	0.40	113.56	
1979	8	27	3	8	34.3	-21.67	183.73	4.46	3.26	60	0.48	113.43	

APPENDIX E

EARTHQUAKES STUDIED IN CHAPTER III

Focal mechanism solutions studied in Chapter 3 are presented as equal-area projections of the lower hemisphere of the focal sphere. Large circles indicate WWSSN long-period P wave first motion data and small circles WWSSN short-period and JMA data. Polarization angles of long-period S waves are indicated by the dashes. Nodal lines are indicated by the thin lines in this figure and their parameters are listed in Table C.2 and C.4.

Events F17, F60 and F68: depths are redetermined for these events of the Tonga double seismic zone, by comparing P-wave first motion waveform of WWSSN long period records with synthetic seismograms. The synthetic seismogram was generated by a method of Kroeger and Geller (1985) and PREM (Dziewonski and Anderson, 1980) was used for the structure near the sources. The source time functions are shown by the trapezoids.

Events F70, F71, F72, and F74: Focal mechanisms are newly determined in this study for these events.

Events H3, H8, H10, H13, H21, H26, H38, and H49: Focal mechanism solutions and the focal depths of CMT solution are compared with WWSSN records. Note that both mechanism and depth of CMT solution are reliable. Event H21 is too small to check either the focal mechanism or the depth by WWSSN seismograms. All the available data from WWSSN are, however, still consistent with the CMT solution. Event H49 is also small and the depth can be checked only at one station (SPA). The model depth 65 km is slightly shallower than CMT depth 70 km.

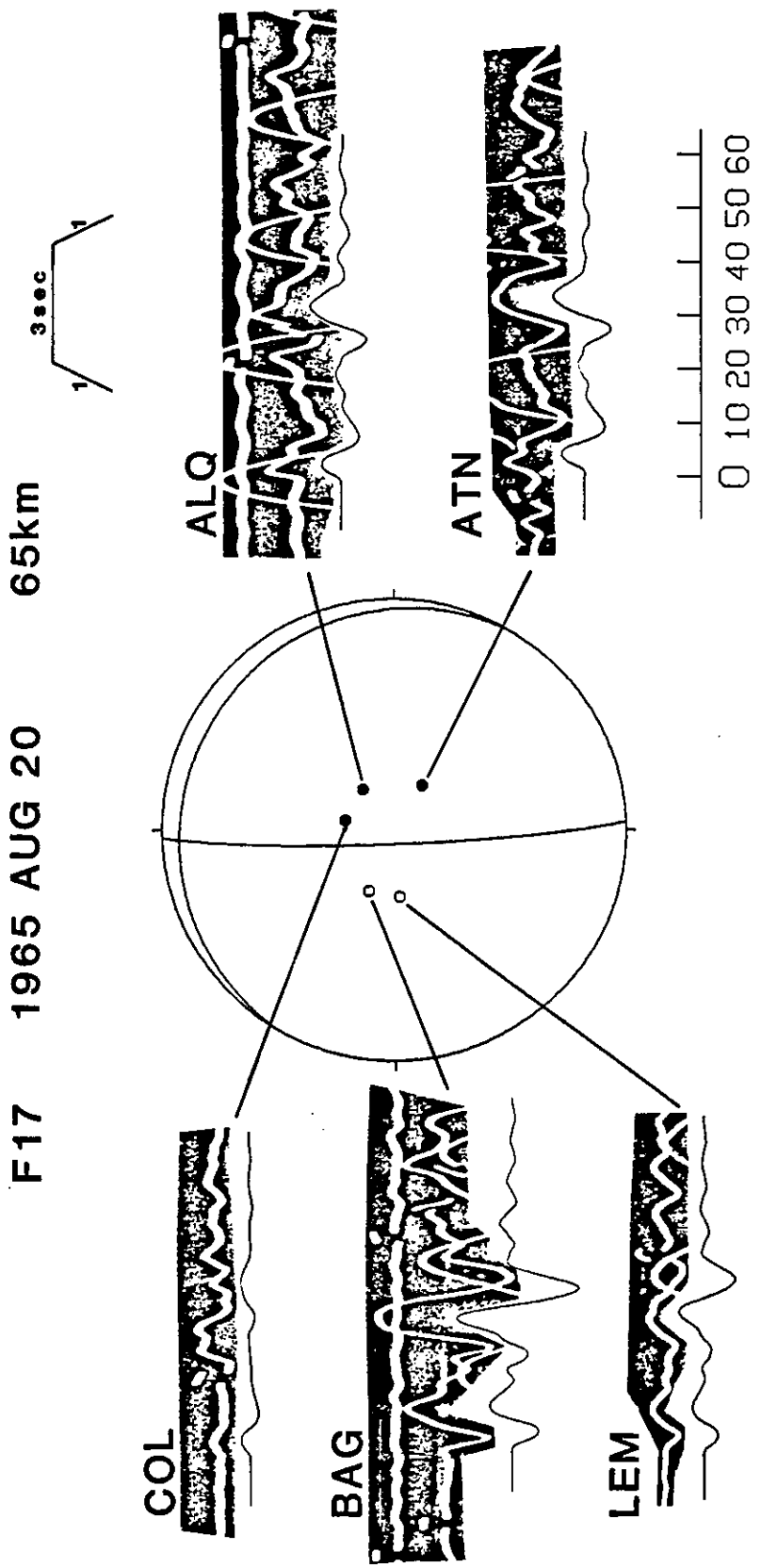
F17 1965 AUG 20 65km
3•••c
1
1
ALQ
ATN
COL
BAG
LEM
0 10 20 30 40 50 60

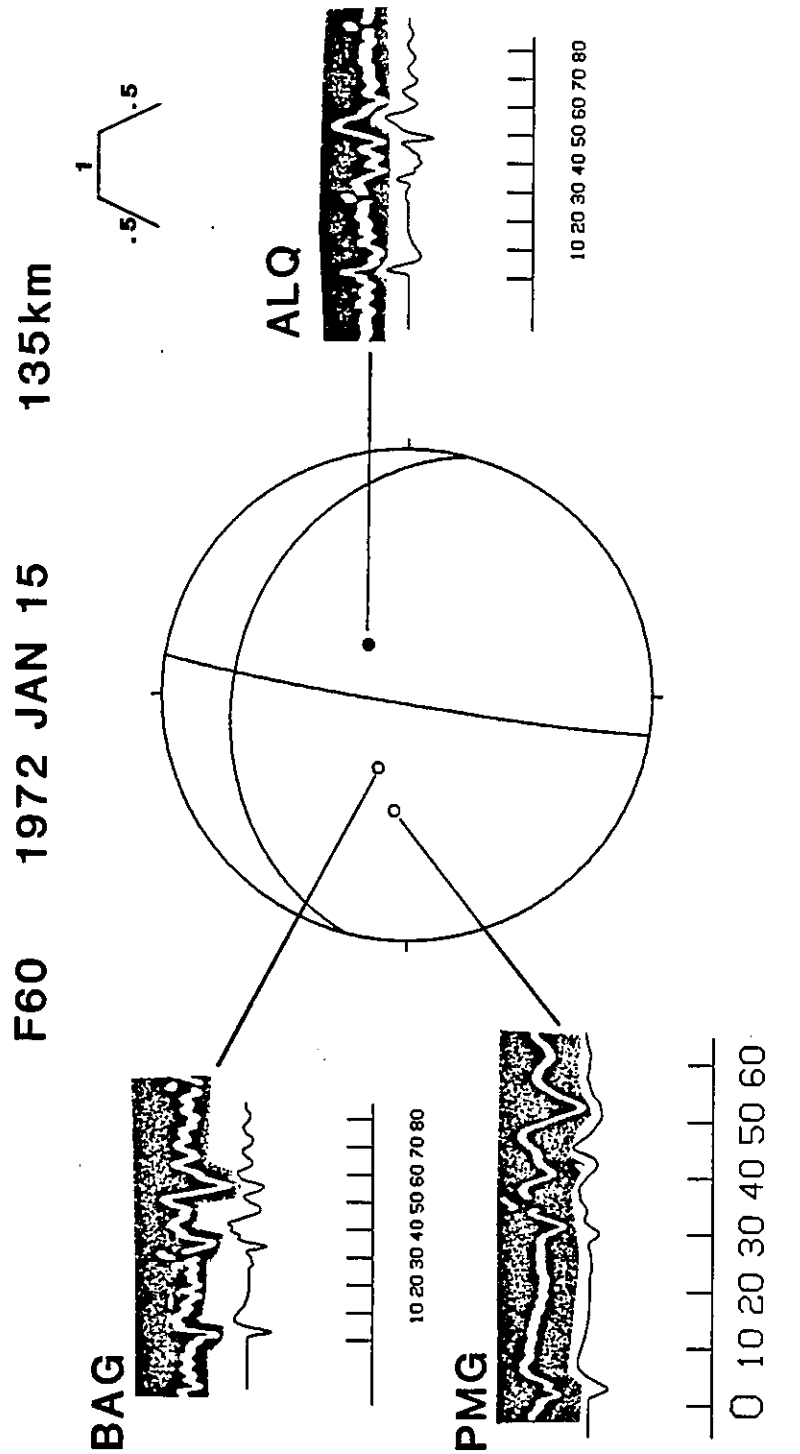
F60 1972 JAN 15 135km
BAG
ALQ
PMG
1
.5
.5
10 20 30 40 50 60 70 80
10 20 30 40 50 60 70 80
0 10 20 30 40 50 60

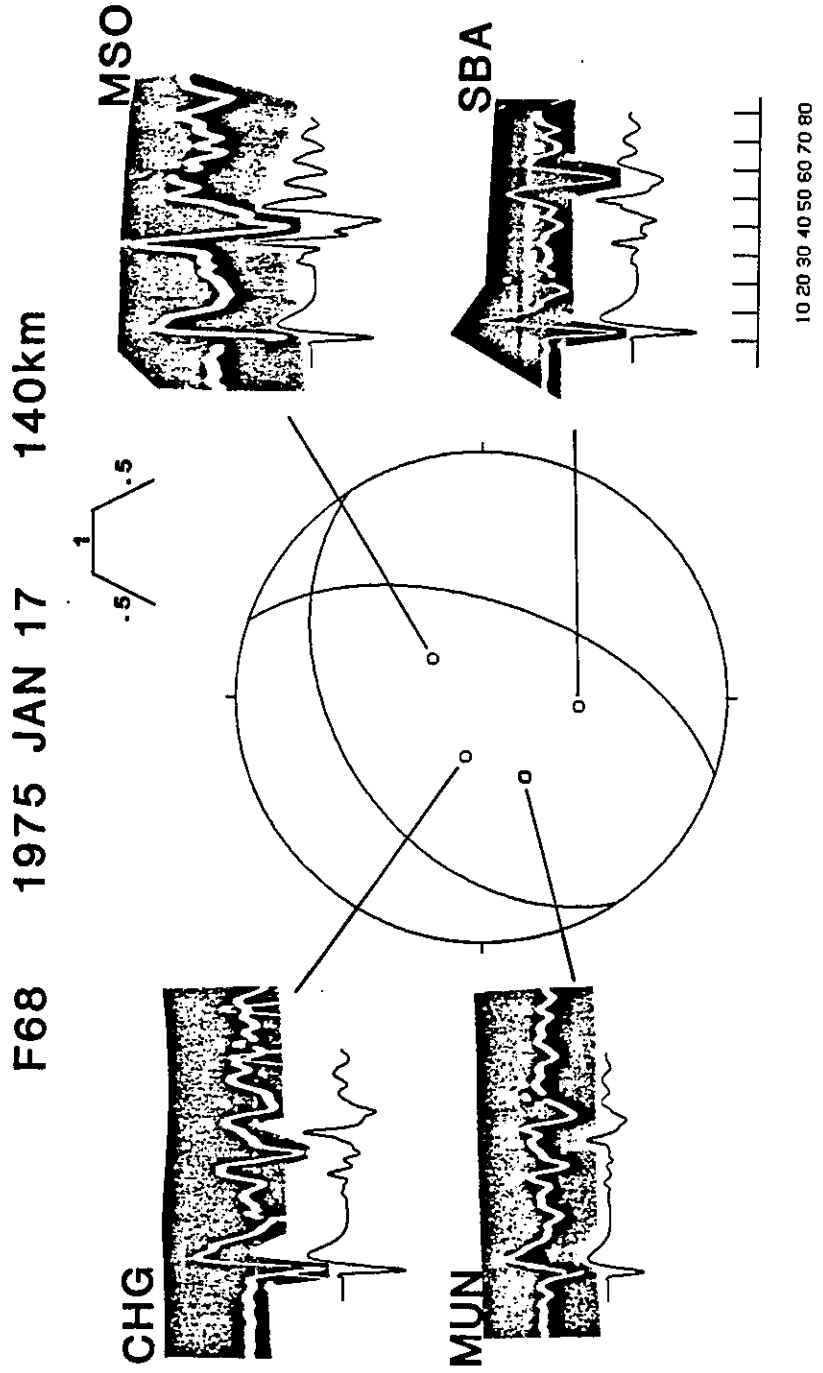
F68 1975 JAN 17 140km
MSO
SBA
CHG
MUN
.5
1
.5
10 20 30 40 50 60 70 80

F70

1976 FEB 14 235km

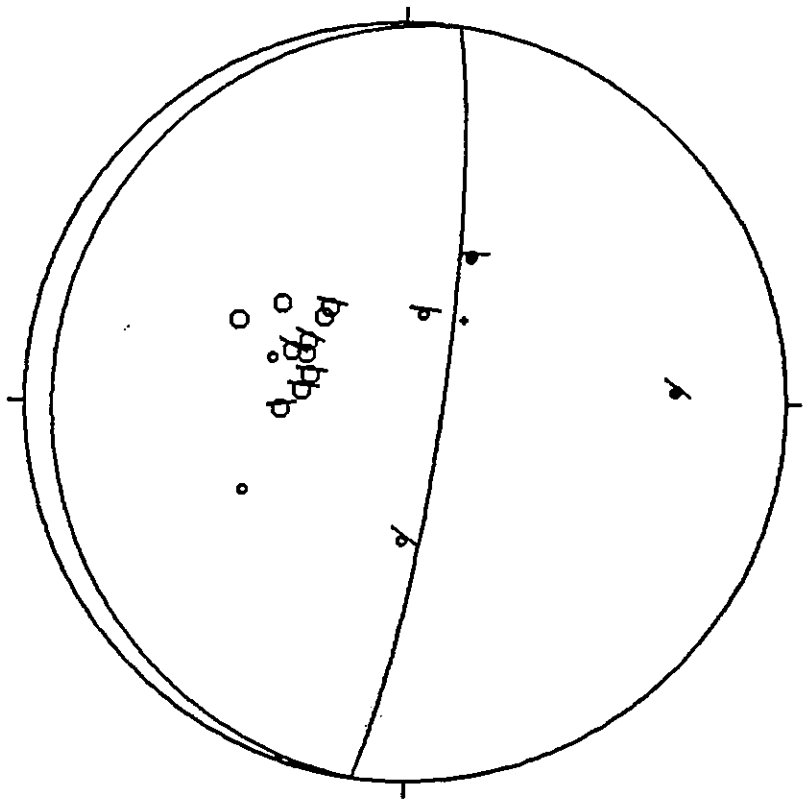

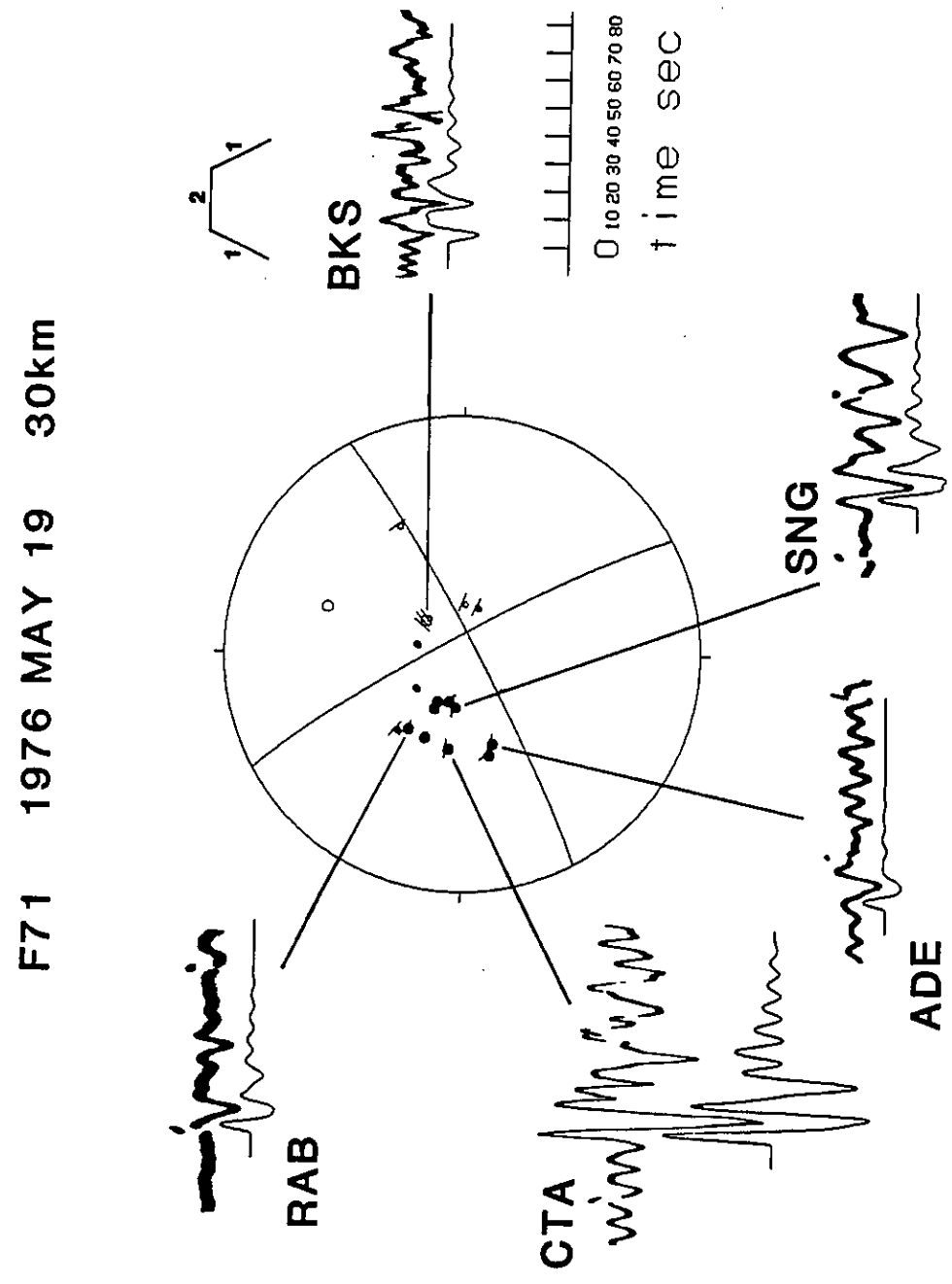
F71 1976 MAY 19 30km
BKS
RAB
CTA
SNG
ADE
0 10 20 30 40 50 60 70 80
time sec

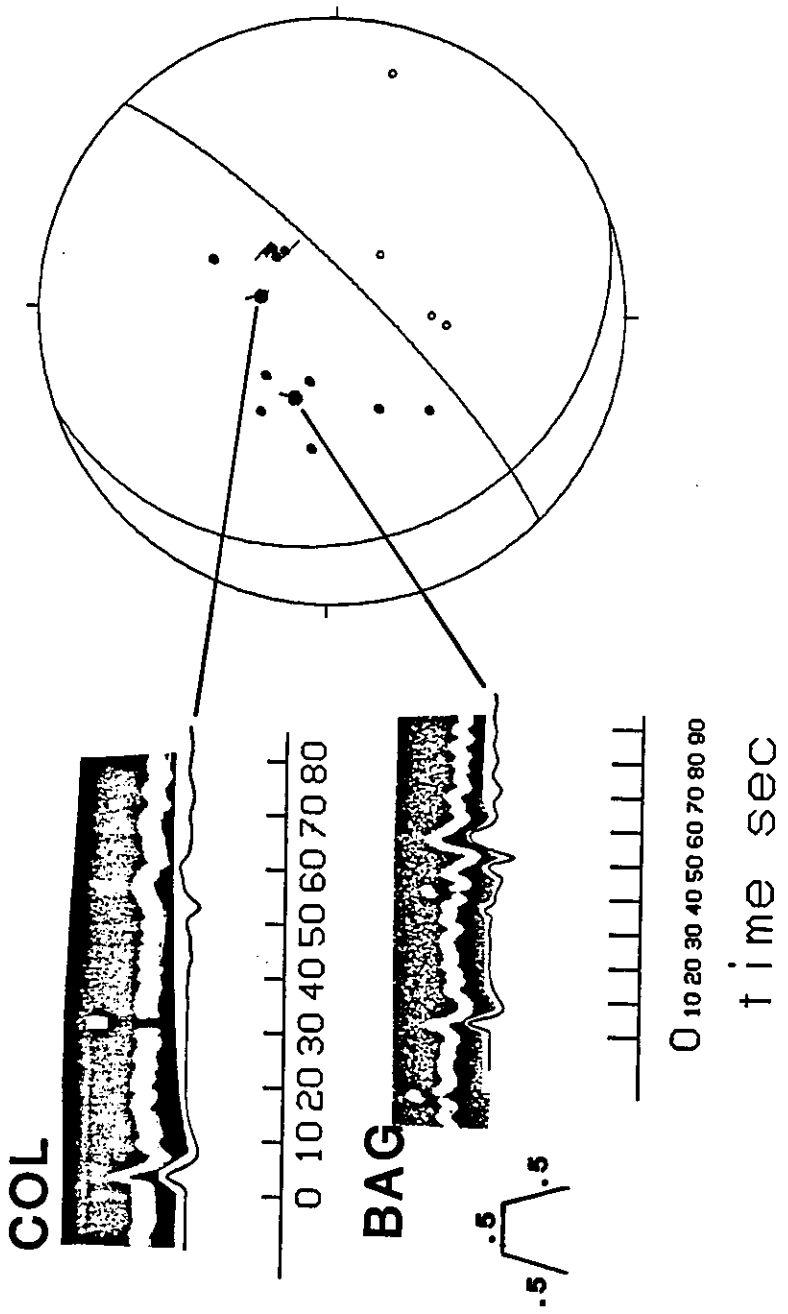
F72 1971 AUG 28 145km
COL
0 10 20 30 40 50 60 70 80
BAG
.5
.5
.5
.5
0 10 20 30 40 50 60 70 80 90
time sec

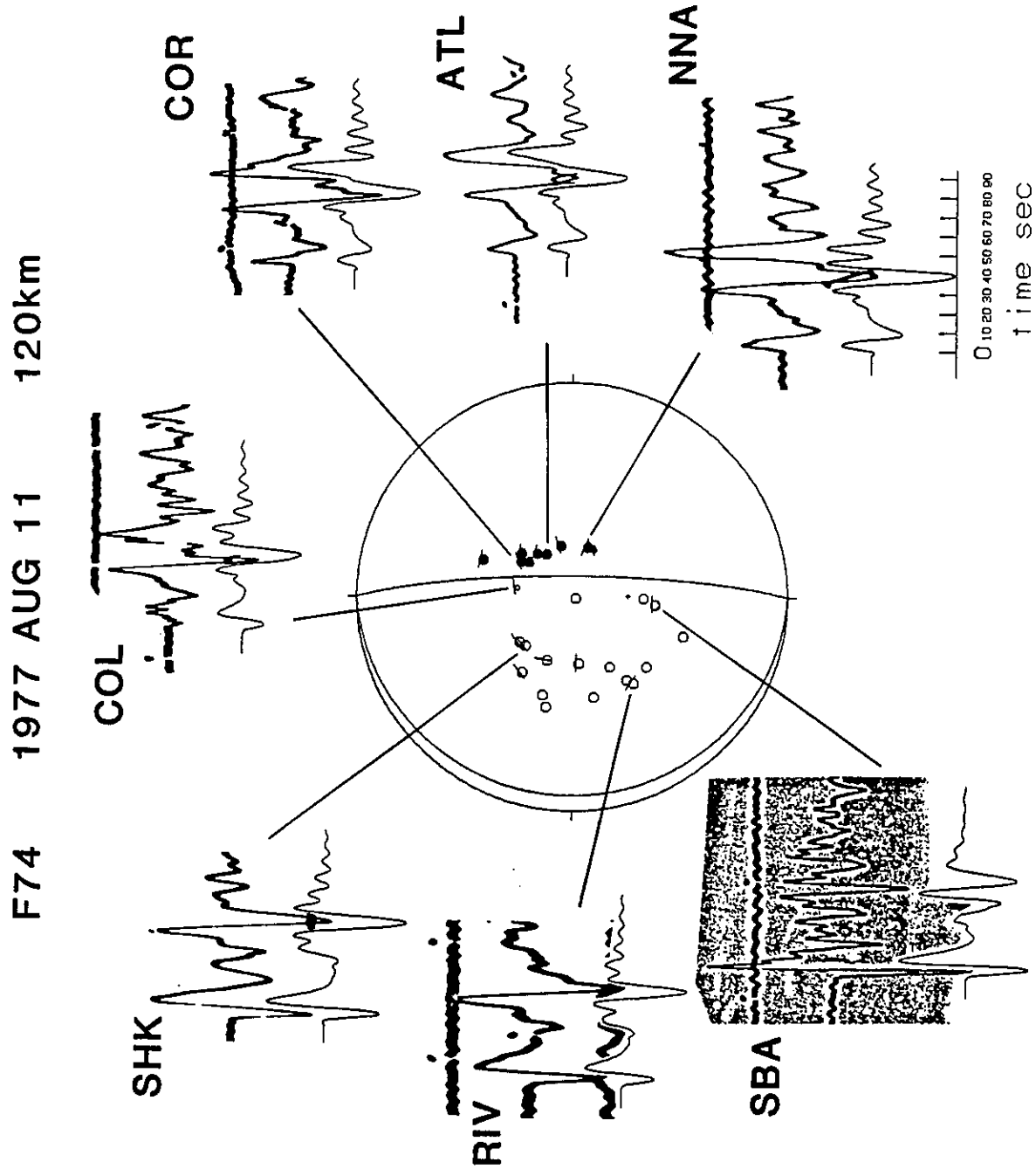
F74 1977 AUG 11 120km
COR
ATL
NNA
COL
SHK
RIV
SBA
0 10 20 30 40 50 60 70 80 90
time sec

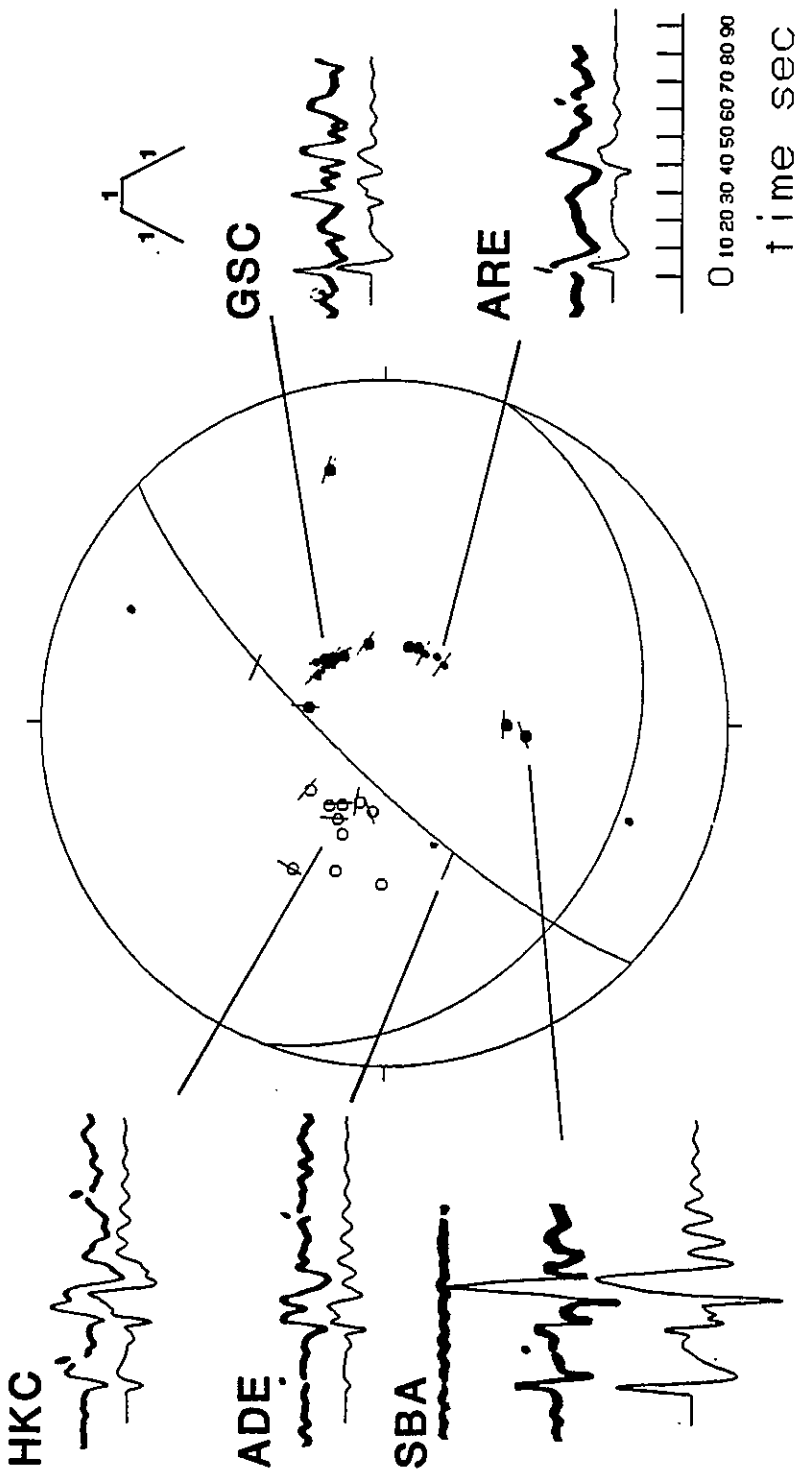
H3 1978 JAN 28 98km
GSC
ARE
HKC
ADE
SBA
0 10 20 30 40 50 60 70 80 90
time sec

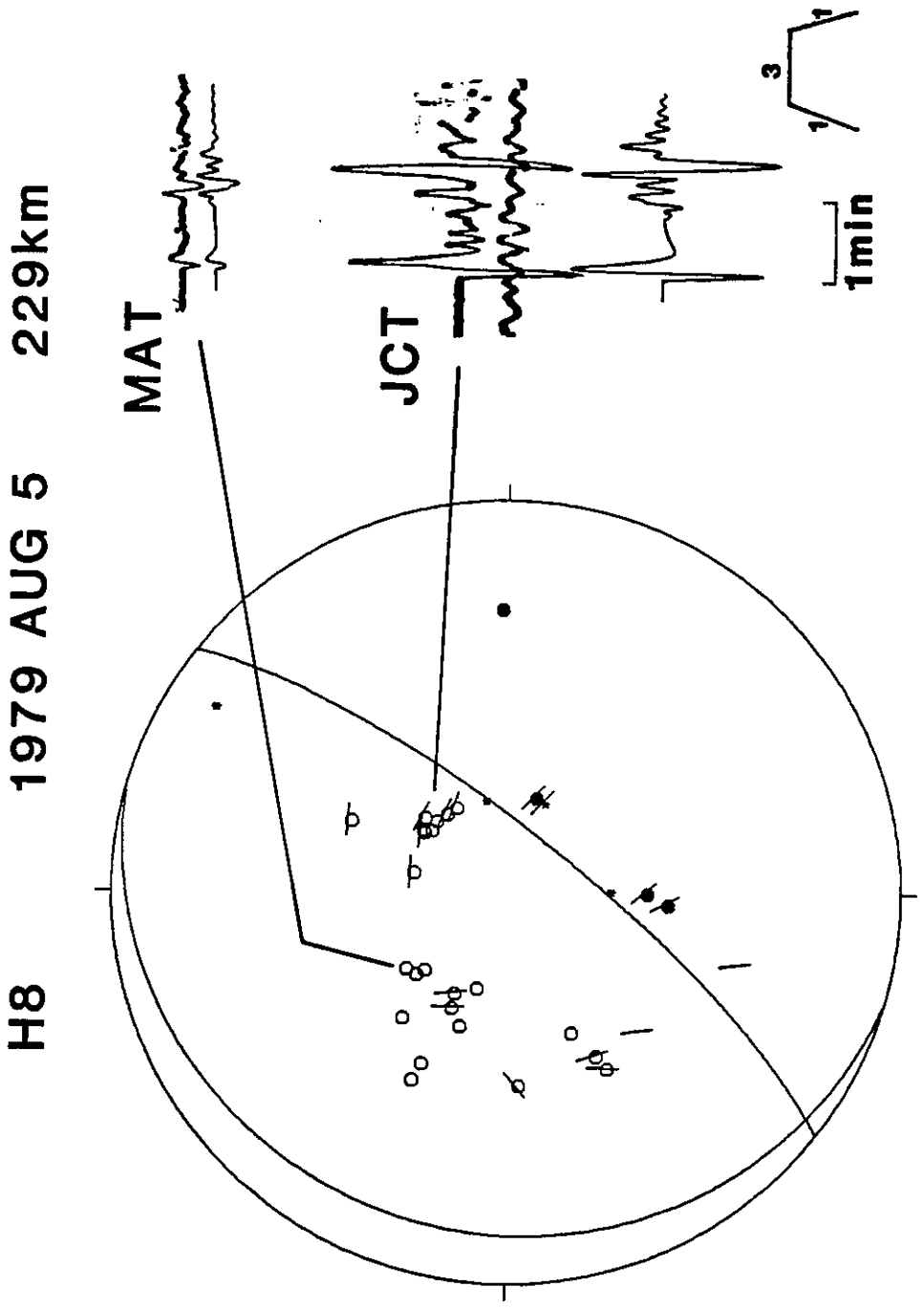
H8 1979 AUG 5 229km
MAT
JCT
3
1
1
1min

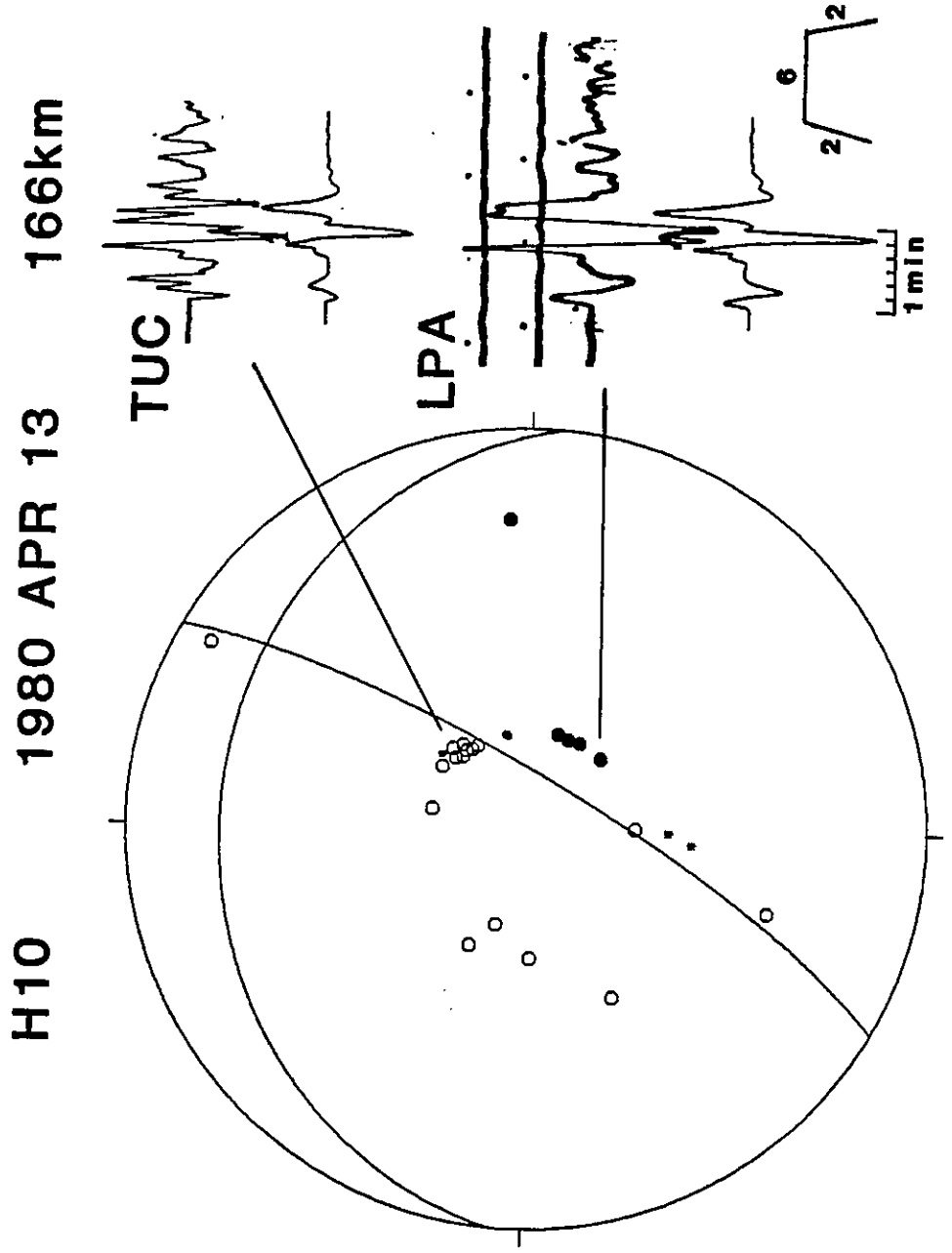
H10
1980 APR 13
166km
TUC
LPA
6
2
2
1 min

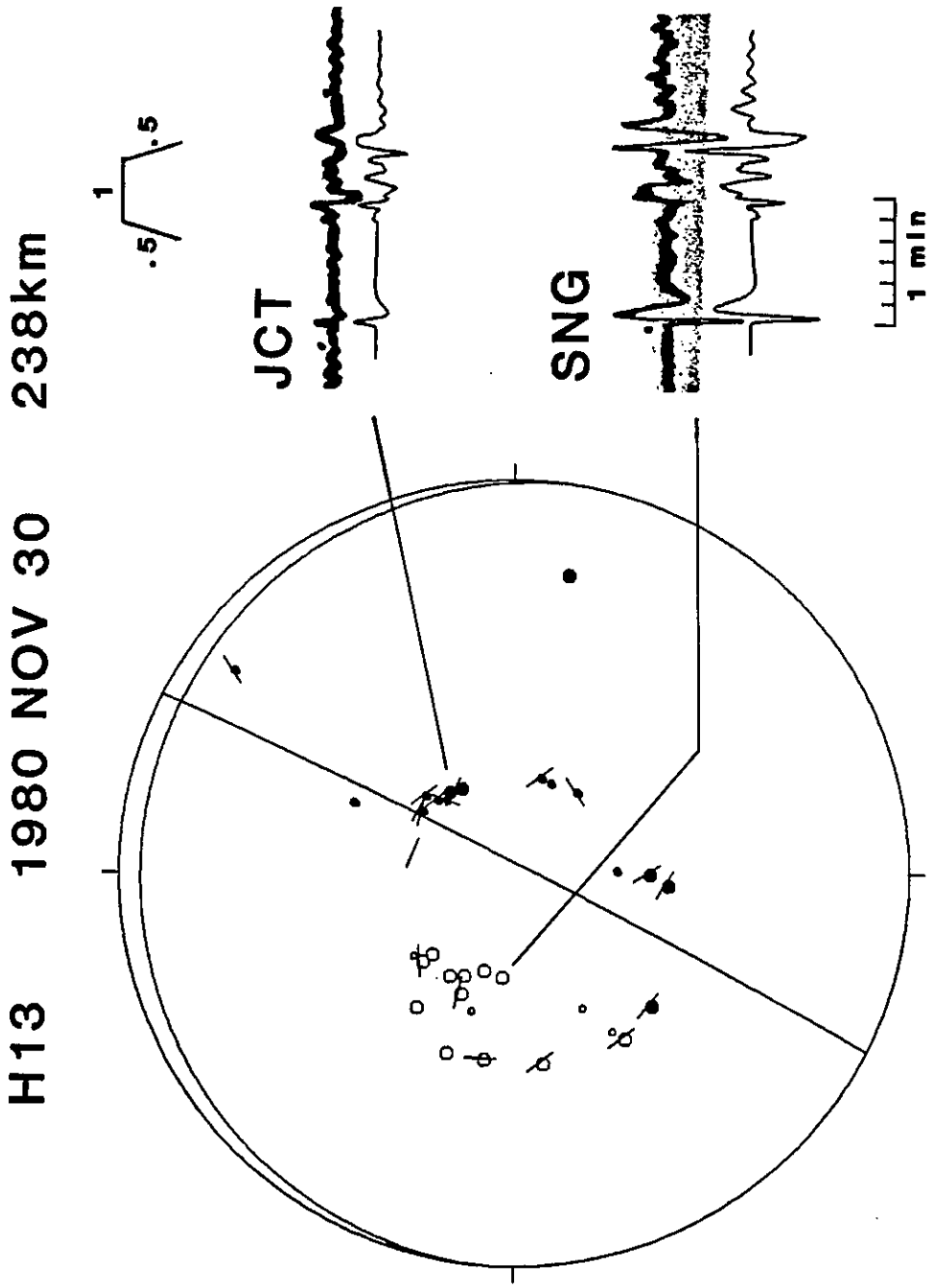
H13 1980 NOV 30 238km
JCT
SNG
1
.5
.5
1 min

H21

1981 AUG 25 108km

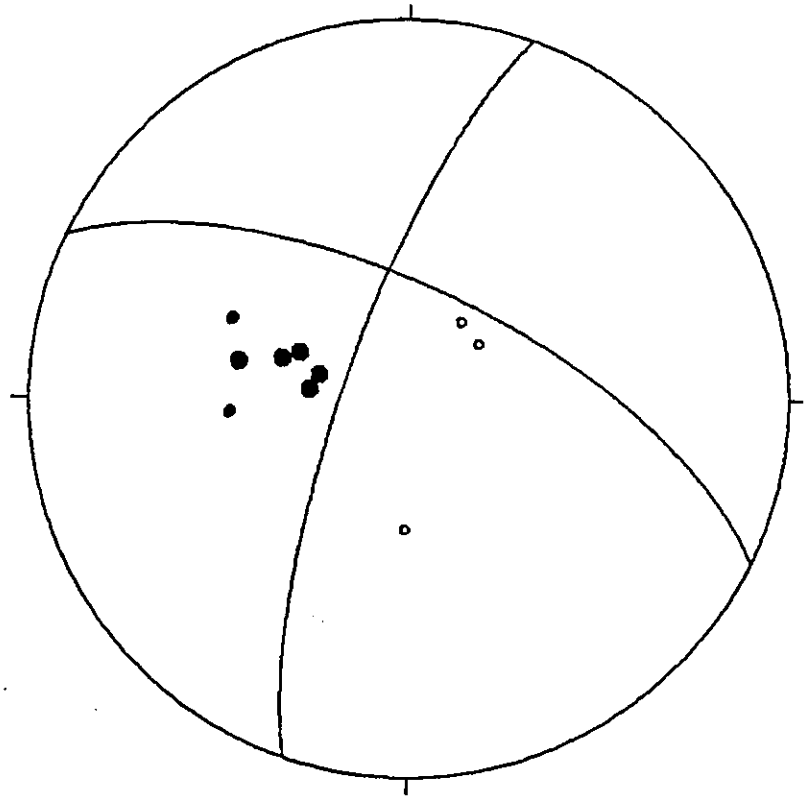

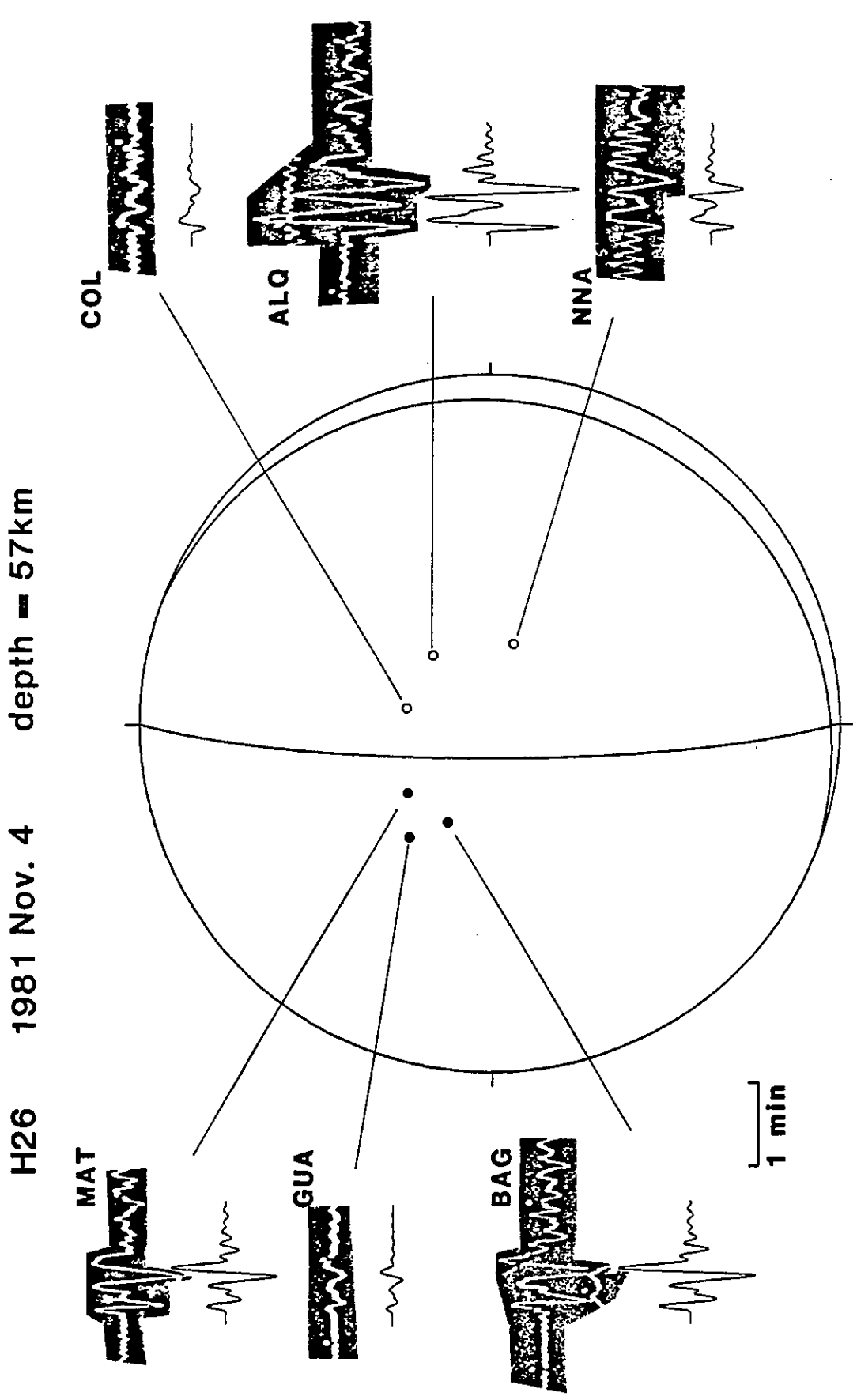
H26 1981 Nov. 4 depth = 57km
COL
ALQ
NNA
MAT
GUA
BAG
1 min

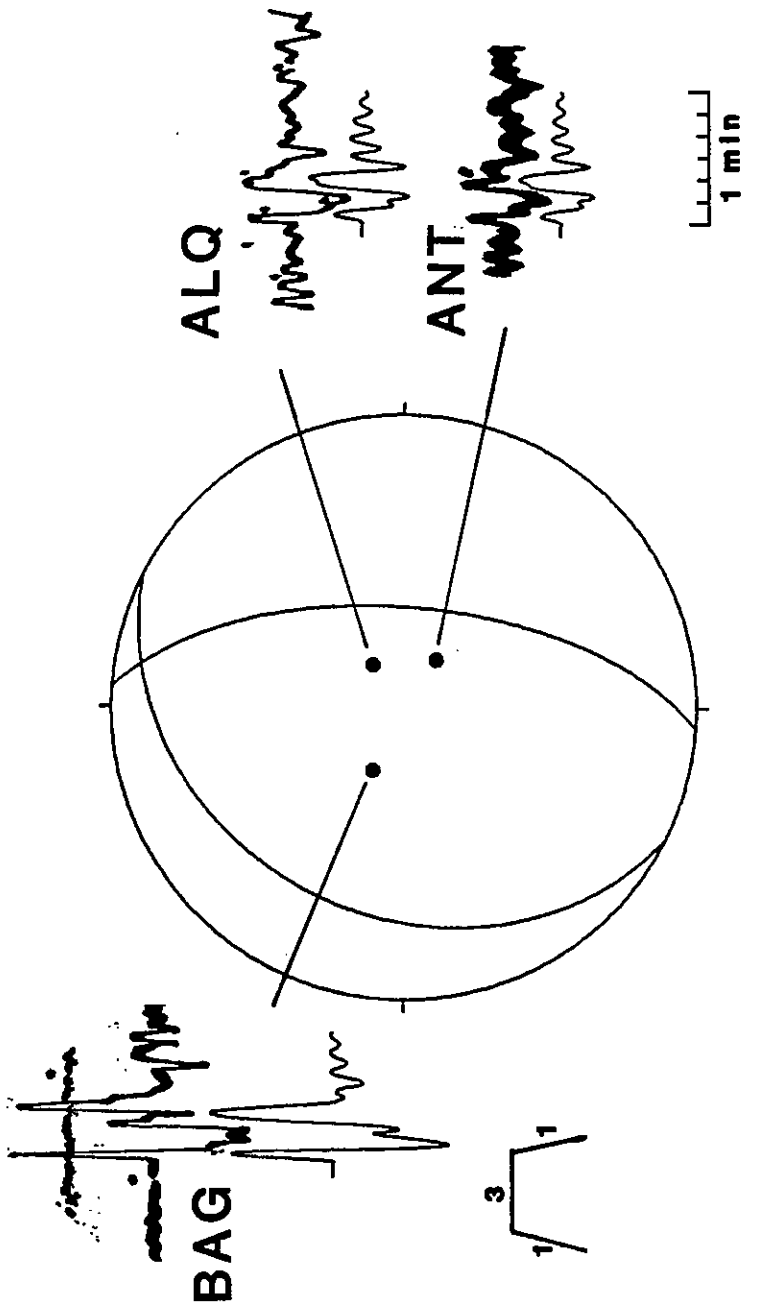
H38 1982 MAR 28 36km
ALQ
ANT
BAG
1 min
3
1
1

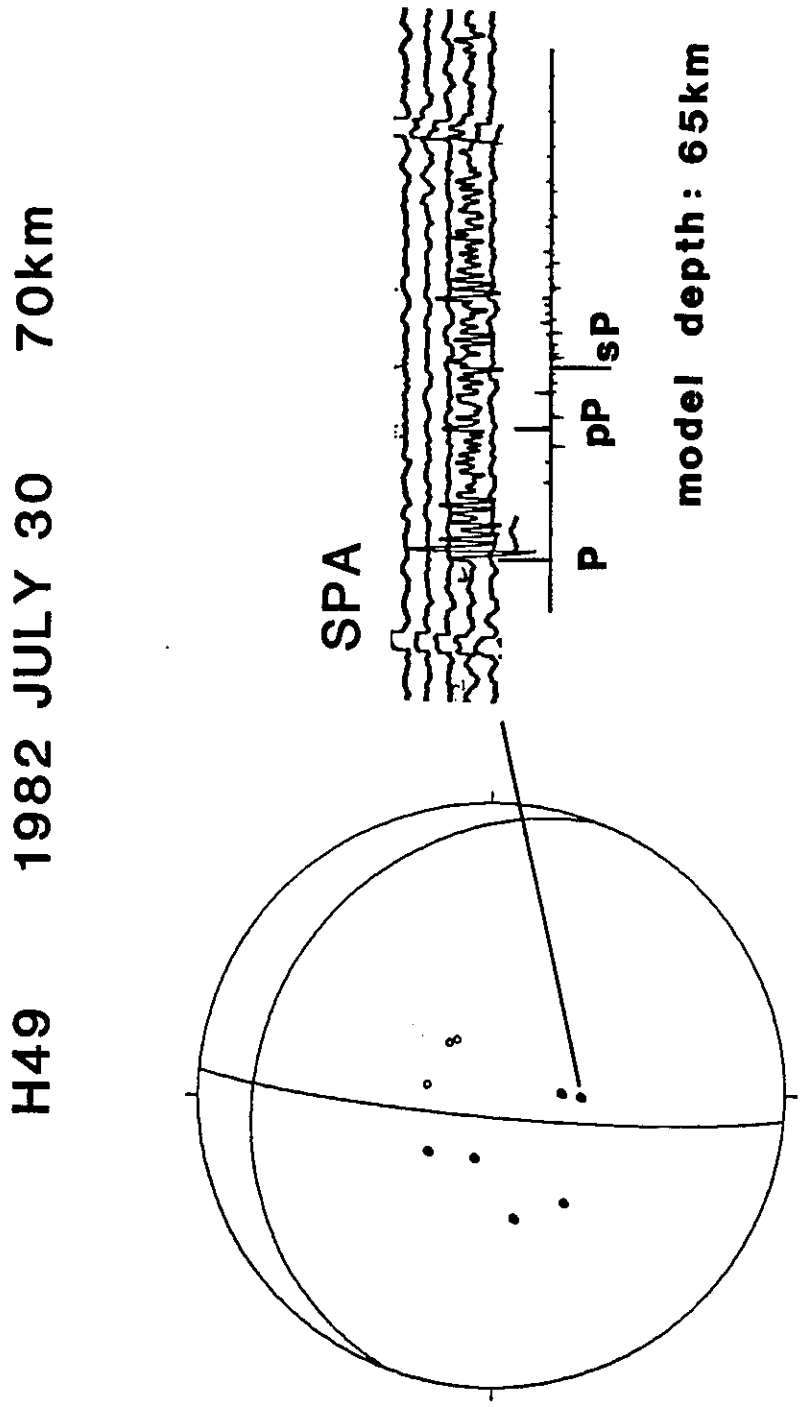
H49 1982 JULY 30 70km
SPA
P
pP
sP
model depth: 65km

REFERENCES

Abe, K., Tectonic implications of the large Shioya-oki earthquakes of 1938, *Tectonophysics*, **41**, 269-289, 1977.

Abe, K., Size of great earthquakes of 1837-1974 inferred from tsunami data, *J. Geophys. Res.*, **84**, 1561-1568, 1979.

Abe, K., Magnitudes of large shallow earthquakes from 1904 to 1980, *Phys. Earth Planet. Inter.*, **27**, 72-92, 1981.

Abe, K., Magnitude, seismic moment and apparent stress for major deep earthquakes, *J. Geophys. Res.*, **30**, 321-330, 1982.

Abe, K., and H. Tsuji, Magnitudes of the Shioya-oki earthquakes, *Annu. Meet. Seismol. Soc. Jpn. Abstr.*, **1**, 24, 1976.

Aida, I., Simulations of large tsunamis occurring in the past off the coast of the Sanriku district (in Japanese), *Bull. Earthquake Res. Inst. Univ. Tokyo*, **52**, 71-101, 1977.

Anderson, R. N., A. Hasegawa, N. Umino, and A. Takagi, Phase changes and the frequency-magnitude distribution in the upper plane of the deep seismic zone beneath Tohoku, Japan, *J. Geophys. Res.*, **85**, 1389-1398, 1980.

Asano, S., T. Yamada, K. Suyehiro, T. Yoshii, Y. Misawa, and S. Iizuka, Crustal structure off northeastern Japan as revealed from refraction method using ocean bottom seismometers (in Japanese), *Annu. Meet. Seismol. Soc. Jpn. Abstr.*, **2**, 104, 1979.

Barazangi, M., and B. L. Isacks, A comparison of the spatial distribution of mantle earthquakes determined from data produced by local and by teleseismic networks for the Japan and Aleutian arc, *Bull. Seismol. Soc. Am.*, **69**, 1763-1770, 1979.

Barazangi, M., B. Isacks, and J. Oliver, Propagation of seismic waves through and beneath the lithosphere that descends under the Tonga Island Arc, *J. Geophys. Res.*, **77**, 952-958, 1972.

Benioff, H. Seismic evidence for crustal structure and tectonic activity, *Geol. Soc. Am., Spec. Papers*, **62**, 67-74, 1955.

Billington, S. The morphology and tectonics of the subducted lithosphere in the Tonga-Fiji-Kermadec region from seismicity and focal mechanism solutions, *Ph. D. thesis*, Univ. of Cornell, 220pp, 1980.

Bolt, B. A., The revision of earthquake epicenters, focal depths and origin times using a high-speed computer, *Geophys. J. R. Astron. Soc.*, **3**, 433-440, 1960.

Chapple, W. M. and D. W. Forsyth, Earthquakes and bending of plates at trenches, **84**, 6729-6749, 1979.

Chen, W.-P., and P. Molnar, Focal depths of intracontinental and intraplate earthquakes and their implications for the thermal and mechanical properties of the lithosphere, *J. Geophys. Res.*, **88**, 4183-4214, 1983.

Creager, K. C. and T. H. Jordan, Slab penetration into the lower mantle, *J. Geophys. Res.*, **89**, 3031-3049, 1984.

Dewey, J. W., Seismicity and tectonics of western Venezuela, *Bull. Seismol. Soc. Am.*, **62**, 1711-1751, 1972.

Douglas, A., Joint epicenter determination, *Nature*, **215**, 47-48, 1967.

Dziewonski, A. M. and D. L. Anderson, Preliminary Reference Earth Model (PREM), *Phys. Earth Planet. Int.*, **25**, 297-356, 1981.

Dziewonski, A. M. and J. H. Woodhouse, An experiment in systematic study of global seismicity: centroid-moment tensor solutions for 201 moderate and large earthquakes of 1981, *J. Geophys. Res.*, **88**, 3247-3271, 1983.

Dziewonski, A. M., T. A. Chou, and J. H. Woodhouse, Determination of earthquake source parameters from waveform data for studies of global and regional seismicity, *J. Geophys. Res.*, **86**, 2825-2852, 1981.

Dziewonski, A. M., A. Friedman, D. Giardini, and J. H. Woodhouse, Global seismicity of 1982: centroid-moment tensor solutions for 308 earthquakes, *Phys. Earth Planet. Int.*, **33**, 76-90, 1983.

Engdahl, E. R., and C. H. Scholz, A double Benioff zone beneath the Central Aleutians and unbending of the lithosphere, *Geophys. Res. Lett.*, **4**, 473-476, 1977.

Engdahl, E. R. and K. Fujita, Comment on 'double seismic zone beneath the Mariana Island arc' by Ilene R. Samowitz and Donald W. Forsyth, *J. Geophys. Res.*, **86**, 7023-7024, 1981.

Engdahl, E. R., N. Umino, and A. Takagi, Seismicity patterns related to the occurrence of interplate earthquakes off the coast of northeastern Japan, *EOS Trans. AGU*, **60**, 312, 1979.

Forsyth, D. W., Fault plane solutions and tectonics of the South Atlantic and Scotia Sea, *J. Geophys. Res.*, **80**, 1429-1443, 1975.

Forsyth, D. W., Comparison of mechanical models of the oceanic lithosphere, *J. Geophys. Res.*, **85**, 6364-6368, 1980.

Fujita, K., and H. Kanamori, Double seismic zones and stresses of intermediate depth earthquakes, *Geophys. J. R. Astron. Soc.*, **66**, 131-156, 1981.

Fujita, K., E. R. Engdahl, and N. H. Sleep, Subduction zone calibration and teleseismic relocation of thrust zone events in the Central Aleutian islands, *Bull. Seismol. Soc. Am.*, **71**, 1805-1828, 1981.

Geller, R. J., Scaling relations for earthquake source parameters and magnitude, *Bull. Seismol. Soc. Am.*, **66**, 1501-1523, 1976.

Geller, R. J., and H. Kanamori, Magnitudes of great shallow earthquakes from 1904 to 1952, *Bull. Seismol. Soc. Am.*, **67**, 587-598, 1977.

Giardini, D., Regional deviation of earthquake source mechanisms from the 'double-couple' model, *Proc. Enrico Fermi Int. Sch. Phys.*, **85**, eds Kanamori, H. and E. Boschi, North-Holland, Amsterdam, 345-353, 1983.

Giardini, D., Systematic analysis of deep seismicity: 200 centroid-moment tensor solutions for earthquakes between 1977 and 1980, *Geophys. J. R. Astron. Soc.*, **77**, 883-914, 1984.

Giardini, D. and J. H. Woodhouse, Deep seismicity and modes of deformation in Tonga subduction zone, *Nature*, **307**, 505-509, 1984.

Goetze, C., and B. Evans, Stress and temperature in the bending lithosphere as constrained by experimental rock mechanics, *Geophys. J. R. Astron. Soc.*, **59**, 463-478, 1979.

Goto, K., Redetermination of the hypocenters of intermediate-depth and deep earthquakes beneath the Tonga arc, *Annu. Meet. Seismol. Soc. Jpn. Abstr.*, **2**, 179, 1984.

Goto, K., and H. Hamaguchi, A double-planed structure of the intermediate seismic zone - Thermal stress within the descending lithospheric slab (in Japanese), *Annu. Meet. Seismol. Soc. Jpn. Abstr.*, **2**, 36, 1978.

Goto, K., and H. Hamaguchi, Distribution of thermal stress within the descending lithospheric slab (in Japanese), *Annu. Meet. Seismol. Soc. Jpn. Abstr.*, **2**, 48, 1980.

Gutenberg, B., and C. F. Richter, *Seismicity of the Earth and Associated Phenomena*, 2nd ed., 130pp., Princeton University Press, N. J., 1954.

Hager, B. H. and R. J. O'Connell, Subduction zone dip angles and flow driven by plates, *Tectonophysics*, **50**, 111-133, 1978.

Hasegawa, A. and N. Umino, Focal mechanisms and the distribution of seismicity in northeast Japan, *Annu. Meet. Seismol. Soc. Jpn. Abstr.*, **1**, 34, 1978.

Hasegawa, A., N. Umino, and A. Takagi, Double-planed structure of the deep seismic zone in the northeastern Japan arc, *Tectonophysics.*, **47**, 43-58, 1978a.

Hasegawa, A., N. Umino, and A. Takagi, Double-planed deep seismic zone and upper-mantle structure in the northeastern Japan arc, *Geophys. J. R. Astron. Soc.*, **54**, 281-296, 1978b.

Hatori, T., Tsunami magnitude and wave source regions of historical Sanriku tsunamis in northeast Japan, *Bull. Earthquake Res. Inst., Univ. Tokyo,* **50**, 397-414, 1975.

Hauksson, E., J. Armbruster, and S. Dobbs, Seismicity patterns (1963-1983) as stress indicators in the Shumagin seismic gap, Alaska, preprint, 1984.

Hong, T. L., and K. Fujita, Modelling of depth phases and source processes of some central Aleutian earthquakes, **53**, 333-342, 1981.

House, L. S., and K. H. Jacob, Thermal stresses in subducting lithosphere can explain double seismic zones, *Nature,* **295**, 587-589, 1982.

House, L. S., and K. H. Jacob, Earthquakes, plate subduction, and stress reversals in the eastern Aleutian arc, *J. Geophys. Res.,* **88**, 9347-9373, 1983.

Isacks, B. L. and P. Molnar, Mantle earthquake mechanisms and the sinking of the lithosphere, *Nature,* **223**, 1121-1124, 1969.

Isacks, B. L. and P. Molnar, Distribution of stresses in the descending lithosphere from a global survey of focal-mechanism solutions of mantle earthquakes, *Rev. Geophys. Space Phys.,* **9**, 103-174, 1971.

Isacks, B. L., and M. Barazangi, Geometry of Benioff zones. Lateral segmentation and downwards bending of the subducted lithosphere, in *Island Arcs Deep Sea Trenchs and Back-Arc Basins, Maurice Ewing Ser.,* vol. **1**, edited by M. Talwani and W. C. Pitman III, pp. 99-114, AGU, Washington, D. C., 1977.

Isacks, B. L., L. R. Sykes, and J. Oliver, Focal mechanisms of deep and shallow earthquakes in the Tonga-Kermadec region and the tectonics of island arcs, *Geol. Soc. Amer. Bull.,* **80**, 1443-1470, 1969.

Johnson, T., and P. Molnar, Focal mechanisms and plate tectonics of the southwest Pacific, *J. Geophys. Res.,* **77**, 5000-5032, 1972.

Kanamori, H., Focal mechanism of the Tokachi-oki earthquake of May 16, 1968: Contortion of the lithosphere at a junction of two trenches, *Tectonophysics.,* **12**, 1-13, 1971a.

Kanamori, H., Seismological evidence for a lithospheric normal faulting - The Sanriku earthquake of 1933, *Phys. Earth Planet. Inter.,* **4**, 289-300, 1971b.

Kanamori, H., Mechanism of tsunami earthquakes, *Phys. Earth Planet. Inter.,* **6**, 346-359, 1972.

Kanamori, H., The energy release in great earthquakes, *J. Geophys. Res.,* **82**, 2981-2987, 1977.

Kanamori, H., and D. L. Anderson, Theoretical basis of some empirical relations in seismology, *Bull. Seismol. Soc. Am.,* **65**, 1073-1095, 1975.

Katsumata, M., and M. Yamamoto, On the seismicity gap off Fukushima prefecture, *Annu.*

Meet. Seismol. Soc. Jpn. Abstr., **1**, 58, 1982.

Kawakatsu, H., and T. Seno, Triple seismic zone and the regional variation of seismicity along the northern Honshu arc, *J. Geophys. Res.*, **88**, 4215-4230, 1983.

Kirby, S. H., Tectonic stresses in the lithosphere: Constraints provided by the experimental deformation of rocks, *J. Geophys. Res.*, **85**, 6353-6363, 1980.

Kirby, S. H., Rheology of the lithosphere, *Rev. Geophys. Space Phys.*, **21**, 1458-1487, 1983.

Kroeger, G. C. and R. J. Geller, A new method for calculating the effects of layered structure on teleseismic body waves, *J. Geophys. Res.*, in press, 1985.

Le Pichon, X., J. Francheteau, and J. Bonnin, *Plate Tectonics* 311pp., Elsevier, Amsterdam, 1976.

Malglange, M. A., and R. Madariaga, Complex distribution of large thrust and normal fault earthquakes in the Chilean subduction zone, *Geophys. J. R. Astron. Soc.*, **73**, 480-505, 1983.

McNutt, M. K., and H. W. Menard, Constraints on yield strength in the oceanic lithosphere derived from observations of flexure, *Geophys. J. R. Astron. Soc.*, **71**, 363-394, 1982.

Mendiguren, J. A., Focal mechanism of a shock in the middle of the Nazca Plate, *J. Geophys. Res.*, **76**, 3861-3879, 1971.

Minear, J. W., and M. N. Toksöz, Thermal regime of a downgoing slab and new global tectonics, *J. Geophys. Res.*, **75**, 1397-1419, 1970.

Mogi, K., Recent seismic activity in the eastern Japan (in Japanese), *Rep. Coord. Comm. Earthquake Predict.*, **21**, 140, 1979.

Nakajima, T., Spatial and sequential distribution of focal mechanisms before and after the Tokachi-oki earthquake of May 16, 1968 (in Japanese), *Geophys. Bull. Hokkaido Univ.*, **32**, 25-42, 1974.

Nieman, T. L., K. A. Wagner, and K. Fujita, Effects of subducting slabs on teleseismic hypocentral determinations - theoretical calculations, *EOS Trans. AGU*, **65**, 234, 1984.

Oliver, J. and B. Isacks, Deep earthquake zones, anomalous structures in the upper mantle, and the lithosphere, *J. Geophys. Res.*, **72**, 4259-4275, 1967.

Parsons, B., and J. Sclater, An analysis of the variation of ocean floor bathymetry and heat flow with age, *J. Geophys. Res.*, **82**, 803-827, 1977.

Reyners, M., and K. S. Coles, Fine structure of the dipping seismic zone and subduction mechanics in the Shumagin islands, Alaska, *J. Geophys. Res.*, **87**, 356-366, 1982.

Richter, F. M., Focal mechanisms and seismic energy release of deep and intermediate earthquakes in the Tonga-Kermadec region and their bearing on the depth extent of mantle

flow, *J. Geophys. Res.*, **84**, 6783-6795, 1979.

Rikitake, T., *Earthquake Prediction*, 357pp, Elsevier, Amsterdam, 1976.

Ruff, L., and H. Kanamori, Seismic coupling and uncoupling at subduction zones, *Tectonophysics*, **99**, 99-117, 1983.

Samowitz, I. R., and D. W. Forsyth, Double seismic zone beneath the Mariana Island arc, *J. Geophys. Res.*, **86**, 7013-7021, 1981.

Sasatani, T., Analysis of two shallow earthquakes based on the body wave data (in Japanese), *Geophys. Bull. Hokkaido Univ.*, **26**, 109-132, 1971.

Seno, T., Intraplate seismicity in Tohoku and Hokkaido and large interplate earthquakes: A possibility of a large interplate earthquake off the southern Sanriku coast, northern Japan, *J. Phys. Earth*, **27**, 21-51, 1979.

Seno, T., and B. Pongsawat, A triple-planed structure of seismicity and earthquake mechanisms off Miyagi prefecture, northeastern Honshu, Japan, *Earth Planet. Sci. Lett.*, **55**, 25-36, 1981.

Seno, T., and G. C. Kroeger, A reexamination of earthquakes previously thought to have occurred within the slab between the trench axis and double seismic zone, northern Honshu arc, *J. Phys. Earth*, **31**, 195-216, 1983.

Seno, T., K. Shimazaki, P. Somerville, K. Sudo, and T. Eguchi, Rupture process of the Miyagi-oki, Japan, earthquake of June 12, 1978, *Phys. Earth Planet. Inter.*, **23**, 39-61, 1980.

Shiono, K., T. Mikumo, and Y. Ishikawa, Tectonics of the Kyushu-Ryukyu arc as evidence from seismicity and focal mechanism of shallow to intermediate-depth earthquakes, *J. Phys. Earth*, **28**, 17-43, 1980.

Silver, P. G., and T. H. Jordan, Total-moment spectra of fourteen large earthquakes, *J. Geophys. Res.*, **88**, 3273-3293, 1983.

Sleep, N. H., Teleseismic P-Wave transmission through slabs, *Bull. Seismol. Soc. Am.*, **63**, 1349-1373, 1973.

Sleep, N. H., The double seismic zone in downgoing slabs and the viscosity of the mesosphere, *J. Geophys. Res.*, **84**, 4565-4571, 1979.

Smith, S. W., Determination of maximum earthquake magnitude, *Geophys. Res. Lett.*, **3**, 351-354, 1976.

Solomon, S. C., and K. T. P. U, Elevation of the olivine-spinel transition in subducted lithosphere: seismic evidence, *Phys. Earth Planet, Int.*, **11**, 97-108, 1975.

Stauder, W., and L. Mualchin, Fault motion in the larger earthquakes of the Kurile-Kamchatka arc and of the Kurile-Hokkaido corner, *J. Geophys. Res.*, **81**, 297-308, 1976.

Suzuki, S., T. Sasatani, and Y. Motoya, Double seismic zone beneath the middle of Hokkaido, Japan, in the southwestern side of the Kurile arc, *Tectonophysics,* **98**, 59-76, 1983.

Sykes, L. R., Seismicity and deep structure of island arcs, *J. Geophys. Res.*, **71**, 2981-3006, 1966.

Sykes, L. R., B. L. Isacks, and J. Oliver, Spacial distribution of deep and shallow earthquakes of small magnitudes in the Fiji-Tonga region, *Bull. Seismol. Soc. Am.*, **59**, 1093-1113, 1969.

Tarandier, J. and E. A. Okal, Human perception of T waves: the June 22, 1977 Tonga earthquake felt on Tahiti, *Bull. Seismol. Soc. Am.*, **69**, 1475-1486, 1979.

Topper, R. E., Fine structure of the Benioff zone beneath the central Aleutian arc, *MS. thesis,* University of Colorado, 148pp, 1978.

Tsuboi, C., Investigation on the deformation of earth's crust found by precise geodetic means, *Jap. J. Astron. Geophys.*, **10**, 93-248, 1933.

Tsukahara, H., Double-planed structure of the deep seismic zone and plasticity for the descending lithosphere (in Japanese), *Annu. Meet. Seismol. Soc. Jpn. Abstr.*, **2**, 149, 1977.

Tsukahara, H., Physical conditions for double seismic planes of the deep seismic zone, *J. Phys. Earth,* **28**, 1-15, 1980.

Tsumura, K., Microearthquake activity in the Kanto district, in *Special Publication for the 50th Annive. of the Great Kanto Earthquake.*, Earthquake Research Institute, pp. 67-87, Tokyo, 1973.

Umino, N., and A. Hasegawa, On the two-layered structure of deep seismic plane in northeastern Japan arc (in Japanese), *J. Seismol. Soc. Jpn.*, **28**, 125-139, 1975.

Usami, T., *Descriptive Catalogue of Disaster Earthquakes in Japan* (in Japanese), 327 pp., University of Tokyo Press, Tokyo, 1975.

Utsu, T., Space-time pattern of large earthquakes occurring off the Pacific coast of the Japanese islands, *J. Phys. Earth,* **22**, 325-342, 1974.

Utsu, T., *Seismology* (in Japanese), 286pp., Kyoritsu, Tokyo, 1977.

Utsu, T., Some remarks on a seismic gap off Miyagi prefecture (in Japanese), *Rep. Coord. Comm. Earthquake Predict.*, **21**, 44-46, 1979a.

Utsu, T., Seismicity of Japan from 1885 through 1925. - A new catalogue of earthquakes of M>6 felt in Japan and smaller earthquakes which caused damage in Japan (in Japanese), *Bull. Earthquake Res. Inst., Univ. Tokyo,* **54**, 253-308, 1979b.

Utsu, T., Spatial and temporal distribution of low-frequency earthquakes in Japan, *J. Phys. Earth,* **28**, 361-384, 1980.

Utsu, T., Seismicity of Japan from 1885 through 1925 (Correction and Supplement) (in Japanese), *Bull. Earthquake Res. Inst., Univ. Tokyo,* **57**, 111-117, 1982.

Veith, K., The relationship of island arc seismicity to plate tectonics, Ph.D. thesis, Southern Methodist Univ., Dallas, Tex., 1974.

Wadati, K., On the activity of deep-focus earthquakes in the Japan Island and neighbourhood, *Geophys. Mag.,* **8**, 305-326, 1935.

Wortel, R., Seismicity and rheology of subducting slabs, *Nature,* **296**, 553-556, 1982.

Yokokura, T. Viscosity of the Earth's mantle: inference from dynamic support by flow stress, *Tectonophysics,* **77**, 35-62, 1981.

Yoshii, T., Proposal of the "aseismic front" (in Japanese), *J. Seismol. Soc. Jpn.,* **28**, 365-367, 1975.

Yoshii, T., Structure of the earth's crust and mantle in northeast Japan, *Kagaku,* **47**, 170-176, 1977.

Yoshii, T., A detailed cross-section of the deep seismic zone beneath Japan, *Tectonophysics,* **55**, 349-360, 1979a.

Yoshii, T., Compilation of geophysical data around the Japanese islands, *Bull. Earthquake Res. Inst., Univ. Tokyo,* **54**, 75-117, 1979b.